Site-directed mutagenesis studies of the GnRH and TRH receptors of the pituitary gland

Julia Vanessa Foskett Cook

Thesis submitted to the University of Edinburgh
for the degree of Doctor of Philosophy

1996

Contents

Declaration

The experiments described in this thesis were the unaided work of the author except where acknowledgement is made by reference. No part of this work has been accepted for any other degree, nor is any part of it being submitted concurrently in candidature for another degree. All experiments were performed at the Medical Research Council Reproductive Biology Unit in Edinburgh.

Julia Cook

February 1996

Acknowledgements

This work has been carried out at the MRC Reproductive Biology Unit, Edinburgh, and I gratefully acknowledge the Medical Research Council and the Ernst Schering Research Foundation for funding my studies.

I would also like to acknowledge the people who contributed to the work in this thesis. The computer derived molecular models of GnRH and its receptor were produced by Dr P L Taylor (MRC, Reproductive Biology Unit, Edinburgh) whilst the helical wheel models of the GnRH-R were generated by Dr J M Baldwin (MRC, Laboratory of Molecular Biology, Cambridge). The Kodak flag tag and HA-tagging systems have been initially developed by Dr K A Eidne, A McGregor and E Faccenda, in the MRC Reproductive Biology Unit, Edinburgh, whilst the triple HA-tagged TRH-R and the HA-tagged Gq protein were obtained from Professor Graeme Milligan, Department of Biochemistry, University of Glasgow. In addition, my thanks go to Dr Lorraine Anderson for calcium imaging data and Dr T A Bramley for kindly producing radiolabelled GnRH analogue tracers.

I would also like to thank those people who have provided both scientific inspiration and emotional support during this study. Firstly, my special thanks goes to my supervisor, Dr Karin Eidne, for her friendship, encouragement and scientific advice throughout the course of my PhD. Secondly, I would like to thank the members of lab GO6: Dr Philip Taylor (for his worldly knowledge on Apple Macintosh computers together with the ability to rescue information from my crashed computer discs), Dr Lorraine Anderson, Dr Bernadette Byrne (for proof reading my thesis), Robin Sellar, Elena Faccenda and Alison McGregor. I would also like to express my gratitude to Ted Pinner and Tom McFetters, in the Graphics department, for producing the great colour figures and photographs.

Finally, I would like to thank my parents and friends (particularly my fellow PhD students) for their everlasting encouragement and support throughout the entire three year period. This thesis could not have been produced without their help and encouragement.

Abstract

Mammalian reproduction is driven by gonadotrophin-releasing hormone (GnRH) - a decapeptide released from hypothalamic neurones into the pituitary portal blood vessels. The aim of this thesis was to study structure-function relationships of the G-protein coupled GnRH receptor (GnRH-R), and has focused on the identification of key amino acids involved in GnRH ligand-receptor interactions as well as the role of putative disulphide bridge formation within the receptor itself. In addition, the role of disulphide bridge formation has also been explored in another G-protein coupled receptor (GPCR), the thyrotrophin-releasing hormone receptor (TRH-R). Comparative sequence analysis and computer molecular modelling approaches were used to target potentially important amino acids for site-directed mutagenesis study. Wild-type and receptor mutants were then expressed in mammalian cells, and receptor binding, expression, and activational properties compared between constructs.

The majority of GPCRs contain two conserved extracellular Cys residues which have been postulated to form a covalently linked disulphide bridge structure. In the GnRH-R, these Cys residues are positioned at Cys114 and Cys195 in the first and second extracellular loops respectively. In addition, the GnRH-R contains two non-conserved Cys residues at Cys14 in the amino terminus and Cys199 in the second extracellular loop. Substitution of these Cys residues to serine resulted in a loss of ligand binding. A comparative study in the TRH-R, substituting the conserved extracellular Cys residues, Cys98 and Cys179, to either serine or alanine, confirmed these findings. This data suggests that extracellular Cys residues, through putative disulphide bridge formation, may maintain the tertiary extracellular structure of the receptor and therefore facilitate ligand-receptor binding. Further studies, using chemical modifying reagents, have indicated that Cys residues with free sulfhydryl groups may also be important in TRH-R binding.

The GnRH-R despite its structural homology to other GPCRs exhibits some unique features. These differences include the interchange of a highly conserved Asp and Asn residue in the transmembrane (TM) domains. Individual substitutions of Asn87

(in TM II) to Asp87 and Asp318 (in TM VII) to Asn318, revealed that Asn87 is important for GnRH agonist and antagonist binding whereas Asp318 is important for receptor activation. To investigate if the function as well as the position of these amino acids were transposed, a double mutation substituting both residues simultaneously was generated. However, this mutant receptor showed only a small degree of GnRH agonist binding, indicating that the functional role of these specific residues is not interchangeable.

Amongst GPCRs, the GnRH-R is particularly suitable for three dimensional molecular modelling and computer aided simulations because of its short extracellular and intracellular domains. Using this approach, it has been possible to predict putative amino acids involved in ligand-receptor interactions. During this study, GnRH molecular models have evolved from a template predicted by the Baldwin model to a series of energy minimised computer generated three dimensional structures. To simulate GnRH ligand-receptor interactions, a model of the native GnRH peptide has also been constructed. The initial Baldwin model highlighted a series of TM located polar amino acids in TM II, TM III, TM IV and TM VII of the GnRH-R. Both the position and nature of these amino acids rendered them capable of interacting with the GnRH ligand. Mutations at these sites identified two residues, His305 located at the TM VII/extracellular interface and Asn314 in TM VII, that were potentially important for GnRH-R binding.

Further modelling studies, using GnRH ligand-receptor computer simulations, predicted that amino acids Phe312 in TM VII and Leu83 in TM II may interact with Trp3 and Leu7 in the GnRH ligand respectively. Substituting these amino acids to residues of either similar, different or neutral hydropathicity, showed that a hydrophobic amino acid was essential for GnRH-R binding at position 312 and for receptor activation at residue 83. Altogether, 15 sites within the GnRH-R have been experimentally modified and the information derived from site-directed mutagenesis studies has been utilised to redefine the structure of the molecular models.

In conclusion, the formation of a putative disulphide bond between extracellular cysteine residues in both the GnRH-R and TRH-R is important in maintaining tertiary protein structure. In addition, amino acids located in TM II and TM VII are essential for binding interactions between GnRH and its receptor. Analysis of structure-function relationships, particularly using this dual biochemical and

molecular modelling approach, will greatly facilitate rational drug design. In the light of the enormous clinical applications of GnRH and its analogues, information regarding the mechanisms of hormone-receptor interactions will be of benefit in the development of new and novel drugs for clinical use in reproductive medicine.

List of Figures

List of Tables and Appendices

Abbreviations

ACTH	adrenocorticotrophic hormone
Ala	alanine(A)
Amp	ampicillin
Arg	arginine (R)
Asn	asparagine (N)
Asp	aspartic acid (D)
β-gal	β-galactosidase
bp	base pair
BSA	bovine serum albumin
$[Ca^{2+}]i$	intracellular calcium
$[Ca^{2+}]e$	extracellular calcium
cAMP	cyclic adenosine monophosphate
cDNA	complementary DNA
cfu	colony forming unit
Chl	chloramphenicol
CMV	cytomegalovirus
COOH	carboxy
CRH	corticotrophic hormone
Cys	cysteine (C)
dATP	deoxyadenosine triphosphate
dCTP	deoxycytidine triphosphate
dGTP	deoxyguanosine triphosphate
dTTP	deoxythymidine triphosphate
DA	dopamine
DAG	diacylglyceride
DNA	deoxyribonucleic acid
DTT	dithiothreitol
EDTA	ethylenediaminetetraacetic acid
el	extracellular loop
ERE	estrogen response element
FSH	follicle stimulating hormone

GH	growth hormone
GHRH	growth hormone releasing hormone
Gln	glutamine (Q)
Glu	glutamic acid (E)
Gly	glycine (G)
GnRH	gonadotrophin-releasing hormone
GnRH-A	gonadotrophin-releasing hormone agonist
GnRH-An	gonadotrophin-releasing hormone antagonist
GnRH-R	gonadotrophin-releasing hormone receptor
GPCR	G-protein-coupled receptor
HEK-293	human embryonic kidney 293 cells
HIFCS	heat inactivated foetal calf serum
His	histidine (H)
IGF	insulin-like growth factor
il	intracellular loop
Ile	isoleucine (I)
$InsP_3$	inositol 1, 4, 5 trisphosphate
IP	inositol phosphate
Kan	kanamycin
kb	kilobase
LB	Luria-Bertani media
Leu	leucine (L)
LH	luteinising hormone
Lys	lysine (K)
Met	methionine (M)
mRNA	messenger RNA
NH_2	amino
OD	optical density
Oligo	oligonucleotide
PBS	phosphate buffered saline
p-CMB	p-chloromercuribenzoic acid
PCR	polymerase chain reaction
PEG	polyethylene glycol
pfu	plaque forming unit
Phe	phenylalanine (F)
PLC	phospholipase C

PRL	prolactin
Pro	proline (P)
RNA	ribonucleic acid
SDS	sodium dodecyl sulphate
Ser	serine (S)
SRIH	somatostatin releasing inhibitory hormone
SSC	sodium salt citrate
SV40	simian virus 40
TBE	tris, borate, EDTA
TE	tris, EDTA
Tet	tetracycline
Thr	threonine (T)
TM	transmembrane
TRH	thyrotrophin-releasing hormone
TRH-A	thyrotrophin-releasing hormone agonist
TRH-R	thyrotrophin-releasing hormone receptor
Trp	tryptophan (W)
tRNA	transfer RNA
TSH	thyrotrophin (thyroid stimulating hormone)
Tyr	tyrosine (Y)
u/v	ultra-violet
Val	valine (V)
VIP	vasoactive intestinal polypeptide
WT	Wild-type
X-gal	5-bromo-4-chloro-3-indolyl-β-D-galactoside

1 Introduction

1.1 Physiological Background

The identification of the gonadotrophin-releasing hormone (GnRH) decapeptide structure in the early 1970s (Burgus et al, 1972; Matsuo et al, 1971) stands as one of the great landmarks in reproductive endocrinology. GnRH and its synthetic analogues are now widely used in clinical endocrinology, not only to treat reproductive disorders but also in the management of hormone-dependent neoplasms. Under normal physiological circumstances, GnRH is released in a pulsatile manner from the hypothalamus and transported to the anterior pituitary gland via the portal blood vessels. GnRH binds to a specific receptor located in gonadotroph cells, the GnRH receptor (GnRH-R), stimulating the synthesis and release of luteinising hormone (LH) and follicle-stimulating hormone (FSH). Moreover, with the elucidation of the GnRH-R amino acid sequence in the 1990s (Tsutsumi et al, 1992) it is now possible to study structure-function relationships in both GnRH and its receptor.

1.2 Aim of the study

The primary aim of this PhD study was to examine structure-function relationships in the GnRH-R and to identify amino acids within the receptor that are crucial mediators of (i) receptor structure, (ii) receptor binding and (iii) receptor activation.

1.3 Importance of the study

It is imperative to understand the normal molecular mechanisms underlying GnRH ligand-receptor activation so that pathological conditions, resulting from imbalances in the normal system, can be recognised and effectively treated. Currently, GnRH and its analogues are widely used clinically, and knowledge regarding the mechanism of GnRH-induced receptor activation could be exploited to further improve treatment regimes. The identification of specific amino acid interactions between the GnRH ligand and receptor has enormous implications for rational drug design. If the atomic

spatial arrangement of residues involved in ligand-receptor binding can be mapped, then drugs can be specifically manufactured to interact with these critical residues. Moreover, this would allow for de novo synthesis of highly specific analogues with greater receptor efficacy. In addition, this approach would also facilitate combinatorial methods of drug design, as existing libraries could be screened for compounds with a complementary structure to the active receptor site. Ultimately, the use of rational drug design will aid in the generation of safer and more clinically acceptable compounds and hopefully extend to the development of orally active, non-peptide, GnRH analogues.

1.4 Fundamental experimental approaches

In this study, site-directed mutagenesis was chosen as a means of accessing the role of targeted amino acids. This technique allows small changes to be incorporated into the receptor cDNA sequence, thereby changing its final protein structure. Any significant alterations in the binding and activational properties of these modified 'mutant' GnRH-Rs were then tested accordingly. Site-directed mutagenesis only permits the concurrent alteration of one or two amino acids. As the rat GnRH-R contains a total of 327 amino acids it would be impractical to modify every individual receptor residue. Therefore, it was important to design a suitable strategy, whereby amino acids located in the positions most likely to affect ligand binding and receptor activation were targeted. Two methods were employed to facilitate this task.

The first method utilised sequence information from other heptahelical G-protein coupled receptors (GPCRs), whilst the second method relied on molecular modelling studies. The GnRH-R belongs to the GPCR superfamily - a family of proteins characterised by seven transmembrane (TM) α helices. These helices are linked together by stretches of hydrophilic amino acids which form intracellular loops (il) and extracellular loops (el). Site-directed mutagenesis studies have been carried out in other GPCRs and as all these receptors share the same overall topographical structure, information derived from one receptor can often be useful in predicting or determining structure-function relationships in other related receptors.

The molecular modelling approach has proved particularly useful in giving insight into the possible three-dimensional structure of GPCRs (Donnelly and Findlay, 1994; Perlman et al, 1994b). Two molecular models of the GnRH-R have been utilised

during the course of this study, the Baldwin model (Baldwin, 1994) and a computer derived model of the GnRH-R (P L Taylor, MRC, Reproductive Biology Unit, Edinburgh). In addition, Dr Taylor has also constructed a computer model of GnRH. Furthermore, these models have been integrated together to allow computer simulations of putative ligand-receptor interactions.

However, whilst molecular modelling approaches are now widely used to predict putative drug-receptor interactions, these models are still only hypothetical. Definitive structural determination can only be achieved by means of two/three-dimensional crystallography which is the ultimate goal of scientific endeavour in this area.

1.5 General experimental procedures

In this study, attention has focused on targeting amino acids which are potential determinants of GnRH tertiary receptor structure or form part of the ligand binding pocket. In total, four experimental studies have been undertaken and these have concentrated on putative bonding interactions between individual receptor residues as well as those between the ligand and its receptor.

1.5.1 Amino acid involvement in receptor tertiary structure

The first study investigated the role of conserved extracellular cysteine (Cys) residues in the GnRH-R and their participation in disulphide bond formation. Four mutant receptors were generated, converting all the extracellular Cys residues to serines (Ser) viz: Cys14Ser, Cys114Ser, Cys195Ser and Cys199Ser. A comparative study was also carried out involving another pituitary GPCR, the thyrotrophin-releasing hormone receptor (TRH-R). In this experimental study, the extracellular Cys residues were substituted for either serine or alanine (Ala) [Cys98Ser, Cys100Ser, Cys179Ser, Cys98Ala, Cys100Ala and Cys179Ala]. In addition, Cys-specific chemical modifying agents were also used to further characterise the role of Cys residues in the TRH-R. The remaining experimental chapters relate to the identification of important residues in the GnRH-R ligand binding pocket.

1.5.2 Amino acid involvement in GnRH ligand binding

The second series of experiments investigated the role of GnRH-R residues asparagine 87 (Asn87) in TM II and aspartic acid 318 (Asp318) in TM VII. These amino acids were targeted because of their unusual positions relative to other GPCRs. In most other GPCRs, an Asp and an Asn residue are located at these TM II and TM VII sites respectively. However, in the GnRH-R these amino acids appear to have transposed positions. To investigate their functional role in ligand-receptor binding, two single mutations were generated substituting the Asn for Asp (Asn87Asp) and the Asp for Asn (Asp318Asn), together with a double reciprocal mutation (Asn87AspAsp318Asn).

The final two experimental investigations have utilised information derived from the Baldwin model and the computer generated models of the GnRH-R respectively. The Baldwin model of the GnRH-R highlights the presence of polar amino acids in the TM domains and TM/extracellular interface of the receptor. Seven amino acid residues were targeted for study, glutamic acid 90 (Glu90) positioned in TM II, two lysine residues (Lys) one at the TM III/extracellular interface (Lys115) and the other in TM III (Lys121), glutamate 174 (Gln174) in TM IV, histidine (His305) at the TM VII/extracellular interface and two Asn residues one at the TM VII/extracellular interface (Asn304) and the other in TM VII (Asn314). The amino acid side chains of these polar residues pointed towards the central channel created by the TM helices and thus were in an ideal position to interact with the ligand. These amino acids were mutated as follows, Glu90 to Gln90 (Glu90Gln), Lys115/Lys121 to arginine (Arg) [Lys115Arg and Lys121Arg], His305 to Arg (His305Arg) and Asn304/Asn314 to Asp (Asn304Asp and Asn314Asp).

The last experimental study examined the role of two GnRH-R amino acids, leucine 83 (Leu83) in TM II and phenylalanine 312 (Phe312) in TM VII. These amino acids were identified as potentially important mediators of receptor binding function through computer-aided ligand-receptor simulations. The position of GnRH in the ligand-receptor simulated models revealed that Leu83 and Phe312 were positioned in close proximity to Leu7 and Trp3 in GnRH respectively. The spatial orientation of these pairs of amino acids was such that hydrophobic interactions might possibly occur between them. To investigate any possible bonding interactions, each site was mutated either to another hydrophobic residue [Leu to valine (Val) and Phe to tyrosine (Tyr)] or to a hydrophilic amino acid [Leu to lysine (Lys) and Phe to Arg]. In

addition, each site was also mutated to a smaller Ala residue. Therefore, in total 6 different mutations were generated i.e. Leu83Val, Leu83Lys, Leu83Ala, Phe312Tyr, Phe312Arg and Phe312Ala.

1.6 Structure of thesis

This introduction has aimed to place the overall study in a much broader context by highlighting the importance and relevance of scientific based structure-function investigations in the field of novel drug design. The following section outlines the structure of the subsequent chapters of this thesis.

Chapter 2 reviews the current literature and is divided into two major parts. Section 1 deals with the role of GnRH as a hypothalamic-pituitary hormone, including the regulation of its synthesis and release from the hypothalamus, its actions at the pituitary gland and the clinical uses of its synthetic analogues. The second section focuses in depth on the precise interactions between GnRH and its pituitary receptor. This section also examines the structure and activational properties of the GnRH-R, the similarities and differences of these features compared to other GPCRs, and GPCR structure-function relationships. Factors regulating GnRH-R gene expression are also discussed. The final part of this section is devoted to the localisation and possible endocrine function of GnRH and its receptor outside the hypothalamic-pituitary axis.

Chapter 3 describes the experimental methodology used in the study, including protocols for standard molecular biology techniques, methods for site-directed mutagenesis, stable/transient expression of DNA, Northern Blot analysis, ligand-induced total inositol phosphate measurements and receptor binding assays.

Molecular models of GPCRs are now widely used to predict ligand-receptor interactions. The basis of these models is the structural determination of two heptahelical proteins, bacteriorhodopsin and rhodopsin. Chapter 4 highlights the structural elucidation of these two proteins, together with their advantages and disadvantages as templates for other GPCRs models. Methods underlying the construction of the Baldwin GnRH-R model and the computer generated models of the GnRH ligand and receptor are also outlined.

The experimental results are contained within Chapters 5-8. Chapter 5 focuses on the role of GnRH-R Cys residues in disulphide bridge formation. A comparative study of another GPCR, the TRH-R, also examines the role of these residues using site-directed mutagenesis. In addition, the role of Cys residues has also been investigated using Cys-specific chemical modifying reagents. Chapter 6 examines the role of GnRH-R amino acids Asn87 and Asp318 in ligand binding and receptor activation. Chapter 7 deals with the function of TM located polar amino acids Glu90, Lys115, Lys121, Gln174, Asn304, His305 and Asn314, identified by the GnRH-R Baldwin model while Chapter 8 analyses the structure-function roles of Leu83 and Phe312, highlighted in the computer-derived model of the GnRH-R.

Chapter 9 focuses on ways of monitoring mutant receptor expression levels and Chapter 10 summarises and concludes the work carried out during the course of this study, outlining future developmental research.

2 Literature Review

2.1 Hypothalamo-Pituitary Interactions

The concept of neuro-endocrine regulation of pituitary function was first suggested by Harris and Green in 1949 (Harris and Green, 1945). Under normal physiological conditions the pituitary gland responds to the endocrine and metabolic needs of the body and releases appropriate hormones into the peripheral circulation. These hormones in turn act to regulate the cellular growth, differentiation and function of specific target organs. Regulation of anterior pituitary hormone secretion is dependent on humoral signals from the hypothalamus, feedback regulation from peripheral hormones, non-humoral neurotransmitter signals, together with paracrine and autocrine action of pituitary growth hormones and factors (Asa et al, 1995). The balance of these chemical and neuronal signals determines the amount and pattern of hormone secretion and allows complex feed-back regulation. The hypothalamus forms the final pathway between the neuronal circuitry of the brain and the endocrine function of the pituitary gland and can thus be regarded as the key regulator of adenohypophyseal hormone release (Yen, 1991).

2.1.1 Hypothalamus

The hypothalamus, a primitive structure largely unchanged throughout evolution, is located at the base of the forebrain. Despite a poorly defined anatomical region, the hypothalamic sulcus is generally regarded as the superior boundary, the lamina terminalis is considered as the anterior border, while the medial forebrain bundle limits its position laterally and the mamillary complex provides the caudal margin. The hypothalamic blood supply is derived from arterial branches of the circle of Willis together with the superior hypophyseal artery. As well as being extensively vascularised, the hypothalamus is also a strongly innervated organ with afferent and efferent fibres connecting the hypothalamus with other regions of the brain including the forebrain, limbic system, visual cortex, thalamus and the brain stem. The regulation of hypothalamic function by chemical signals from the blood and/or

cerebrospinal fluid (CSF) along with neurotransmitters released locally from afferent neurons, is only possible due to these neuronal and vascular networks.

The concept of neurosecretory cells was first proposed by Ernst Scharrer and co-workers in the 1930's (for review see Reichlin, 1987). Neurons in the hypothalamus form clusters, known as nuclei, which are responsible for the production and secretion of hypothalamic-releasing and inhibitory factors (Figure 2.1). The hormones oxytocin and vasopressin are produced in the magnocellular cell bodies of the supraoptic (SON) and paraventricular nuclei (PVN) and are transported along the nerve axons, constituting the hypothalamic-hypophyseal tract, to the neurohypophysis. Smaller parvocellular secretory neurons, responsible for the secretion of hypophysiotrophic hormones, are primarily found in the preoptic area, arcuate nucleus and ventromedial nucleus; although a few such cells are also present in the SON and PVN. The tuberoinfundibular tract arises from the parvocellular neurons and carries hypophysiotrophic hormones to the median eminence where they are released into the primary portal plexus and travel in the hypophyseal portal veins to a secondary plexus overlying the anterior pituitary gland (Figure 2.1).

Figure 2.1 Diagrammatic representation of the hypothalamic-pituitary axis (following page)

The blood supply to the median eminence is derived from the superior hypophyseal artery. This artery forms a primary capillary plexus in the medium eminence and hypophyseal portal vessels arising from it terminate in the anterior pituitary gland. The posterior pituitary is supplied directly from the inferior hypophyseal artery. Axons from the parvocellular neurons, carrying hypophysiotrophic hormones, terminate close to the primary capillary plexus. Axons from the magnocellular neurons of the PVN and SON terminate directly in the posterior pituitary gland. Adapted from Johnson and Everitt, 1995.

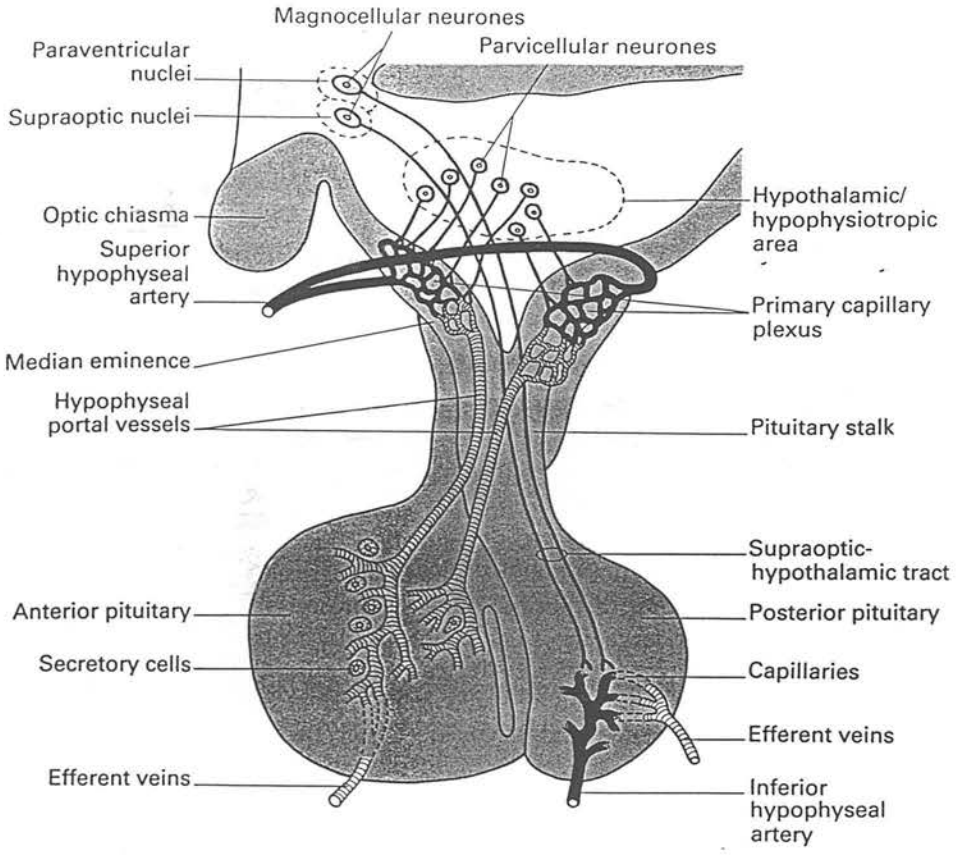

To date five classical hypophysiotrophic peptide hormones, thyrotrophin-releasing hormone (TRH) (Guillemin et al, 1971), gonadotrophin-releasing hormone (GnRH) (Burgus et al, 1972; Matsuo et al, 1971), somatostatin or somatotroph-releasing inhibitory hormone (SRIH) (Brazeau et al, 1973), corticotrophin-releasing hormone (CRH) (Vale et al, 1981) and growth hormone-releasing hormone (GHRH) (Guillemin et al, 1982) have been isolated, and their role in the regulation of anterior pituitary hormone synthesis and secretion extensively studied. Other factors, e.g., neurotransmitters and neuropeptides, shown to influence anterior pituitary hormone release include catecholamines (dopamine (DA), adrenaline, noradrenaline, serotonin and histamine), acetylcholine, γ-aminobutyric acid (GABA), opioid peptides and vasoactive intestinal peptide (VIP). The precise action of many of these factors is unknown but the roles of dopamine and VIP in the regulation of prolactin (PRL) secretion have been more precisely established (Abe et al, 1985; Jonathan, 1985).

Many of the hypothalamic-releasing hormones have also been localised outside the hypothalamic-pituitary axis including the brain, spinal cord, autonomic nervous system, gastrointestinal, respiratory and reproductive tracts (Yen, 1991). A potential role for these peptides in cellular communication prior to the development of the neuronal or endocrine systems has been postulated by Kreiger (1983).

2.1.2 The pituitary gland

The pituitary gland, positioned in the sella turcica, is derived from two ectodermal components. Rathke's pouch, formed from the roof of the buccal cavity, develops into the anterior pituitary and intermediate lobe whilst the floor of the third ventricle forms the pituitary stalk and posterior pituitary.

The posterior lobe is composed of magnocellular neurosecretory nerve endings. Oxytocin and vasopressin with their corresponding neurophysin molecules are synthesised in the SON and PVN, packaged into granules and transported through the nerve axons, via the pituitary stalk, to the posterior pituitary. When stimulated, the neurosecretory cells fire action potentials and exocytose hormones directly into the capillary vessels of the inferior hypophyseal artery. Cholinergic and noradrenergic fibres synapse with the SON and PVN and have been shown to stimulate hormone release, while inhibitory regulation occurs by dopaminergic and opioidergic pathways. Purification of oxytocin and vasopressin by du Vingneud et al (1954) revealed that both these hormones have a nonapeptide structure requiring a disulphide bond between cysteine residues (at positions 1 and 6) for biological activity. Oxytocin is released in response to peripheral stimuli from cervical stretch receptors or from suckling stimulus at the breast, and its action in the cervix promotes foetal expulsion during labour whereas in the mammary gland it causes milk release. The main physiological stimulus for the release of vasopressin is provided by alterations in body fluid balance, an increase in osmotic pressure being counterbalanced by the action of vasopressin on water reabsorption from the kidneys.

In contrast, the anterior lobe is made up of different endocrine cell types namely somatotrophs, corticotrophs, lactotrophs, gonadotrophs and thyrotrophs. Hypothalamic-releasing/inhibiting hormones bind to specific anterior pituitary cell surface receptors and in doing so alter their structural conformation. This change in receptor structure triggers a second messenger cascade system, causing an increase in intracellular calcium levels ($[Ca^{2+}]i$), and ultimately hormone exocytosis.

Regulation of anterior pituitary hormone secretion by hypothalamic-releasing and inhibitory factors together with their downstream target action is illustrated in Figure 2.2.

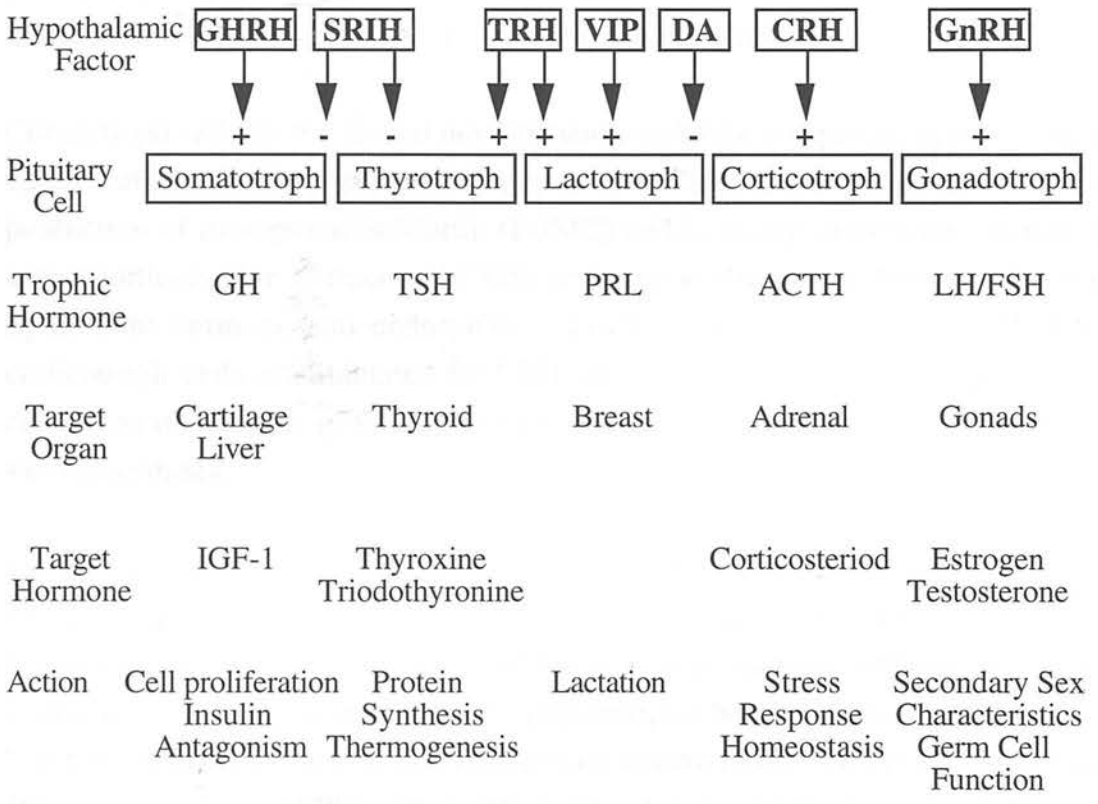

Figure 2.2 Control of anterior pituitary hormone release

Control of anterior pituitary hormone secretion by hypothalamic-stimulatory/inhibitory factors and the ensuing regulation of trophic hormone secretion. The effect of trophic hormones on their downstream target tissues is also highlighted. Adapted from (Asa et al, 1995).

ACTH, adrenocorticotrophic hormone; CRH, corticotrophic hormone; DA, dopamine; FSH, follicle-stimulating hormone; GHRH, growth hormone-releasing hormone; GnRH, gonadotrophin-releasing hormone; IGF-1, insulin-like growth factor 1; LH, luteinising hormone, PRL, prolactin; SRIH, somatostatin-releasing inhibitory hormone; TRH, thyrotrophin-releasing hormone; TSH, thyrotrophin; VIP, vasoactive intestinal polypeptide.

Somatotroph cells constitute approximately 50% of the cells in the adenohypophysis and are responsible for the production of growth hormone (GH). GH synthesis and secretion is regulated by two hypophysiotrophic factors, GHRH stimulates its release whereas SRIH has an inhibitory action. Once released into the circulation GH promotes the growth of bone, soft tissue and viscera either directly or indirectly through the stimulation of insulin-like growth factor 1 (IGF-1).

Corticotroph cells are the second most numerous cell type comprising approximately 15-20% of the adenohypophyseal cell population. These cells are responsible for the production of pro-opiomelanocortin (POMC) and its many derivatives, including adrenocorticotrophin hormone (ACTH), melanocyte-stimulating hormone (MSH), lipotrophic hormone and endorphins. Synthesis and release of ACTH from corticotroph cells is stimulated by CRH, and once released into the peripheral circulation its action is generally confined to the adrenal cortex where it stimulates steroid synthesis.

Lactotrophs represent approximately 15% of the total anterior pituitary cell population and are responsible for the production of PRL. Unlike other adenohypophyseal hormones their regulation is controlled primarily through the tonic inhibitory actions of a catecholamine, DA, rather than a hypophysiotrophic hormone. However, TRH and VIP have been shown to stimulate PRL release *in vitro* (Kosh et al, 1977; Nagy et al, 1988). The actions of PRL are mainly in breast tissue where it is responsible for stimulating the growth of mammary tissue and supporting milk secretion.

Gonadotroph cells constitute approximately 10% of adenohypophyseal cells and produce the gonadotrophin glycoprotein hormones, LH and FSH, which have a critical function in reproduction. The structure of gonadotroph genes is discussed in section 2.3.2. The rate of gonadotrophin synthesis and secretion is primarily controlled by the one factor, GnRH. LH stimulates steroid hormone production in the gonads whilst FSH stimulates follicle growth and estrogen production in the ovary. FSH also regulates Sertoli cell function together with the maturation of developing spermatids in the testis. A more detail description of gonadotrophin secretion and its regulation is discussed in section 2.3.3.

The least common cell type in the anterior pituitary gland are the thyrotroph cells, constituting only 5% of the total cell population. Thyrotroph cells produce thyroid-

stimulating hormone (TSH), also known as thyrotrophin, and this glycoprotein hormone, like LH and FSH, consists of a common α subunit and a hormone specific β subunit. Its production is stimulated by TRH and inhibited by SRIH and once released from the anterior pituitary, TSH travels to the thyroid gland promoting the synthesis and secretion of thyroid hormones.

2.2 Gonadotrophin-releasing hormone (GnRH)

The mammalian form of GnRH (mGnRH) was first isolated from porcine (Matsuo et al, 1971) and ovine (Burgus et al, 1972) brains in the 1970s. Since then six different forms have been identified and named according to the animals they were isolated from: chicken I (cGnRH-I), catfish (cfGnRH), chicken II (cGnRH-II), dogfish (dfGnRH), salmon (sGnRH) and lamprey (lGnRH). Their structures are illustrated in Table 2.1. Present throughout vertebrates from cartilaginous fish to primitive placental mammals, c-GnRH II is the longest conserved, arising over 500 million years ago (Sherwood et al, 1993). The mammalian form appeared 'more recently', approximately 400 million years ago, and can be found in the descendants of primitive bony fish. Non-mammalian vertebrates express multiple forms of GnRH and each form is characterised by a tissue-specific distribution pattern, suggesting different peptides have different regulatory roles. Mammals are unusual as only one form of GnRH has been identified (King et al, 1988): however, other GnRH forms are capable of causing the release of mammalian LH and FSH but, generally with much less potency. cGnRH-I, structurally the closest to the mammalian form, shows only a 3% LH releasing activity compared with mGnRH. Paradoxically cGnRH-II and dfGnRH, with 3 amino acid substitutions compared to mGnRH, show a greater ability to release gonadotrophs compared to cGnRH-I (Sherwood et al, 1993).

2.2.1 Embryonic development and migration of GnRH neurons

GnRH immunoreactive cells originate in the olfactory placode and during foetal life migrate from the nasal region towards the anterior forebrain in association with the nerve terminalis and vomeronasal nerve (Schwanzel-Fukuda and Pfaff, 1989). Neural cell adhesion molecules provide a scaffold along which the clusters of GnRH neurons migrate to their final destination shortly before birth (Schwanzel-Fukuda et al, 1992). Failure of GnRH migration from the olfactory epithelium results in Kallman's

Syndrome, a disease characterised by hypogonadotrophic hypogonadism and anosmia (Schwanzel-Fukuda et al, 1989).

Species	Amino acid	1	2	3	4	5	6	7	8	9	10
Mammalian	mGnRH	pGlu	His	Trp	Ser	Tyr	Gly	Leu	Arg	Pro	Gly-NH_2
Chicken I	cGnRH-I	pGlu	His	Trp	Ser	Tyr	Gly	Leu	Gln	Pro	Gly-NH_2
Catfish	cfGnRH	pGlu	His	Trp	Ser	His	Gly	Leu	Asn	Pro	Gly-NH_2
Chicken II	cGnRH-II	pGlu	His	Trp	Ser	His	Gly	Trp	Tyr	Pro	Gly-NH_2
Dogfish	dfGnRH	pGlu	His	Trp	Ser	His	Gly	Trp	Leu	Pro	Gly-NH_2
Salmon	sGnRH	pGlu	His	Trp	Ser	Tyr	Gly	Trp	Leu	Pro	Gly-NH_2
Lamprey	lGnRH	pGlu	His	Tyr	Ser	Leu	Glu	Trp	Lys	Pro	Gly-NH_2

Table 2.1 Structure of GnRH peptide from different species

Structure of the mammalian (m), chicken (c) I and II, dogfish (df), catfish (cf) and lamprey (l) GnRH. All the species identified to date share 50% homology with the same amino acids in positions 1, 2, 4, 9 and 10.

2.2.2 Localisation of GnRH neurons in the brain

GnRH immunoreactive cells are diffusely scattered in the brain. In primates, the highest concentration of GnRH neurons can be seen in the arcuate nucleus of the mediobasal hypothalamus and the preoptic area of the anterior hypothalamus (Yen, 1991). Two prominent nerve bundles, the infundibular and preopticoterminal tract, are formed from the projection of these fibres to the median eminence and organosum vasculosum of the lamina terminalis (OVLT) respectively. In total, approximately 50-75% of all GnRH neurons terminate in the median eminence, releasing their hypophysiotrophic hormones into the primary pituitary portal plexus (Merchenthaler et al, 1990). GnRH neurons tend to be distributed in a species-specific pattern and in rodents the most prominent clusters of cell bodies are present in the dorsal and medial septal nuclei, the nucleus of the diagonal band of Broca, the anterior hypothalamic nucleus and the OVLT (Silverman et al, 1979). Immunocytochemical techniques have also localised GnRH neurons in the olfactory bulb, amygdala and hippocampus. Direct synaptic connections between these and other neuronal systems suggest that GnRH may function as a neurotransmitter and/or neuromodulator. In addition to its

well established role in the control of anterior pituitary hormone secretion, GnRH is also thought to regulate female sexual behaviour. Evidence supporting this hypothesis has been presented by Pfaff and co-workers who demonstrated infusion of GnRH into the rat medial preoptic area, arcuate nucleus, ventromedial hypothalamus, midbrain central grey and spinal cord facilitates lordosis (Pfaff et al, 1994). In particular, the ventromedial hypothalamic nuclei have been implicated in co-ordinating female sexual behaviour. Steroidogenic factor-1 (SF-1), an important factor in pituitary-specific expression of gonadotrophins, appears critical in the formation of the ventromedial hypothalamic nuclei (Ikeda et al, 1995).

2.2.3 Gene structure and regulation

GnRH is cleaved from a larger precursor molecule composed of a signal peptide, GnRH decapeptide sequence, a processing site (Gly-Lys-Arg) and a 56 amino acid peptide, known as the GnRH associated peptide (GAP) (Seeburg and Adelman, 1984). GnRH and GAP co-localise in hypothalamic neurons, and pituitary cell culture experiments have shown that low doses of GAP promote the release PRL *in vitro* (Seeburg et al, 1987). GAP may also be involved in the packaging and processing of the GnRH hormone, a role illustrated by the hypogonadal mouse model. These animals lack the region of the GnRH gene that codes for GAP, and as a result do not release GnRH and so are sexually immature (Seeburg et al, 1987).

The mammalian GnRH gene contains 4 exons. The first exon codes for the 5' untranslated region with the second exon coding for the signal peptide, the GnRH decapeptide sequence and the processing signal, and the third/fourth for GAP and the 3' untranslated region (Seeburg and Adelman, 1984). Regulation of gene transcription occurs through the activation of transcription factors, and analysis of the rat GnRH gene sequence reveals DNA binding elements for transcription factors similar to Oct-1, Tst-1 and Pit-1 (Kepa et al, 1992). Although these binding sites are present in the gene structure there is no direct evidence regarding their regulatory function. An estrogen response element (ERE) has now also been identified in the human GnRH gene (Radovick et al, 1994).

2.2.4 GnRH secretion from hypothalamic neurons

Knobil in 1980, demonstrated that GnRH was released from the hypothalamus in a pulsatile fashion - a process initiated, controlled and regulated by the GnRH pulse generator. Studies examining the mechanism of action of the pulse generator have been difficult as hypothalamic GnRH neurons are few in number, highly dispersed and difficult to identify. The development of an immortalised GnRH hypothalamic neuronal cell line, GT-1 (Mellon et al, 1990), has resolved this problem but care should be taken in extrapolating information from tumour-derived cell lines to normal physiological situations. However, much of the knowledge obtained from GT-1 cell lines has been substantiated by other experimental approaches using primary foetal hypothalamic cell cultures, hypothalamic tissue and *in vivo* animal models. In addition to neuronal regulation, glial cells are also thought to regulate the GnRH pulse generator (Melcangi et al, 1995).

2.2.5 Regulation of GnRH pulse generator activity

Autoregulation by GnRH

The ability of GT-1 cells to survive independently in culture and secrete synchronised pulses of GnRH, in the absence of other cell types, implies that the pulse generator activity endogenously resides in the GnRH neurons. Several lines of evidence suggest that this system may be autoregulated by GnRH. Experiments using a perfused culture system, have demonstrated that treatment of GT-1 neurons with GnRH results in a transient increase in peptide release followed by suppression of basal pulsatility (Stojilkovic et al, 1994a). The Ca^{2+} dependent nature of these effects suggests a receptor-mediated process. Moreover, GnRH-R protein and mRNA have been detected in these cells (Krsmanovic et al, 1993). Together, these findings imply that regulation of the pulse generator activity is primarily controlled by the autoregulatory actions of GnRH.

GT-1 cells provide a good *in vitro* model to study hypothalamic hypophysiotrophic regulation, as neuronal activity can be modulated to mimic physiological situations. Continuous infusion of GnRH into a GT-1 cell perfusion system results in patterns of GnRH pulse frequency activity and amplitude similar to that observed during the preovulatory LH surge (Stojilkovic et al, 1994a).

Modulation of GnRH secretion by other factors

Neurotransmitters, hormones and other factors have also been postulated to modulate GnRH gene expression and secretion, either directly, through specific cell surface receptors or indirectly, through interconnecting neuronal pathways.

Factors thought to act directly through receptor specific interactions include GABA, excitatory amino acids, catecholamines, neuropeptide Y and endothelin (Spergel et al, 1994; Stojilkovic et al, 1994a). It is also well documented that steroids, in particular estrogens, have an important role to play in regulating GnRH secretion. A direct action of estrogen in regulating GnRH gene expression, is suggested by the presence of an ERE in the human GnRH gene (Radovick et al, 1994). In addition, the identification of estrogen receptors in GnRH neurons further suggests that this steroid can regulate the activity of GnRH neurons directly (Radovick et al, 1994). Other steroids are also thought to be involved in modulating GnRH neuronal activity and studies of GT-1 neurones have identified both androgen (Poletti et al, 1994) and glucocorticoid receptors (Chandran et al, 1994).

Steroids have also been shown to influence GnRH regulation through the activation of interconnecting neuronal systems. The progesterone metabolite tetrahydroprogesterone, for example, stimulates GnRH release in GT-1 cells via the neurotransmitter GABA (El Etr et al, 1995). Endogenous opioids have also been implicated in GnRH regulation and are thought to inhibit GnRH release through suppression of excitatory adrenergic influence (Nazian et al, 1994). Furthermore, Calogero and co-workers have shown that the inhibitory actions of both PRL and CRH on GnRH pulsatile release involves the activation of opioid interneurons (Calogero et al, 1994). *In vivo* studies have also demonstrated the involvement of opioid interneurons, as the effects of estrogen on GnRH secretion in ovariectomised monkeys (Grosser et al, 1993) together with the action of neuropeptide Y on GnRH release in rats (Xu et al, 1993), can be blocked by the opioid antagonist naloxone.

GnRH pulsatile secretion can be modulated by many factors and this diverse regulation is also reflected in the signal transduction pathways activated. Protein kinase A and C activation are responsible for many of the Ca^{2+} dependent events and recently, nitric oxide has been postulated as having an important second messenger function (Mahachoklertwattana et al, 1994).

2.3 GnRH - Its action at the pituitary

Once released into the portal circulation GnRH travels to the anterior pituitary where it binds to specific receptors located on pituitary gonadotroph cell membranes (section 2.6). Ligand-receptor binding induces micro-aggregation and dimerisation of receptor molecules (Conn et al, 1984) and the resulting receptor conformational change triggers a complex series of intracellular signal transduction events. These signals stimulate gonadotrophin hormone synthesis and their packaging into secretory granules. LH and FSH are finally exocytosed from the gonadotroph cells into general circulation and transported to their target organs - the gonads.

2.3.1 Structure of gonadotroph cells

Immunoperoxidase staining of gonadotrophs reveals that many of these cells are immunopositive for both hormones (Horvath and Kovacs, 1995). However, the existence of monohormonal producing cells and variations in the number of cells staining for both LH and FSH suggests that gonadotrophin production alters with functional demand. As yet, it is unclear whether these observations reflect different cell subpopulations or merely cells in different secretory phases. At the ultrastructural level gonadotrophs are large oval cells, with short profiles of dilated rough endoplasm reticulum (ER), containing an electron lucent substance, a ring-like Golgi complex and secretory granules. Gonadotrophins are localised within secretory granules and are categorised by cell size and granin content. Small (150-250 nm in diameter) electron dense granules contain primarily LH and secretogranin II, while large granules (350-450 nm) contain mostly FSH, with a small amount of LH, together with chromogranin A (Asa et al, 1995; Farnworth, 1995).

The mechanisms controlling the differential secretion of LH/FSH from gonadotroph cells are largely unknown. Gonadotrophs phasically secrete LH and FSH in response to a GnRH-induced rise in $[Ca^{2+}]i$. FSH (but not LH) secretion is also regulated independently of GnRH, in a tonic manner, via mechanisms involving non-steroidal factors. The existence of different regulatory systems may be indicative of separate signal transduction networks and their independent activation could provide the stimulus for physically distinct exocytosis pathways. It has been postulated that the large, mainly FSH-containing secretory granules or possibly the synaptic-like vacuoles selectively respond to activin, inhibin and follistatin. In this way, non-

steroidal factors may differentially regulate FSH secretion (Farnworth, 1995). The potential mechanisms underlying such regulation, however, have still to be elucidated.

2.3.2 Structure of gonadotroph genes

Each glycoprotein hormone consists of a common α subunit and a different β subunit which is responsible for conferring hormone specificity. α and β subunits are linked by covalent disulphide bonds and are only biologically active in this heterodimeric structural form. The α subunit gene contains four exons and three introns. Cyclic adenosine monophosphate (cAMP) regulates gene transcription by binding to a specific DNA sequence. A 18 bp palindromic cAMP response element (CRE) together with a cAMP protein binding site have been identified in the 5' flanking region of the gene (Gharib et al, 1990). Mellon and co-workers have identified a region in all mammalian α subunit genes responsible for conferring gonadotroph specificity. The accordingly named gonadotrophin specific element (GSE) binds a 54 kDa protein, known as GSE-binding protein 1 (GSEB1) (Horn et al, 1992), and this has recently been identified as the orphan nuclear receptor SF-1 (Barnhart and Mellon, 1994). Experiments, incorporating the proximal 1.6 kb 5' flanking sequence of the human gene into primary pituitary cell cultures and transgenic mice, have shown that this portion of the gene is responsible for its expression (Burrin and Jameson, 1989).

The LH β and FSH β subunit genes each contain 3 exons and 2 introns. Sequence analysis reveals that an ERE is present in the 5' flanking regions of each gene but, apart from this consensus sequence, the two β subunits share little homology (Gharib et al, 1990). The region of the LH β or FSH β gene responsible for conferring biological specificity has still be to identified (Fallest et al, 1995; Kumar and Low, 1994).

2.3.3 Regulation of gonadotrophin secretion

Regulation of gonadotrophin secretion occurs at various sites along the hypothalamic-pituitary axis. Direct modulation of anterior pituitary function can either increase (positive feedback) or decrease (negative feedback) the sensitivity of gonadotrophs to GnRH. Alternatively, regulation of the hypothalamic GnRH pulse generator activity (see section 2.2.5) directly, or indirectly through modulation of interconnecting neuronal systems, affects FSH and LH secretion from the pituitary. In many

instances regulation at both these sites is known to occur and steroid factors, in particular, play a fundamental role in the regulation of gonadotrophin release.

Regulation by GnRH

GnRH-mediated regulation of gonadotrophin synthesis and secretion has been studied extensively in animal models *in vivo* and in pituitary cell cultures *in vitro*. Knobil showed that gonadotrophin secretion could be re-established in rhesus monkeys lacking endogenous GnRH (as a result of hypothalamic lesions) by exogenous pulsatile administration of the hormone (Knobil, 1980). In addition to its affects on hormone secretion GnRH also alters the level of gonadotrophin gene expression. In cell culture systems the effects of GnRH are controversial but it is generally thought to stimulate the transcription of all gonadotrophin subunits (Ben-Menahem and Noar, 1994; Shupnik, 1990). The rate of transcription of each subunit is however differentially regulated by GnRH with faster pulse frequencies increasing α and LH β subunit expression, whereas slower frequencies stimulate only the expression of the FSH β subunit gene (Bhasin and Swerdloff, 1995). This observation has led to speculation that the differential secretion of LH and FSH from the anterior pituitary gland is dependent on the pattern of GnRH pulses.

Regulation by steroids

In primates and rats, estradiol both inhibits and stimulates gonadotrophin gene expression and hormone secretion (Gharib et al, 1990). It has been postulated that the inhibitory actions of estrogens are mediated mainly through the hypothalamus (Wray et al, 1989; Yamaji et al, 1992; Shupnik et al, 1989), whereas the stimulatory actions occur at the anterior pituitary gland (Knobil, 1980; Kamel et al, 1987). However, negative effects of estrogens at the level of the pituitary gland have also been demonstrated by Knobil (1980), who observed that estrogen treatment of hypothalamic-lesioned monkeys resulted in a suppression of LH secretion. Evidence to support a hypothalamic site for positive estrogen regulation has also been shown (Kamel et al, 1987).

A great deal of uncertainty surrounds the role of progesterone in the control of gonadotrophin secretion. During the luteal phase of the human, monkey and sheep menstrual cycle, when progesterone concentrations are at their highest, LH pulse frequency is decreased (Hauger et al, 1977; Soules et al, 1984; Van-Vugt et al, 1984).

In the rat, however, progesterone appears to alter GnRH pulse amplitude (Weick and Noh, 1984). Hypothalamic regulation of GnRH release by progesterone is thought to involve opioidergic pathways (El Etr et al, 1995; Van-Vugt et al, 1984). Progesterone may also act to enhance both the stimulatory and inhibitory effects of estradiol on gonadotrophin regulation (Bhasin and Swerdloff, 1995).

Non-steroidal regulation

Additional non-steroidal factors have been identified that are capable of modifying FSH gene expression and secretion. The hormones inhibin, activin and follistatin were first isolated in the gonads but have since been discovered in the anterior pituitary gland. Their localisation within the pituitary gland suggests that local paracrine and autocrine feedback mechanisms may be in operation (Bhasin and Swerdloff, 1995).

2.4 GnRH analogue design

The manufacture of GnRH analogues was made possible by the development of solid phase peptide synthesis (Merrifield, 1963) and more than 3000 analogues have been made to date. The majority of work has endeavoured to generate more potent 'super-agonist' compounds, with an increased receptor affinity and a reduction in peptide degradation.

2.4.1 GnRH agonists

GnRH agonists with an increased potency are achieved by replacing the glycine (Gly) amide at position 10 with an ethylamide (Fujino et al, 1972) or substituting the Gly at position 6 with a D-amino acid (Monahan et al, 1973). The most clinically used analogues are [D-Leu^6, Pro^9, NEt]-GnRH (Leuprolide, Abbott Laboratories), [D-Trp^6, Pro^9, NEt]-GnRH (Salk Institute), [N-Bzl-D-His^6, Pro^9, NEt]-GnRH (Histrelin, Ortho Population Council), [D-Nal(2)^6]-GnRH (Nafarelin, Syntex), [D-Ser(Bu^t)^6, Pro^9, NEt]-GnRH (Buserelin, Hoechst-Roussel) and [D-Ser(Bu^t)^6, Aza-Gly^{10}]-GnRH (Zoladex, ICI), which are 50-200 times more potent than GnRH. Analogues with modifications in other positions are generally uncommon but [N-Me-Leu^7]-GnRH and [1-l-Nal^3]-GnRH also show agonist properties (Karten and Rivier, 1986). Although many compounds have been synthesised with amino acid substitutions in positions 1, 2, 4, 5, 8 and 9 none of these compounds show an increase in receptor affinity compared to the native peptide (Karten and Rivier, 1986).

2.4.2 Antagonists

Antagonists bind to the recognition site within the receptor but prevent the conformational structural changes that activate the signal transduction pathway. The rationale behind the design of GnRH antagonists is their potential use as safe, non-steroidal female contraceptive agents and in 1972, Vale and co-workers manufactured the first antagonist [des-His^2]-GnRH (Vale et al, 1972). The next major breakthrough came with the manufacture of [D-Phe^2, D-Ala^6]-GnRH (Corbin and Beatty, 1975) which was the first antagonist to inhibit ovulation in rats. Additional modifications at position 3, [D-Phe^2, D-Trp^3, D-Lys^6]-GnRH (Seprodi et al, 1978), further increased the antagonist affinity but none of these compounds could be clinically used due to their histaminic side effects. The second generation of antagonists, known as the 4-F antagonists, contained a substitution at position 1 ([Ac-2-D-Nal^1, 4-F-D-Phe^2, D-Trp^3, D-Arg^6]-GnRH) together with further substitutions at positions 2, 3, and 6. This greatly enhanced potency, but the anaphylactic side effects remained (Karten and Rivier, 1986). More recently designed analogues such as Antide ([Nal-Lys,(Ac-D-Nal^1, D-4-Cl-Phe^2, D-Pal^3, Nic-Lys^5, D-Nic-Lys^6, Ip-Lys^8, D-Ala^{10}]-GnRH) and Cetrorelix ([Ac-D-Nal^1, D-4-Cl-Phe^2, D-Pal^3, D-Cit^6, D-Ala^{10}]-GnRH) cause much lower levels of histamine release and are particularly promising for clinical use.

With advances in protein technology it is now possible to synthesise antagonists with a very high biological potency. Structure-activity studies have shown that the most potent analogues contain D-Nal or D-Qal in position 1, D-pClPhe in position 2, D-Pal in position 3, cPzACAla or PicLys in position 6, ILys or Arg in position 8 and D-AlaNH_2 in position 10 (Janecka et al, 1994). When designing drugs, clinical tolerance is also an important factor to consider. In the case of GnRH antagonists, side effects have greatly limited their therapeutic use and studies have shown that histamine release results from the presence of a D-amino acid at position 6 combined with a highly basic Arg at position 8 and a cluster of hydrophobic residues at the amino terminus (Schmidt et al, 1984). It is now possible to reduce the histaminic effects by substituting Arg8 with isopropyllysine (ILys) (Janecka et al, 1994).

2.5 Clinical uses of GnRH

The clinical applications of GnRH and its analogues has been comprehensively reviewed by Barbieri (1992), Conn and Crowley (1994) and Sandow (1983). Therefore only directly relevant information will be covered in this section.

The pulsatile secretory nature of endogenous GnRH allows dual manipulation of gonadotrophin secretion by exogenously administered GnRH or its analogues. Pulsatile administration of low doses of GnRH/GnRH agonists results in the stimulation of gonadotrophin secretion and has important clinical applications in conditions requiring activation of the pituitary-gonadal system. In contrast, continuous administration of high doses of GnRH agonists desensitises pituitary GnRH-Rs, so preventing gonadotrophin release ('selective medical hypophysectomy'), and consequently inhibiting ovarian and testicular steroid production ('medical castration'). Chronic GnRH administration can therefore be applied to medical situations requiring suppression of the pituitary-gonadal axis. The main problem associated with GnRH agonist-induced pituitary/gonadal suppression is the initial stimulation of LH and FSH secretion before receptor desensitisation occurs. In many cases it can take upto 14 days to fully suppress the pituitary-gonadal axis and the gonadotrophins initially released can aggravate certain disease states which is particularly undesirable in the treatment of hormone dependent neoplasms.

GnRH treatment has been successfully used to restore normal reproductive function to patients suffering from hypogonadotrophic hypogonadism, characterised by a complete absence of GnRH secretion. Exogenous administration of GnRH, at rates of ~ 12 pulses / 24 hours in males and ~ 18-24 pulses / 24 hours during the follicular phase or ~ 6-10 pulses / 24 hours during the mid-luteal phase of the cycle in menstruating females, establishes normal gonadotrophin secretory patterns (Crowley et al, 1985). Activation of the pituitary-gonadal axis by pulsatile administration of GnRH has also been successfully employed to accelerate gonadal development in cryptorchidism and to induce ovulation in women suffering from primary /secondary amenorrhea.

GnRH agonist-induced suppression of the pituitary gonadal axis has many clinical applications being successfully used to delay gonadal maturity in children with precocious puberty, decrease the incidence of spontaneous LH surges in *in vitro* fertilisation programmes as well as in the treatment of polycystic ovarian disease and

pre-menstrual syndrome. Additionally, GnRH agonists have important therapeutic value in treating diseases stimulated by sex hormones. Estrogen-dependent conditions such as endometriosis and uterine fibroids can be effectively treated by GnRH agonists: however, the hypoestrogenic state produced by prolonged medical castration results in post-menopausal like symptoms. Recent evidence suggests that the hot flushes and bone density loss can be alleviated by the reintroduction of small doses of estrogen/progestin without compromising the overall outcome of the treatment regime (Lemay et al, 1994).

2.5.1 Treatment of hormone-dependent neoplasms

GnRH agonists are now widely used in the treatment of hormone-dependent prostate and breast cancers and may also have beneficial effects in the treatment of ovarian epithelial cancer, ovarian sex cord stromal tumours and endometrial cancer (clinical trials ongoing) (Emons and Schally, 1994). In addition to the withdrawal of sex steroids, the antiproliferative action of GnRH on neoplastic tissue may be direct through GnRH-Rs present in the tumour cells (see subsections 2.13.2-5).

The main disadvantage of GnRH agonist-induced pituitary-gonadal suppression is the initial aggravation, known as 'disease flare', resulting from gonadotrophin stimulation of steroid production. However, it is possible to immediately reduce gonadotrophin secretion by using GnRH antagonists to directly block the pituitary GnRH-R ligand binding site. Realisation of the therapeutic potential of GnRH antagonists resulted in the synthesis of many antagonist compounds but their clinical use has been complicated by severe histaminic side effects. Recently new antagonists have been developed and clinical trials have shown that Cetrorelix is effective in the treatment of advanced carcinoma of the prostate (GonzalesBarcena et al, 1994). The potential use of GnRH antagonists for the treatment of other gynaecological disorders, including polycystic ovarian disease, endometriosis and uterine fibroids, is also under review (Reissmann et al, 1994).

2.6 The pituitary GnRH-R

GnRH binds with high affinity to receptors located in pituitary gonadotroph cell membranes. Whilst the amino acid structure of the ligand was identified in the early 1970s (Burgus et al, 1972; Matsuo et al, 1971) it took another 20 years to elucidate the structure of the receptor. The main problem was the low concentration of protein

receptor in pituitary tissue but this was successfully resolved with the development of αT3-1 cells, a gonadotroph cell line containing approximately 2-5 pmols GnRH-R per mg of protein (Horn et al, 1991). A cDNA library was generated from αT3-1 mRNA and this provided the starting material for the cloning of the mouse GnRH-R cDNA.

2.6.1 Molecular cloning of mammalian GnRH-R

In 1992, Tsutsumi et al, cloned the mouse GnRH-R cDNA using a polymerase chain reaction (PCR) based homologous screening strategy. Degenerate oligonucleotides with consensus sequences to TM III and TM VI domains of other GPCRs were used as primers in PCR reactions with an αT3-1 derived DNA template. The novel PCR sequences were then tested for their ability to block GnRH-R expression using a Xenopus oocyte hybrid arrest expression system. This experimental approach relies on an antisense oligonucleotide (derived from the sequence obtained in PCR) blocking the expression of the appropriate receptor in Xenopus oocytes. One of the oligonucleotides generated fulfilled this criteria and was used as a probe to isolate a full length clone from an αT3-1 cDNA library. The mouse GnRH-R cDNA sequence derived using this method has since been confirmed by two other independent groups (Perrin et al, 1993; Reinhart et al, 1992). Sequences of the rat (Eidne et al, 1992; Kaiser et al, 1992; Perrin et al, 1993), human (Chi et al, 1993; Kakar et al, 1992), cow (Kakar et al, 1993) and sheep GnRH-Rs (Brooks et al, 1993; Illing et al, 1993) have also been determined. The sequences of the five different species of GnRH-R isolated to date are illustrated in Figure 2.3.

2.6.2 Primary amino acid structure of the mammalian GnRH-R

The mouse and rat GnRH-R is composed of 327 amino acids but the human, sheep and cow sequences contain an additional amino acid in the second extracellular domain. Interestingly, the GnRH-R shares the greatest sequence homology with the interleukin-8 receptor and not with any other hypophysiotrophic releasing-hormone receptor. The GnRH-R is classified as a member of the G-protein coupled receptor (GPCR) superfamily and contains certain characteristics common to this group.

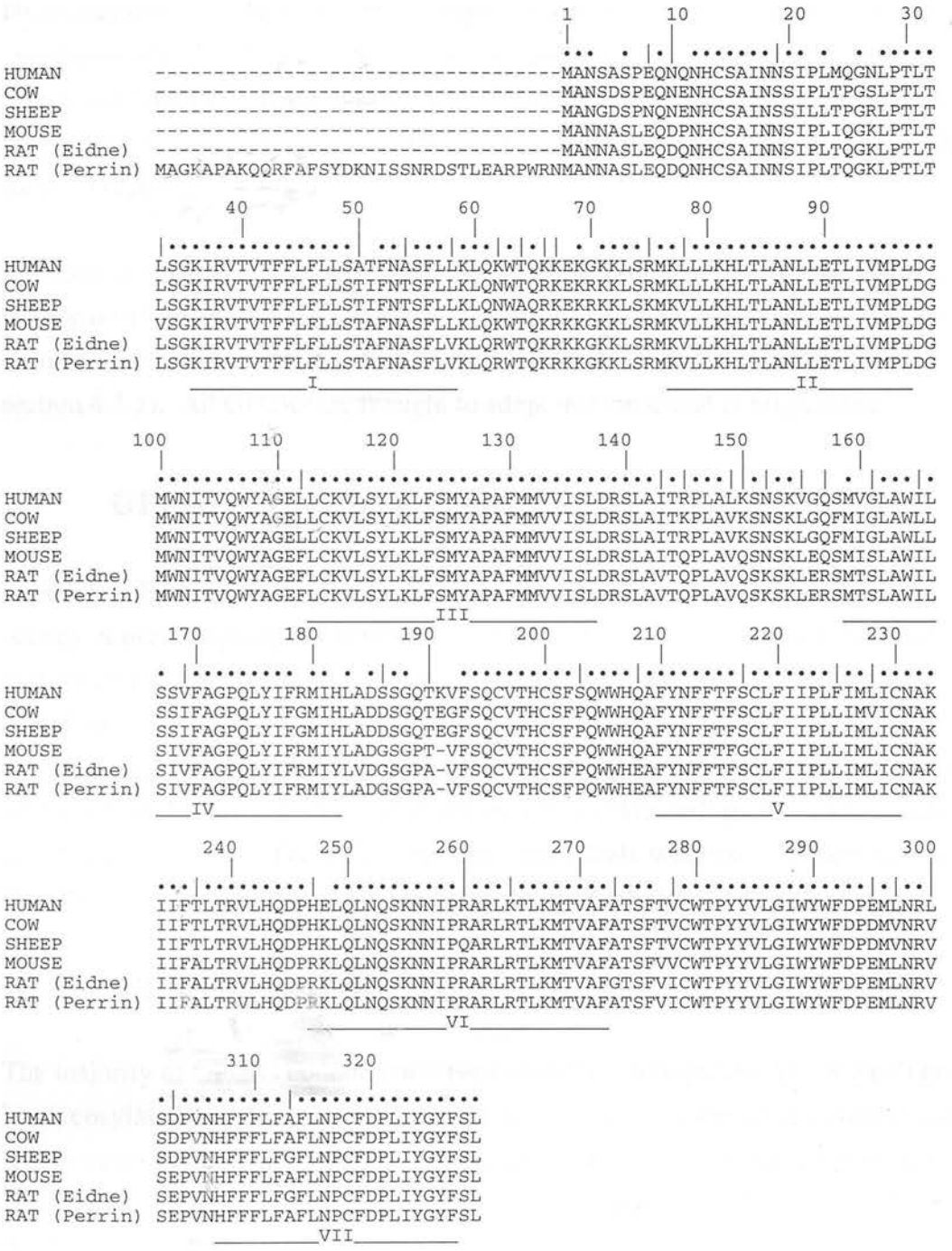

Figure 2.3 Amino acid sequence of the GnRH-R in different mammalian species

Amino acid sequence of the human (Kakar et al, 1992), cow (Kakar et al, 1993), sheep (Brooks et al, 1993), mouse (Tsutsumi et al, 1992) and rat GnRH-R (Eidne et al, 1992; Perrin et al, 1993). Identical amino acids are represented as • and conservative substitutions by |. Position of the TM domains are based on the alignment of Henderson's bacteriorhodopsin model (Henderson et al, 1990).

Hydropathicity analysis of the receptor structure reveals seven stretches of approximately 20-25 hydrophobic amino acids which are thought to cross the membrane bilayer. Linked to these TM domains are an amino (NH_2) terminus, three hydrophilic extracellular loops (el), three intracellular loops (il) and a carboxy (COOH) terminal region.

Electron diffraction studies of two heptahelical proteins, bacteriorhodopsin and rhodopsin (Henderson et al, 1990; Schertler et al, 1993), have shown that the TM domains form α helices and are arranged together around a hydrophilic pore (see section 4.1.1). All GPCRs are thought to adopt this structural configuration.

2.7 GPCRs - Common structural features

Sequence alignment of many GPCRs has shown that certain amino acid residues occupy conserved positions (Probst et al, 1992). Furthermore, it has been suggested that these conserved residues mediate common structural changes ensuing from ligand-receptor activation (Baldwin, 1994). A great deal of information can be derived by comparing the common and unique features of one receptor subgroup with another and much of the early work on structure-function relationships was carried out in β adrenergic receptors. The following subsection deals with the common features of GPCRs and those features which are unique to the GnRH-R.

2.7.1 Glycosylation sites

The majority of GPCRs contain conserved consensus sequences (Asn-X-Ser/Thr) for N-glycosylation of Asn residues. The role of glycosylation in structure-function relationships has been examined in catecholamine and glycoprotein receptor subtypes. In the β adrenergic receptor two glycosylation sites have been identified, at Asn6 and Asn15 (Rand et al, 1990), and the substitution of either Asn for Gln results in a receptor with normal binding properties but at a reduced level of expression. From these experiments it was postulated that receptor glycosylation may have a role in protein trafficking to the cell surface. A role for N-linked glycosylation in glycoprotein hormone binding has also been proposed, as substitution of glycosylated Asn residues in TSH/LH receptors results in a loss of hormone binding (Russo et al, 1991; Zhang et al, 1991). However, further studies in this receptor group have revealed that loss of receptor binding is mediated directly by the Asn residue itself and

not from a failure of carbohydrate attachment (Lui et al, 1993). All mammalian forms of the GnRH-R contain two potential glycosylation sites at Asn18, in the NH_2 terminus of the receptor, and at Asn 102 in el 1. The mouse and rat form of the GnRH-R contain an additional site at Asn4. Photoaffinity labelling studies have shown that the mouse GnRH-R is glycosylated at Asn4 and Asn18 but not at Asn 102. Substitution of Asn4, Asn18 or Asn102 with Gln yielded mutant receptors with normal binding affinities for GnRH analogues but reduced receptor expression. Glycosylation of the GnRH-R therefore appears critical in expression and stability of the receptor structure (Davidson et al, 1995). These results together with those obtained from studies in the β adrenergic receptor suggest that the main role of Asn-linked oligosaccharides is in the regulation of cell surface protein expression. However, in some receptors, such as the muscarinic M_2 receptor, glycosylation is not involved in hormone binding or receptor expression suggesting that the effects of N-linked receptor glycosylation are receptor specific.

2.7.2 Disulphide bridge formation

A striking feature of most GPCRs is a pair of conserved cysteine (Cys) residues in the el 1 and el 2. These Cys residues are thought to form a covalently linked 'disulphide bridge' structure and their function has been studied in many heptahelical receptor proteins. Site-directed mutagenesis studies in rhodopsin have indicated that conserved extracellular Cys residues are involved in receptor expression (Karnik et al, 1988) and the stabilisation of the light-activated protein (Davidson et al, 1994). Similar studies have been carried out with the muscarinic M_1 (Savarese et al, 1992), β adrenergic (Dohlman et al, 1990) and angiotensin II receptors (Yamano et al, 1992). Many GPCRs also contain non-conserved Cys residues in their extracellular domains. The β adrenergic receptor contains four extracellular Cys residues and it is thought that these residues form two disulphide bridges with, paradoxically, each bond occurring between a conserved Cys and a non-conserved Cys residue (Noda et al, 1994). Although it is not known exactly which Cys residues in the extracellular domains of the GPCRs are able to form disulphide bonds, it has been proposed that extracellular disulphide links are important in stabilising the three-dimensional inter-helical receptor structure (Baldwin, 1994). The rat GnRH-R contains four extracellular Cys residues with the two conserved residues at positions 114 and 195 in the el 1 and el 2 respectively. The additional non-conserved two Cys residues lie at position 14 in the

NH_2 terminus and position 199 in the el 2 (Eidne et al, 1992). The role of these Cys residues in putative disulphide bond formation will be investigated in Chapter 5.

2.7.3 Amino acids involved in ligand-induced conformation changes

Following ligand-receptor binding all GPCRs activate a specific concert of G-proteins present on the inside of the cell membrane. Whilst the actual mechanisms responsible for transducing the signal across the membrane are unknown, it is postulated that ligand activation induces a conformational change in the receptor structure triggering a signal transduction cascade mechanism. It is reasonable to presume that there are common features of GPCRs which could facilitate this process and helix breaking proline (Pro) residues, commonly present in the TM domains of many GPCR, may fulfil this function (Probst et al, 1992). The rat GnRH-R contains a series of conserved Pro residues at positions Pro173 (TM IV), Pro222 (TM V), Pro281 (TM VI) and Pro315 (TM VII) and these amino acids are thought to be involved in the transfer of energy from agonist binding to conformational changes in the intracellular domain (Millar et al, 1993). Additional Pro residues are also located at Pro96 (TM II) and Pro 128 (TM IV) and these together with an Asn 53 (TM I), the sequence Phe-X-X-Cys-Trp-X-Pro (TM VI) and Asp-Asn-Ser (TM III/il 3) (Sealfon and Millar, 1995) have also been implicated as potential molecular switches in the GnRH-R binding-transduction relay mechanisms (Millar et al, 1993).

2.7.4 Ligand binding in GPCRs

Amino acids contained within TM III appear to be particularly important in ligand-receptor binding. In the α adrenergic, β adrenergic, and muscarinic M_1 receptors an Asp in TM III is necessary for the maintenance of high affinity agonist and antagonist binding. This amino acid is thought to interact with the positively charged amine head group of the ligand (Savarese and Fraser, 1992). In the GnRH-R, a Lys residues lies in TM III, at a position analogous to Asp113 in the β adrenergic receptor, and this residue may also be important in agonist-induced receptor binding. Site-directed mutagenesis studies show that substitution of Lys to Arg in both the rat (see Chapter 7) and human (Zhou et al, 1995) GnRH-R does not affect receptor function. However, substitution of Lys121 to Gln (in the human GnRH-R) resulted in a receptor with a decreased agonist affinity but with an apparently intact high affinity

antagonist binding site. The function of Lys121 in GnRH-R binding is further considered in Chapter 7.

2.7.5 Relationship between GnRH and the GnRH-R structure

Site-directed mutagenesis studies often highlight key amino acids within a receptor structure that are important for ligand binding. However, to fully map a receptor ligand binding domain it is also essential to examine the structure of the ligand so that specific interactions between residues in the ligand and those in the receptor can be identified. Analysis of the GnRH amino acid sequences (Table 2.1, pg14) reveals a 50% homology between the 6 different species with position 8 as the most variable. Chemical studies have indicated that mGnRH interacts with at least 2 carboxyl groups in the receptor (Hazum, 1987) and the positively charged nature of Arg8, in the mammalian peptide, makes it a likely candidate for such interactions. Recently, ionic binding between Arg8 in the peptide and Glu301 in the GnRH-R has been proposed (Davidson et al, 1994) and it has been postulated that this interaction conforms the ligand into a special structural entity which facilitates receptor binding. Tyr and Trp residues within the GnRH-R structure have also been implicated in GnRH binding (Keinan and Hazum, 1985) and these two amino acids could participate in aromatic stacking or in charge-transfer interactions. The indole nucleus of the Trp is electron rich and could feasibly interact with a protonated imidazole ring of histamine while the phenolic Tyr hydroxyl group could also be involved in hydrogen bonding (Janecka et al, 1994).

Rivier and co-workers proposed that in its biologically active state GnRH binds to its receptor in a hairpin configuration with residues 4-7 (Ser-Tyr-Gly-Leu) (Karten and Rivier, 1986), creating a β turn. The alignment of the NH_2 and COOH termini together (Monahan et al, 1973) ensures that only the ends of the GnRH peptide will interact directly with the receptor. Residues at the NH_2 terminus of GnRH are thought to be important in receptor activation whilst those at the COOH end are crucial for high affinity binding (Nikolics et al, 1988). The role of amino acids at positions 4-7 are probably structural. However, it is possible that certain residues participate in both receptor binding and functional activation and that individual amino acids do not act alone but as a structural unit.

2.7.6 Residues important in signal transduction

Following ligand-receptor binding in GPCRs, a three-dimensional conformational change within the structure of the receptor activates a specific G-protein system located on the intracellular surface of the membrane. Like the amino acids involved in receptor binding function, both conserved and uniquely positioned receptor residues are likely to participate in G-protein activation. Site-directed mutagenesis and receptor chimera studies have implicated intracellular regions of GPCRs, especially the il 2, il 3 and occasionally the COOH tail, in ligand-receptor activation processes (Caron and Lefkowitz, 1993; Probst et al, 1992; Savarese and Fraser, 1992). In particular, a conserved motif sequence Asp-Arg-Tyr (DRY), located at the TM III/il 2 interface, is thought to be involved in signal transduction mechanisms. Mutation of the Asp part of the sequence in the β adrenergic, muscarinic M_1 and α_2 adrenergic receptors results in mutant receptors that display a high affinity binding site but, reduced or absent G-protein coupling (Savarese and Fraser, 1992). In rhodopsin, the corresponding Gln is also thought to be involved in signal transduction mechanisms (Savarese and Fraser, 1992).

In the muscarinic receptor, a Leu lying in close proximity to the DRY sequence in il 2 has been implicated as an important residue in both signal transduction and receptor sequestration (Moro et al, 1993; 1994). A corresponding positioned Leu residue (Leu147) in the GnRH-R also appears important in G-protein activation and second messenger production. A study by Arora et al (1995) has demonstrated that substitution of Leu147 to either Ala or Asp significantly alters second messenger production whilst retaining normal receptor binding function. However, in these studies some second messenger production was still detected implying that other receptor residues must also be involved.

2.8 Unique features of the GnRH-R

The GnRH-R exhibits unique features which make it distinct from other members of the GPCR family including the replacement of the Tyr residue in the conserved DRY motif in il 2, together with the interchange of a conserved Asp and Asn in helix 2 and helix 7 respectively. The most striking feature, however, is the total absence of a COOH tail making it the only GPCR cloned to date missing this structure.

2.8.1 Role of DRS sequence in the GnRH-R

As highlighted in section 2.7.6, the DRY motif has been implicated in signal transduction mechanisms. In the GnRH-R this motif is altered to DRS thus generating a potential phosphorylation site. Site-directed mutagenesis studies, substituting a Tyr residue in place of Ser140 (the Ser residue in the DRS sequence) has shown that Ser140Tyr does not affect G-protein coupling but significantly increases receptor affinity and the rate of GnRH-R internalisation (Arora et al, 1995).

2.8.2 Asp and Asn interchange

An Asp in TM II and an Asn in TM VII are conserved in 98% and 95% of GPCRs respectively but in GnRH-R the positions of these two conserved amino acids are interchanged with Asn87 in TM II and Asp318 in TM VII. The role of the Asp in TM II has been examined in many neurotransmitter receptors. Site-directed mutagenesis studies replacing Asp with other amino acids has resulted in a wide variety of functional effects including reduced agonist/antagonist binding, diminished or loss of receptor activation and a loss of receptor modulation by pH, sodium, or GTP analogues (Zhou et al, 1993). The involvement of Asn in TM VII in ligand binding and receptor activation has not been so extensively studied. However, an experimental investigation in the 5-HT_{1A} receptor, substituting Asn396 (TM VII) to Ala/Phe/Val, has shown that this amino acid is essential for receptor binding (Chanda et al, 1993).

The role of Asn87 in TM II and Asp318 in TM VII in the GnRH-R will be investigated in Chapter 6.

2.8.3 Absence of COOH tail

In other GPCRs the intracellular COOH domain is involved in the maintenance of receptor stability and phosphorylation-mediated receptor desensitisation (Savarese and Fraser, 1992). An increase in receptor stability occurs through palmitoylation of Cys residues, a process that facilitates interactions between the COOH tail and the membrane bilayer resulting in remodelling of the receptor structure to create another il (O'Dowd et al, 1989). As the GnRH-R lacks a COOH tail some of its functions

(stabilisation and receptor desensitisation) may be taken over by amino acids located in other parts of the receptor. Regions within the receptor involved in membrane stabilisation have yet to be identified but there are eight consensus phosphorylation sites (putative targets for protein kinases), at threonine (Thr) 64 and Ser 74 in the il 1, Ser140, Ser151, Ser153 and Ser158 in the il 2 and Thr238 and Thr264 in the il 3 in the rat GnRH-R.

2.9 Receptor desensitisation and down-regulation mechanisms

Desensitisation is generally defined as the attenuation of a biological response upon prolonged exposure to agonists. The ability to suppress the pituitary-gonadal axis through desensitisation of the GnRH-R underlies the clinical use of GnRH agonists and it is, therefore, vital to understand the mechanism by which such events arise.

Exposure of the GnRH-R to its agonist induces a state of homologous desensitisation that results in a functional uncoupling of the receptor from its G-protein and effector system. Moreover, the responsiveness of other receptors utilising the same G-protein/effector system are unaffected by this desensitisation mechanism. In other GPCRs protein kinase dependent phosphorylation of Ser and Thr residues, in the il 3 and COOH terminal tail, are important in G-protein uncoupling events. Specific receptor kinases in the β adrenergic (Benovic et al, 1987) and rhodopsin (Hargrave and McDowell, 1992; Savarese and Fraser, 1992) systems have been shown to mediate these events. In the GnRH/GnRH-R system phosphorylation of Ser/Thr residues in the il 3 are also thought to be important but the mechanisms underlying receptor phosphorylation and the possible sites of action in the signal transduction cascade pathway are largely unknown.

Studies in αT3-1 cells have shown that rapid exposure of these cells to GnRH does not affect the production of the second messenger inositol 1,4,5 trisphosphate ($InsP_3$), implying that agonist-induced G-protein uncoupling processes are mediated at sites down-stream of phospholipase C (PLC) membrane hydrolysis (Anderson et al, 1995) (see subsection 2.12). Further experiments in αT3-1 cells have revealed that a single high dose pulse of GnRH rapidly desensitises GnRH-induced biphasic Ca^{2+} release and, therefore, it is possible that G-protein uncoupling events are related to alterations in Ca^{2+} mobilisation (Anderson et al, 1995). Several other hypotheses have been put

forward with Milligan and co-workers suggesting that as multiple G-proteins can be stimulated by a single receptor type, G-protein uncoupling may result from preferential desensitisation of one G-protein over another (Milligan, 1993).

The loss of G-protein coupling leads to the attenuation of gonadotrophin release from secretory granules. It has been further suggested that the decrease in LH secretion might result from a decrease in LH movement from non-releasable to releasable stores, with this movement being progressively diminished as agonist exposure time is increased, causing an eventual loss of gonadotrophin secretion (Janovick and Conn, 1993).

In addition to the influence on G-protein coupling and hormone secretion continuous agonist exposure directly affects the specific receptor that is responsible for the mediation of its actions. Continuous exposure of GnRH to the GnRH-R results in receptor sequestration, a process involving the removal of the receptor from the cell surface by internalisation. This loss in receptor number occurs in minutes to hours and is reversible on removal of GnRH. Arora and co-worker identified two sites within the GnRH-R that are involved in mediating receptor internalisation processes, Ser140 (part of the DRS motif) and Leu147. The substitution of these amino acids, Ser140 by Tyr and Leu147 by either Ala or Asp, affected levels of receptor internalisation. The Ser140Tyr mutation increased internalisation rates whilst both Leu147Ala and Leu147Asp mutations showed a 50% reduction in receptor internalisation compared to the wild-type (Arora et al, 1995). Chronic exposure to agonist, however, eventually results in the degradation of internalised receptors. This process is irreversible and thus, the restoration of receptor number must occur by de novo protein synthesis.

It is clear from the studies highlighted in this section that a complex series of processes underlies receptor desensitisation and many of these issues still have to be explored.

2.10 GnRH-R gene structure

The GnRH-R belongs to a small subset of intron-containing GPCRs that include the glycoprotein, opsin and endothelin receptor families (Probst et al, 1992). Within this subset receptors can be further categorised by the position of their introns. However, the GnRH-R gene stands alone as no other GPCR has a gene structure with a similar

intron/exon pattern. Both the mouse (Albarracin et al, 1994; Zhou and Sealfon, 1994) and human (Fan et al, 1994) GnRH-R genes have been cloned and consist of at least three exons and two introns, with the human gene localised as a single copy to chromosome 4 (Fan et al, 1994; Morrison et al, 1994).

Analysis of the human gene structure shows that the first exon contains the 5' untranslated region and the open reading frame encoding for TM I-III and part of TM IV, the second exon codes for the remainder of TM IV and TM V and the third exon encodes the rest of the open reading frame and the 3' untranslated region. Of the two introns, the first (4.2 kb) is positioned between Gln174 and Leu175 (TM IV) and the second (5 kb) is between Glu248 and Leu 249 (il 3). The sequence of the mouse gene also appears to contain the same intron/exon pattern. Alternative spliced variants have been identified although these do not code for functional active receptors (Zhou and Sealfon, 1994).

Albarracin et al (1994) have recently characterised part of the 5' flanking region of the mouse GnRH-R gene. A major transcription start site was identified 62 nucleotides upstream of the translational start site; however, the promoter region of the GnRH-R gene does not appear to contain a TATA box sequence. This TATA-less phenomenon has also been observed in the other GPCR genes including the LH, FSH (Huhtaniemi et al, 1992) and the somatostatin-1 (Hauser et al, 1994) receptors. Putative sites for the transactivation factor AP-1 and a 8 bp element, TGTCCTTG, homologous to part of the 30 bp GSE (Horn et al, 1992), were also identified (Albarracin et al, 1994). Additional studies analysing the mouse GnRH-R gene promoter region by Clay and co-workers have reported the presence of another transcription start site approximately 200 bp in the 5' direction of the initiation codon. This more distal transcription initiation site appears to be associated with a consensus TATA motif. Further experiments have revealed the presence of putative cell specific regulatory elements between -400 and -500 bp relative to the translational ATG start site (Clay et al, 1995).

2.11 Regulation of the GnRH-R

Regulation of GnRH-R biosynthesis is dependent on mechanisms controlling gene transcription, mRNA production and stability along with translational/post translational processes. Receptor degradation, sequestration and recycling of receptors between accessible and non-accessible pools, together with the

responsiveness of the GnRH-R to its ligand, can also affect the outcome of ligand-receptor coupling mechanisms.

2.11.1 GnRH regulation of the GnRH-R

The action of GnRH on the GnRH-R can result in both up- and down-regulation of the receptor depending on the duration and level of GnRH exposure. *In vitro* experiments, using dispersed rat pituitary cells, have shown that administration of low doses of GnRH result in an initial loss of GnRH-Rs but after 6 hours the receptor number increases above basal levels (Conn et al, 1984). In contrast, exposure to high concentrations of GnRH only results in receptor down-regulation (Conn et al, 1984). Additional studies have indicated that, within this system, receptor down-regulation occurs via processes that do not require RNA or protein synthesis, whereas the ensuing up-regulation appears dependent on both synthesis of mRNA and receptor protein (Sealfon and Millar, 1995). The role of extracellular calcium ($[Ca^{2+}]e$) in receptor up-regulation events is controversial. Early studies highlighted the importance of Ca^{2+} cell entry (Conn et al, 1984), but recent experiments suggest that $[Ca^{2+}]e$ is not required for de novo receptor synthesis (Braden and Conn, 1990).

Treatment of αT3-1 cells with a low dose of GnRH (0.1-10nM) results in an initial decrease followed by an increase in receptor number. However, receptor up-regulation is not accompanied by changes in GnRH-R mRNA levels or RNA stability (Tsutsumi et al, 1993). Chronic exposure of αT3-1 cells to GnRH (1μM) decreased the number of GnRH binding sites by 75% after 24 hours. In these studies GnRH-R mRNA levels were not altered but RNA translational efficiency was reduced, suggesting that receptor down-regulation in αT3-1 cells is in part mediated by changes in receptor translation mechanisms (Tsutsumi et al, 1995). These results contrast with those obtained in pituitary cell culture studies which indicate that up-regulation of the GnRH-R, following pulsatile administration of GnRH, corresponds to an increase in receptor mRNA production (Kaiser et al, 1993). The reasons underlying these differences are at present unknown.

Many *in vivo* studies have also been carried out to monitor the regulatory effects of GnRH and its analogues on GnRH-R levels. These experiments have highlighted that the mode of GnRH presentation to the GnRH-R is the most important determining factor. Katt and co-workers demonstrated that GnRH-induced GnRH-R up-regulation

is dependent on the frequency of GnRH pulses administered (Katt et al, 1985). Other experimental studies in sheep have indicated that pulsatile administration of a low dose of GnRH increases both mRNA levels and GnRH-R numbers (Turzillo et al, 1995). In contrast, administration of high doses of a potent GnRH agonist suppresses both GnRH-R mRNA and receptor levels in rats and sheep (Clayton and Catt, 1980; Lerrant et al, 1995; Wu et al, 1994).

2.11.2 Regulation of GnRH-R levels during the estrous cycle

The rate of gene transcription and the number of GnRH-Rs change during the estrous cycle. Northern Blot analysis of the rat GnRH-R mRNA has shown that transcription levels increase during diestrus I reaching a 3-fold maximum increase at diestrus II and then decline to a 2-fold increase by the late proestrus stage of the cycle (Kakar et al, 1994). A similar pattern has also been seen during the estrous cycle of the sheep (Brooks et al, 1993) with changes in mRNA in accord with changes in receptor numbers (Clayton et al, 1980). The changes observed in mRNA and receptor levels throughout the estrous cycle probably reflect alterations in the hormonal milieu with the actions of both steroidal and non-steroidal factors having important regulatory roles. GnRH-R gene regulation has been well characterised in both rats and sheep. Removal of gonadal steroids by castration results in an increase in GnRH-R mRNA levels in the rat anterior pituitary, which can be reversed by the introduction of exogenous steroids (Kaiser et al, 1993; Kakar et al, 1994). Non-steroidal factors activin and inhibin are also important regulators with activin A increasing the rate of GnRH-R synthesis (as measured by density shift techniques) (Braden and Conn, 1992) and inhibin decreasing receptor numbers in rat primary pituitary cultures (Wang et al, 1988). Studies in ovine pituitary cell cultures revealed that estradiol, progesterone and inhibin alter GnRH-R responsiveness, as determined by GnRH-stimulated LH release (Sealfon and Millar, 1995). These changes correspond to receptor content, with the lowest receptor number present during treatment with progesterone and the highest number observed following co-administration of estradiol with inhibin. Further studies have revealed that the changes in receptor number are linked to gene transcription (Wu et al, 1994).

2.12 Activation of the GnRH-R and signalling pathways in pituitary gonadotrophs and αT3-1 cells

The binding of GnRH to its pituitary receptor is associated with G-protein coupling, activation of PLC, followed by Ca^{2+} mobilisation and finally exocytosis of secretory hormones from the cell. Many studies examining intracellular signalling events utilise αT3-1 cells, a clonally derived cell line of gonadotroph lineage, as a representative model (Horn et al, 1991). αT3-1 cells were established from embryonic cells before the development of the gonadotrophin β subunit and are therefore unable to secrete gonadotrophins. This limits their use to the study of events leading up to exocytosis but not the mechanisms underlying exocytosis itself. Figure 2.4 illustrates signal transduction pathways activated by the interaction of GnRH with its receptor.

2.12.1 G-protein coupling

Ligand-receptor binding induces conformational changes in the GnRH-R which are responsible for the activation of a G-protein complex - a heterotrimeric structure located on the cytoplasmic surface of the plasma membrane. G-proteins are composed of three individual subunits. The α subunit is receptor specific, containing a receptor activation site whereas the β and γ subunits exist as a common pool interchangeable between the different α subunits. In the inactive state, G-proteins have guanosine diphosphate (GDP) bound to the α subunit. Receptor activation creates membrane perturbations and stimulates the replacement of GDP for guanosine triphosphate (GTP), resulting in the dissociation of the complex into α and βγ subunit components (Speigel et al, 1992). The free α subunit can now stimulate an appropriate second messenger system but this activation is only temporary as GTPase activity, intrinsic to the α subunit, rapidly leads to G-protein inactivation. α subunits are categorised by function and bacterial toxin sensitivity. GnRH-R ligand binding activates the pertussis toxin insensitive G-proteins, $G\alpha_q$ and $G\alpha_{11}$ (Anderson et al, 1993; Naor, 1990). Studies in αT3-1 cells have shown that the GnRH-induced second messenger activity can be blocked with an antiserum raised against $G\alpha_q$ and $G\alpha_{11}$ (Hsieh and Martin, 1992). A role for the dissociated βγ subunits has also been implicated in GnRH-R activation in GGH3-1 cells (GH3 cells stably transfected with the rat GnRH-R cDNA). GnRH-stimulated increases in second messenger production and hormone secretion in GGH3 cells can be attenuated by co-transfection of GnRH-R cDNA with part of the β adrenergic receptor kinase (βARK) cDNA. βARK1 contains an 125

amino acid sequence that directly binds to the βγ subunits and thus allows the distinction between Gα and Gβγ activated pathways (Guo et al, 1995).

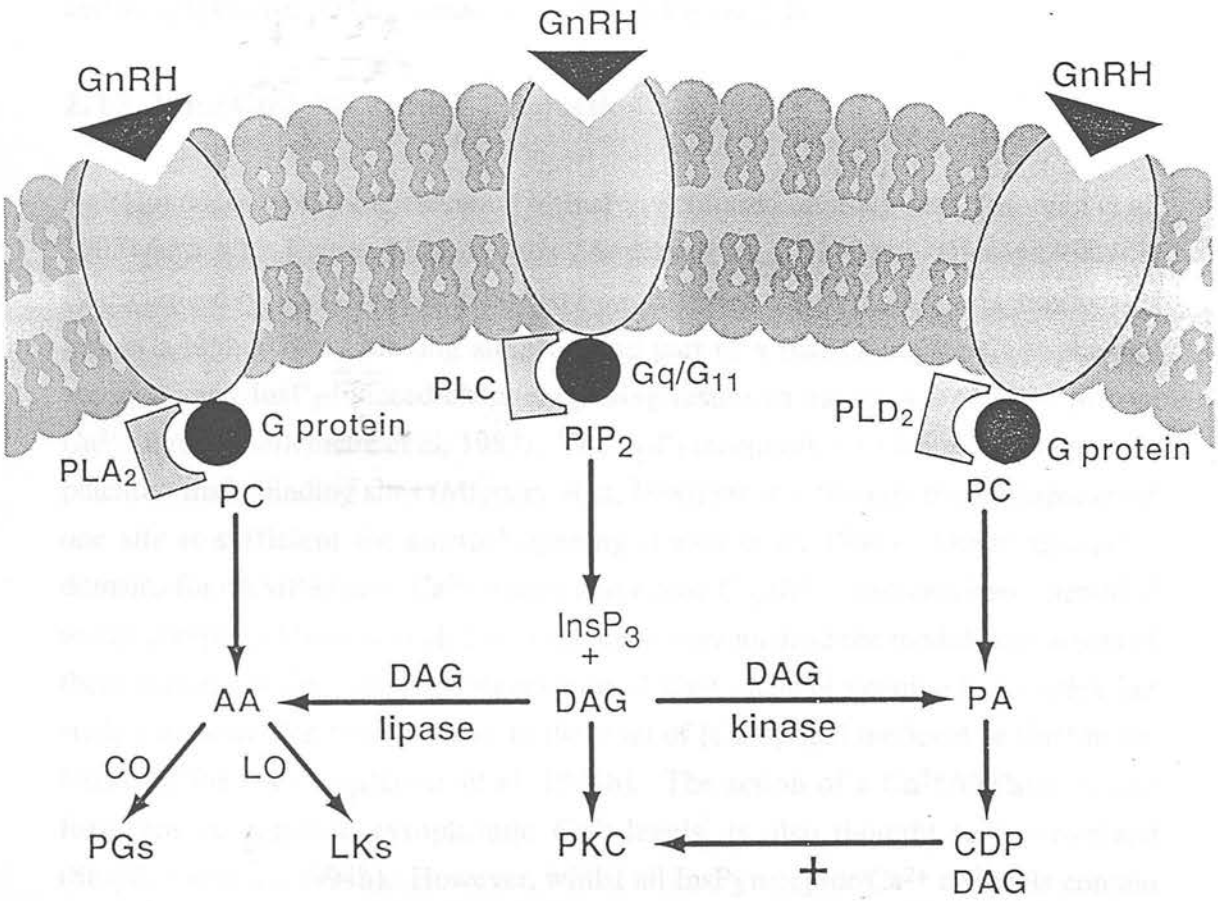

Figure 2.4 Multiplicity of GnRH-induced intracellular signalling in pituitary gonadotrophs

Illustration of 3 major interconnecting signal transduction pathways activated by GnRH in gonadotroph cells. GnRH interactions with its receptor activates a G-protein effector system. This results in the production of two major second messenger molecules $InsP_3$ and DAG via the action of PLC. $InsP_3$ is responsible for the mobilisation of Ca^{2+} whilst DAG further activates PKC. DAG production may also arise from the stimulation of the PLD_2 pathways and this alternative pathway prolongs the activation of PKC. PKC activation has a positive feedback effect on PLD_2 and PLA_2 signalling pathways. The production of AA is thought to arise from the activation of PLA_2. AA can be further metabolised by cycloxygenase (CO) and lipoxygenase (LO) to prostaglandins (PGs) and leukotrienes (LKs) respectively.

$G\alpha_q$ and $G\alpha_{11}$ activates the β1 and β2 PLC isoforms promoting the hydrolysis of phosphatidylinositol 4,5 bisphosphate (PIP_2). The activation of PIP_2 results in the formation of two important signalling molecules inositol 1, 4, 5 trisphosphate ($InsP_3$) and diacylgylcerol (DAG) (Limor et al, 1989) (Figure 2.4).

2.12.2 Inositol Phosphate Production

GnRH induces a biphasic elevation of $InsP_3$ in cultured pituitary cells (Morgan et al, 1987) and αT3-1 gonadotroph cells (Anderson et al, 1992). This response is characterised by an early peak followed by a sustained rise in $InsP_3$ production. $InsP_3$ acts at a high affinity binding site, forming part of a $InsP_3$ receptor/Ca^{2+} channel complex, and $InsP_3$-induced channel opening results in the release of $[Ca^{2+}]i$ from Ca^{2+} stores (Guillemette et al, 1987). The $InsP_3$ receptor/Ca^{2+} channel contains four potential $InsP_3$ binding sites (Mignery et al, 1990) but it is thought that occupation of one site is sufficient for channel opening (Finch et al, 1991). Other regulatory domains for cAMP kinase, Ca^{2+} and protein kinase C (PKC) have also been identified on the complex (Mignery et al, 1990) and these may mediate the modulatory action of these factors on Ca^{2+} release. Regulation of Ca^{2+} channel opening is complex but studies indicate that it is sensitive to the level of $[Ca^{2+}]i$ and the level of Ca^{2+} in the lumen of the ER (Stojilkovic et al, 1994b). The action of a Ca^{2+}ATPase, which functions to regulate cytoplasmic Ca^{2+} levels, is also thought to be involved (Stojilkovic et al, 1994b). However, whilst all $InsP_3$ receptor/Ca^{2+} channels contain $InsP_3$ binding sites not all of them are sensitive to $InsP_3$ thus resulting in a large non-releasable Ca^{2+} pool.

Once activated $InsP_3$ is rapidly metabolised either by 5' phosphatase activity to inositol 1,4 bisphosphate or by 3-kinase activity to inositol 1, 3, 4, 5 tetraphosphate ($InsP_4$) (Shears, 1992). Dephosphorylation prevents any further activation of the system whereas phosphorylation may further propagate signal transduction via the production of $InsP_4$. $InsP_4$ is thought to control Ca^{2+} entry into the cell and may also act as a precursor for $InsP_5$ or $InsP_6$ production. Controversy surrounds the role of $InsP_4$ and the action of 'higher inositol phosphates', $InsP_5$ and $InsP_6$, in gonadotroph cell signalling. Nevertheless, it is clear that agonist-induced PLC activation is the main positive regulatory component of $InsP_3$ production and the duration of signalling is dependent on its rate of activation compared to the action of its metabolising enzymes. Studies have revealed that 3-kinase activity is positively regulated by increasing

$[Ca^{2+}]i$ and inhibited by PKC activity. Tyrosine kinase has also been implicated in its regulation (Johnson et al, 1989). The regulation of 5' phosphatase enzyme in gonadotrophs cells has been less well studied although in other systems it is thought to be receptor regulated (Stojilkovic et al, 1994b).

2.12.3 Diacylglyceride signalling

Receptor-induced PIP_2 hydrolysis also results in the activation of DAG in both pituitary gonadotrophs and αT3-1 cells, with an initial rapid stimulation followed by a sustained rise in DAG (Stojilkovic et al, 1994b). PLC activation is thought to account for the initial rapid increase in DAG formation although the sustained DAG response is thought to be mediated by PKC activation of another membrane phospholipase, phospholipase D_2 (PLD_2) (Zheng et al, 1994). PLD_2 hydrolyses phosphatidylcholine (PC) to phosphatidic acid (PA) which can then be converted to DAG (see Figure 2.4).

DAG can also be metabolised to arachidonic acids (AA) by DAG lipase and GnRH has been shown to stimulate AA release in pituitary cell cultures (Naor et al, 1985). AA formation can also occur through GnRH activation of another phopholipase, PLA_2. Both AA and several of its metabolites, prostaglandins (PGs) and leukotrienes (LKs) have been shown to stimulate LH and FSH release from gonadotrophs *in vitro* (Hunting et al, 1985; Naor et al, 1985).

2.12.4 Protein Kinase C activation

The formation of DAG and the increase in $[Ca^{2+}]i$ are primarily responsible for the activation of PKC isotypes α and β II in pituitary gonadotroph cells. PKC acts in the membrane to modulate receptor number, ion channel function, phospholipase activity and endocytosis (Stojilkovic et al, 1994b). In the cytoplasm it is responsible for the control of Ca^{2+} signalling via its regulation of PLC, voltage sensitive Ca^{2+} channels (VSCC) and the $InsP_3$ receptor/Ca^{2+} channel (Stojilkovic et al, 1994b) and in the nucleus PKC regulates cell growth and differentiation. The action of PKC in the nucleus involves the transcription of primary response genes which in turn regulate late response genes, required for cell growth and differentiation (MaMahon and Monroe, 1992).

2.12.5 Mechanism of exocytosis

Secretion of LH and FSH from pituitary gonadotrophs is an energy dependent process requiring Ca^{2+}. In gonadotroph cells biphasic LH secretion occurs rapidly and can be correlated to changes in $[Ca^{2+}]i$ (Stojilkovic and Catt, 1992). Despite the apparent link between changes in $[Ca^{2+}]i$ and hormone secretion the underlying mechanisms are still unknown. Leong and Thorner (1991) devised a model to explain their relationship, and suggest that the GnRH-induced biphasic rise in $[Ca^{2+}]i$ is associated with gonadotrophin secretion alongside an inhibition of LH β subunit mRNA and a decrease in GnRH-R levels. This model also proposes that agonist-induced Ca^{2+} oscillations are responsible for increases in both LH β subunit mRNA and GnRH-R levels but these actions are not sufficient to activate a secretory response. PKC and calmodulin have also been implicated in the modulation of exocytosis (Stojilkovic and Catt, 1992).

2.12.6 Adenyl-cyclase signalling

The role of GnRH-induced adenyl-cyclase activity in gonadotroph intracellular signalling processes is unclear. An increase in cAMP and cGMP levels has been observed in prolonged agonist stimulation of pituitary cell cultures (Naor et al, 1979) but these factors do not appear to be involved in exocytosis. A role in the modulation of gonadotrophin synthesis (Lui and Jackson, 1981) has also been proposed.

2.12.7 Plasma membrane oscillations

Gonadotroph cells and αT3-1 cells contain many different types of ion channels and the flow of various ions through these channels at any one time determines the membrane potential of the cell (Vm). Several different types of voltage gated K^+ channels, T and L-type Ca^{2+} channels and tetrodotoxin-sensitive Na^+ channels have been identified in these cell types (Stojilkovic and Catt, 1992). Gonadotroph cells have a basal pace-maker activity (Stojilkovic and Catt, 1992) and the base line firing of action potentials (APs) is dependent on the magnitude and frequency of the transient hyperpolarisation which ensues after each AP. Non-stimulated pituitary gonadotrophs show fluctuations in $[Ca^{2+}]i$ but these spontaneous $[Ca^{2+}]i$ fluctuations are not sufficient to cause gonadotrophin secretion (Iida et al, 1991).

2.12.8 GnRH-induced Vm changes

GnRH causes dramatic changes in the electrical activity of cultured pituitary gonadotroph cells with variations in voltage/current profiles largely dependent on agonist concentration. Administration of nanomolar concentrations of GnRH causes periodic hyperpolarisation of Vm, altering the resting Vm (~ -35 mV to -45 mV) to hyperpolarising values (~ -75 mV to -95 mV) before returning to baseline levels. This slow depolarisation leads to the firing of multiple APs via the influx of Na^+ and Ca^{2+} ions through voltage dependent channels and these changes in Vm appear to be dependent on a rise in $[Ca^{2+}]i$. The periodic hyperpolarisation that follows depolarisation occurs as a result of continual opening and closing of small conductance Ca^{2+}-activated K^+ channels and these ion sensitive channels are probably regulated by GnRH-induced $[Ca^{2+}]i$ oscillations (Hille et al, 1995).

2.12.9 GnRH-induced biphasic calcium response

In pituitary gonadotrophs and αT3-1 cells, treatment with GnRH results in a biphasic rise in $[Ca^{2+}]i$ that is characterised by a rapid initial Ca^{2+} spike followed by a prolonged secondary plateau phase (Anderson et al, 1993). These non-oscillatory responses are dose-dependent, a sign indicative of an amplitude-modulated Ca^{2+} response i.e. increased receptor occupancy results in a Ca^{2+} response with an increased amplitude. The use of chemical agents that specifically modify different aspects of Ca^{2+} mobilisation, have allowed the differential contribution of $[Ca^{2+}]i$ versus $[Ca^{2+}]e$ to be studied during GnRH-induced biphasic Ca^{2+} responses.

Thapsigargin, a sesquiterpene lactone, selectively inhibits ER Ca^{2+}ATPase activity, thereby depleting $InsP_3$ regulated $[Ca^{2+}]i$ stores, and can be used to indicate the importance of $[Ca^{2+}]i$ release. The pretreatment of primary gonadotrophs and αT3-1 cells with thapsigargin abolishes the initial GnRH-induced Ca^{2+} spike phase (Anderson et al, 1992; Iida et al, 1991). This evidence, together with the observation that the rapid Ca^{2+} spike phase occurs independently of changes in the Vm and/or the activation of PKC in pituitary gonadotrophs, is consistent with the hypothesis that GnRH-induced fast Ca^{2+} transients are dependent on the release of Ca^{2+} from intracellular stores (Stojilkovic et al, 1994b). In addition, the close temporal relationship between $InsP_3$ production and the rapid Ca^{2+} spike suggests it provides the trigger for the initial phase of the response (Anderson et al, 1993; 1995; Morgan et

al, 1987; Zheng et al, 1994). Following either the reduction of $[Ca^{2+}]e$ by EGTA or the blockage of the L-type VSCC with nifedipine or cobalt, the secondary plateau phase in GnRH treated pituitary gonadotrophs is either substantially reduced or abolished (Anderson et al, 1992; McCardle and Poch, 1992). An influx of $[Ca^{2+}]e$ via L-type VSCC therefore appears to be involved in the Ca^{2+} plateau phase. Further studies have shown that this secondary phase, which occurs at baseline levels of $InsP_3$, is dependent on changes in the Vm, and can be modulated by PKC (Stojilkovic et al, 1994b). However, Hille et al (1995) have provided a different model based on the observation that there is no sharp distinction between the two phases of GnRH-induced Ca^{2+} response. These authors suggest that $InsP_3$ is continually synthesised during agonist exposure and that cyclic release of Ca^{2+} from intracellular stores is primarily responsible for $[Ca^{2+}]i$ increases. They also propose that there is a concurrent slow entry of Ca^{2+} into the cell to replenish the loss from the intracellular stores.

2.12.10 GnRH-induced Ca^{2+} oscillations

Gonadotrophs are examples of excitable endocrine cells which exhibit both spontaneous and agonist-induced Ca^{2+} oscillations. However, no such oscillations have been reported in αT3-1 cells although Anderson and co-workers have observed infrequent Ca^{2+} oscillation in these cells when treated with low concentrations of GnRH (unpublished observations). The pattern of these oscillations is known to be frequency modulated and increasing agonist concentrations cause a decrease in the response latency but an increase in frequency of spiking (Iida et al, 1991). Continuous exposure to higher concentrations of GnRH (10nM) causes the amplitude of these spikes to wane and eventually reach a steady state plateau, an effect attributable to the gradual depletion of the agonist sensitive Ca^{2+} pool (Stojilkovic et al, 1993). The mobilisation of $[Ca^{2+}]i$ and $[Ca^{2+}]e$ appears to be responsible for these Ca^{2+} oscillations.

2.12.11 Mechanism of Ca^{2+} oscillations

In electrically excitable cells, Ca^{2+} oscillations can be divided into two classes depending on the primary Ca^{2+} source; namely via the plasma membrane [$(Ca^{2+}]e$) or cytoplasmic Ca^{2+} oscillators ($[Ca^{2+}]i$) (Berridge, 1988). In pituitary gonadotroph cells it is now generally regarded that cytoplasmic oscillations are of primary

importance in the generation of Ca^{2+} oscillations. Several different models have been proposed to explain GnRH-induced Ca^{2+} oscillations in pituitary cells. A currently favoured $InsP_3$ controlled model involves the sequential positive and negative feedback of $InsP_3$ on Ca^{2+} release (Finch et al, 1991; Iino and Endo, 1992). Studies by Finch et al (1991) have shown that the $InsP_3$ receptor/channel opening is sensitive to levels of $[Ca^{2+}]i$. The existence of a bell-shaped Ca^{2+} dependent sensitivity curve has been proposed whereby low levels of $InsP_3$-induced $[Ca^{2+}]i$ facilitates the opening of more $InsP_3$ receptor/Ca^{2+} channels, but as the level of $[Ca^{2+}]i$ continues to rise these channels close. The channel remains shut for several seconds to allow Ca^{2+}ATPases, located on the membranes of the intracellular ER stores, to pump the Ca^{2+} from the cytoplasm back into the stores. The concentration of Ca^{2+} within the lumen of the ER is also thought to modulate Ca^{2+} release for these vesicles (Nunn and Taylor, 1992).

Stojilkovic and co-workers have developed a mathematical model to describe several aspects of agonist-induced Ca^{2+} signalling in GnRH-stimulated gonadotrophs (Li et al, 1994). This model is based upon rapid activation of the $InsP_3$ receptor/Ca^{2+} channel at low $[Ca^{2+}]i$, and slow activation at high $[Ca^{2+}]i$ levels. These gating properties, when combined with the action of the ER Ca^{2+}ATPase and the enhancement of channel opening in the presence of reduced ER luminal Ca^{2+} levels, predicts many of the Ca^{2+} profiles seen during experimental procedures.

2.13 Extrapituitary localisation of GnRH and its receptor

GnRH and its specific receptor have been localised outside the hypothalamic-pituitary system in other brain regions and also in breast tissue, placenta, ovary, prostate and testes. Studies have documented a direct action of GnRH on extrapituitary tissues both *in vivo* and *in vitro* and GnRH has also been shown to have a regulatory effect on tumour cell proliferation (Prevost et al, 1993). The detection of local GnRH production or GnRH-like substances in these areas together with the expression of its receptor suggests that this hormone may have paracrine or autocrine functions. These potential actions, at tissues distal to the pituitary, may be mediated directly through receptor specific interactions or may operate indirectly through the modulation of other hormone systems.

2.13.1 GnRH and GnRH-Rs in the brain

Autoradiographic studies using iodinated GnRH agonists Buserelin (Jennes et al, 1988), [D-Ala^6, Des, Gly^{10}-NHEt]-GnRH (Le Blanc et al, 1988) and [D-Ala^6, N$^{\alpha}$MeLeu^7, Pro^9, Des, Gly^{10}-NHEt]-GnRH] (Reubi et al, 1987) have localised GnRH binding sites to a variety of regions in the rat brain. High affinity GnRH-R binding sites have been identified in rat olfactory regions, frontal cortex (sulcus rhinalis), lateral septum, arcuate nucleus, interpeduncular nucleus, central gray area, superior colliculus, cingulate cortex, amygdala, but the greatest number of receptors is found in the hippocampus. These regions correlate well with the localisation of immunoreactive GnRH (Jennes and Conn, 1994). The brain localisation of the rat GnRH-R mRNA has also been carried out and as expected its distribution closely follows that of the autoradiographic localisation of GnRH-R binding sites (Jennes and Conn, 1994). The only deviation from these dual localisation patterns is in the arcuate nucleus and ventromedial nucleus of the hypothalamus, along with the periventricular nucleus of the thalamus and the medial habenula of the epithalamus. These areas all contain GnRH-R mRNA but show no receptor binding sites. There are also a few areas that bind radiolabelled GnRH analogues but lack GnRH neurons to express the receptor mRNA and these sites include the interpeduncular nucleus and the central periaqueductual gray. In these areas it has been suggested that the receptors are synthesised in another location and then transported to the required destination (Jennes and Conn, 1994).

2.13.2 GnRH and GnRH-Rs in the placenta

GnRH mRNA (Seeburg and Adelman, 1984) and peptide (Tan and Rousseau, 1982) together with GnRH-like peptides have all been identified in human placental tissue. *In vitro* studies using primary placental cultures have shown that GnRH stimulates hCG, αhCG, progesterone and estrogen production (Khodr and Siler-Khodr, 1978) but these responses are largely confined to the mid-term placenta. It has been suggested that these effects are receptor-mediated, as specific GnRH-Rs have been identified and characterised in placental cells using iodinated radiolabelled GnRH analogues. The receptor, unlike its pituitary equivalent, displays a low affinity binding site with a receptor dissociation constant in the μM range (Currie et al, 1981). The physiological significance of GnRH and its receptor in the foetal-placental unit together with any functional regulatory role they may play has yet to be established.

2.13.3 Breast tissue and human breast tumour cells

Bovine and human milk contains an immunological substance similar to GnRH (Amarant et al, 1982). GnRH-like immunoreactive peptides and GnRH mRNA have also been identified in human breast cancer cell lines (Eidne et al, 1985; Harris et al, 1991) but the action of GnRH agonists in these cell lines has yielded contradictory findings. In 1985, Miller et al reported that low doses of Buserelin could inhibit the growth of MCF-7 cells but later studies failed to reproduce these findings. Results from *in vitro* GnRH antagonist experiments have been clearer with the treatment of MCF-7 cells, ZR-75-1 and MDA-MB-231 cell lines with GnRH antagonists resulting in either a decrease of ^{3}[H] thymidine incorporation into DNA or an inhibition of cell growth (Eidne et al, 1987). The presence of both high (Baumann et al, 1993; Fekete et al, 1989; Milovanovic et al, 1992) and low affinity (Eidne et al, 1987; Fekete et al, 1989; Milovanovic et al, 1992) GnRH-R binding sites in a variety of human breast cancer tumour tissue prompts the question of possible autocrine regulation of tumour cell growth. In addition, Kakar and co-workers PCR-amplified a product of comparable size to the GnRH-R from RNA derived from human breast tissue and MCF-7 breast cancer cell lines (Kakar et al, 1992). However, these GnRH-R mRNA transcripts appear to be expressed at very low levels as they could not be detected using Northern Blot analysis.

2.13.4 Ovary

GnRH has been shown to have a wide range of effects on rat ovarian tissue. In both hypophysectomised rats and *in vitro* culture systems, reported effects of GnRH are variable and appear dependent upon: (i) the gonadotrophin environment, (ii) the duration of exposure to GnRH analogues and (iii) the degree of follicular development (Fraser and Eidne, 1989). Acute responses to GnRH result in an increase in ovarian steroidogenesis, induction of meiosis and germinal vesicle breakdown, whilst chronic administration of GnRH has been shown to inhibit ovarian steroidogenesis (Fraser and Eidne, 1989). GnRH-induced cytodifferentiation in immature rat granulosa cells has also been described (Fraser and Eidne, 1989). The direct effects of GnRH on the ovary however vary between species and although distinct effects on rat ovarian physiology have been observed, these effects are less evident in other species. The presence of GnRH-like substances (Aten et al, 1986), a high affinity binding site

(Popkin et al, 1983) and GnRH-R mRNA (Whitelaw et al, 1995) in rat tissue provides additional evidence as to the importance of GnRH signalling in this species.

In human epithelial ovarian cancer tissue and human ovarian cell lines both low and high affinity GnRH-R binding sites have been detected (Emons et al, 1993; Thompson et al, 1991). Although the biological significance of these binding sites is unclear, GnRH analogues have been reported to reduce cell proliferation in a number of ovarian tumour cell lines *in vitro* (Thompson et al, 1991). GnRH has also been shown to cause regression of human ovarian epithelial tumours transplanted into nude mice (Schally et al, 1984).

2.13.5 Prostate

Both GnRH-like peptides (Quyam et al, 1990a) and GnRH-Rs (Quyam et al, 1990b) have been identified in the prostate and prostatic cancer tissue. Once again, GnRH has been implicated in prostatic epithelial cell growth and it has been suggested that the effects of GnRH analogues in these cancers are mediated by specific GnRH tumour receptors.

2.13.6 GnRH and apoptosis

A current theory put forward to explain the presence of GnRH in extrapituitary tissue is its possible involvement in apoptosis. Hormone-sensitive tissue, implicated in apoptosis, has been shown to produce both GnRH (or GnRH-like peptides) along with the GnRH-R. In addition, apoptotic tumour regression has been observed in female mice bearing mammary carcinomas following treatment with GnRH and the GnRH antagonist Cetrorelix (SB-75) (Redding et al, 1992). These effects in animal models may be indirect due to suppression of the pituitary-gonadal axis and may not be a direct result of a receptor mediated process. However, Billing et al (1994) have recently shown that GnRH can directly induce apoptotic death in ovaries from hypophysectomised rats, further suggesting that GnRH may be involved in programmed cell death.

2.14 Summary

This chapter has examined the physiological actions of GnRH, and highlighted its importance as the key regulatory element in mammalian reproduction. The isolation of the GnRH peptide by Burgus and Guillemin in 1971, initiated many investigations into the mechanisms underlying the function of this hypothalamic-releasing hormone. Since the 1970s, a great deal of information has been assimilated and this knowledge, in turn, has been exploited for use in reproductive medicine. GnRH is now widely used in the treatment of a variety of reproductive endocrine conditions/disorders ranging from contraception to hormone-dependent breast and prostate cancer. However, a lot remains unknown especially about the interaction of GnRH with its target pituitary receptor, the GnRH-R.

It was only recently, in 1992, that the GnRH-R cDNA structure was identified and characterised. With the cloning of the receptor, it is now possible to study structure-function relationships within the GnRH-R and identify specific areas important for ligand-receptor interactions. Such investigations will aid in further understanding the molecular mechanisms governing the action of GnRH at the pituitary. Moreover, this information can be used in rational design of novel GnRH analogues.

This study has utilised a technique known as site-directed mutagenesis. Using this procedure, the receptor cDNA sequence can be altered, and the properties of genetically engineered 'mutant' receptors analysed. This approach therefore allows the comparison of wild-type receptor properties (receptor binding function, receptor expression and second messenger coupling) with those of the mutant receptors. Moreover, alterations in the normal receptor function, displayed by receptor mutants, provides important information about possible structure-function relationships. For example, if a mutant receptor shows a decrease in ligand-receptor binding, then this implies that the normally positioned amino acid is an important mediator of receptor function. In this way, the properties of the mutant receptors can be related back to the function of the receptor residues initially altered to create the mutation. With this strategy, the role of specifically targeted amino acids in the rat GnRH-R, isolated and characterised by Eidne et al (1992) have been investigated. The methodology utilised to generate mutant GnRH-Rs and analyse their functional properties is described in the following chapter.

3 Materials and methods

3.1 Introduction

The techniques described in this chapter include general molecular biology techniques and specific methods used to (i) generate point mutations in receptor DNA, (ii) express these 'mutant' constructs in eukaryotic cells, (iii) monitor ensuing RNA transcription levels and (iv) assess the functional properties of the translated mutant proteins.

Site-directed mutagenesis is commonly used to examine structure-function relationships in DNA and its encoded proteins. This technique allows small alterations to be introduced in the wild-type receptor (TRH-R/GnRH-R) cDNA and thus into its translated protein. Following mutagenesis, the receptor cDNA was expressed in a mammalian cell culture system using either a transient or stable expression system. In the transient method, the cDNA is localised in the cytoplasm and expressed episomally for 48-72 hours post transfection, whereas in the stable expression system the cDNA is incorporated into the cell genome. Stable transfection systems have the advantage that DNA expression is maintained as the cell divides. The functional properties of the receptor mutants were subsequently analysed and compared to the wild-type receptor. The effects of receptor mutants on RNA transcription levels were monitored using Northern Blot analysis. The ligand binding and second messenger activational properties of the mutant receptors were assessed using receptor binding assays and ligand-stimulated total inositol phosphate measurements respectively.

A detailed list of buffers and chemical suppliers is included in Appendix I and Appendix II respectively and additional methodology is detailed in Appendix III.

3.2 DNA preparation and purification

3.2.1 Plasmid DNA preparation

A single bacterial colony was used to inoculate 10ml of LB broth containing antibiotics. The *E.Coli* culture was grown overnight with shaking at 37°C and the DNA extracted using a Promega Wizard™ Mini-prep DNA purification system as follows. Bacterial cells were pelleted by centrifugation at 12000 rpm for 5 minutes, resuspended, lysed and neutralised with 300µl of resuspension, lysis and neutralisation solutions respectively. Following further centrifugation at 12000 rpm for 5 minutes, the clear supernatant was removed, divided into 2x 0.4ml aliquots and 0.5ml of Mini-prep DNA purification resin added to each tube. The DNA/resin mixture was then incubated at room temperature for 5 minutes and subsequently filtered through Miniprep columns using a vacuum manifold. Finally, the columns were washed with ethanol, dried, and the DNA eluted with 100µl of TE buffer by centrifugation at 12000 rpm for 1 minute. Approximately 30µg of plasmid DNA was obtained from a 10ml *E.Coli* bacterial culture. Larger scale plasmid DNA preparations were carried out using a Promega Wizard™ Maxi-prep kit. Using this procedure, a 10ml *E. Coli* starter culture was used to inoculate 300ml of antibiotic-containing LB broth and the DNA extracted using a similar but scaled up version of the Mini-prep procedure described above. Approximately 600µg of DNA was obtained using this method.

3.2.2 Agarose gel electrophoresis

Agarose gel electrophoresis is a method of separating, identifying and purifying DNA fragments. A 0.9% agarose gel (Boehringer Mannheim) was routinely used to analyse DNA samples, as this gives high resolution of DNA fragments between 500 bp and 7 kb. The agarose was melted in 1xTBE buffer, 0.3µg/ml ethidium bromide added and when hand hot, the gel was cast into a casting tray and allowed to set. Meantime, samples containing 50ng to 1µg of DNA were prepared in sterile water, electrophoresis loading dye added, to approximately 10% of the total volume, and the samples loaded into the wells. In addition, DNA markers, HindIII/EcoR1 and pGEM (Promega), were prepared and run alongside the samples so as to ascertain the size of the DNA fragments. The gel was run in 1xTBE buffer at a constant voltage of 50V for several hours until the dye front reached the bottom of the gel.

DNA visualisation was carried out under ultra violet (u/v) light using a u/v transluminator (Vilber Lourmat).

Low melting point agarose (Sea Plaque agarose, Flowgen) gels were used to extract DNA samples for further purification. This method is similar to the protocol described above except that the 1% low melting point agarose gels were set and run at 4°C. In addition, to prevent any damage to the DNA, ethidium bromide staining occurred following electrophoresis. The DNA fragments were then viewed under u/v light, the position of the required fragment(s) ascertained and the correct DNA bands excised with a scalpel blade for further purification.

3.2.3 Phenol/chloroform DNA purification

Phenol/chloroform extraction separates nucleic acids from proteins, and is a widely used technique for the removal/inactivation of enzymes or the purification of DNA from agarose gels. The excised agarose fragment was melted at 65°C in 5 volumes of 20mM Tris-HCl pH 8.0. An equal volume of TE-saturated phenol was added and the sample vortexed for 1 minute followed by centrifugation at 10000 rpm for 5 minutes. The upper aqueous phase was removed into a separate tube and the vortexing and centrifugation procedure repeated, first with an equal volume of phenol/chloroform and finally with an equal volume of chloroform. The DNA was extracted from the chloroform phase using a salt/ethanol precipitation method.

3.2.4 DNA/ RNA salt and ethanol precipitation methods

Nucleic acids were concentrated by precipitation, with ethanol, in the presence of monovalent cations. Ammonium acetate (10M) or sodium acetate (3M, pH 5.4) was added to a final concentration of 2.5M or 0.3M respectively, together with 3 volumes of 100% ethanol. The samples were precipitated at -70°C for 30 minutes and centrifuged at 12000 rpm for 20 minutes at 4°C. The liquid was then removed, the DNA pellet washed in 75% ethanol and resuspended in TE buffer/water.

3.2.5 Sphectrophotometric DNA/RNA quantitation

The concentration of a 1:200 dilution of a DNA/RNA preparation was determined by measuring the optical density (OD) at 260 nm and 280 nm in a Kontron Analytical spectrophotometer. An OD 260 reading equivalent to one corresponds to 50µg/ml for double-stranded DNA, 40µg/ml for either single-stranded DNA or RNA and 20µg/ml for single-stranded oligonucleotides. An OD 260:280 ratio of 1.8 for DNA and 2.0 for RNA indicates good sample purity.

3.2.6 Restriction enzyme digestion

Restriction digests were used to release cDNA receptor inserts from plasmids or to linearise circular plasmid DNA. Restriction enzymes (Boehringer Mannheim) bind to, and cleave, specific sequences in double-stranded DNA; for example, EcoR1 (a commonly used enzyme) recognises the five nucleotide sequence G/AATTC. 1-5µg of purified DNA was digested with 10 units of restriction enzyme, in 1x enzyme buffer at 37°C for 1 hour, and the digestion products subsequently analysed by gel electrophoresis.

3.3 Site-directed mutagenesis

3.3.1 General methodology

DNA mutations were introduced in the GnRH-R and TRH-R using a method adapted from Kunkel (Kunkel, 1987) and performed using a Muta-Gene™ phagemid *in vitro* mutagenesis kit (Bio-Rad). The gene of interest was cloned into a eukaryotic expression vector and the DNA replicated within a *dut*, *ung* double mutant *E. Coli* bacterium. The *dut* mutation inactivates dUTPase whereas the *ung* mutation inactivates the enzyme uracil-N-glycosylase. Together these mutations result in the incorporation of uracils into the DNA. This 'parental' DNA strand was then used as a template to anneal an oligonucleotide with the desired mutation. A complementary non-uracil containing DNA strand, identical except that it carried the mutation, was subsequently synthesised. The double-stranded DNA construct was transformed into cells containing an efficient uracil-N-glycosylase enzyme system and this resulted in the inactivation of the parental DNA strand, thus permitting only

the DNA strand carrying the mutation to replicate. The basic principle of this specific site-directed mutagenesis protocol is summarised in Figure 3.1

3.3.2 Isolation of receptor cDNA

The rat TRH-R, a 3.3 kb clone, was isolated from a rat anterior pituitary cDNA library (lamba Zap) and cloned into the EcoR1 polylinker site in the eukaryotic expression vector pcDNA 1(Sellar et al, 1993). The rat GnRH-R, a 2.2 kb clone, isolated from the same library, was also cloned into pcDNA 1 as well as into another eukaryotic expression vector pcDNA 3, again at the EcoR1 polylinker site (Eidne et al, 1992).

3.3.3 Eukaryotic expression vectors

The plasmid pcDNA 1 (Invitrogen) is a 4.0 kb vector derived from pCDM8. The vector contains a CMV promoter and enhancer, splice segments and a polyadenylation signal, together with SV40 and polyoma virus eukaryotic origins of replication. It also includes an M13 origin for the rescue of single-stranded DNA, essential for this mutagenesis protocol, SP6 and T7 promoters for the production of sense/antisense RNA transcripts and an phiVX (ColE1 like) high copy plasmid origin. The presence of the Sup F gene confers ampicillin (Amp) and tetracycline (Tet) resistance in the *E.Coli* strain MC1061/P3.

The plasmid pcDNA 3 (Invitrogen) is a 5.4 kb vector derived from pRc/CMV. The vector contains a CMV promoter and enhancer, SV40 origin for transient episomal replication of cells expressing the SV40 large T antigen, and a bovine growth hormone polyadenylation signal. It also contains an f1 origin for the rescue of single-stranded DNA, T7 and SP6 promoters for the production of sense/antisense RNA transcripts, and a ColE1(from pUC 19) high copy number origin. The β-lactamase gene confers Amp resistance in the *E.Coli* strain TOP 10F'. In addition, this vector has the advantage of a neomycin resistance marker, expressed from the SV40 early promoter, for the selection of stable transformants in the presence of G418.

3.3.4 *E.Coli* bacterial strains (Table 3.1)

MC1061/P3 is a bacterial strain designed to support the replication of plasmid DNA encoding the tyrosine tRNA suppressor (Synthetic Sup F gene). The P3 plasmid carries kanamycin (Kan), Amp and Tet drug resistance markers but these genes are inactivated, during normal bacterial growth, by the presence of amber mutations carried on the P3 plasmid. Tet and Amp resistance properties are, however, restored upon the introduction of pcDNA 1 plasmids carrying the Sup F gene.

TOP 10F' is a recombinant negative strain for stable replication of high copy number plasmids. It carries the F' episome which is required for pili formation and thus for single-stranded DNA rescue by helper phage superinfection. The F' episome carries the Tet resistance gene marker and cells can therefore be selected with this antibiotic.

CJ263/P3 is a strain used for uracil incorporation. The *dut* and *ung* phenotypes result in the occasional substitution of thymidine by uracil. This strain carries the F' episome and therefore can be used for the isolation of single-stranded DNA. It also contains the P3 gene.

CJ263 has the same features as CJ263/P3 except that it does not contain the P3 gene.

Figure 3.1 Site-directed mutagenesis method (following page)

The rat GnRH-R and TRH-R were electroporated into a *dut ung E. Coli* bacterial strain and this resulted in the incorporation of uracils into the DNA. A mutagenic oligonucleotide was designed and annealed to this uracil-containing template, with the complementary strand generated incorporating the desired mutation. The double-stranded DNA construct was transformed into cells containing an efficient uracil-N-glycosylase enzyme system which resulted in the inactivation of the parental DNA strand, permitting only the DNA strand carrying the mutation to replicate.

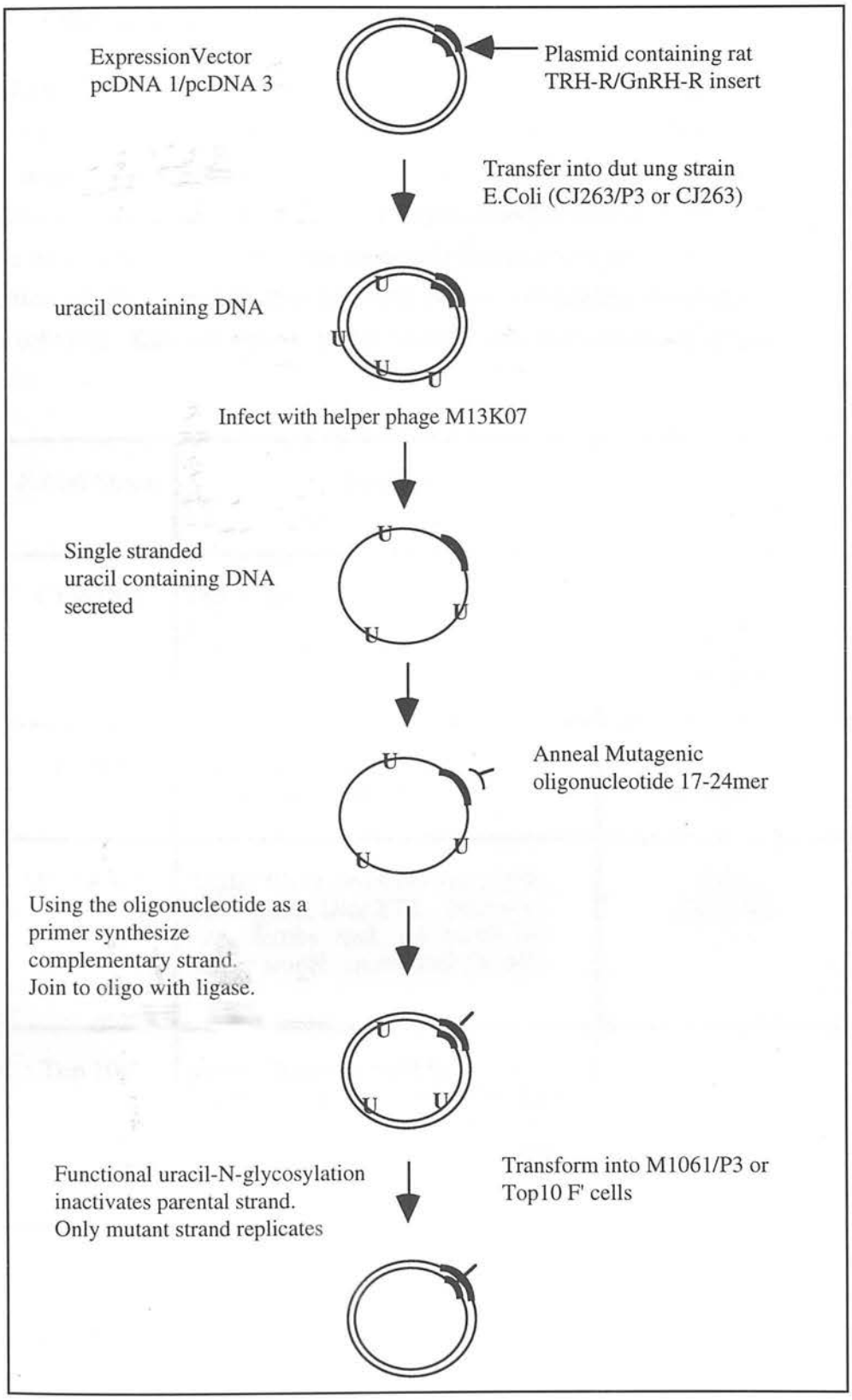
ExpressionVector
pcDNA 1/pcDNA 3
Plasmid containing rat
TRH-R/GnRH-R insert
Transfer into dut ung strain
E.Coli (CJ263/P3 or CJ263)
uracil containing DNA
U
Infect with helper phage M13K07
Single stranded
uracil containing DNA
secreted
Anneal Mutagenic
oligonucleotide 17-24mer
Using the oligonucleotide as a
primer synthesize
complementary strand.
Join to oligo with ligase.
Functional uracil-N-glycosylation
inactivates parental strand.
Only mutant strand replicates
Transform into M1061/P3 or
Top10 F' cells

3.3.5 Helper phage

M13KO7 (Invitrogen) is a single-stranded interference resistance helper phage carrying the mutant gene II. Phage infection of plasmids containing either an f1 or M13 origin (for the rescue of single-stranded DNA) results in the preferential replication, packaging and extrusion of single-stranded plasmid DNA. M13KO7 had a titre of $2.6x10^{10}$ plaque forming units (pfu)/ml and was added at a multiplicity of infection of 20:1 (phage:cells) to a cell culture containing $1x10^{8}$ colony forming units (cfu)/ml. Kan was used to select for cells infected with helper phage.

E.Coli Strain	Genotype	Antibiotic LB agar/broth
CJ263/P3	Dut-1, ung-1, th/-1, relA-1, deoR+, pCJ105(camR, F'), {p3: amber ampR, amber tet R, KmR}	Chl 15/30µg/ml Kan 70µg/ml
CJ263	Dut-1, ung-1, th/-1, rel A1/pCJ105(cmR), F'	Chl 15/30µg/ml
MC1061/P3	AraD139, D (araABC-leu), 7696, galU, galK, DlacX74, (rk,m+k), strA, deoR+, rpsL, thi, mcrB,{p3: amber ampR, amber tetR, KmR}	Kan 70µg/ml
Top 10F'	mcrA, D(mrr-hsddRMS-mcrBC), F'800DlacZDM15, DlacX74, deoR, recA1, ara D 139, D(ara,leu). 7697, galU, galK, I-, rpsL, endA1, nupG, F'	Tet 15µg/ml

Table 3.1 ***E.Coli*** **bacterial strains used in the site-directed mutagenesis procedure**

E.Coli cell stains (Invitrogen), CJ263/P3 and MC1061/P3 were used in the site-directed mutagenesis procedure to construct mutant receptors expressed in the eukaryotic expression vector pcDNA 1. CJ263 and Top10F' cells were used to generate mutant receptors in pcDNA3. The individual cell genotypes and their corresponding antibiotic growing conditions are also highlighted.

3.3.6 Preparation of uracil containing template

CJ263 cells were streaked onto LB agar plates containing 30μg/ml chloramphenicol (Chl) and single colonies selected for further use. In contrast, CJ263/P3 cells were streaked onto LB agar plates containing 30μg/ml Chl and 70μg/ml Kan, then single colonies were picked and subsequently replated on separate plates containing either 15μg/ml Tet, 50μg/ml Amp or 30μg/ml Chl plus 70μg/ml Kan. Only colonies that grew on the Chl plus Kan plates were picked for further use. Individual colonies were subsequently grown in an appropriate antibiotic environment and electrocompetent cells prepared as follows. Cells in mid-log phase (200ml) were chilled on ice, pelleted by centrifugation at 4000 rpm for 5 minutes, washed twice with ice cold sterile water and twice with ice cold 10% glycerol. Following production of the final pellet, 400μl of ice cold 10% glycerol was added to yield approximately 1.1ml of electrocompetent cells. These cells were stored in 100μl aliquots at -70°C. Electrocompetent CJ263P3/CJ263 cells (40μl) were electroporated, using a Gene Pulser™ (Bio-Rad), with 2μl of DNA and incubated in SOC media, containing Chl, Amp and Tet, for 45 minutes to allow antibiotic resistance to develop. The transformed cells were plated onto LB agar plates, containing appropriate antibiotics, incubated overnight at 37°C and single colonies picked. The DNA plasmids were then extracted and the presence of inserts checked by EcoR1 restriction digests.

3.3.7 Single-stranded DNA preparation

Selected colonies were grown in 2xYT broth, containing appropriate concentrations of Chl, Amp and Tet, for 4 hours until an OD reading (at 600 nm) of 0.3 was reached. M13KO7 helper phage was added, the incubation continued for 1 hour prior to the addition of Kan (70μg/ml) and then continued overnight. The *E Coli* cells were pelleted by centrifugation and the supernatant treated with 10μg/ml RNase and 10μg/ml DNase at 37°C for 10 minutes. One quarter of the total volume of 3.5M ammonium acetate/20% polyethylene glycol was added, the solution precipitated on ice for 10 minutes, and the DNA repelleted by centrifugation at 12000 rpm for 20 minutes. The DNA was resuspended in TE buffer and purified using a phenol/chloroform extracted method. The single-stranded uracil-containing DNA was then used as a template to anneal mutagenic oligonucleotides.

3.3.8 Oligonucleotide design

Mutagenic oligonucleotides, complementary to the receptor DNA except containing internal base mismatches, were designed to the targeted area of the receptor (Table 3.2 and 3.3) and synthesised on an Applied Biosystems PCR Mate synthesiser. The oligonucleotides were deprotected in 1ml of ammonia solution at 55°C overnight, purified by salt/ethanol precipitation, and subsequently phosphorylated using T4 polynucleotide kinase. These phosphorylated oligos were then annealed to a uracil-containing template in a 25:1 primer to template ratio. A complementary strand of DNA was synthesised from dNTPs using T7 DNA polymerase and the ends of this de novo DNA strand ligated together with T4 DNA ligase.

Mutation	TRH-R Wild-Type/mutagenic DNA sequence	TRH-R Wild-Type/mutagenic protein sequence	Nucleotide length/ position
Cys98Ser	ATGTTGGC**T**GCCTCTGC ATGTTGGC**A**GCCTCTGC	Val-Gly-**Cys**-Leu-Cys Val-Gly-**Ser**-Leu-Cys	17 284-300
Cys179Ser	TGATATCC**T**GTGGCTAC TGATATCC**A**GTGGCTAC	Ile-Ser-**Cys**-Gly-Tyr Ile-Ser-**Ser**-Gly-Tyr	17 527-543
Cys100Ser	GCTGCCTC**T**GCATCACG GCTGCCTC**A**GCATCACG	Cys-Leu-**Cys**-Ile-Thr Cys-Leu-**Ser**-Leu-Thr	17 290-306
Cys98Ala	TGTTGGC**TG**CCTCTGCA TGTTGGC**GC**CCTCTGCA	Val-Gly-**Cys**-Leu-Cys Val-Gly-**Ala**-Leu-Cys	17 285-301
Cys179Ala	GATATCC**TG**TGGCTACAA GATATCC**GC**TGGCTACAA	Ile-Ser-**Cys**-Gly-Tyr Ile-Ser-**Ala**-Gly-Tyr	18 528-545
Cys100Ala	CTGCCTC**TG**CATCACGT CTGCCTC**GC**CATCACGT	Cys-Leu-**Cys**-Ile-Thr Cys-Leu-**Ala**-Leu-Thr	17 291-307

Table 3.2 TRH-R mutant constructs

Oligo-directed mutagenesis of the rat TRH-R showing the location of the mutation(s) in the DNA and amino acid sequence. The design and length of the oligonucleotides are also highlighted. These mutations were generated in the eukaryotic expression vector pcDNA 1.

Table 3.3 GnRH-R mutant constructs (following page)

Oligo-directed mutagenesis of the rat GnRH-R showing the location of the mutation(s) in the DNA and amino acid sequence. The design and length of the oligonucleotides are also highlighted. These mutations were generated in the expression vector pcDNA 3 with the exception of mutations highlighted (*) which were made in pcDNA 1. Mutations created in both expression vectors are indicated (•).

Mutation	GnRH-R Wild-Type/mutagenic DNA sequence	GnRH-R Wild-Type/mutagenic protein sequence	Nucleotide position
Cys14Ser	AAAATCAC**T**GCTCAGCC	Asn-His-**Cys**-Ser-Ala	17
*	AAAATCAC**A**GCTCAGCC	Asn-His-**Ser**-Ser-Ala	32-48
Cys114Ser	AGTTCCTT**T**GCAAAGTT	Phe-Leu-**Cys**-Lys-Val	17
*	AGTTCCTT**A**GCAAAGTT	Phe-Leu-**Ser**-Lys-Val	332-348
Cys195Ser	TCTCGCAA**T**GTGTGACC	Ser-Gln-**Cys**-Val-Thr	17
*	TCTCGCAA**A**GTGTGACC	Ser-Gln-**Ser**-Val-Thr	575-591
Cys199Ser	TGACCCAC**T**GCAGCTTT	Thr-His-**Cys**-Ser-Phe	17
*	TGACCCAC**A**GCAGCTTT	Thr-His-**Ser**-Ser-Phe	587-603
Asn87Asp	ACCTTAGCC**A**ACCTCCTTG	Thr-Leu-Ala-**Asn**-Leu-Leu	19
•	ACCTTAGCC**G**ACCTCCTTG	Thr-Leu-Ala-**Asp**-Leu-Leu	250-268
Asp318Asn	CCGTGCTTC**G**ACCCACTT	Thr-Leu-Ala-**Asn**-Leu-Leu	18
	CCGTGCTTC**A**ACCCACTT	Thr-Leu-Ala-**Asp**-Leu-Leu	943-960
Asn87Asp	ACCTTAGCC**A**ACCTCCTTG	Thr-Leu-Ala-**Asn**-Leu-Leu	18
Asp318Asn	ACCTTAGCC**G**ACCTCCTTG	Thr-Leu-Ala-**Asp**-Leu-Leu	943-960
•	CCGTGCTTC**G**ACCCACTT	Thr-Leu-Ala-**Asn**-Leu-Leu	
	CCGTGCTTC**A**ACCCACTT	Thr-Leu-Ala-**Asp**-Leu-Leu	
Glu90Gln	ACCTCCTT**G**AGACTCTA	Leu-Leu-**Glu**-Thr-Leu	17
	ACCTCCTT**C**AGACTCTA	Leu-Leu-**Gln**-Thr-Leu	260-276
Lys115Arg	CCTTTGCA**A**AGTTCTCA	Leu-Cys-**Lys**-Val-Leu	17
	CCTTTGCA**G**AGTTCTCA	Leu-Cys-**Arg**-Val-Leu	336-352
Lys121Arg	CTATCTGA**A**GCTCTTCT	Tyr-Leu-**Lys**-Phe-Ser	17
	CTATCTGA**G**GCTCTTCT	Tyr-Leu-**Arg**-Phe-Ser	354-370
Gln174Glu	CGGGACCA**C**AGTTATAT	Gly-Pro-**Gln**-Leu-Tyr	17
	CGGGACCA**G**AGTTATAT	Gly-Pro-**Glu**-Leu-Tyr	512-528
Asn211Asp	CCTTCTAC**A**ACTTTTTC	Phe-Tyr-**Asn**-Phe-Phe	17
	CCTTCTAC**G**ACTTTTTC	Phe-Tyr-**Asp**-Phe-Phe	623-639
Asn304Asp	AGCCAGTC**A**ATCACTTC	Pro-Val-**Asn**-His-Phe	17
	AGCCAGTC**G**ATCACTTC	Pro-Val-**Asp**-His-Phe	902-918
His305Arg	AGTCAATC**A**CTTGTTGT	Val-Asn-**His**-Phe-Phe	17
	AGTCAATC**G**CTTCTTCT	Val-Asn-**Arg**-Phe-Phe	906-922
Asn314Asp	GGTTTCTA**A**ACCCGTGC	Phe-Leu-**Asn**-Pro-Cys	17
	GGTTTCTA**G**ACCCGTGC	Phe-Leu-**Asp**-Pro-Cys	932-948
Phe312Tyr	TCTTTGGTT**T**TCTAAAC	Phe-Gly-**Phe**-Leu-Asn	17
	TCTTTGGTT**A**TCTAAAC	Phe-Gly-**Tyr**-Leu-Asn	926-939
Phe312Ala	TCTTTGGT**TT**TCTAAAC	Phe-Gly-**Phe**-Leu-Asn	17
	TCTTTGGT**GC**TCTAAAC	Phe-Gly-**Ala**-Leu-Asn	926-942
Phe312Arg	TCTTTGGT**TT**TCTAAAC	Phe-Gly-**Phe**-Leu-Asn	17
	TCTTTGGT**CG**TCTAAAC	Phe-Gly-**Arg**-Leu-Asn	926-942
Leu83Val	TTAAAGCAT**T**TGACCTTAGCC	Leu-Lys-His-**Leu**-Thr-Leu-Ala-Asn	21
	TTAAAGCAT**G**TGACCTTAGCC	Leu-Lys-His-**Val**-Thr-Leu-Ala-Asn	238-258
Leu83Ala	TTAAAGCAT**TT**GACCTTAGCC	Leu-Lys-His-**Leu**-Thr-Leu-Ala-Asn	21
	TTAAAGCAT**GC**GACCTTAGCC	Leu-Lys-His-**Ala**-Thr-Leu-Ala-Asn	238-258
Leu83Arg	TTAAAGCAT**TT**GACCTTAGCC	Leu-Lys-His-**Leu**-Thr-Leu-Ala-Asn	21
	TTAAAGCAT**AA**GACCTTAGCC	Leu-Lys-His-**Lys**-Thr-Leu-Ala-Asn	238-258

3.4 Tissue Culture Procedures

3.4.1 Cell lines and reagents

Tissue culture reagents were purchased from Gibco BRL and Advanced Protein Products Ltd. COS-1 cells (Monkey kidney, SV40 transformed fibroblasts) and HEK-293 cells (Human embryonic kidney epithelial cells) were obtained from the American Type Culture Collection and αT3-1 cells (immortalised anterior pituitary cells of gonadotroph lineage) were a gift from Dr. Pamela Mellon (The Salk Institute, La Jolla, CA, USA). Cells were routinely maintained and passaged in complete Dulbecco's modified Eagle's medium (DMEM), containing 10% (v/v) heat inactivated foetal calf serum (HIFCS), glutamine (0.3mg/ml), penicillin (100IU/ml) and streptomycin (100μg/ml), and incubated at 37°C in a humidified atmosphere of 5% (v/v) $C0_2$ in air. COS-1 cells were used for the transient tranfection procedures and HEK-293 cells for the generation of stably expressing rat GnRH-R WT or mutant cell lines.

3.5 Transfection Procedures

3.5.1 Liposome-mediated transfections

Liposome-mediated transient transfection protocols using lipofectin™ (Gibco BRL), N-[1-(2,3-dioleyloxy) propyl]-N, N, N-trimethylammonium chloride (DOTMA)/dioleoyl phosphatidylethanolamine (DOPE) and Transfectam™ (Promega), a synthetic lipopolyamine, are described below. Both these compounds have a high affinity for DNA, forming an outer cationic lipid layer to facilitate DNA entry into the cell.

3.5.2 Preparation of cells for transfection

COS-1 cells in 175cm^2 flasks were trypsinised with 0.5% Trypsin-EDTA solution and plated into 60mm/100mm culture dishes at concentrations of 0.5/2x10^6 cells per dish.

3.5.3 Lipofectin™

DNA (12µg) was diluted into 50µl of sterile water, mixed gently with 50µl of lipofectin and incubated for 15 minutes at room temperature. 100mm culture dishes, approximately 80% confluent, were washed twice with DMEM and the lipofectin/DNA mixture added dropwise to dishes containing 3ml of media. The plates were gently swirled and incubated for 16 hours overnight. The following day the transfection solution was removed and replaced with complete DMEM media.

3.5.4 Transfectam™

60mm culture dishes, approximately 60% confluent, were washed twice with DMEM. DNA (3µg) was diluted in 0.5ml DMEM, combined with 10µl of transfectam in 0.5ml DMEM and pipetted dropwise into dishes containing 0.5ml media. The plates were incubated for 6 hours, washed and replaced with complete DMEM media.

3.5.5 β-galactosidase transfections

To monitor the efficiency of the transfection procedure, COS-1 cells were transfected with 3µg of pSV-β galactosidase control vector (Promega) using 10µl of transfectam per 60mm culture plate, and stained *in-situ* for β-galactosidase activity 72 hours later. The cells were washed twice in PBS, fixed with 2ml of 0.25% glutaraldehyde solution and incubated at 37°C for 15 minutes. This solution was removed by washing with PBS, followed by the addition of 1ml of X-gal (5-bromo-4-chlor-3-indolyl-β-D-galactopyranoside) β-galactosidase substrate. The incubation was continued for a further 4-6 hours, with cells expressing the β-galactosidase enzyme appearing blue under an Olympus CK2 inverted microscope. Figure 3.2 highlights the number of COS-1 cells incorporating the pSV-β galactosidase control vector.

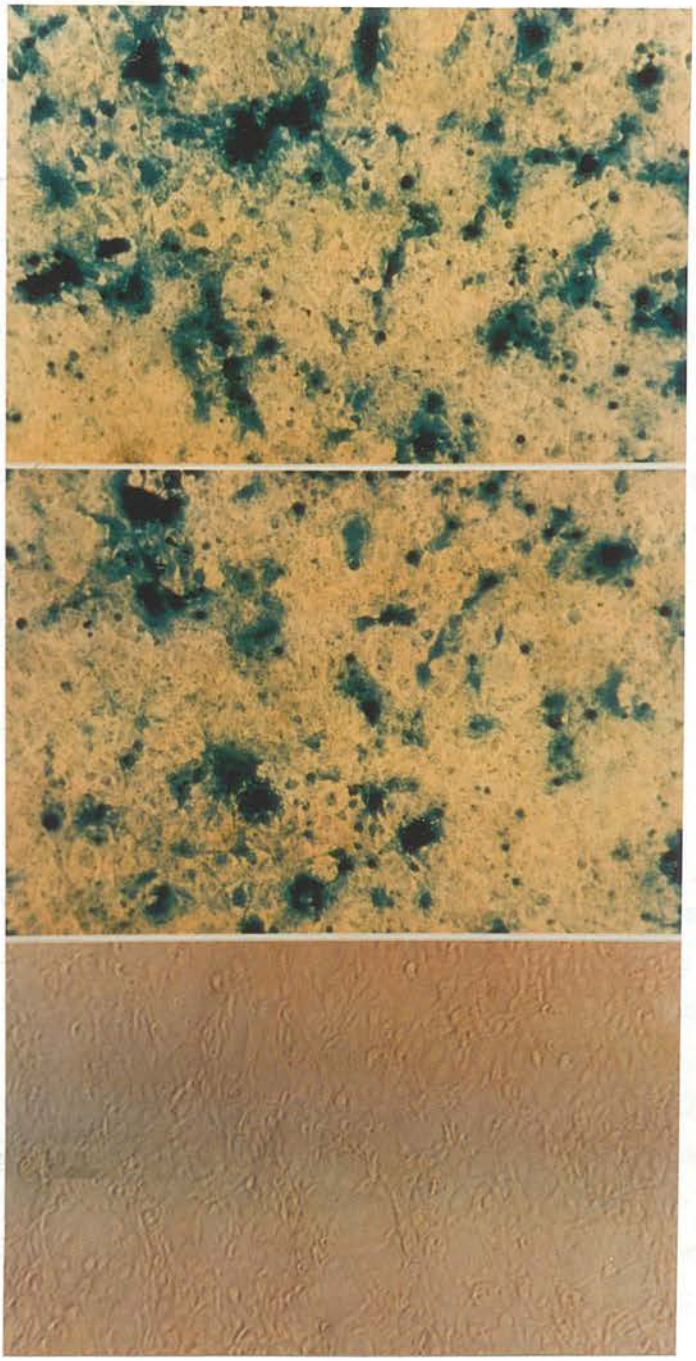

Figure 3.2 **Photomicrographs of β-galactosidase transfections using Transfectam reagent**
COS-1 cells transiently transfected with (a) 3μg of control pSV-β galactosidase vector (b) 3μg of control pSV-β galactosidase vector + 3μg GnRH-R (pcDNA 3) and (c) sham untransfected COS-1 cells. The uptake of DNA is represented by the blue coloration and approximately 25-35% of the cells incorporate and express the transfected DNA.

3.5.6 Stable transfection procedure

Stable cell lines of the rat GnRH-R WT and mutants were generated in HEK-293 cells. The receptor DNA (600ng) was linearised using the Not 1 restriction enzyme (Boehringer Mannheim) and transfected in HEK-293 cells, plated into 6 well dishes, (Falcon) using 30µl of lipofectin. Once the cells were approximately 90% confluent, they were trypsinised and transferred first into 75cm^2 flasks (Costar) and subsequently into 175cm^2 flasks. The pcDNA 3 expression vector contains a neomycin resistance gene marker and thus cells incorporating DNA, expressed in this vector, were selected through antibiotic resistance. When cells in the 175cm^2 flasks were 50% confluent, Geneticin G418 sulphate (Gibco BRL) was added at a concentration of 1mg/ml. Individual receptor-expressing clones were isolated, expanded from single cell colonies and maintained in complete DMEM media containing 800ng/ml G418.

3.6 Northern Blot Analysis

3.6.1 Isolation of total RNA from mammalian cells

Total RNA was extracted from confluent 2x 60mm cell culture dishes using TRI reagent (Molecular Research Centre). Cells were initially lysed with 6ml of TRI reagent and left for 5 minutes at room temperature to allow nuclear protein dissociation. Lysed cells were then mixed vigorously with 1.2ml chloroform, incubated at room temperature for 15 minutes, centrifuged at 12000 rpm for a further 15 minutes at 4°C and the RNA-containing upper aqueous phase removed. RNA was precipitated with 4ml of isopropanol for 30 minutes at -70°C, again pelleted by centrifugation at 12000 rpm for 15 minutes at 4°C, washed with 75% ethanol, and resuspended in DEPC treated water. Approximately 2-6µg/µl of total RNA was obtained from 2x 60mM dishes using this method.

3.6.2 Analysis of RNA by formaldehyde gel electrophoresis

A 1.5% agarose gel was prepared by dissolving agarose in H_20, cooling to 60°C, and then adding 5xformaldehyde gel running buffer (RB), together with formaldehyde to final concentrations of 1x and 2.2M respectively. The gel was cast in a chemical fume hood and allowed to set for 30 minutes. Meantime, the samples were prepared by adding 10µl formamide, 3.5µl of a 37% formaldehyde solution and 5xRB to

15µg of RNA. The mixture was then denatured by heating at 65°C for 10 minutes. Following sample cooling, on ice, 8µl of sample loading buffer was added and the samples loaded onto the gel. The gel was run in 1x RB, at a low voltage of 50 V overnight, and stained with ethidium bromide. The position of the 18S and 28S RNA bands were noted and the RNA blotted onto a Hybond-N (Amersham) nylon membrane as described in section 3.6.3.

3.6.3 RNA transfer to nylon membrane

The apparatus is depicted in Figure 3.3. Two pieces of 3mm Whatman filter paper were cut, soaked in 20xSSC, and laid over a glass plate raised on rubber bungs. The gel was placed on top of the wicks and the air bubbles removed with a glass rod. Hybond-N nylon membrane (Amersham), cut to size, was placed over the gel, autoradiographic film inserted beneath the sides, to ensure buffer transfer through the gel, and 4 pieces of filter paper positioned on top. Paper towels and a heavy weight were finally placed over the filter paper and the blot left overnight. After RNA transfer, the positions of the wells were marked with a needle, the RNA fixed by u/v cross linking, and the blot stored at 4°C until hybridisation.

3.6.4 Preparation of radiolabelled probes

Plasmid GnRH-R and TRH-R cDNA was digested with EcoR1 restriction enzyme, to release a 2.2 kb and a 3.3 kb DNA insert respectively. The inserts were separated from the plasmids on a low melting point gel, excised, placed in eppendorf tubes with 5 volumes of 20mM Tris pH 8.0/1mM EDTA and melted by heating at 65°C for 5 minutes. When cool, an equal volume of TE-saturated phenol was added to the tubes, they were vortexed for 2 minutes, and then centrifuged at 10000 rpm for 1 minute. The clear supernatant was removed and transferred to a fresh tube, where an equal volume of phenol/chloroform was added and the tubes vortexed, centrifuged and the supernatant extracted. Finally, an equal volume of chloroform was added and following vortexing and centrifugation, the supernatant was collected and precipitated with 0.2 volumes of 10M ammonium acetate and 2 volumes of 100% ethanol at -70°C for 30 minutes. The purified DNA was pelleted by centrifugation at 12000 rpm for 20 minutes and resuspended in TE buffer.

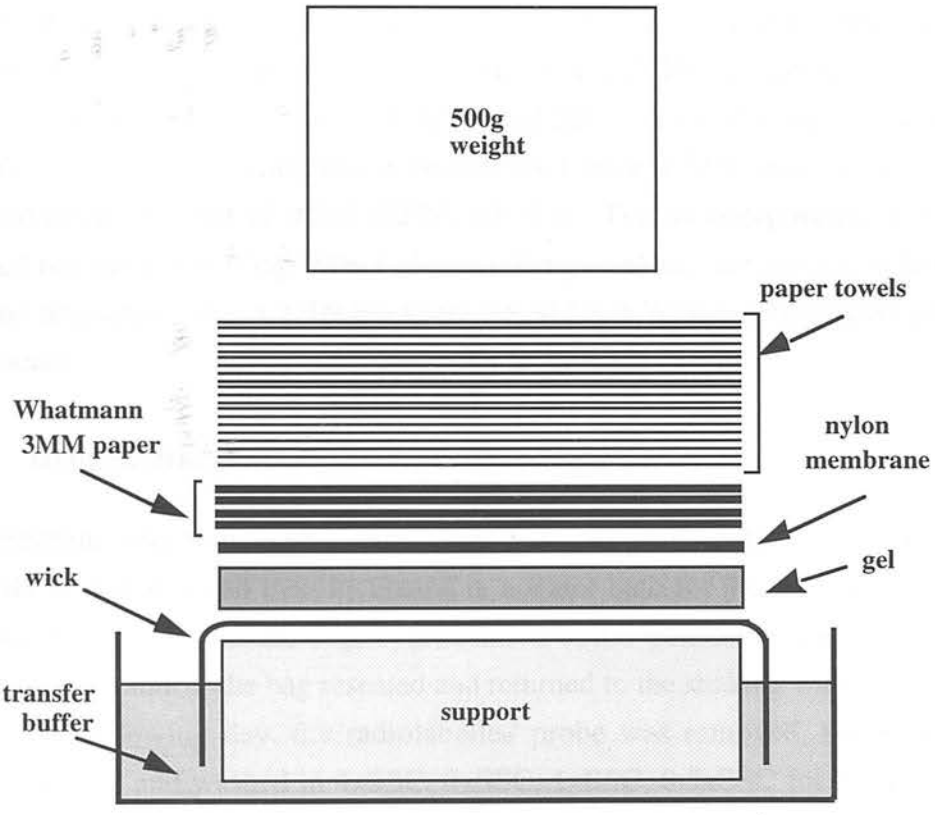

Figure 3.3 Northern Blot apparatus

Capillary transfer of RNA from agarose/formaldehyde gel to a nylon membrane. Transfer buffer is drawn from the reservoir through the gel, via the wick, and into a stack of paper towels. The RNA is eluted from the gel by the moving stream of buffer and is deposited onto the nylon membrane. The weight applied to the top of the paper towels ensures a tight connection between the layers of material used in the transfer system.

The purified cDNA insert was labelled with [α^{32}P]dCTP (Amersham) by the random primer method (Feinburg and Vogelstein, 1983; Feinburg and Vogelstein, 1984), using a random primer DNA labelling kit (Boehringer Mannheim). DNA (100ng) was denatured by boiling for 5 minutes and placed on ice to prevent renaturation. Label mix containing 1µl of dGTP, dATP, dCTP and dTTP was added to the DNA together with 50µCi of radiolabelled dCTP and 2µl of Klenow enzyme (in a total volume of 20µl). The reaction was incubated for 1 hour at 37°C and finally stopped by the addition of 0.5µl of 0.5M EDTA, pH 8.0. The unincorporated label was separated out using a NuTrap Push Column (Stratagene) and the specific activity of the probe measured using a 1209 Rackbeta liquid LKB Wallac scintillation counter (Pharmacia).

3.6.5 Hybridisation and washing

The membrane was transferred into a polythene bag, 7ml of hybridisation buffer added, the bag sealed and then incubated in a water bath for 4 hours at 42°C. The liquid was removed from the bag, hybridisation buffer containing 1x10^6cpm/ml of denatured probe added, the bag resealed and returned to the shaking water bath for 16 hours. The following day, the radiolabelled probe was removed, the membrane rinsed in 4xSSC and washed in 4xSSC, 2xSSC, 1xSSC, 0.5xSSC for 30 minutes at each buffer concentration.

3.6.6 Autoradiography

The plastic enclosed membranes were placed in cassettes with two intensifying screens, overlaid with two X-OMAT™ S scientific imaging films (Kodak), and exposed for 24 hours at -70°C. The first film was developed with LX 24 X-ray developer (Kodak), fixed with FX-40 X-ray liquid fixer (Kodak) (according to the manufacturer's instructions), and left to dry. If the positive signals were not visible at this time point then the second film was left for a longer exposure period.

3.6.7 RNA loading

To check for even RNA sample loading, the membranes were stripped by boiling in 0.1% SDS and reprobed using an end-labelled anti-18S RNA oligonucleotide probe (Chang et al, 1984). The oligonucleotide was labelled with [γ^{32}P]dATP using T4 polynucleotide kinase for 45 minutes at 37°C (in a total volume of 10µl). The

unincorporated radiolabelled nucleotides were then removed through a NuTrap column and the probe's specific activity measured. The membrane was transferred into a polythene bag, 7ml of hybridisation buffer added, sealed and incubated for 4 hours at 65°C. The liquid was removed from the bag, hybridisation buffer containing $1x10^6$ cpm/ml of probe added and the bag resealed prior to returning to the shaking water bath for 16 hours. The following day, the radiolabelled probe was removed, the membrane rinsed in oligonucleotide hybridisation washing buffer and washed twice for 30 minutes before exposing to autoradiographic film.

Details of the composition of hybridisation buffers and washing solutions for the cDNA and oligonucleotide labelled probes are given in Appendix I.

3.7 Receptor Binding Assays

3.7.1 Radiolabelled ligands

3-methyl-his^2, [L-his-4-^{3}H, L-pro-3, 4-^{3}H] TRH (^{3}H[3-Me-His^2]TRH) was purchased from NEN Dupont. The specific activity of ^{3}H[3-Me-His^2]TRH (TRH-A) was 62.8Ci/mmol. In contrast, the GnRH-R binding assays were carried out using an iodinated radiolabelled GnRH agonist (GnRH-A, [des Gly^{10}, D-Trp^6, Pro^9 NEt]-GnRH) and antagonist (GnRH-An, [Ac-3,4-dehydro-Pro^{1}D-p-F-Phe^2, D-Trp^{3,6}]-GnRH). These GnRH analogues (Sigma) were labelled with I^{125} using the lactoperoxidase-glucose oxidase method, chromatographed on a 1x 60cm Sephadex G-25 column and eluted with 0.01N acetic acid/0.1% BSA (Sharpe and Fraser, 1980). Fractions corresponding to the monoiodinated hormone peaks were pooled and frozen in 2ml aliquots at -20°C. Preparations of radiolabelled tracer were tested for high affinity binding on membranes prepared from HEK-293 cells stably expressing the rat GnRH-R.

3.7.2 Preparation of cell membranes

Seventy-two hours post-transfection, cells were washed twice with PBS, scraped from 60mM culture dishes using cell scrapers (Falcon) and pelleted by centrifugation at 1000 rpm for 5 minutes. The cell pellets were resuspended in 20mM Tris, pH 7.2, and left to lyse on ice for 10 minutes. The cell suspensions were homogenised using a glass homogeniser (BDH) and centrifuged at 14000 rpm for 20 minutes at 4°C. The

buffer was removed by aspiration and the cell membranes aliquoted and stored at -70°C until further use.

3.7.3 TRH-R (displacement) binding assays

Displacement curves were generated using 500pM ^{3}H-[3-Me-His^{2}]-TRH and [3-Me-His^{2}]-TRH (Peninsula) at concentrations ranging from 0.1nM to 10μM (Lee et al, 1995). Glass test tubes containing 100μl of ^{3}H[3-Me-His^{2}]-TRH, 100μl [3-Me-His^{2}]-TRH, 100μl of membrane preparation (20-50μg of total protein resuspended in TRH RBA buffer) and 200μl TRH RBA buffer, were incubated for 2 hours at 4°C. The samples were filtered onto Whatman GFB glass filters (pre-treated in 0.5% polyethylenimine) using a Brandell cell harvester (Semat), washed three times with TRH RBA buffer, and the filter papers shaken overnight in EcoScint scintillant (Pharmacia) before counting. Maximum binding (Bo) was measured from tubes containing no displacing [3-Me-His^{2}]-TRH, non-specific binding from tubes containing 10^{-5}M [3-Me-His^{2}]-TRH and blank values from tubes with no membranes.

3.7.4 TRH-R saturation binding assays

Saturation assays were performed using concentrations of ^{3}H[3-Me-His^{2}]-TRH between 40pM-40000pM. Glass test tubes containing 200μl of ^{3}H[3-Me-His^{2}]-TRH, 100μl of membrane preparation (20μg total protein resuspended in TRH RBA buffer) and 200μl TRH RBA buffer, were incubated for 2 hours at 4°C prior to filtration. Non-specific binding was calculated in the presence of 10μg of [3-Me-His^{2}]-TRH and blank values in tubes incubated without membranes. Saturation assays were also performed in the presence of the cysteine-modifying compounds dithiothreitol (DTT) and p-chloromercuribenzoic acid (p-CMB). These chemicals, obtained from Sigma, were added to final concentrations of 20mM and 0.05mM respectively for DTT and p-CMB.

3.7.5 Pre-equilibrium TRH-R binding assays

Cell membrane preparations were preincubated with DTT at concentrations of 1mM, 2.5mM, 5mM, 10mM and 20mM or p-CMB at concentrations of 0.01mM, 0.05mM, 0.1mM, 0.2mM and 0.5mM, on ice for 30 minutes. 100μl of membrane preparation (20μg total protein resuspended in TRH RBA buffer) were added to tubes containing

100µl (2nM) ^{3}H[3-Me-His^{2}]-TRH, 300µl TRH assay buffer and ± 1µg [3-Me-His^{2}]-TRH (Bo or NSB values). The assay was incubated for 2 hours at 4°C. Specific binding was calculated as Bo-NSB and expressed per µg of protein.

3.7.6 Post-equilibrium TRH binding studies

Glass tubes containing 100µl of membranes (20µg total protein resuspended in TRH RBA buffer), 100µl (2nM) ^{3}H-[3-Me-His^{2}]-TRH, 300µl TRH assay buffer and ± 1µg [3-Me-His^{2}]-TRH (Bo or NSB values) were incubated for 2 hours at 4°C. Chemical modifying agents, DTT or p-CMB, were then added at concentrations of 1mM, 2.5mM, 5mM, 10mM and 20mM for DTT and 0.01mM, 0.05mM, 0.1mM, 0.2mM and 0.5mM for p-CMB, for a further 30 minutes. The assays were then filtered and counted. Specific binding was calculated as Bo-NSB and expressed per µg of protein.

3.7.7 Specific activity of GnRH-A/An tracers

Specific activities of the radiolabelled tracers were calculated from self displacement assays using either female rat pituitary homogenates or cell membrane preparations from either HEK-293 cells stably expressing the WT GnRH-R or COS-1 cells transiently expressing the receptor. Specific activities ranged from 16 to 75µCi/µg.

3.7.8 GnRH saturation binding assays

GnRH receptor binding assays were set up on ice, in order to minimise degradation of the unbound tracer and dissociation of the tracer bound to the membranes. Glass tubes containing between 200µl of ^{125}I GnRH tracer (5000 cpm to 200000 cpm), 50µl of 1% BSA solution, 150µl GnRH RBA buffer and 100µl of membranes (20-50µg of total protein resuspended in GnRH RBA buffer) were incubated for 2 hours at 4°C (Bramley et al, 1985). The samples were filtered onto Whatman GFB glass filters (pre-treated in 0.5% polyethylenimine) using a Brandell cell harvester (Semat) and washed three times with 5ml of GnRH RBA buffer containing 0.1% BSA. The filter papers were counted on a LBK Wallac γ counter at 75% efficiency. Non-specific binding was calculated in the presence of 10µg of GnRH-A and blank values from tubes incubated without membranes.

3.7.9 GnRH displacement binding assays

Glass tubes containing 100µl of ^{125}I GnRH tracer (100000 cpm), 100µl of unlabelled GnRH-A at final concentrations of between 10^{-11}M to 10^{-5}M, 50µl of 1% BSA solution, 150µl GnRH RBA buffer and 100µl of membranes (20-50µg of total protein resuspended in GnRH RBA buffer) were incubated for 2 hours at 4°C. These tubes were filtered and counted. Specific binding was measured from tubes containing no unlabelled GnRH-A, non-specific binding from tubes containing 10^{-5}M GnRH-A and blank values from tubes with no membranes.

3.7.10 Protein assays

To determine the concentration of protein in each sample, protein assays were carried out in 96 well microtitre plates (Nunc). A protein BSA standard (Biorad) was diluted to concentrations of 7µg/ml, 14µg/ml, 21µg/ml, 35µg/ml, 70µg/ml, 105µg/ml, 140µg/ml for standard curve measurements. The samples were diluted accordingly (1:5 and 1:10) in sterile water and 50µl of standard or sample added into the individual wells of the microtitre plates. In addition, 150µl of sterile water, 100µl of 0.2M NaOH and 50µl of Farbstoff-Konzentrat dye reagent (Biorad) were added to the plates. The plates were mixed for 20 minutes and the colour absorbance measured at 620 nm in a Labsystems plate reader. Data was analysed using the computer program Assay Zap.

3.7.11 Data analysis

Receptor dissociation constant (Kd) and receptor number (B max) were calculated from Scatchard analysis or Cheng and Prussoff analysis (DeBlasi et al, 1989) using Sigma Plot. Scatchard analysis involves the calculation of the amount of radioactivity bound (B) to cell membranes versus the non-bound amount, or free (F), radioactivity. A Scatchard plot involves the plotting of B/F verses B. A linear relationship indicates a single affinity binding site with a Kd value calculated from the slope of this line and a B max value from its x-intercept. Cheng and Prussoff analysis involves the calculation of Kd and B max from measurements of the concentration of unlabelled ligand required to displace half the specific binding (IC50 values). This analysis is only appropriate when the same compound is used as both the radioligand and competitor. Assays were carried out on a minimum of three

independent occasions, unless otherwise specified, with individual assay points representing the mean of triplicate or duplicate samples.

3.8 Total Inositol Phosphate (IP) Production

3.8.1 General methodology

Total IPs, containing inositol monophosphates-$InsP_1$, inositol bisphosphates-$InsP_2$ and inositol trisphosphates-$InsP_3$, were extracted and separated according to the method developed by Pelvin and Boarder (1988). Cells expressing the receptor were labelled with myo [^{3}H]-inositol and then stimulated with ligand. The assays were carried out in the presence of lithium ions in order to prevent the recycling of monophosphates to inositol. Total IPs produced were extracted, using perchloric acid (PCA), and separated on a column containing an anion exchange resin. Water was used to elute off free inositol, followed by elution of any glycerophosphoinositols with sodium tetraborate/ammonium formate. Finally, the total IPs were retrieved by elution with formic acid/ammonium formate solution and counted with liquid scintillation counting.

3.8.2 Incubation with radiolabelled myo-inositol

Twenty-four hours post-transfection, COS-1 cells were trypsinised from 60mm dishes and transferred into 12 well plates. Cells were labelled with ^{3}[H]myo-inositol (1.5µCi/well, Amersham) in inositol-free DMEM containing 1% dialysed HIFCS, glutamine (0.3mg/ml), penicillin (100IU/ml) and streptomycin (100µg/ml), then incubated for a further 48 hours (Anderson et al, 1993).

3.8.3 Total IP Extraction

COS-1 cells were washed with Buffer A (Appendix I F) and incubated for 20 minutes in Buffer A containing 20mM LiCl. Cells were subsequently stimulated with ligand, at final concentrations between 10^{-11}M and 10^{-2}M, for 45 minutes at 37°C. The peptides were purchased from Cambridge Research Biochemicals (TRH), Peninsula (GnRH) or Sigma (GnRH). The buffer was then aspirated off, 500µl of 2% PCA/5mM EDTA and 50µl of 1.8mg/ml phytic acid solution added, and the plates incubated for a further 10 minutes at 4°C. This solution containing IPs was transferred into polystyrene tubes, neutralised with 450µl of neutralisation solution

and centrifuged at 3000 rpm for 10 minutes at 4°C. The supernatant was then transferred into a fresh tube containing 500µl Ag 1-X8 anion exchange resin (Biorad), vortexed, the resin allowed to settle and the clear upper liquid aspirated off. The resin was washed with 1ml of sterile water, vortexed, and the supernatant again removed. This procedure was repeated with 1ml 60mM ammonium formate/5mM sodium tetraborate solution. Finally, the total IPs were released into solution following the addition of 1ml of 1M ammonium formate/0.1M formic acid. An 800µl aliquot was removed, dissolved in 4ml Optiphase Hisafe scintillant (Pharmacia) and counted using a 1209 Rackbeta liquid scintillation counter.

3.8.4 Total Counts

The total incorporation of ^{3}[H]myo-inositol into COS-1 cells was measured to allow standardisation of the number of cells in each well. Cells in the 12 well plates were washed twice with 2% PCA/5mM EDTA solution, solubilised with 500µl 0.2M NaOH and then neutralised with 400µl of 0.66% acetic acid. Optiphase Hisafe scintillant was added and total radioactivity in the cells counted as in section 3.8.3.

3.8.5 Expression of results

Results are expressed either as dpm or dpm/100000 Total Counts (Tc) with assay points representing the mean of triplicate or duplicate samples. Assays were carried out on at least three independent occasions unless otherwise stated.

3.9 Computer and statistical analysis of experimental data

3.9.1 Computer hardware and software packages

All the computer software programmes were run on a Power Macintosh 6100/66 except were otherwise stated. Individual software packages are specified in the text as relevant.

3.9.2 Analytical techniques and significance levels

The statistical significance of experimental data was analysed by Student's t test using Statview. Significance of the calculated t values was assessed against the Student t distribution tabulated values at the 95% probability level (p values < 0.05).

This chapter has outlined the specific methodology used during the course of this study. Chapter 4 now considers the use of molecular models as a means of targeting amino acids for site-directed mutagenesis procedures.

4 Molecular modelling of the GnRH-R and GnRH ligand

4.1 Introduction

To assist in the understanding of the construction of the three-dimensional molecular models, a brief review of the recent developments in this area has been included at the beginning of the chapter. This background information is considered vital in order that the generation of the models used in this study can be viewed against other GPCR molecular modelling approaches. The introductory section encompasses a synopsis of the structural determination of bacteriorhodopsin and rhodopsin, together with the advantages and disadvantages of their use as templates in GPCR molecular modelling studies. The results section deals with the construction of the GnRH ligand and receptor models.

The information derived from these studies was critical in analysing results obtained from site-directed mutagenesis studies carried out in Chapters 6 and 7, and in the targeting of potentially important GnRH-R amino acids involved in ligand-receptor function in Chapter 8.

4.1.1 Structural determination of heptahelical proteins

A wealth of data on structure-function relationships in GPCRs has been derived from biochemical studies, but it is increasingly important to view this information within a three-dimensional structural framework. Bacteriorhodopsin was the first heptahelical protein structure to be determined (Henderson et al, 1990), and the structural elucidation of a closely related protein, halorhodopsin (Havelka et al, 1995) has subsequently followed. Both these proteins are similar in structure to GPCRs but do not couple to G-proteins. The first major breakthrough in the structural determination of a GPCR was the low resolution 9Å projection map of bovine rhodopsin reported by Schertler and colleagues (1993). Rhodopsin still remains the only GPCR for which hard structural data has been obtained. Two-dimensional crystals of frog rhodopsin have also now been purified and 6Å and 7Å resolution projection maps, generated

from these crystals, have provided further insight into the arrangement and tilts of TM domains (Schertler and Hargrave, 1995). To date, the structural determination of these heptahelical proteins has been limited to the TM domains, primarily due to the use of two-dimensional crystals for crystallography. Further advances in crystallography techniques, however, should permit the development of three-dimensional crystals and hence provide the necessary starting material to determine the entire GPCR structure.

Bacteriorhodopsin functions as a light-driven proton pump and is found naturally as a two-dimensional crystalline protein in the membrane of the *Halobacterium halobium.* In 1990, Henderson and co-workers constructed a high resolution (3.5 Å), three-dimensional map, using electron cryo-microscopy techniques (Henderson et al, 1990). The model of bacteriorhodopsin revealed the importance of kink-inducing Pro residues and highlighted the tilted positions of the helices relative to each other and to the membrane. With such a high degree of resolution it was possible to visualise the amino acids involved in chromophore binding and proton pump activation. A total of 21 amino acids constituted the retinal binding pocket and the binding of the chromophore, perpendicular to the plane of the helices, was localised to a position approximately half way down the central channel. The structural information derived from the model was in accord with earlier bacteriorhodopsin site-directed mutagenesis studies, and many of these characteristic features have now been extrapolated to encompass the entire GPCR family.

More recently, a three-dimensional structure of the α helices of halorhodopsin, a light-driven chloride pump, has been determined from two-dimensional crystals. The 7Å resolution map generated by Hevelka and co-workers (Havelka et al, 1995), revealed that the arrangement of the seven TM helices was similar to bacteriorhodopsin although the orientation of the protein framework within the membrane appeared rotated by approximately three degrees.

The low resolution (9Å) projection map of bovine rhodopsin reported by Schertler et al (1993) revealed that each rhodopsin molecule displayed an elongated arc-shaped feature together with four resolved density peaks. Each high density peak was thought to represent a TM domain orientated perpendicular to the membrane (helices IV, V, VI, VII) with the arc-like feature corresponding to the tilted arrangement of the remaining three α helices (helices I, II and III). Comparative structural analysis of

bacteriorhodopsin and rhodopsin indicates that whilst both proteins share a common heptahelical structure, they differ with respect to the position and tilts of the individual helices, as illustrated in Figure 4.1. In bovine rhodopsin, the protein structure appears less elongated and slightly wider relative to bacteriorhodopsin, with helix III deeply buried between helix II, IV, V and VII. Helix IV and VII are parallel in orientation and occupy a position approximately equidistant from helix III. In bacteriorhodopsin, helix IV appears roughly parallel to helix II and III, whilst helix III lies closer to helix IV than to helix VII (Donnelly and Findlay, 1994). Two projection maps of frog rhodopsin at significantly higher resolution have since been reported (Schertler and Hargrave, 1995). The 6Å and 7Å resolution projection maps closely resembled the 9Å bovine rhodopsin structure but show that helix V carries a much stronger tilt than previously realised (Figure 4.1). This information further supports the distinct structural differences between rhodopsin and bacteriorhodopsin.

4.1.2 Molecular Modelling of GPCRs

The availability of structures for bacteriorhodopsin and rhodopsin together with biochemical/biophysical data regarding G-protein structure-function relationships, and the technical developments in molecular modelling software has lead to rapid advancements in receptor modelling. Many three-dimensional models of GPCRs have been constructed, but their degree of adherence to the bacteriorhodopsin/rhodopsin template structures varies enormously thus producing markedly different results.

Homology modelling is now a widely used approach in molecular modelling. This technique relies on identifying a known protein sequence that bears a common three-dimensional structure with an unknown protein and can, therefore, be used as a suitable template. Bacteriorhodopsin provides the basic structural framework for the construction of many GPCR models, but these models tend to vary in their degree of adherence to its structure. GPCR models, including those of the β_2 adrenergic receptor, adenosine A_1 receptor, muscarinic M_1 receptor and thromboxane A_2 receptor (Yamamoto et al, 1993) have closely followed the co-ordinates of bacteriorhodopsin whereas other models, including those for the dopamine D_2 receptor, the $C5_a$ receptor and the opsin receptor, have only utilised the overall topology of the seven TM helices (Grotzinger et al, 1991). In this latter receptor group, additional information on the structure of other membrane bound proteins together with biochemical data has been amalgamated in order to optimise the model's structure.

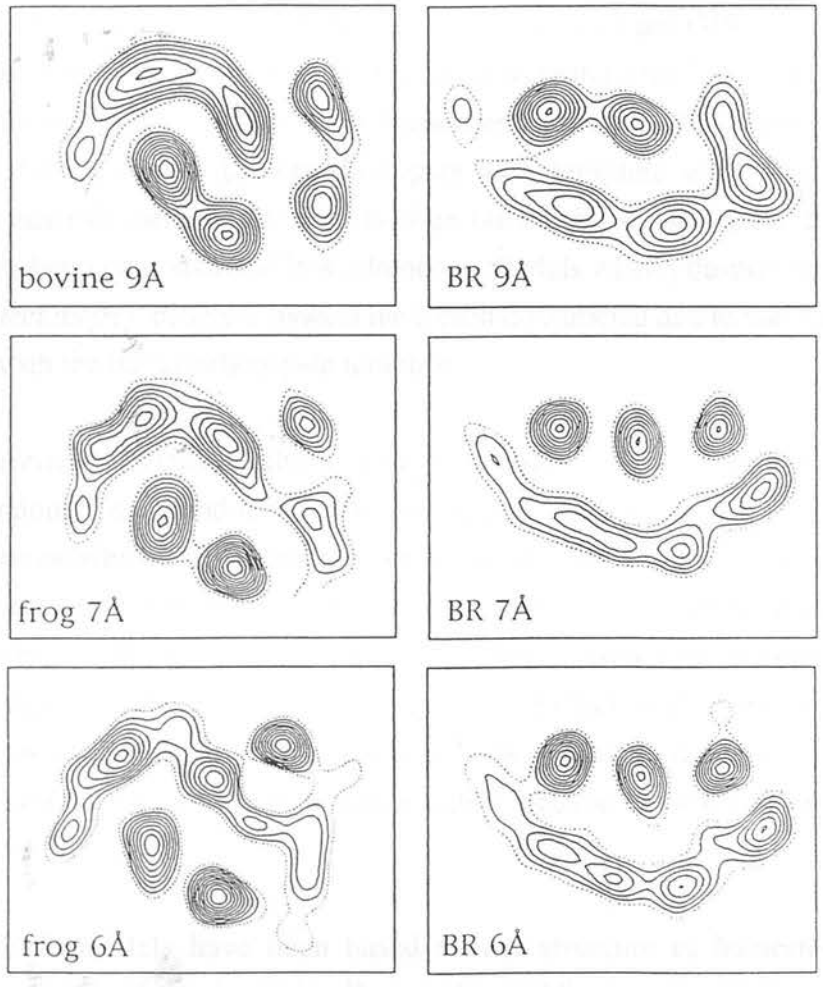

Figure 4.1 Structural comparison of frog and bovine rhodopsin with bacteriorhodopsin

Projection density maps of bovine rhodopsin (9Å) and frog rhodopsin (7Å and 6Å) compared to bacteriorhodopsin (BR, 9Å, 7Å and 6Å) (Schertler and Hargrave, 1995). These projection maps highlight the structural differences between rhodopsin and bacteriorhodopsin. This figures is printed with the permission of Dr G F X Schertler.

Bacteriorhodopsin, however, may not prove an ideal template as although structurally similar to GPCRs, it does not couple to a G-protein effector system, and has little sequence homology with other GPCRs. Many sequence analysis methods fail to show any significant alignment between bacteriorhodopsin and GPCRs but use of the Clustal algorithm (Thompson et al, 1994) reveals that whilst the homology is low, it is sufficient to align GPCR amino acid sequences to bacteriorhodopsin. Molecular models of GPCRs using bacteriorhodopsin as a template will clearly differ if alternative analysis methods are used to align the GPCR to bacteriorhodopsin. This problem has been demonstrated in β adrenergic models where, despite similarities in modelling techniques, different models have been constructed due to variations in their alignment with the bacteriorhodopsin template.

The differences between the electron diffraction patterns obtained for bacteriorhodopsin and rhodopsin have also lead to speculation that it is a model of limited value on which to base predications about GPCRs. Others groups have argued that bacteriorhodopsin and rhodopsin have the same TM three-dimensional structure and that differences in their electron diffraction patterns result from altered tilting in the protein structures of the two-dimensional crystals (Hoflack et al, 1994) or differences in crystal formation per se. This however, now seems unlikely as two different crystals of frog rhodopsin have generated a similar electron density map (Schertler and Hargrave, 1995).

Not all GPCR models have been based on the structure of bacteriorhodopsin. Alternative models of the dopamine D_2 receptor and the β_2 adrenergic receptor have also been constructed and both models appear as the mirror image of bacteriorhodopsin (Donnelly and Findlay, 1994). Zhang and Weinstein, initially favoured a model of the 5HT receptor, derived from molecular dynamic studies, that displayed a non-sequential order rather than a clockwise or anticlockwise arrangement of the helices: however, they have now adopted the more conventional sequential arrangement (Zhang and Weinstein, 1993; 1994).

4.1.3 The Baldwin model of GPCRs

The Baldwin model of GPCRs was based on structural information derived from detailed sequence analysis of 204 members of the GPCR family (Baldwin, 1993). This model predicts that each TM domain is spatially close to its neighbour in sequence and that helix III is deeply buried in the membrane, whereas helices I, IV and V are most exposed to the lipid. The observations on helix positioning were deduced from the knowledge that certain GPCRs contain very short interhelical loops. If all members have an identical helical arrangement, the only feasible structure must position helix I beside helix II and helix II beside helix III and so on. The predications concerning the relative exposure of each helix to the surrounding lipid surfaces were derived from analysis of the hydrophobic nature of the amino acid side chains. By assigning each residue into a class, non-lipid interacting polar residues or lipid interacting non-polar residues, and then viewing the structure of the helices in a wheel shaped model, it was apparent that helices I, IV, V and VI had a large surface area without polar residues whereas helices II, III and VII had a much smaller non-polar surface area. This information, in conjunction with the position of conserved amino acids and positional differences between closely related sequences, has lead to speculation that helices I, IV and V are the most exposed to the lipid and that helix III is buried deep in the membrane.

Baldwin's analysis has allowed a tentative assignment of the order of the helices to the peaks observed in the rhodopsin projection map. This proposed arrangement appeared similar to the middle region of the membrane-embedded part of bacteriorhodopsin, although further analysis revealed differences in the helical tilts. These structural differences have been postulated to arise from the presence of a disulphide bridge, between a conserved Cys residue in the el 1 and el 2, and the altered positions of Pro residues in GPCRs relative to bacteriorhodopsin. Additional evidence supporting these findings has been provided from the binding of small amine peptides. In these receptors, the helical residues that interact with the ligand, as identified by site-directed mutagenesis, are not in an appropriate position in bacteriorhodopsin to permit such an interaction. However, the potential mobility of the protein must also be taken into consideration and whilst in their unbound state the receptors may adopt different orientations, upon ligand-receptor binding there may be a high degree of internal conformational change. Receptor mobility, together with the different nature of the ligands in GPCRs, suggests that every receptor will have a

certain degree of structural diversity and that no one model will accurately predict the nature of the binding site.

A model of rhodopsin, in agreement with Baldwin's model, has been constructed by Donnelly using a method that detects helical periodicity in sequence alignments from known protein structures (Donnelly et al, 1994). Zhang and Weinstein have used the alternative approach of polarity-conserved positioning to determine the orientation of GPCR TM helices. Whilst their results are not identical to Baldwin's, they do predict that helices III and VII are buried deep within the membrane (Zhang and Weinstein, 1994).

4.2 Results

4.2.1 Structure of the Baldwin model of the GnRH-R

The Baldwin model of the GnRH-R consists of three cross-sectional wheel diagrams through different regions of the TM domains (Figure 4.2). The first diagram depicts the position of amino acids located nearest to the TM/intracellular interface (Figure 4.2a), the second is a view of residues in the middle regions of the α helices (Figure 4.2b) and the third represents amino acids positioned proximal to the TM/extracellular interface (Figure 4.2c).

Figure 4.2 The Baldwin model of the GnRH-R (following page)

(a) The Baldwin wheel diagrams of the rat GnRH-R amino acid sequence, viewed from the intracellular surface of the receptor. The model shows a cross-sectional view through (a) the intracellular face 11 amino acids (b) the middle TM domain 12 amino acids and (c) the extracellular surface 11 amino acids. Each large circle represents a TM domain with the position of the α carbon atoms represented as dots around the periphery and numbered in accordance with the protein sequence of the GnRH-R. The size of the dot indicates its depth within the TM domain with the largest dots closest to the intracellular face and the smallest dots closest to the extracellular face. These templates were generated by Dr J M Baldwin.

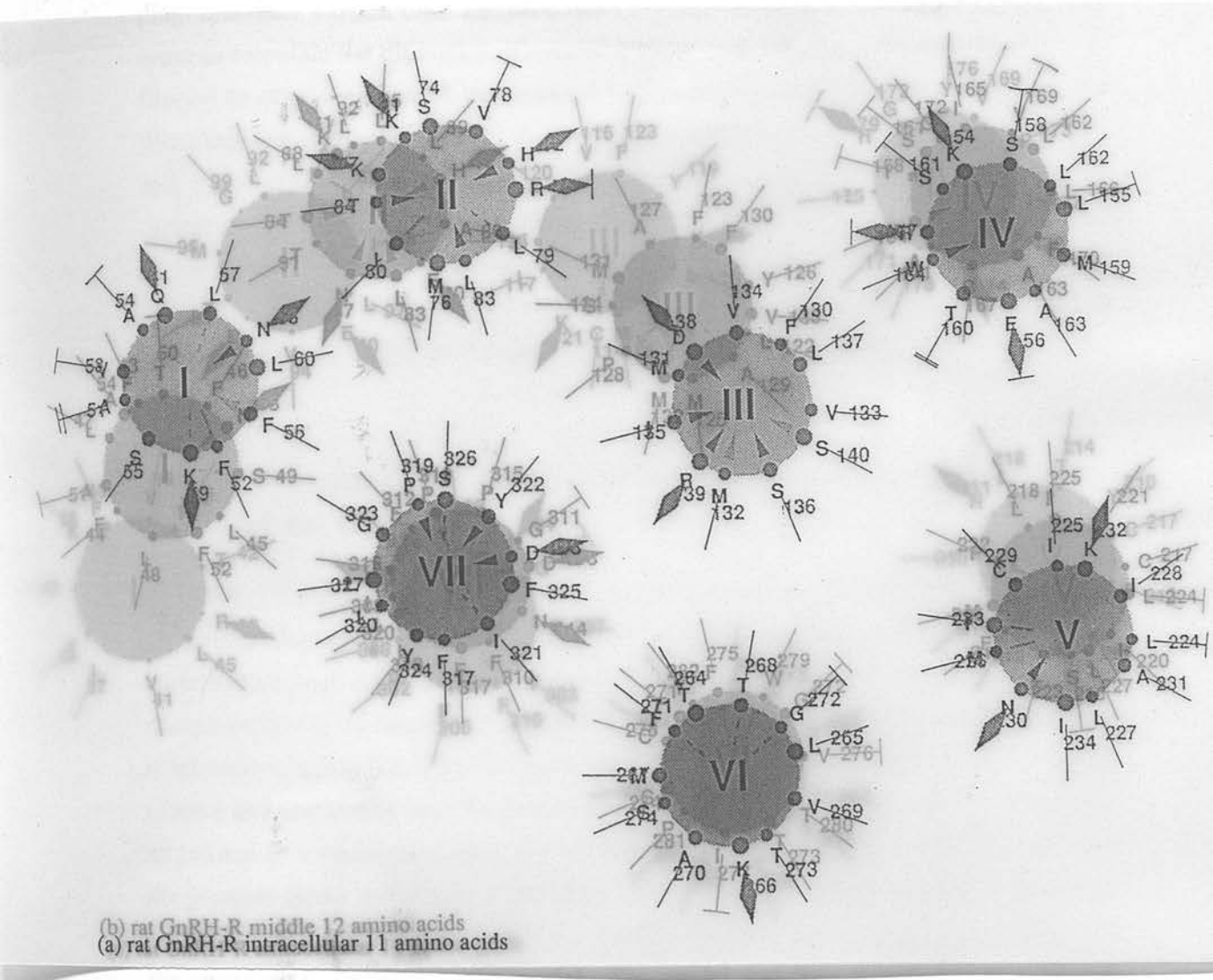

(b) rat GnRH-R middle 12 amino acids
(a) rat GnRH-R intracellular 11 amino acids

Legend:

A 70	Location and number of residue (size of circle indicates depth).
	Polar residue conserved in more than 10% of GPCRs
	Bars indicate non-conserved residues. More bars = more variable.
	Solid triangle indicates residue conserved in > 85% of cases.
	Shaded triangle indicates residue conserved in > 75% of cases
	Shaded bar indicates residue conserved in > 65% of cases
	Broken bar indicates one of a pair of related residues, conserved in > 75% of cases.

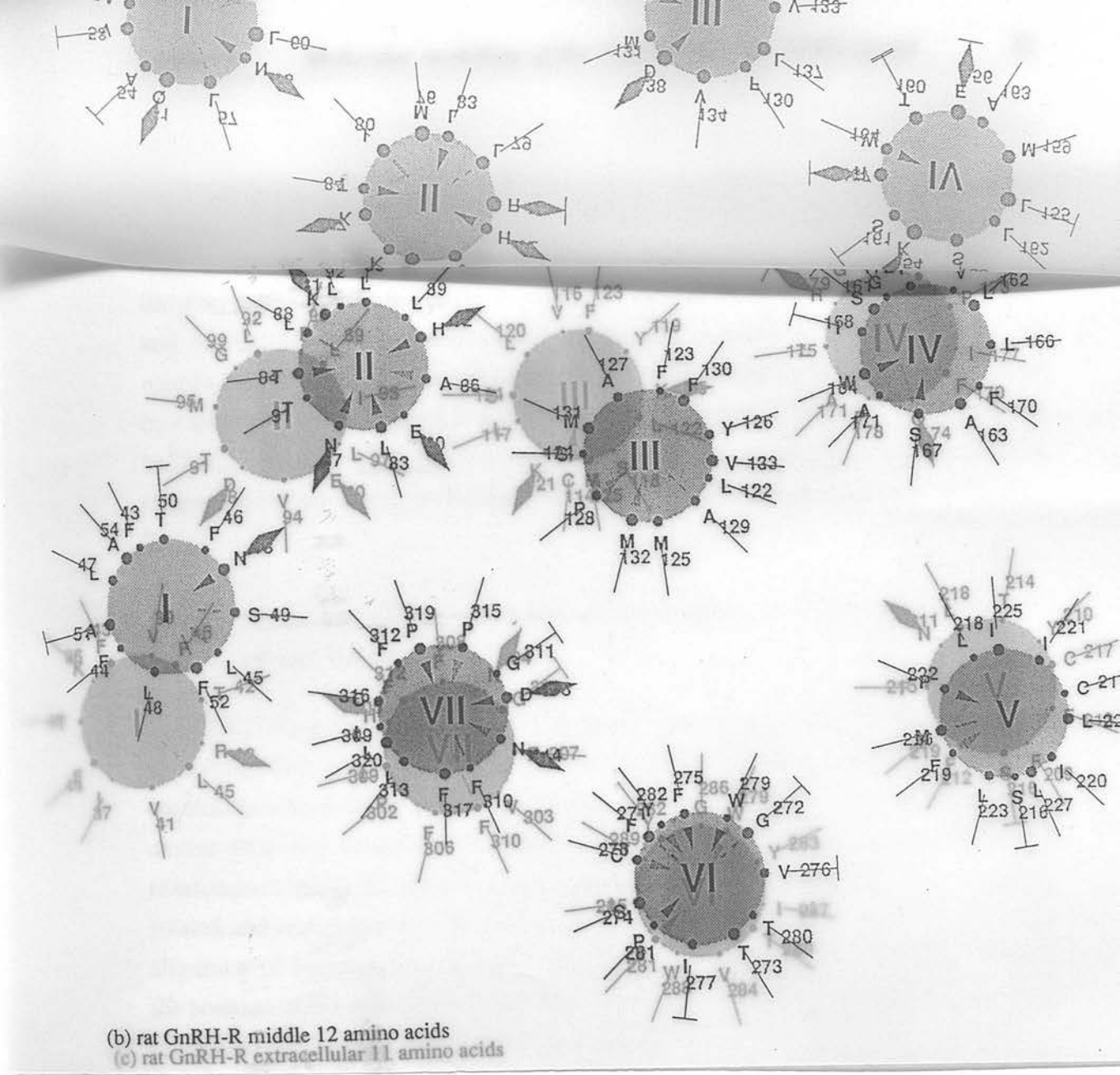

(b) rat GnRH-R middle 12 amino acids

(c) rat GnRH-R extracellular 11 amino acids

Legend:

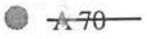

Location and number of residue (size of circle indicates depth).

Polar residue conserved in more than 10% of GPCRs

Bars indicate non-conserved residues. More bars = more variable.

Solid triangle indicates residue conserved in > 85% of cases.

Shaded triangle indicates residue conserved in > 75% of cases

Shaded bar indicates residue conserved in > 65% of cases

Broken bar indicates one of a pair of related residues, conserved in > 75% of cases.

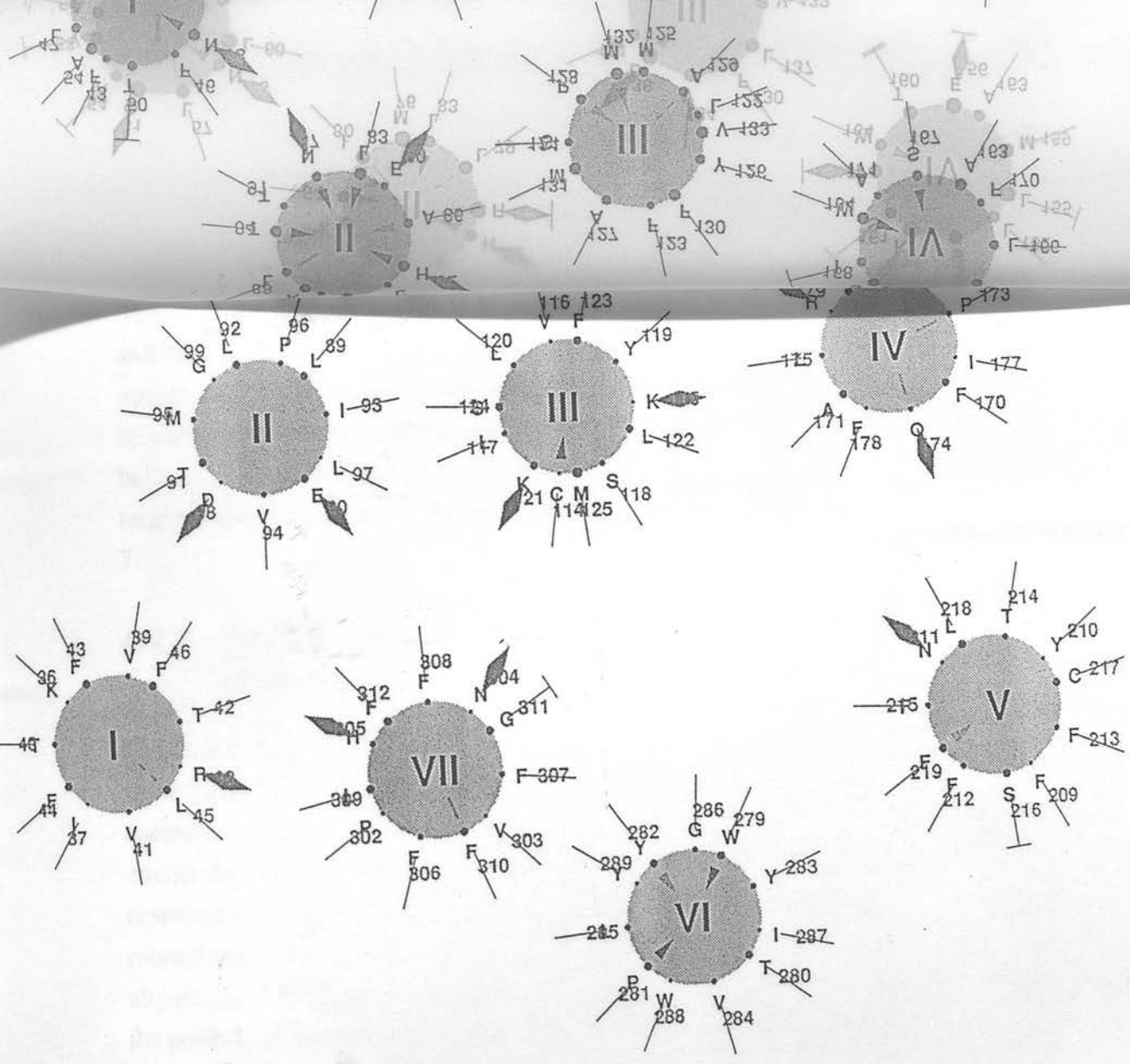

(c) rat GnRH-R extracellular 11 amino acids

Legend:

- A 70 — Location and number of residue (size of circle indicates depth).
- Polar residue conserved in more than 10% of GPCRs
- Bars indicate non-conserved residues. More bars = more variable.
- Solid triangle indicates residue conserved in > 85% of cases.
- Shaded triangle indicates residue conserved in > 75% of cases
- Shaded bar indicates residue conserved in > 65% of cases
- Broken bar indicates one of a pair of related residues, conserved in > 75% of cases.

To generate a three-dimensional GnRH-R model, further modulations of the wheel diagrams were carried out. Initially, the individual diagrams were superimposed in order to calculate the tilt angles of each TM helix. The TM helices were subsequently flipped to obtain a view of the receptor from the extracellular surface. Figure 4.3 illustrates the composite GnRH-R model, as viewed from the extracellular surface, and highlights the relative positions of the TM domains as they transverse the membrane. A noticeable feature of this model is the markedly different tilt displayed by each helix. Helix I, helix II and helix III show dramatic tilts, helix IV, helix V and helix VII have only slight tilts whereas helix VI is relatively straight. The amino acids targeted for study using the Baldwin model of the GnRH-R are described in Chapter 7.

4.2.2 Structure of the computer-derived three-dimensional model(s) of the GnRH-R

The GnRH-R model was constructed using information derived from the structure of bacteriorhodopsin and the Baldwin model of GPCRs (Figure 4.4a and 4.4b). The bacteriorhodopsin co-ordinates were used as an initial template and the amino acid side chains removed to leave the peptide backbone. The skeleton model was then reassembled using the modelling computer programme MacMimic and each helix rotated and translated into the position predicted by the Baldwin model. Sequence alignment of bacteriorhodopsin and the GnRH-R, as illustrated in Table 4.1, allowed the position of the individual amino acids in each GnRH-R helix to be located relative to their position in bacteriorhodopsin. Amino acid side chains were then assigned to the appropriate Cα atom in the model. The model was then transferred to a Silicon Graphics workstation where further manipulations were performed using Sybyl (Tripos Associates). The configuration of the Pro residues were adjusted according to the main-chain torsion angle as suggested by Sankararamakrishnan, 1991 (Sankararamakrishnan et al, 1991). The initial locations of the helices left large gaps, and these were closed by manually condensing the model, rotating and translating the helices to obtain the best fit between the amino acid side chains. The model was finally subjected to energy minimisation using the Kollman all-atom energy model. An initial round of ten iterations of steepest-descent energy minimisation was followed by repeated conjugate-gradient minimisation, to a final energy gradient of 0.05 kCal/mol.

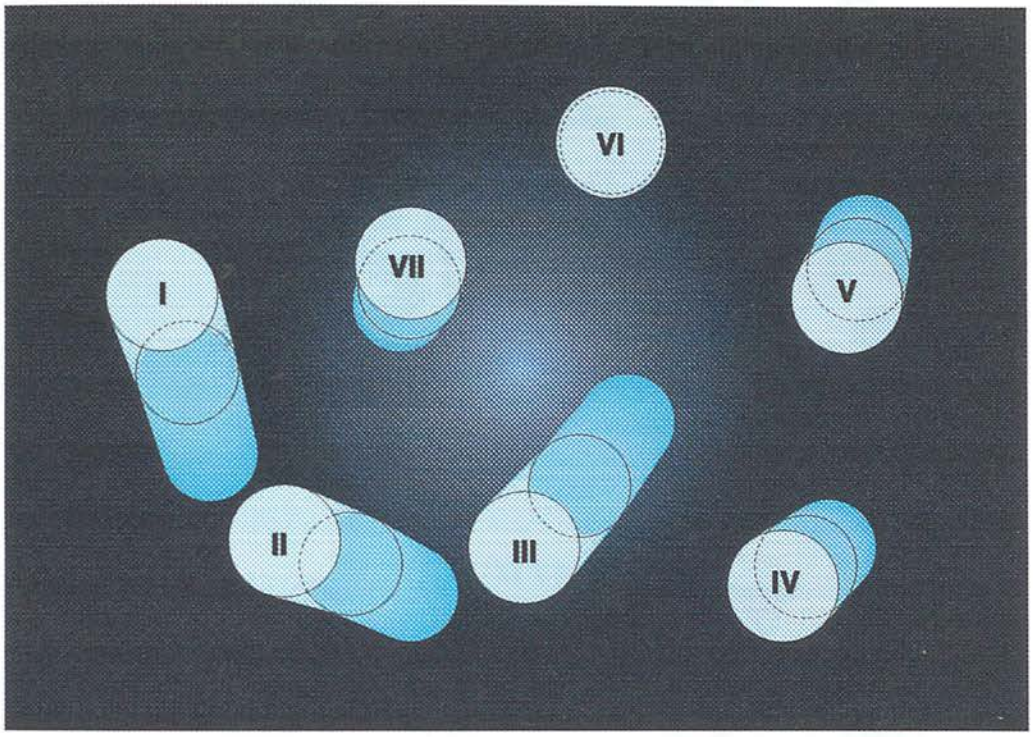

Figure 4.3 The composite Baldwin model of the GnRH-R

Structural model of the TM domains of the rat GnRH-R as predicted by the Baldwin model. The model has been flipped and is a view from the extracellular surface of the receptor, looking inwards down the central receptor pore, towards the intracellular face. The TM domains are represented as cylinders and the amino acids have been removed in order to give a clear three dimensional view of TM domain tilts.

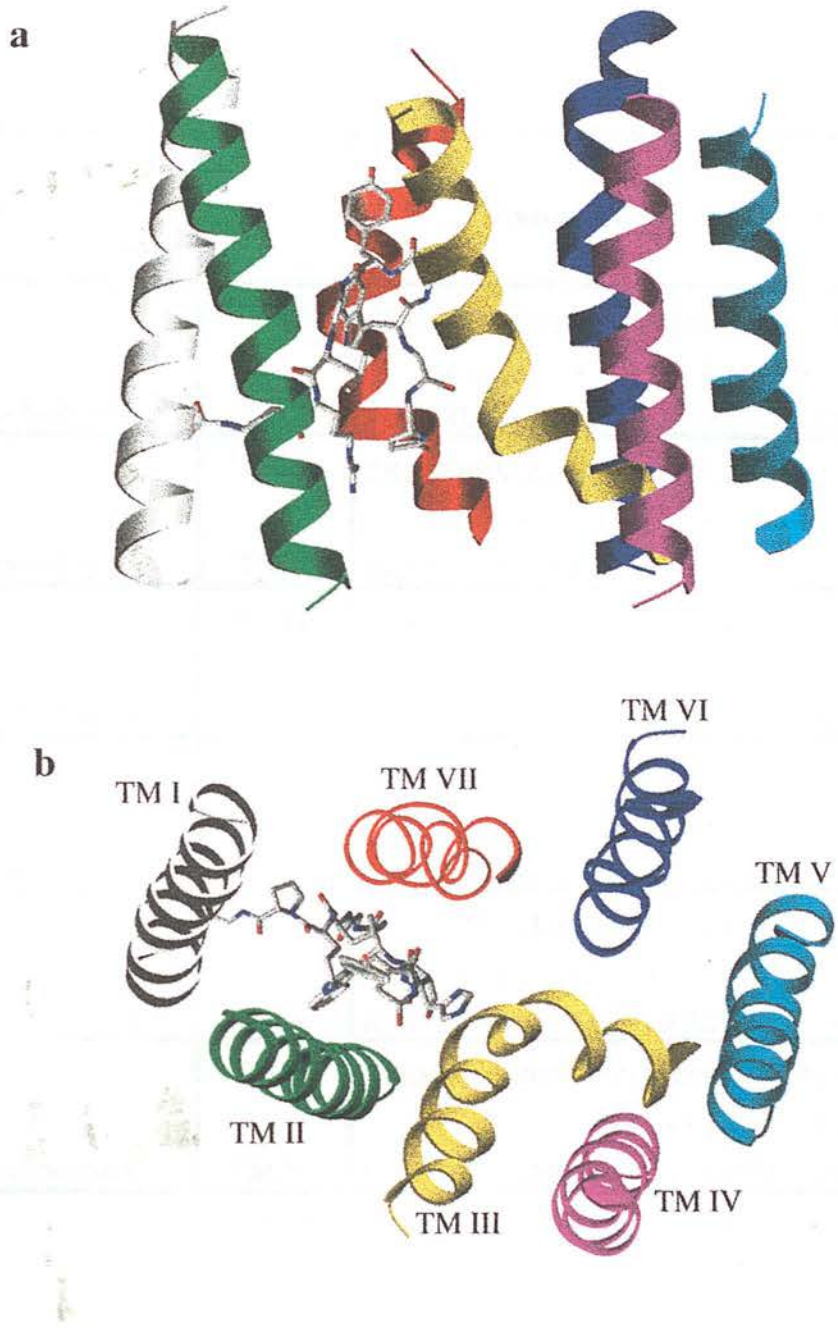

Figure 4.4 Computer-derived model of the GnRH-R

Computer model of the TM domains of the GnRH-R with GnRH inserted into a putative binding location. (a) side view from within the membrane (b) plan view looking into the pore from outside the cell. The TM domains are represented as ribbons so that the individual tilts of the helices and their positions relative to other helices can be observed.

Receptor	TM	Amino Acid Sequence
GnRH	TM I	SGKIRVTVTFFLFLLSTAFNASFLVK---
		| •|||| • •|• | ••••
Bacteriorhodopsin	TM I	PEWIWLALGTALMGLGTLY---FLVKGMG
GnRH	TM II	KKLSRMKVLLKHLTLANLLETLIV
		•| |||| • •|
Bacteriorhodopsin	TM II	DAKFYAITLVPAIAFTMYLSMLLG
GnRH	TM III	LCKVLSYLKLFSMYAPAFMMVVISLD
		| | | |||• ||| | •
Bacteriorhodopsin	TM III	EQNPIYWARYAWLFTPLLLLDLALLV
GnRH	TM IV	FRMIYLVDGSGPAVFSQCVTHCS
		|| ••|| • | | • |
Bacteriorhodopsin	TM IV	GTILALVGADGIMIGTGLVGALT
GnRH	TM V	FYNFFTFSCLFIIPLLIMLICN
		| • | •| |•| | |
Bacteriorhodopsin	TM V	WWAISTAAMLYILYVLFFGFTS
GnRH	TM VI	RTLKMTVAFGTSFVICWTPYYVLGIWYW-
		•| •||• • |•
Bacteriorhodopsin	TM VI	EVASTFKVLRNVTVVLWSAYPV--VWLIG
GnRH	TM VII	HFFFLFGFLNPCFDPLIYGYFSL-COOH
		||•| •| | |• | •
Bacteriorhodopsin	TM VII	TLLFMV--LDVS-AKVGFGLILLRS

Table 4.1 **Sequence alignment of the rat GnRH-R and bacteriorhodopsin**

Identical amino acids are represented as • and conserved homologous residues represented |.

Sequence homology was analysed using the Clustal algorithm on Gene jockey II.

4.2.3 The GnRH computer-derived model

A model of the GnRH peptide in its biologically active state has been constructed by Gupta et al (1993) using an homology modelling approach. Twenty protein templates containing at least 5 consecutive amino acids in the GnRH peptide were identified, energy minimised models constructed, and the protein segments further categorised based on their broad conformational features. Two classes of structure emerged either folded or extended, and whilst the extended category displayed structural diversity, many of the folded structures contained a common β-III type turn motif around the Trp-Ser-Tyr-Gly segment - a prediction that has also been made for the structure of GnRH. Utilising biochemical GnRH structure-function information, one molecular structure from Streptomyces griseus proteinase A (Sielecki et al, 1979) had an appropriate conformation and was used as the basis for the GnRH model. This molecule appeared folded bringing the N- and C-termini close together in a hairpin configuration. It is known that a D- amino acid following a β-III turn stabilises the turn and an extensive family of GnRH super-agonists incorporate a D-amino acid at position 6, serving to confirm the model. The location of the Gly at position 6 in the Gupta model, in close proximity to the β-III turn, would allow such a substitution. The side chains of Trp3 and Arg8 are exposed suggesting their importance for receptor interactions. Arg8 has a high positive electrostatic potential in keeping with the hypothesis that it is the critical residue involved in species-specific GnRH binding. In addition, analogues substituted at position 8 with the amino acids, Lys, Orn or Leu showed a reduced positive electrostatic potential in agreement with their decrease in biological activity. The Gupta model was used as the basis for the computer-derived model of GnRH (MRC, Reproductive Unit, Edinburgh) and this computer model is illustrated in Figure 4.5

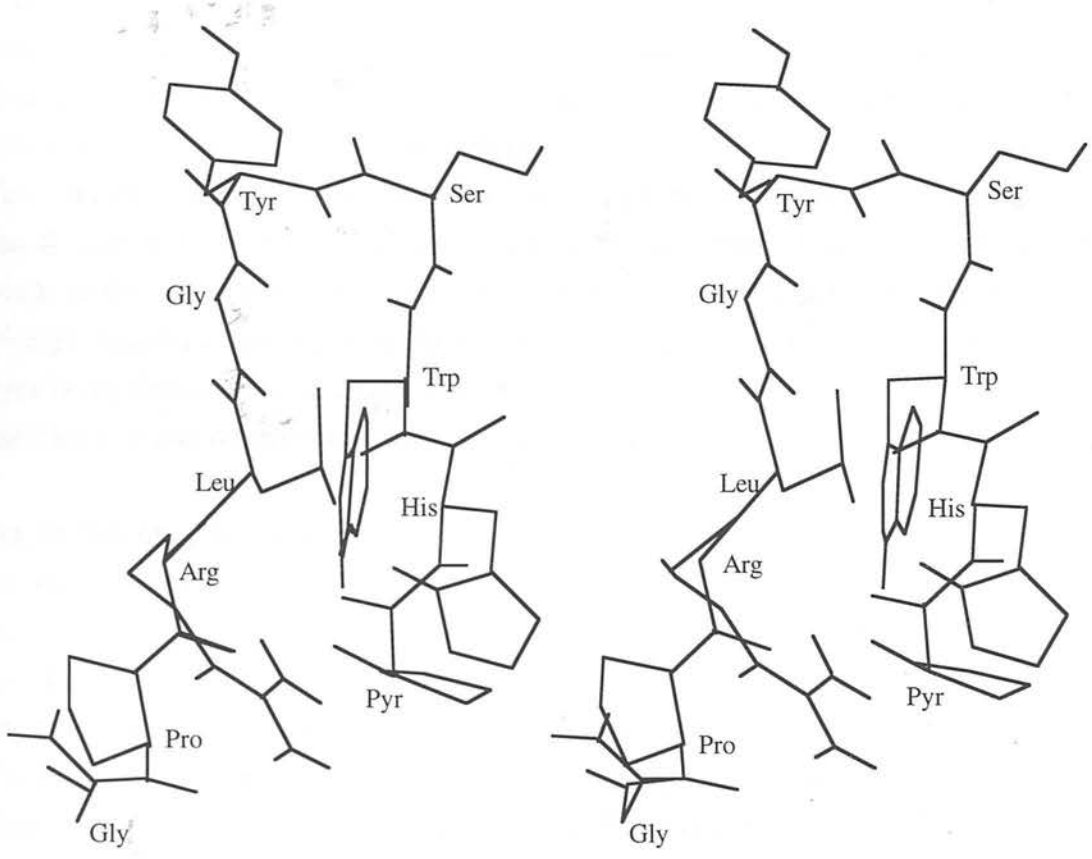

Figure 4.5 The computer-derived GnRH model

A model of the GnRH ligand derived from the Gupta model. This is a stereo pair and can be seen as a three-dimensional image if the GnRH structure is viewed cross eyed. The position of the β-turn around the Trp3-Ser4-Tyr5-Gly6 amino acids can be clearly seen.

4.2.4 GnRH ligand and receptor interactions

The GnRH model was docked into the computer-derived model of the receptor. It was immediately apparent that there was only one possible location within the receptor structure, between TM II, TM III and TM VII, where GnRH could be located (Figure 4.4a and 4.4b). However, at this site it is possible to orientate the GnRH decapeptide either with the ends of the hairpin configuration or with the Tyr at position 5 going in first. Based on the design of GnRH analogues, and the biochemical evidence linking the C- and N- termini with receptor binding and activation, it is likely that GnRH binds to the receptor with the ends of the molecule entering the receptor pore first. Energy minimisation was carried out with the ligand located in this position as previously described in section 4.2.2. A space-filling model showing the position of the ligand within the receptor structure is illustrated in Figure 4.6.

As yet it is uncertain as to how far down the pore the ligand will penetrate but based on the observation of retinal binding in rhodopsin and bacteriorhodopsin, it is reasonable to presume that the binding and activation sites are roughly in the middle of the TM regions. Using the simulated model structures, two amino acids in the receptor appear in appropriate positions to interact with GnRH. Leu at position 83 (Leu83) and Phe at position 312 (Phe312) occupy positions allowing potential interactions with Leu7 and Trp3 respectively in the GnRH ligand. To test the potential importance of these highlighted residues they were mutated either to amino acids of similar hydropathicity, different hydropathicity or the small hydrophobic residue Ala (see Chapter 8).

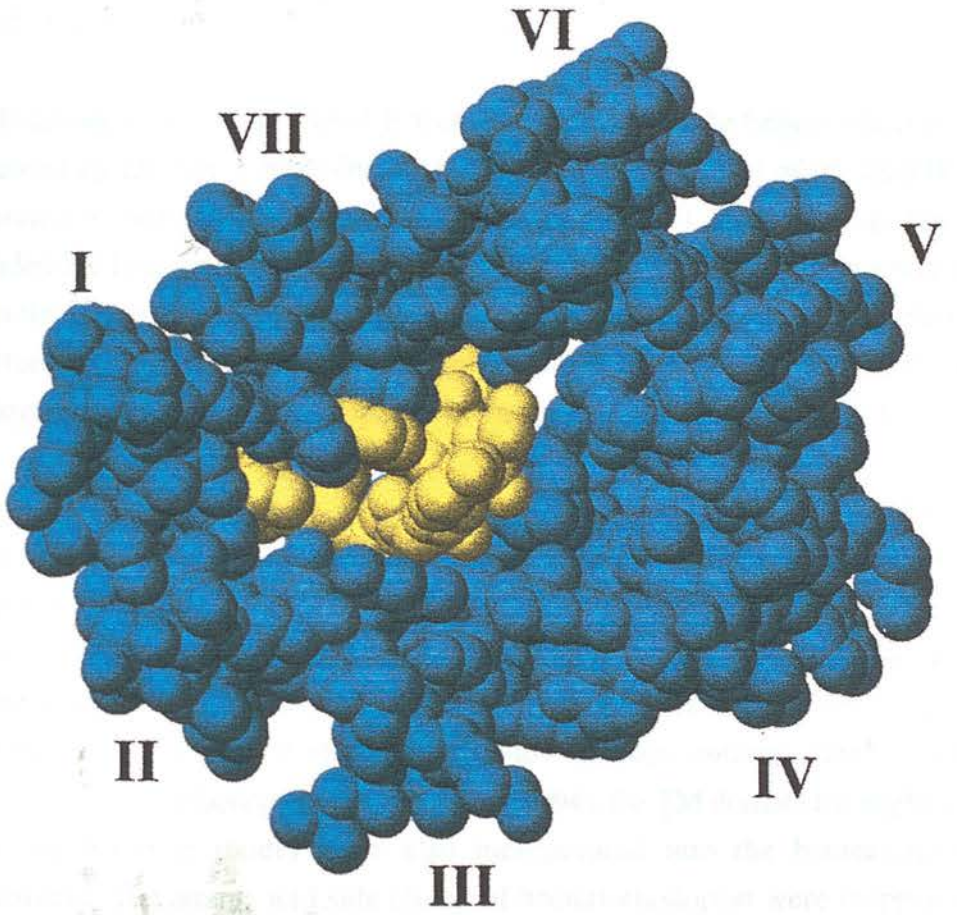

Figure 4.6 Space-filling model of GnRH-R/GnRH

Space filling model of the GnRH-R showing a possible arrangement between the TM domains of the GnRH-R (blue) and GnRH (yellow). GnRH is in a hairpin configuration with the β turn nearest Tyr5.

4.3 Discussion

During the course of this study, three-dimensional models of the GnRH-R, the Baldwin model and a computer-derived model, together with a computer model of the GnRH ligand were constructed and utilised to predict potential amino acids involved in ligand-receptor interactions.

The Baldwin model of the GnRH-R was constructed from the helical wheel diagrams generated by Dr. Joyce Baldwin. A three-dimensional model of the GnRH-R was generated by superimposing the three individual wheel diagrams together. This provided the first spatial view of the GnRH-R structure and was subsequently used to aid in the targeting of polar amino acids for site-directed mutagenesis (Chapter 7). In addition, this model allowed the tentative calculation of the TM domain tilt angles, information utilised in the development of the computer-derived model of the receptor.

In order to construct a three-dimensional computer model of the GnRH-R, it was necessary to collate and interpret all the information currently available on GPCR molecular modelling techniques. The co-ordinates of bacteriorhodopsin were used as a starting point as this is the only heptahelical protein whose structure has been determined to near atomical resolution. In addition, as recent evidence suggests that the structure of the GPCR rhodopsin provides a more suitable template structure (relative to bacteriorhodopsin) (Hoflack et al, 1994), the TM domain tilt angles derived from the Baldwin model were also incorporated into the bacteriorhodopsin framework. The amino acid side chains of bacteriorhodopsin were stripped off the template and those of the GnRH-R subsequently superimposed. Further adjustments were then carried out with the Pro residues altered in accordance with the angles suggested by Sankararamakrishnan and the TM domains rotated into an optimal minimum energy position.

A computer model of the GnRH ligand was also generated based on the structure proposed by Gupta and co-workers. With computer models of both the ligand and receptor, it was possible to combine these models and hence predict possible interacting sites. From these studies, two amino acids in the GnRH-R, Leu83 in TM II and Phe312 in TM VII were targeted for site-directed mutagenesis study, discussed in Chapter 8. The ligand-receptor simulation studies were carried out with the NH_2 and COOH ends of the hairpin GnRH structure penetrating furthest into the receptor pore. This particular ligand orientation was adopted as the chromophore ligand in

bacteriorhodopsin binds in the middle regions of the TM domains (Henderson et al, 1990). Furthermore, it has been postulated that the COOH and NH_2 termini of GnRH are principally involved in receptor binding and activation respectively (Nikolics et al, 1988) and, therefore, it is likely that the ends of the ligand penetrate deepest into the receptor pore. However, it is also possible that GnRH is orientated in the opposite direction with the residues clustered around the hairpin (Ser4-Leu7) entering the receptor TM domains first. This arrangement seems more unlikely and to date no simulation studies have been carried out with GnRH orientated in this alternative configuration.

The computer-derived GnRH-R model has evolved through many different stages from the original template structure. The initial position of the TM helices have been re-orientated and rotated and the α helices now occupy different positions when compared to the starting framework. These alterations are largely as a result of the change in the torsion angle of the kink-inducing Pro residues, together with the extensive energy minimisation procedures carried out. The present space-filling model of the GnRH-R is illustrated in Figure 4.6.

The modelling approach has proved extremely useful in this study as it has enabled structural alterations of the model, based on the information derived from site-directed mutagenesis experiments. Furthermore, this permits the reciprocal exchange of information, whereby the model can be used to predict amino acids potentially important in ligand-receptor binding and the site-directed mutagenesis studies then used to assess the accuracy of the model and subsequently redefine its structure accordingly.

The computer modelling and subsequent ligand-receptor simulation studies have provided a good framework from which to base predictions about putative ligand-receptor amino acid interactions. This approach helped to localise sites within the receptor structure where the ligand is most likely to bind, thereby eliminating the necessity to mutate every individual receptor residue. Together the molecular modelling and site-directed mutagenesis studies create a very powerful targeting approach, whereby the models can be used as hypothetical indicators of amino acid function and the site-directed mutagenesis data used to provide hard biochemical evidence for these predications.

Molecular models of the GnRH-R TM domains have been utilised in Chapters 6, 7 and 8 to predict amino acids involved in ligand-receptor interactions and to analyse site-directed mutagenesis data. However, no molecular models of the extracellular and intracellular loop structures of GPCRs have been generated and, therefore, examining the role of such residues must be carried out without the use of these models. Chapter 5 has focused on the function of extracellular Cys residues in disulphide bond formation and this study is based on comparative sequence information from other GPCRs.

5 Role of extracellular Cys residues in the GnRH-R and the TRH-R

5.1 Introduction

Sequence analysis of many GPCRs has identified the presence of two conserved Cys residues in the extracellular domain. Cys residues contain sulfhydryl groups (-SH) which are involved in the formation of disulphide bridges (Figure 5.1). Furthermore, it has been postulated that these disulphide bonds function to stabilise the three dimensional intra-helical receptor structure (Baldwin, 1994). The orientation and folding of the receptor within the membrane is vital so that the ligand can gain entry into the TM domains and interact with the appropriate receptor residues in the ligand binding pocket.

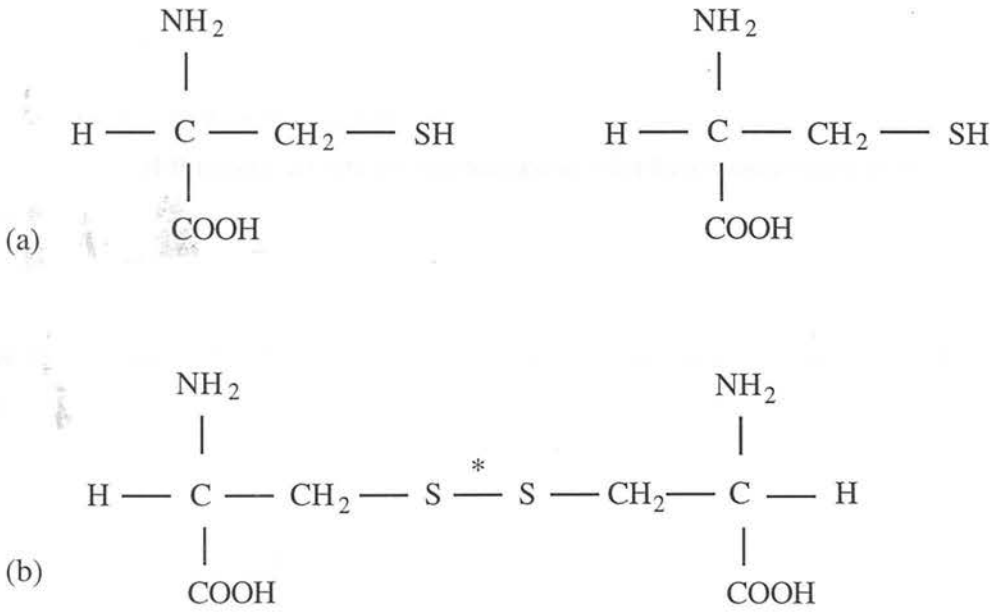

Figure 5.1 Structure of cysteine residues and the formation of disulphide bonds (a) Chemical structure of Cys residues showing their free sulfhydryl (SH) groups and (b) the formation of a disulphide bond (*) between closely positioned extracellular Cys residues.

The rat GnRH-R contains 4 extracellular Cys residues with two conserved residues positioned at Cys114 in the el between TM II and TM III (el 1) and Cys195 in the el between TM IV and TM V (el 2). The other two extracellular Cys residues occupy non-conserved positions at Cys14 and Cys199 in the NH_2 terminus and el 2 respectively. In order to investigate the role of extracellular Cys residues in the GnRH-R and examine their potential involvement in disulphide bond formation, all the GnRH-R extracellular Cys residues were replaced by Ser. The amino acids targeted for study are illustrated in Table 5.1. Figure 5.2 shows a schematic diagram of the GnRH-R highlighting the position of these four Cys residues together with their potential involvement in disulphide bond formation.

GnRH-R Mutant	TM Position	Amino acid modification
Cys14Ser	NH_2	C to S
Cys114Ser	el 1	C to S
Cys195 Ser	el 2	C to S
Cys199Ser	el 2	C to S

Table 5.1 GnRH-R Cys/Ser mutations

Amino acids in the GnRH-R targeted for site-directed mutagenesis and their corresponding amino acid substitutions.

To assess the functional role of these GnRH-R mutants, the mutant DNA was expressed in an *in vitro* culture system. COS-1 cells, a monkey kidney fibroblast cell line, were transiently transfected, with either the WT or mutant GnRH-R constructs and subsequently tested for their ability to bind a radiolabelled GnRH agonist (GnRH-A), and elicit an appropriate GnRH-induced second messenger response. Following the failure of the GnRH-R Cys to Ser mutations to produce any ligand binding response (see Results 5.2.1) it was decided, for comparison, to conduct a similar study in another pituitary peptide receptor, the TRH-R.

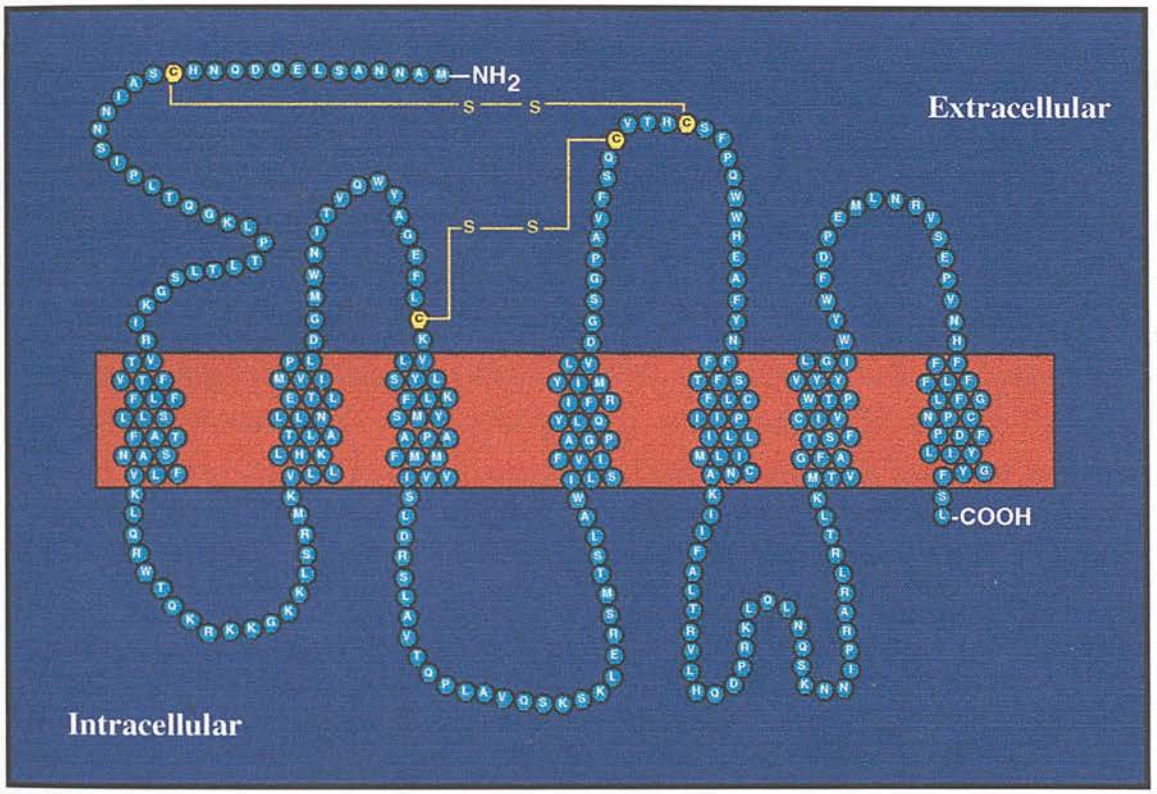

Figure 5.2 Structure of the rat pituitary GnRH-R

Schematic representation of the rat pituitary GnRH-R showing the classical heptahelical structure of a GPCR. Conserved extracellular Cys114 and Cys195 and non-conserved extracellular Cys14 and Cys199 are shown in putative disulphide bond formations.

The TRH-R provides a good comparative model as it has many similarities to the GnRH-R. TRH-R regulates the action of TRH, a hypothalamic neuropeptide, responsible for controlling the synthesis and release of TSH and PRL from the anterior pituitary gland (Metcalf and Jackson, 1989). Like the GnRH-R, ligand-induced activation of the TRH-R is mediated through the G-proteins, G_q and G_{11} (Aragay et al, 1992; Hsieh and Martin, 1992).

The rat TRH-R contains two conserved extracellular Cys residues, Cys98 (el 1) and Cys179 (el 2). In addition, another extracellular Cys residue lies in close proximity to Cys98 at position Cys100 at the el 1/TM III interface (Sellar et al, 1993). To assess the disulphide bonding role of TRH-R Cys residues, these amino acids were mutated to Ser (Cys98Ser, Cys179Ser and Cys100Ser). Furthermore, these sites were also mutated to Ala (Cys98Ala, Cys179Ala and Cys100Ala) as studies in rhodopsin revealed that substitution of extracellular Cys residues with non-polar amino acids maintains normal levels of receptor expression (Davidson et al, 1994). The amino acids targeted for study are summarised in Table 5.2 and their positions within the TRH-R are illustrated in Figure 5.3. A putative disulphide bonding interaction between the two conserved Cys residues, Cys98 and Cys179, together with the position of Cys100 at the el 1/TM III interface is highlighted (Figure 5.3).

TRH-R Mutant	TM Position	Amino acid modification
Cys98Ser	el 1	C to S
Cys179Ser	el 2	C to S
Cys100Ser	el 1/TM III	C to S
Cys98Ala	el 1	C to A
Cys179Ala	el 2	C to A
Cys100Ala	el 1/TM III	C to A

Table 5.2 TRH-R Cys/Ser and Cys/Ala mutations

Amino acids in the TRH-R targeted for site-directed mutagenesis and their corresponding amino acid substitutions.

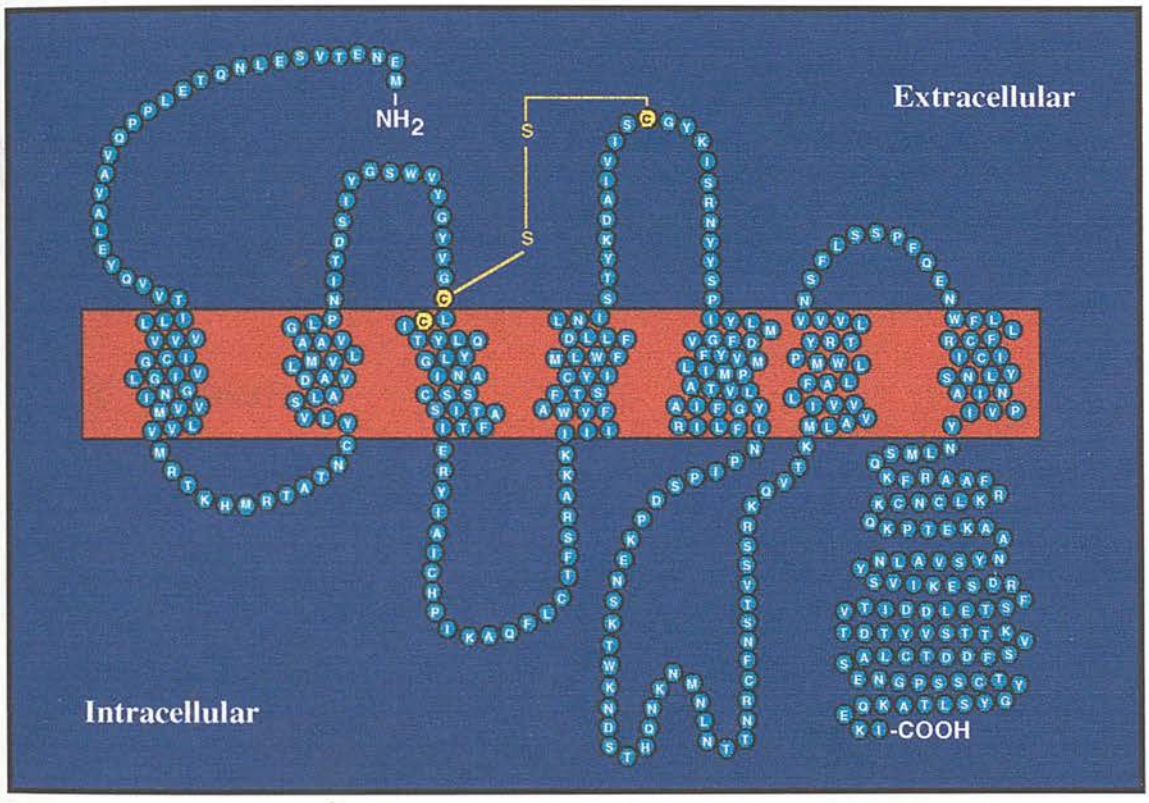

Figure 5.3 Structure of the rat pituitary TRH-R

Schematic representation of the rat pituitary TRH-R (the 411 amino acid long form) (Sellar et al, 1993) showing the classical heptahelical structure of a GPCR. Conserved extracellular Cys98 and Cys179 are highlighted in a putative disulphide bond formation. The position of the non-conserved extracellular Cys100 at the extracellular/ TM interface is also highlighted.

To complement the site-directed mutagenesis data, a further investigation into the role of extracellular Cys residues in TRH-R disulphide bonding interactions was carried out using the disulphide-reducing chemical agent dithiothreitol (DTT). In addition, as evidence suggests that Cys residues carrying free sulfhydryl groups (i.e. those not involved in disulphide bond formation) may also participate in receptor binding processes, parallel studies were conducted using p-chloromercuribenzoic acid (p-CMB) - a chemical compound that reacts with Cys residues carrying free sulfhydryl groups (Lu et al, 1993). The aim of these chemical modification studies was to investigate the effects of specific reagents on Cys residues, either those involved in disulphide bonding (using DTT) or Cys residues carrying free sulfhydryl groups (using p-CMB), and to determine how chemical modification interferes with normal receptor binding mechanisms.

5.2 Results

5.2.1 Cys residues in the GnRH-R

Scatchard analysis of competitive receptor binding assays revealed that the GnRH-R WT had a Kd (± SEM) value of 3.8 ± 0.38 nM and a B max (± SEM) value of 1.60 ± 0.49 pmol/mg protein (Figure 5.4).

Ligand-induced total IP production measurements, in COS-1 cells transiently expressing the GnRH-R WT, showed a two fold increase when stimulated with 1μM GnRH (Figure 5.5). In contrast, GnRH-R mutants Cys14Ser, Cys114Ser, Cys195Ser and Cys199Ser exhibited no receptor binding when compared to the WT and hence failed to display a ligand-induced second messenger response as shown in Figure 5.5.

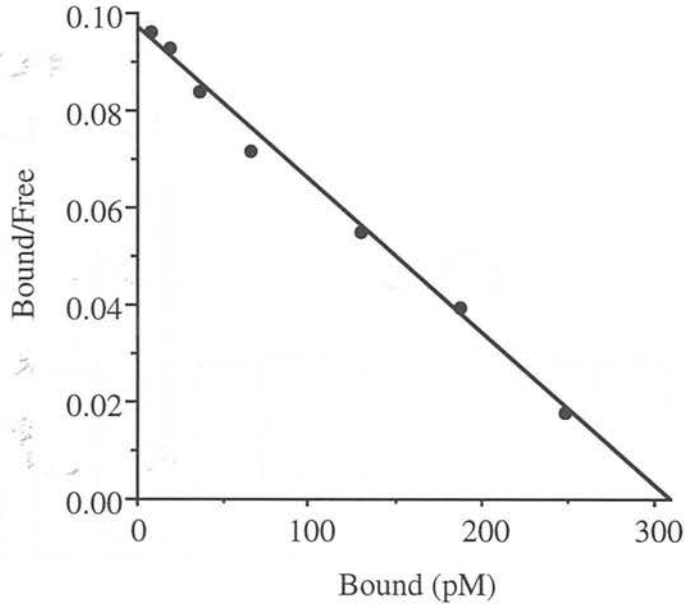

Figure 5.4 WT GnRH-R agonist binding data

Scatchard analysis of GnRH-A binding to COS-1 cells transiently expressing the WT GnRH-R. Competition receptor binding assays were performed using an iodinated GnRH-A [des Gly^{10}, D-Trp^{6}, Pro^{9} NEt]-GnRH on membrane preparations. Data points are the mean of duplicate/triplicate samples and the graph is a representative example from n=4 experiments.

Figure 5.5 GnRH-R WT and Cys/Ser mutants total inositol phosphate production (following page)

Total IP production in COS-1 cells transiently expressing the GnRH-R WT and mutants Cys14Ser, Cys114Ser, Cys195Ser and Cys199Ser. The open bars represent the basal stimulation following the addition of Buffer A only whilst the hatched bars represent IP production with 1μM GnRH. Each bar is the mean of duplicate/triplicate samples (± SEM) and the graph is an average of n=3 experiments.

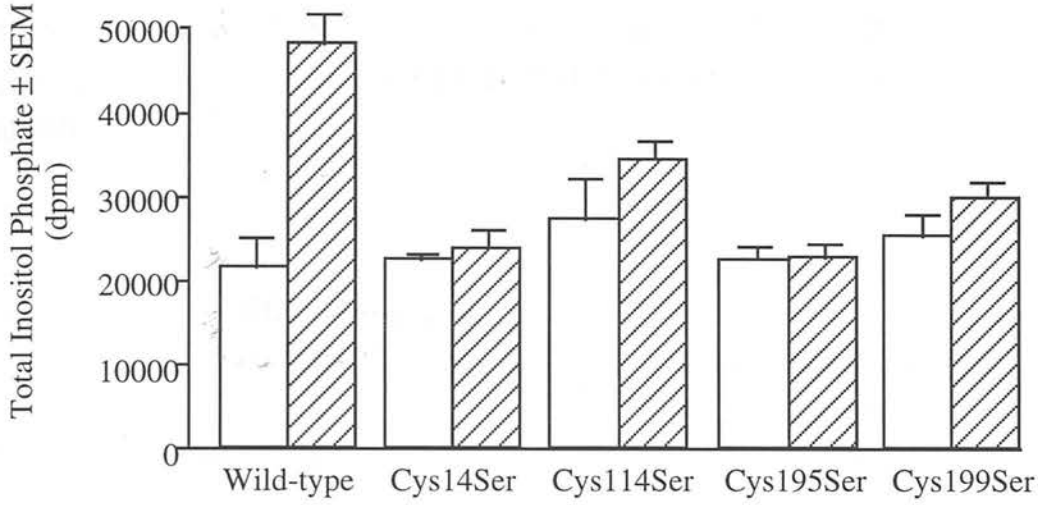

The Cys to Ser substitutions prevented ligand binding and receptor activation, indicating that extracellular Cys residues have an important role in receptor function. The loss of ligand-receptor binding displayed by GnRH-R mutants Cys14Ser, Cys114Ser, Cys195Ser and Cys199Ser probably arises from alterations in disulphide bonding patterns, resulting in destabilisation of the receptor's three dimensional extracellular structure.

In rhodopsin, substitution of Cys residues with hydrophilic Ser residues decreased levels of receptor expression (Karnik et al, 1988). Therefore, it is possible that the loss of receptor binding and second messenger coupling in the GnRH-R Cys/Ser mutations may reflect a lack of functionally active cell surface GnRH-Rs. The next logical step was hence to measure mutant GnRH-R expression levels, but at this stage a receptor specific antibody was unavailable. To overcome this problem it was decided to generate GnRH-R antibodies (see section 9.2.1). However, this proved more difficult then initially perceived and is still an ongoing project.

5.2.2 Cys residues in the TRH-R

The Kd and B max of TRH-R mutants Cys100Ser and Cys100Ala, calculated from displacement curves (Figure 5.6), were comparable to WT (Table 5.3) and both these mutants showed WT levels of ligand-induced total IP production (Figure 5.7 a and b). TRH-R mutants Cys98Ser, Cys179Ser, Cys98Ala and Cys179Ala expressed in COS-1 cells showed no ^{3}H[3-Me-His^{2}]-TRH (TRH-A) receptor binding when compared with WT.

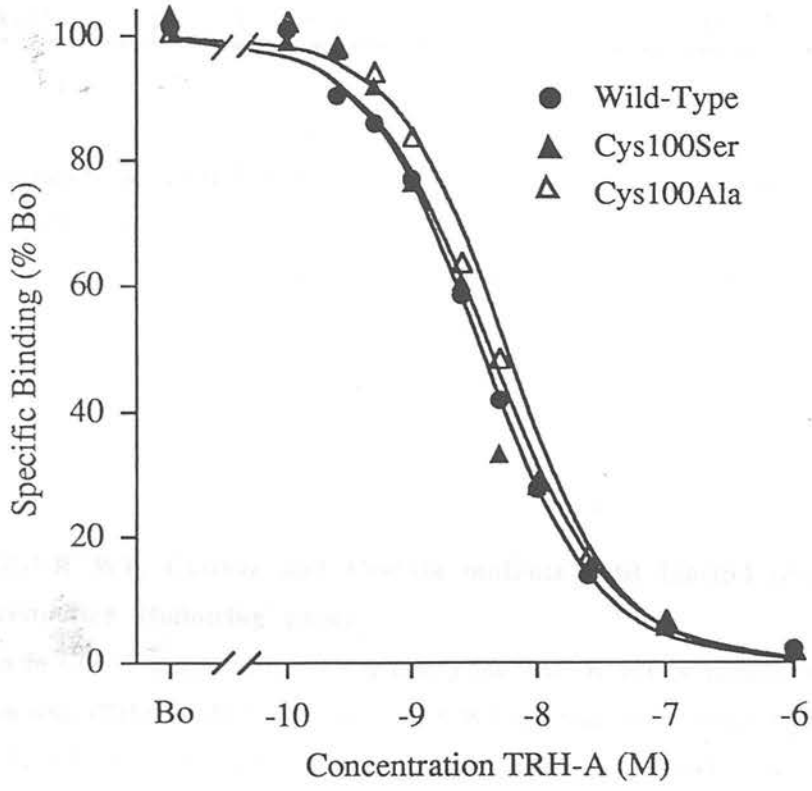

Figure 5.6 TRH-R WT and Cys100 mutants agonist binding data

Displacement of ^{3}H[3-Me-His^{2}]-TRH (500pM) binding to COS-1 cell membranes transiently expressing the TRH-R wild-type or mutants Cys100Ser and Cys100Ala by unlabelled [3-Me-His^{2}]-TRH (0.1nM to 1μM). Data points represent the mean of duplicate/triplicate samples and the graph is a representative example from n=3 individual experiments.

TRH-R Construct	Kd ± SEM (nM)	B max ± SEM (pmol/mg protein)
Wild-Type	2.73 ± 0.68	2.13 ± 0.80
Cys98Ser	no binding	—
Cys98Ala	no binding	—
Cys179Ser	no binding	—
Cys179Ala	no binding	—
Cys100Ser	2.23 ± 0.22	1.79 ± 0.75
Cys100Ala	3.56 ± 0.42	1.40 ± 0.55

Table 5.3 Summary of TRH-R WT, Cys/Ser and Cys/Ala mutant binding data

Table summarising TRH-R binding assay data. Receptor dissociation constant (Kd) and receptor number (B max) were calculated from Scatchard analysis of competition receptor binding assays. Kd and B max values are the average ± SEM of at least n=3 individual experiments.

Figure 5.7 TRH-R WT, Cys/Ser and Cys/Ala mutants total inositol phosphate production (following page)

Total IP production in COS-1 cells transiently expressing the TRH-R WT or mutant receptors following stimulation with TRH (100pM-10mM) (**a**) TRH-R WT and mutants Cys98Ser, Cys179Ser, and Cys100Ser (**b**) TRH-R WT and mutants Cys98Ala, Cys179Ala and Cys100Ala. Untransfected COS-1 cells were used as a negative control. Data points represent the mean of duplicate/triplicate samples and the graph is a representative example from n=3 individual experiments.

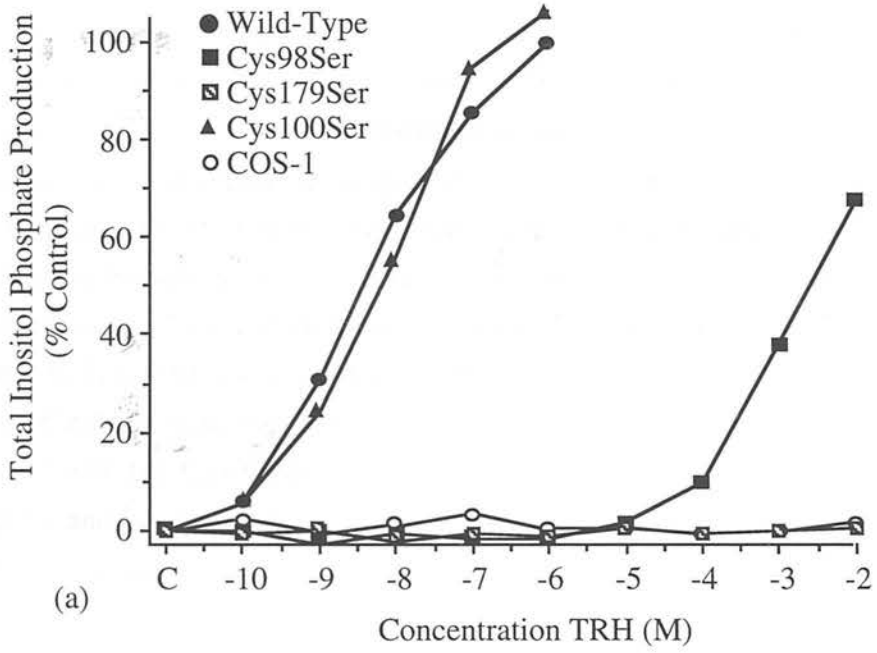
Wild-Type
Cys98Ser
Cys179Ser
Cys100Ser
COS-1
Total Inositol Phosphate Production
(% Control)
100
80
60
40
20
0
C
-10
-9
-8
-7
-6
-5
-4
-3
-2
Concentration TRH (M)

(a)

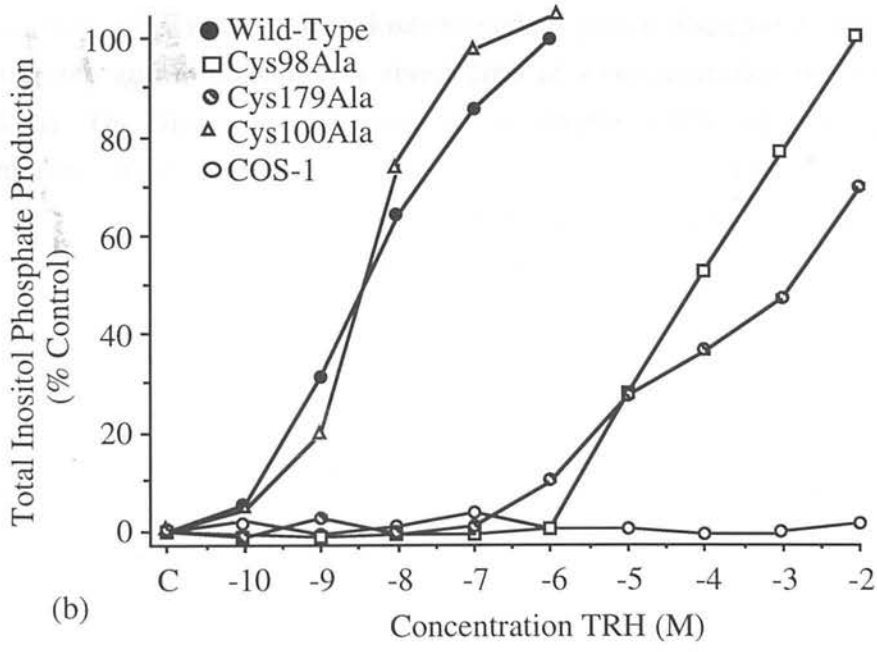
Wild-Type
Cys98Ala
Cys179Ala
Cys100Ala
COS-1
Total Inositol Phosphate Production
(% Control)
100
80
60
40
20
0
C
-10
-9
-8
-7
-6
-5
-4
-3
-2
Concentration TRH (M)

(b)

These results were similar to those obtained for the GnRH-R, but again the lack of receptor-specific antibodies hindered the measurement of receptor expression levels. However, experiments by Gershengorn and co-workers have overcome these problems by measuring TRH-R mutant IP responses in the presence of high concentrations of TRH (Perlman et al, 1994a,b; 1995). Their results have shown that it is possible to elicit a functional response in some mutant receptors, with non-detectable levels of receptor binding, using concentrations of stimulating ligand between 1μM and 10mM. Furthermore, from these experiments the potency of mutant receptors can be estimated. A similar experiment was thus conducted in the six TRH-R mutant constructs. The EC50 values of total IP stimulation by TRH for cells expressing WT, Cys98Ser, Cys98Ala and Cys179Ala were 0.004μM, 1000μM, 60μM and 60μM respectively. Maximum levels of IP stimulation were 70% for Cys98Ser, 100% for Cys98Ala and 70% for Cys179Ala when compared to WT (Figure 5.7 a and b). In contrast, Cys179Ser showed no IP stimulation with TRH at any of the concentrations used (Figure 5.7a).

The chemical modification studies (with DTT and p-CMB) were conducted using cell membranes prepared from either COS-1 cells transiently expressing the TRH-R or from a stably expressing cell line, HEK-293 E2 cells (as both cell types gave similar results in receptor binding experiments). Cell membranes were either pre-treated with each of the reagents for 30 minutes on ice (pre-equilibrium), or added to the receptor binding assay after equilibrium had been reached (post-equilibrium). Pre-incubation of membranes with DTT resulted in a dose-dependent partial decrease of radiolabelled TRH-A binding and inhibition was about 20% at a concentration of 20mM DTT (Figure 5.8a). The effects of DTT were fully reversible as WT values were restored after membranes were washed with assay buffer. Addition of DTT for 30 minutes to the receptor binding assay, post-equilibrium, did not alter the dose-dependent decrease in TRH-A receptor binding when compared to membrane pre-treatment (Figure 5.8a). Following pre-treatment of membranes with p-CMB, a dose-dependent decrease in specific binding of TRH-A was observed (Figure 5.8b). The action of p-CMB was irreversible as removal of the chemical agent, by washing membranes twice in assay buffer, did not significantly alter the dose response profile. However, addition of p-CMB for 30 minutes, post-equilibrium, at concentrations of 0.1mM and higher was significantly less effective in reducing specific binding relative to the pre-incubated membrane treatment (Figure 5.8b). Non-specific binding was not affected in these experiments.

Figure 5.8 Chemical modification of the rat TRH-R WT (following page)

(a) The effect of DTT on ^{3}H[3-Me-His^{2}]-TRH (250pM) binding to HEK-293 E2 cell membranes (20-50μg total protein) expressing the rat TRH-R. Membranes were pre-treated for 30 minutes on ice with DTT (1mM to 20mM) (open bars) before addition to the assay or the DTT added for 30 minutes after the assay had reached equilibrium (hatched bars). Assays were incubated for 2 hours at 4°C and the data points represent the mean of duplicate/triplicate samples ± SEM.

(b) The effect of p-CMB on ^{3}H[3-Me-His^{2}]-TRH (250pM) binding to HEK-293 E2 cell membranes (20-50μg total protein) expressing the rat TRH-R. Membranes were pre-treated for 30 minutes on ice with p-CMB (0.01mM to 0.5mM) (open bars) before addition to the assay or the p-CMB added for 30 minutes after the assay had reached equilibrium (hatched bars). Assays were incubated for 2 hours at 4°C and the data points represent the mean of duplicate/triplicate samples ± SEM.

p values represent * $p<0.05$ and ** $p<0.01$.

Saturation analysis of TRH-A binding was conducted in the absence or presence of p-CMB (0.05mM) or DTT (20mM). Membranes were incubated with buffer (control) or in the presence of these reagents for 30 minutes before the addition of radiolabelled TRH-A in the range 40-8000pM. Receptor number for DTT-treated membranes was significantly reduced (B max ± SEM of 3.8 ± 0.2 pmol/mg protein, $p<0.05$), while receptor affinity (Kd ± SEM = 4.5 ± 1.0) was comparable to control values. The presence of p-CMB decreased receptor number values (B max ± SEM of 2.3 ± 0.2 pmol/mg protein, $p< 0.01$) compared to control values (B max ± SEM of 4.8 ± 0.6 pmol/mg protein). Receptor affinity (Kd ± SEM = 5.0 ± 0.7) was not significantly different when compared to the control (Kd ± SEM = 3.8 ± 0.5).

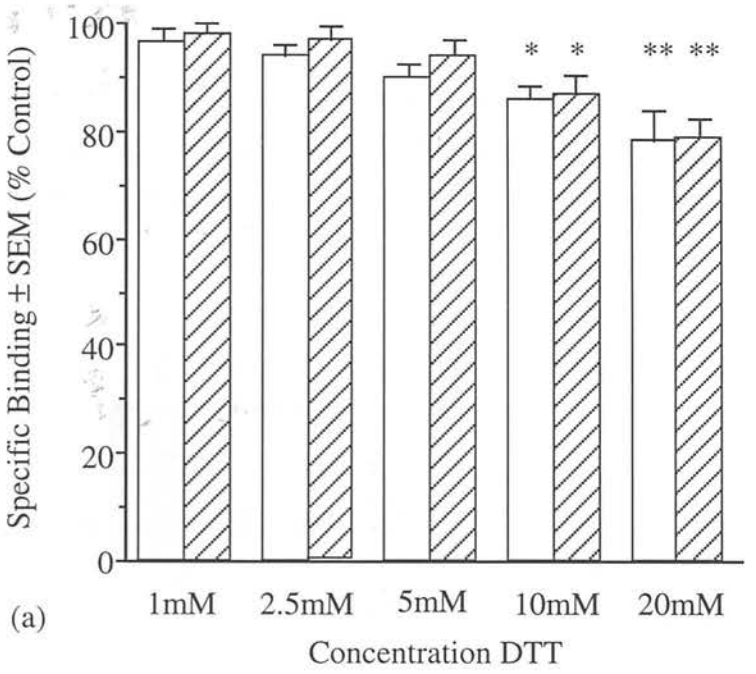
Specific Binding ± SEM (% Control)
100
80
60
40
20
0
* *
** **
1mM
2.5mM
5mM
10mM
20mM
Concentration DTT

(a)

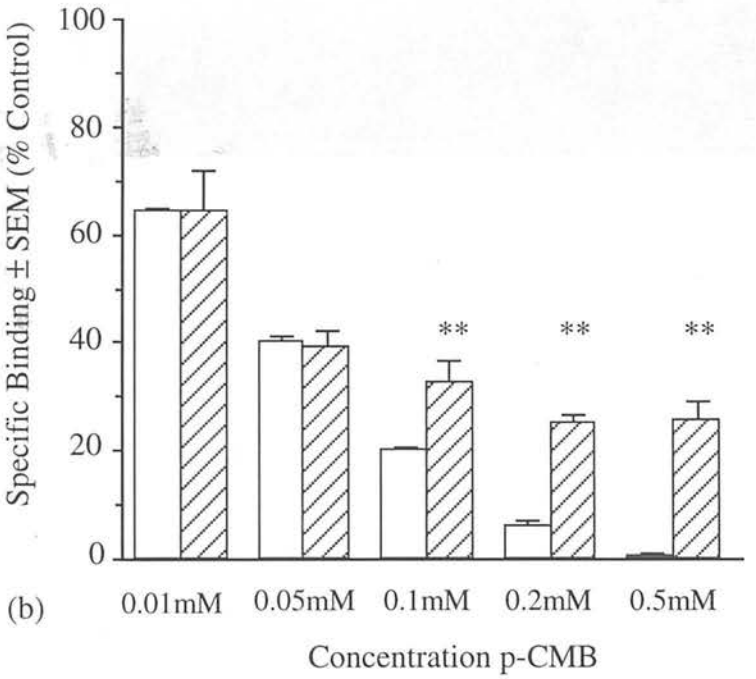
Specific Binding ± SEM (% Control)
100
80
60
40
20
0
** ** **
0.01mM
0.05mM
0.1mM
0.2mM
0.5mM
Concentration p-CMB

(b)

Northern Blot analysis was used to compare the expression of TRH-R mutant RNA with WT RNA. Figure 5.9 shows a Northern Blot of total RNA extracted from COS-1 cells transiently expressing the WT and mutant TRH-Rs. RNA extracted from HEK-293 E2 cells is a positive control and RNA from untransfected HEK-293 and COS-1 cells are negative controls. The size of the TRH-R mRNA transcript is approximately 4 kb (Figure 5.9a). Hybridisation of a radiolabelled 18S oligonucleotide probe with a 1.9 kb band corresponding to 18S RNA showed equivalent amounts of RNA were loaded into each well (Figure 5.9b).

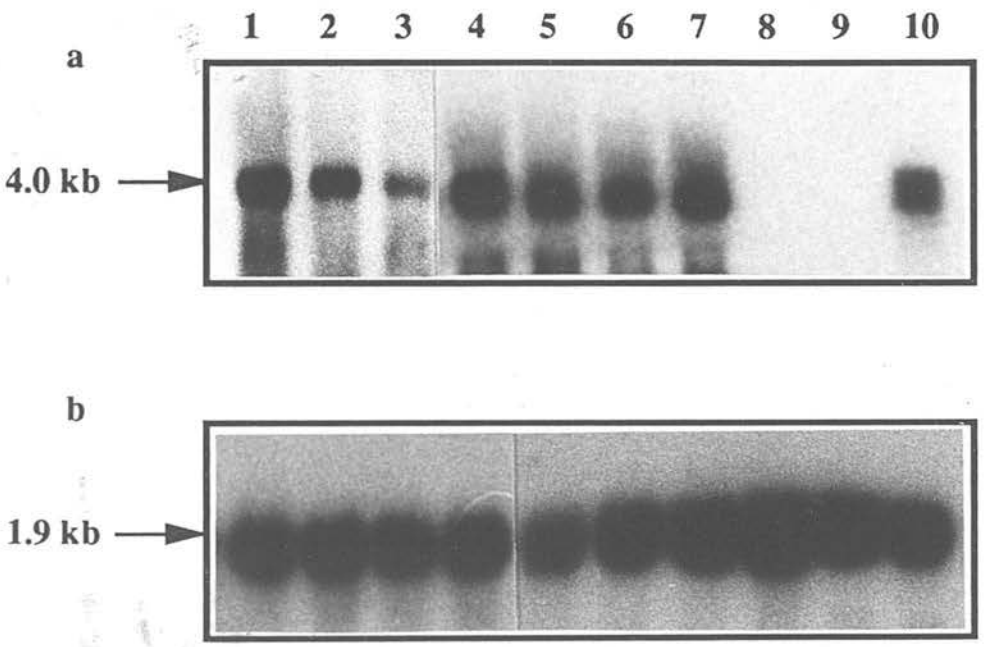

Figure 5.9 Northern Blot of TRH-R WT, Cys/Ser and Cys/Ala mutants

(a) Northern blot probed with a [^{32}P]αdCTP labelled 2.5 kb rat TRH-R insert showing RNA expression levels in total RNA (15μg) from COS-1 cells transiently expressing TRH-R Cys mutations (Cys100Ala, Cys179Ala, Cys98Ala, Cys100Ser, Cys179Ser, Cys98Ser) (lane 1-6), wild-type (lane 7), untransfected COS-1 cells (lane 8), and HEK-293 cells (lane 9), and HEK-293E2 cells (lane 10).

(b) Northern Blot probed with [^{32}P]γ dATP labelled anti-18S oligonucleotide to check for the presence of even RNA loading in the corresponding wells.

Experiments were carried out on at least n=3 independent occasions using different batches of RNA.

5.3 Discussion

Sequence alignment of over 200 members of the GPCR family show that there are two conserved Cys residues found in el 1 and el 2 of 92% of these receptors (Baldwin, 1994; Probst et al, 1992). In the GnRH-R, these conserved Cys residues are found at Cys114 in el 1 and Cys195 in el 2. Another pair of non-conserved Cys residues are also present in the el domains at Cys14 in the NH_2 terminus and Cys199 in the el 2 (Eidne et al, 1992). Extracellular GPCR Cys residues, potentially involved in disulphide bridge formation, are thought to be important in stabilising three dimensional receptor conformation and facilitating ligand-induced receptor activation (Baldwin, 1994). Substitution of these Cys residues with other amino acids should prevent disulphide bond formation and therefore destabilise the tertiary receptor structure. This receptor destabilisation may alter the path of the ligand to its recognition site within the TM domain or disrupt the recognition site itself, resulting in a loss of binding activity.

In the GnRH-R, substitution of Cys14, Cys114, Cys195 and Cys199 with Ser residues resulted in a loss of measurable ^{125}I GnRH-A binding and this may be due to prevention of disulphide bridge formation. Furthermore, the failure of all four Cys/Ser mutations to bind GnRH suggests the presence of at least two disulphide bonds.

The loss of receptor binding activity displayed by the GnRH-R Cys to Ser mutants may also reflect a decrease in mutant receptor expression. To address this possibility, GnRH-R antibodies were developed. However, the initial antibodies raised against the GnRH-R, in the rabbit, proved non-specific. A different strategy using epitope tagging has now been adopted. A hemagglutinin (HA) epitope tag sequence has been positioned at the amino acid terminus of the GnRH-R WT sequence. The receptor binding and second messenger properties of the HA-tagged GnRH-R have been characterised and suitable detection methods established. Presently, this tag construct is being incorporated into the GnRH-R Cys/Ser mutations to monitor levels of cell surface GnRH-R protein (see section 9.2.3).

The role of extracellular Cys residues in the TRH-R was also examined using site-directed mutagenesis and chemical modification studies. The decision to investigate the function of these residues was based on the following. Firstly, the majority of work regarding GPCR extracellular Cys residues, and their role in disulphide bridge formation, has been carried out on catecholamine receptors and rhodopsin, with very few studies in peptide receptors. The TRH-R is a pituitary peptide receptor, displaying similar receptor coupling properties to the GnRH-R, and hence makes an ideal comparative model. Secondly, receptor expression levels can be monitored in TRH-R mutants lacking receptor binding function by measuring second messenger production in the presence of high concentrations of stimulating ligand. A method of monitoring levels of mutant receptor expression, in the absence of a specific TRH-R antibody, has been described by Gershengorn and co-workers (Perlman et al, 1994a, b; 1995). These workers have mutated a number of sites within the ligand binding pocket of the TRH-R. Some of these mutant receptors exhibit very low affinities for TRH analogues and thus are difficult to measure in binding experiments. For such mutants, relative affinities were assessed by measuring potencies of second messenger stimulation, and the magnitude of the TRH-stimulated IP responses directly correlated to levels of TRH-R expression. Attempts to utilise this experimental approach in the GnRH-R Cys to Ser mutants was hampered due to low levels of receptor expression. For this reason, GnRH-stimulated IP responses could not be correlated to levels of GnRH-R expression.

In the TRH-R, conserved extracellular Cys residues are found at Cys98 in el 1 and Cys179 in el 2. Another Cys, Cys100, is located at the el 1/TM III interface (Sellar et al, 1993). Substitution of Cys98 and Cys179 to either Ser or Ala resulted in a loss of measurable TRH-A binding. The relative affinity of Cys98Ser, Cys179Ser, Cys98Ala and Cys179Ala TRH-R mutants was assessed by measuring the potencies of TRH-stimulated IP second messenger production. The potency of these mutants was shown to decrease by 4-5 orders of magnitude. Cys179Ser showed no IP production at any of the concentrations used and this may be representative of a loss of receptor expression. Alternatively, as Cys179 is located in the middle of the el 2 any structural alterations in this region may affect the three dimensional folding of the receptor.

Substitution of Cys98 and Cys179 to Ser showed a decrease in maximum TRH-induced IP formation compared to their Cys to Ala counterparts. This may result from the hydrophilic nature of the Ser residue. The choice of substituting residue appears

critical in site-directed mutagenesis studies. Extracellular Cys residues are commonly replaced with hydrophilic Ser residues and these have been shown to impair receptor expression in the muscarinic receptor (Savarese et al, 1992) and in rhodopsin (Karnik et al, 1988). A further study in rhodopsin (Davidson et al, 1994), mutating the Cys residues to non-polar Ala, demonstrated a protein with normal expression levels but a defective signal transduction pathway. The function of disulphide bridge formation in rhodopsin therefore appears to be the stabilisation of the active receptor state. In this study, both extracellular Cys to Ala substitutions resulted in higher expression levels of the receptor protein when compared to Cys to Ser mutations. Northern Blot analysis of Cys to Ser and Cys to Ala TRH-R mutants showed similar expression of all these mutants at the RNA level, indicating that translational and/or post-translational factors could be responsible for the observed results. The level of protein cell surface receptor expression displayed by these mutant receptors has now also been carried out (See Appendix V).

TRH-R mutants at the extracellular/membrane interface, Cys100Ser and Cys100Ala, did not affect the receptor binding site as receptor binding parameters and signal transduction measurements were similar to the WT receptor. Although Cys100 lies in close proximity to Cys98, its position close to the TM domain makes it an unlikely candidate for extracellular disulphide bridge formation.

Covalent chemical modification of proteins with reagents specific for Cys residues can be a useful approach to examine structure-function relationships in GPCRs. DTT, a disulphide-reducing agent, and p-CMB, a sulfhydryl-modifying agent, were used to further investigate the role of extracellular disulphide bond formation and free sulfhydryl groups respectively (Fonseca et al, 1991; Lu et al, 1993). The effects of DTT in both pre- and post-equilibrium studies resulted in a small reduction in binding which was due to an apparent loss in receptor numbers. These effects were fully reversible following removal of DTT. The modest effect of DTT suggests that the disulphide bridge could be buried within the TM domain and therefore not fully accessible to the action of this reducing reagent. Studies carried out with rhodopsin (Karnik and Khorana, 1990) and the α_2 adrenergic receptor (Parini et al, 1987) have showed that prior treatment with denaturants could greatly enhance the effects of DTT.

Modification of sulfhydryl groups in the TRH-R with p-CMB resulted in a loss of specific receptor binding. Scatchard analysis carried out in the presence of 0.05M p-

CMB revealed that there was a loss of available receptor binding sites. Both pre- and post-equilibrium incubations with p-CMB resulted in an irreversible reduction of TRH analogue binding, in a dose-dependent manner. However, there was a greater loss of specific binding following pre-equilibrium incubations with p-CMB at concentrations of 0.1mM and above. Incubation of the membranes with [3-Me-His^2]-TRH therefore conveys some protection against the action of p-CMB. In the rat TRH-R there are a total of 16 Cys residues, 14 of which are potentially available for modification by p-CMB (the Cys residues involved in disulphide bridge formation would be unavailable) and 7 lie within the TM domains. If the ligand is bound to the receptor prior to the addition of p-CMB, the receptor will have adopted a ligand-activated conformational state and therefore not all these Cys residues may be available for modification. A model of the ligand binding pocket within the TM domains, involving Tyr106, Asn110, Arg283 and Arg306 has been proposed by Perlman et al, 1994a, b; 1995. TRH binding within this site could conceivably block the action of p-CMB on the free sulfhydryl groups of Cys residues lying in close proximity to the active site.

In summary, site-directed mutagenesis evidence suggests that disulphide bonding interactions occur between the extracellular Cys residues Cys14, Cys114, Cys 195 and Cys199 in the GnRH-R. Site-directed mutagenesis and chemical modification studies in the TRH-R provide further evidence that extracellular Cys residues (Cys98 and Cys179) are involved in a disulphide bonding interaction. Extracellular disulphide bridges appear important in maintaining the correct tertiary structure of the receptor and therefore hold the receptor in a conformational state to permit ligand-receptor interactions. Chemical modification of other TRH-R Cys residues suggests that some of the TM located residues may lie in close proximity to the TRH recognition site.

This chapter has investigated the role of conserved extracellular Cys residues in GPCRs. The following chapter (Chapter 6) focuses on the role of two uniquely positioned TM domain residues, Asn87 and Asp318, in GnRH ligand binding and receptor activation mechanisms.

6 Role of amino acids Asn87 and Asp318 in the GnRH-R

6.1 Introduction

The rat GnRH-R despite its structural homology to other GPCRs exhibits some unique features. These differences include the replacement of a highly conserved Asp residue in TM II with an Asn, Asn87. This charged residue has been shown to be important in mediating receptor binding in monoamine receptors (Strader et al, 1988) as well as in receptor coupling (Probst et al, 1994). The reverse substitution occurs in TM VII where a highly conserved Asn residue is replaced by an Asp, Asp318, suggesting that the function performed by these residues is transposed. Therefore to investigate the role of these amino acids and determine whether this apparent amino acid inversion has a specific functional role, site-directed mutagenesis experiments were carried out. Two single mutations substituting Asn87 to Asp (Asn87Asp) and Asp318 to Asn (Asp318Asn) were generated together with a double mutation in which both these sites were substituted simultaneously to recreate the situation observed in the majority of other GPCRs (Asn87AspAsp318Asn). The amino acids targeted are summarised in Table 6.1.

GnRH-R Mutant	TM Position	Amino acid modification
Asn87Asp	TM II	N to D
Asp318Asn	TM VII	D to N
Asn87AspAsp318Asn	TM II and TM VII	N to D and D to N

Table 6.1 GnRH-R Asp/Asn mutations

Amino acids targeted for site-directed mutagenesis and their corresponding amino acid substitutions.

6.2 Results

6.2.1 GnRH-R Asp/Asn mutations

Alignment between various GPCRs shows the GnRH-R to be virtually unique in its possession of an Asn87 residue in TM II and an Asp318 residue in TM VII (Table 6.2).

Receptor	Species	TM II	TM VII
GnRH-R	Rat	VLLKHLTLA N LLETLIVMPL	LNPCF D PLIYGYF
GnRH-R	Mouse	VLLKHLTLA N LLETLIVMPL	LNPCF D PLIYGYF
GnRH-R	Human	LLLKHLTLA N LLETLIVMPL	LNPCF D PLIYGYF
TRH-R	Mouse	CYLVSLAVA D LMVLVAAGLP	-NSAI N PVIYNLM
TRH-R	Rat	CYLVSLAVA D LMVLVAAGLP	-NSAI N PVIYNLM
Dopamine D1-R	Rat	FFVISLAVS D LLVAVLVMPW	ANSSL N PIIYAF-
B Adrenergic-R	Human	YFITSLACA D LVMGLAVVPF	VNSGF N PLIYCR-
B Adrenergic-R	Rat	YFITSLACA D LVMGLAVVPF	VNSAF N PLIYCR-
B Adrenergic-R	Hamster	YFITSLACA D LVMGLAVVPF	VNSAF N PLIYCR-
Substance P	Rat	YFLVNLAFA E ACMAAFNTVV	SSTMY N PIIYCCL
Substance K	Rat	YFIVNLALA D LCMAAFNAAA	SSTMY N PIIYCCL
Cannabinoid-R	Rat	HFIGSLAVA D LLGSVIFVYS	LNSTV N PIIYALR
Endothelin B-R	Rat	ILIASLALG D LLHIIIDIPI	LNSCI N PIAL-YL
Endothelin ET1-R	Rat	ALIASLALG D LIYVVIDLPI	MNSCI N PIAL-YF
Bombesin-R	Rat	LFISSLALG D LLLLVTCAPV	TNSCV N PFAL-YL

Table 6.2 Position of conserved TM II Asp residue and TM VII Asn residue in GPCRs

Alignment of the amino acid sequences in TM II and TM VII regions of members of the GPCR family. The position of Asn87 (N) in TM II and Asp318 (D) in TM VII is virtually unique to the GnRH-R.

Scatchard analysis of competition receptor binding assays revealed that the GnRH-R WT and mutant Asp318Asn have similar receptor affinities with Kd values (± SEM) of 3.8 ± 0.38 nM and 3.9 ± 0.03 nM respectively (Table 6.3). The B max value (± SEM) of mutant Asp318Asn was 1.65 ± 0.63 pmol/mg protein, similar to the 1.60 ± 0.49 pmol/mg protein value calculated for the WT receptor. The displacement of radiolabelled GnRH-A with unlabelled GnRH-A is illustrated in Figure 6.1. Unlabelled native GnRH peptide was also used to displace the iodinated GnRH-A (Figure 6.1) and a ratio of the ED50 values (ED50 GnRH : ED50 GnRH-A) of 10.1 and 13.4 were calculated for the WT (Figure 6.1a) and Asp318Asn (Figure 6.1b) respectively.

GnRH-R Construct	**Kd ± SEM (nM)**	**B max ± SEM (pmol/mg protein)**
Wild-Type	3.8 ± 0.38	1.60 ± 0.49
Asn87Asp	no binding	—
Asp318Asn	3.9 ± 0.03	1.65 ± 0.63
Asn87AspAsp318Asn	no binding	—

Table 6.3 Summary of GnRH-R WT and Asp/Asn mutant agonist binding data

Table summarising receptor binding assay data. Receptor dissociation constant (Kd) and receptor number (B max) were calculated from Scatchard analysis of competitive receptor binding assays. Kd and B max values are the average ± SEM of at least n=3 individual experiments.

Figure 6.1 GnRH-R WT and Asp318Asn mutant agonist binding data (following page)

Displacement curves of GnRH-A binding to (a) GnRH-R WT and (b) mutant Asp318Asn. Competitive binding assays were performed using an iodinated GnRH-A [des Gly^{10}, D-Trp^{6}, Pro^{9} NEt]-GnRH, in the presence of different concentrations of either cold GnRH-A or GnRH, on membrane preparations from COS-1 cells transiently expressing the GnRH WT or Asp318Asn. Specific binding is expressed as a % of the maximum binding (Bo) minus the non-specific binding (NSB). Data points are the mean of triplicate samples and the graphs are representative examples from at least n=3 individual experiments.

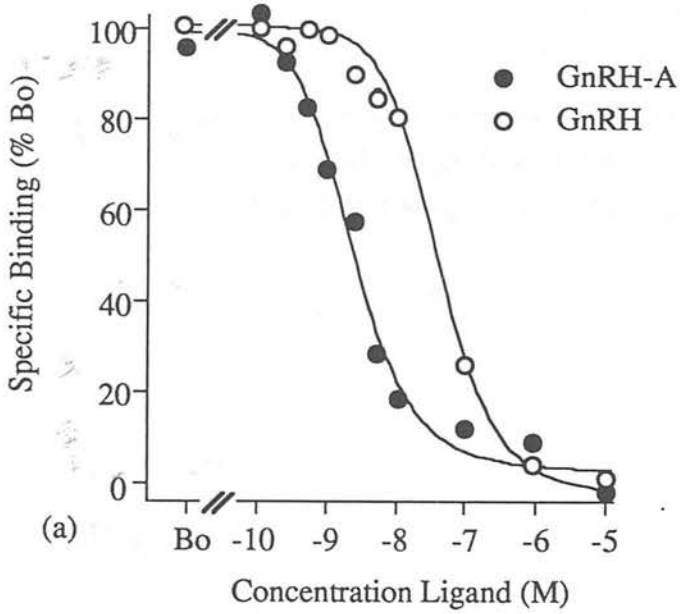
Specific Binding (% Bo)
100
80
60
40
20
0
GnRH-A
GnRH
(a)
Bo -10 -9 -8 -7 -6 -5
Concentration Ligand (M)

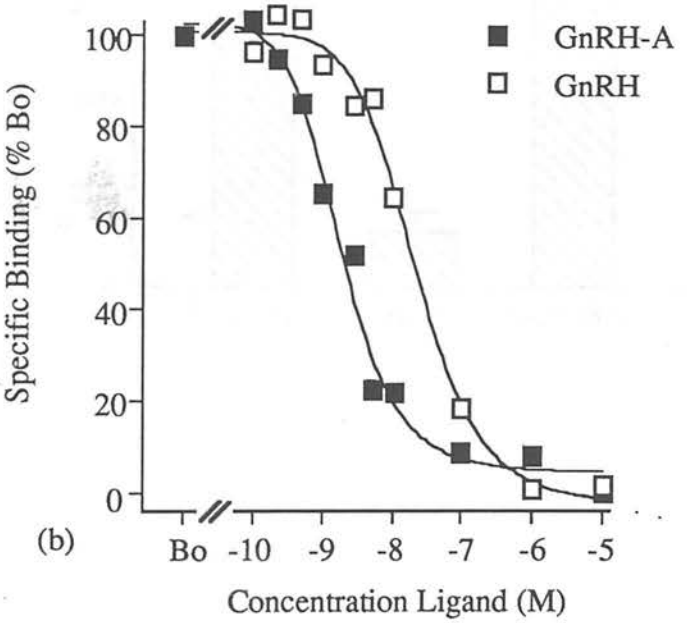
Specific Binding (% Bo)
100
80
60
40
20
0
GnRH-A
GnRH
(b)
Bo -10 -9 -8 -7 -6 -5
Concentration Ligand (M)

Both the WT GnRH-R and Asp318Asn also showed similar levels of specific binding when membrane preparations were incubated with the radiolabelled GnRH antagonist ^{125}I [Ac-3,4-dehydro-Pro^{1}-D-p-F-Phe^{2},D-Trp^{3,6}]-GnRH as illustrated in Figure 6.2. In contrast, COS-1 cells transiently expressing the GnRH-R single mutant Asn87Asp and the double mutation, Asn87AspAsp318Asn, exhibited no GnRH-A binding (Figure 6.2). These mutants also showed no significant GnRH-An binding compared to WT. Table 6.3 summarises the GnRH-R agonist binding data for the WT and receptor mutants.

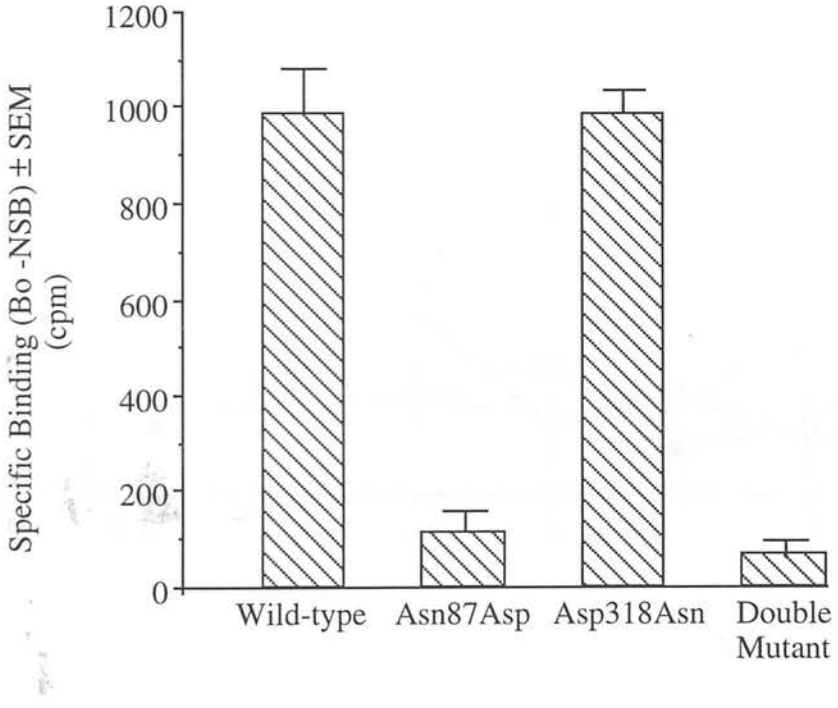

Figure 6.2 GnRH-R WT and Asp/Asn mutants antagonist binding data

Specific binding of the GnRH-An ^{125}I [Ac-3,4-dehydro-Pro^{1}-D-p-F-Phe^{2},D-Trp^{3,6}]-GnRH to membrane preparations of COS-1 cells transiently transfected with GnRH-R WT or mutants Asn87Asp, Asp318Asn and Asn87AspAsp318Asn. Specific binding is expressed as maximum binding (Bo) minus non-specific binding (NSB). Data points are the mean of triplicate samples and the graph represents the average of n=2 individual experiments.

Second messenger function of the WT and mutant receptors was ascertained through the measurement of GnRH-stimulated total IP production (Figure 6.3). COS-1 cells transiently expressing the WT receptor displayed a GnRH-induced dose-dependent increase in total IP accumulation. However, both single mutants, Asn87Asp and Asp318Asn, together with the double mutation failed to produce an IP response when stimulated with GnRH (10 pM-1 μM).

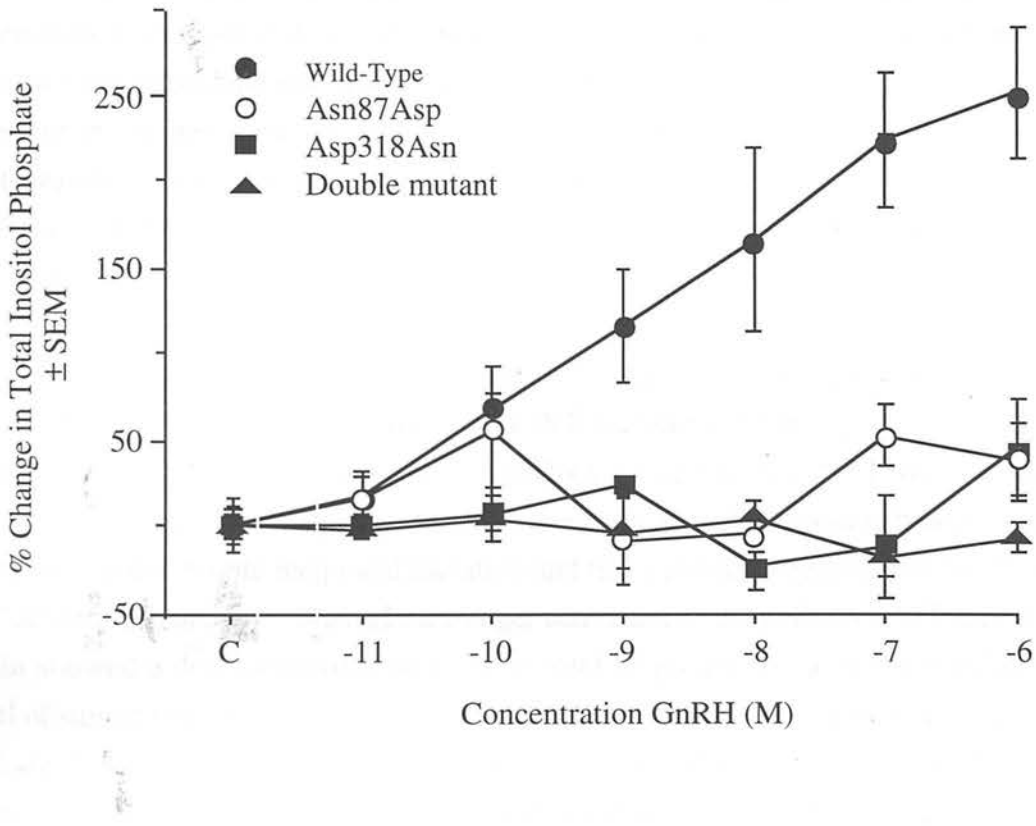

Figure 6.3 GnRH-R WT and Asp/Asn mutants total inositol phosphate production

Total IP production in COS-1 cells transiently expressing the GnRH-R WT or mutants Asn87Asp, Asp318Asn and Asn87AspAsp318Asn following stimulation with GnRH (10 pM-1 μM). Untransfected COS-1 cells used as a negative control (data omitted for clarity) showed only basal stimulation at all concentrations of GnRH. Data points are the mean of triplicate samples (± SEM) and the graph is a representative example from n=3 individual experiments.

6.2.2 Improving expression levels in GnRH-R Asn/Asp mutant

In general the maximum levels of receptor binding and second messenger total IP production observed in the WT GnRH-R were quite low. To improve the transfection efficiency several alternative chemical transient transfection methods were tested. These included $CaPO_4$ (Sambrook et al, 1989), DEAE-Dextran (Sambrook et al, 1989) and lipofectamine (GIBCO BRL). In addition, pilot studies utilising a non-chemical method of DNA incorporation, electroporation, (Andreason and Evans, 1988) were also carried out. All of the above DNA transfer methods proved ineffective in increasing receptor expression levels and therefore attention was focused on an alternative vector expression system. Studies this far, utilised the eukaryotic expression vector pcDNA 1. The WT, Asp318Asn and the double mutant were subsequently subcloned into a new vector, pcDNA 3 (Invitrogen), with a reportedly stronger promoter activity and hence potentially higher expression levels. Furthermore, a new transfection reagent, Transfectam (Promega), when used together with the pcDNA 3 expression system resulted in a three-fold increase in receptor expression levels.

The results using the new expression system were largely similar to those described in section 6.2.1. The binding properties of the WT receptor and the Asp318Asn mutant were comparable to those observed using pcDNA 1 (see Figure 6.4). However, with the improved expression system a small amount of specific receptor binding was detectable in the double reciprocal mutation and this equated to approximately 5% of WT activity (Figure 6.4). Second messenger activation of the pcDNA 3 WT receptor again showed a dose-dependent increase in total IP production with the maximum level of stimulation at 1μM approximately seven-fold that of the basal value (compared with the 2-3 fold stimulation above basal levels seen in the WT receptor in pcDNA 1). None of the receptor mutants showed a GnRH-induced total IP production (Figure 6.5).

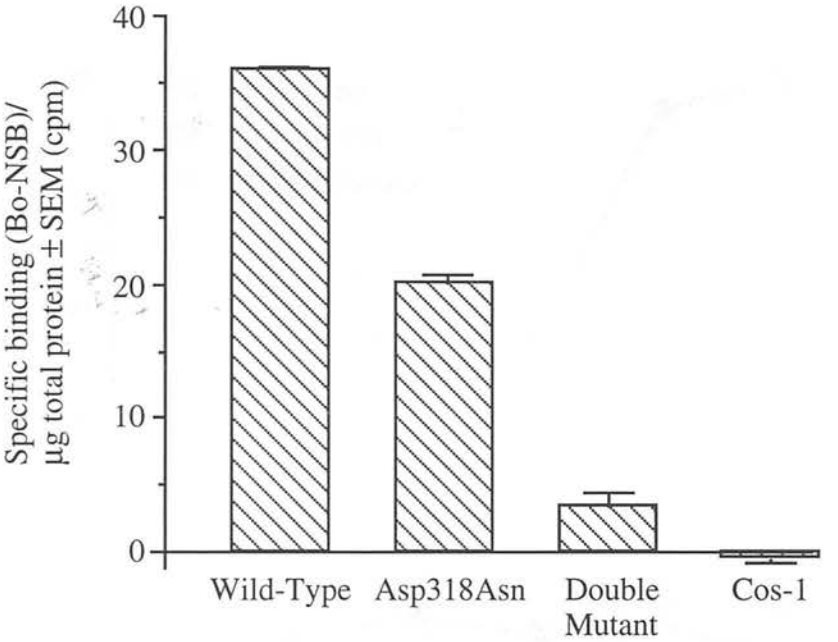

Figure 6.4 GnRH-R WT and Asp/Asn (pcDNA 3) mutants receptor agonist binding data

Specific binding of iodinated GnRH-A [des Gly^{10}, D-Trp^{6}, Pro^{9} NEt]-GnRH in COS-1 cells transiently expressing the WT and mutants Asp318Asn and Asn87AspAsp318Asn expressed in the eukaryotic expression vector pcDNA 3. Specific binding is expressed as maximum binding (Bo) minus non specific binding (NSB) ± SEM per µg of total protein. Binding assays were performed using an iodinated GnRH-A on membrane preparations. Data points are the mean of triplicate samples and the graph represents an average of n=2 individual experiments.

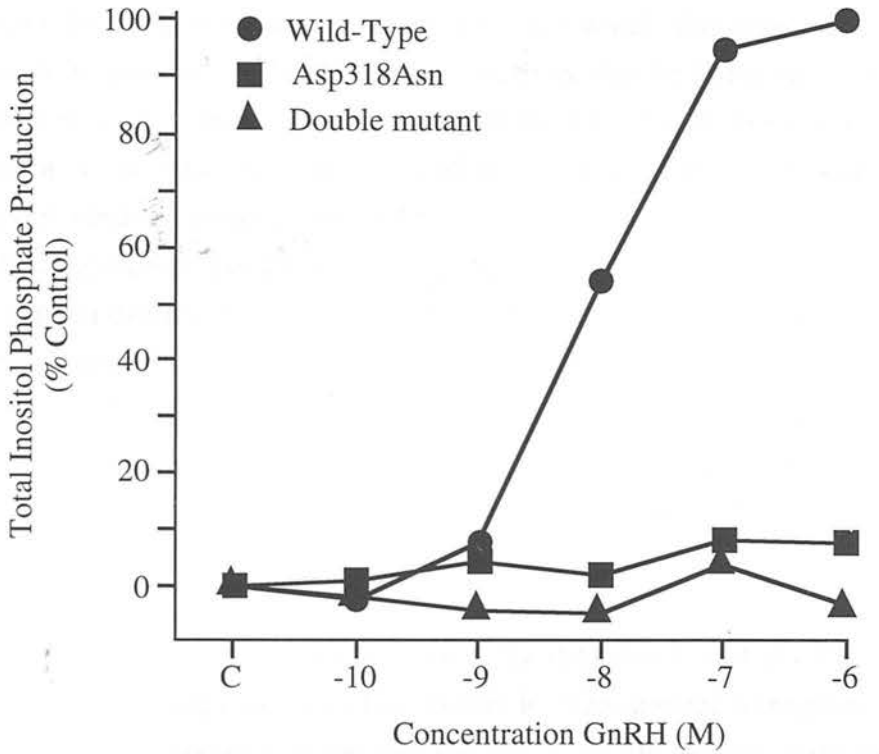

Figure 6.5 GnRH-R WT and Asn/Asn (pcDNA3) mutants total inositol phosphate production

Total IP production in COS-1 cells transiently expressing the GnRH-R WT and mutants Asp318Asn and Asn87AspAsp318Asn (subcloned into the eukaryotic expression vector pcDNA 3) following stimulation with GnRH (10 pM to 1μM). Untransfected COS-1 cells used as a negative control (data omitted for clarity) showed only basal stimulation at all concentrations of GnRH. Data points are the mean of triplicate samples and the graph is a representative example from n=2 individual experiments.

6.3 Discussion

These results suggest that Asn87 is essential for GnRH ligand binding whereas Asp318 is not required for binding, but is necessary for signal transduction. The data also indicates that these two amino acids must be located in their natural positions to maintain full receptor binding and second messenger coupling activity. However, caution must be exercised in the interpretation of results obtained for receptors using site-directed mutagenesis studies, since a mutant which abolishes receptor binding may do so for any one of several reasons. Activity may be lost because the mutation is located in a site which is in contact with the ligand and directly involved with binding, or because it is in a remote site which nonetheless affects the size or shape of the ligand binding pocket. In addition, the mutation may interfere with post-translational processing or the insertion of the receptor into the cell membrane. In this study, indirect distortions of the ligand binding pocket are likely to be low as Asp and Asn are of similar size and their high frequency of evolutionary substitution would suggest that they are readily interchangeable. Furthermore, the near universal occurrence of Asp87 in TM II of other GPCRs, implies that there is no reason to expect this substitution will interfere with protein processing and/or membrane assembly.

These experiments highlight the necessity for the presence of Asn87 in TM II to mediate ligand binding functions of the GnRH-R. Site-directed mutagenesis studies in other GPCRs have shown that the Asp residue, normally located in the homologous TM II position, is also a crucial mediator of receptor binding and function. In the β adrenergic receptor it has been suggested that the negative charge carried by the TM II Asp residue is involved in both ligand binding and the transfer of information across the cell membrane (Chung et al, 1988; Strader et al, 1988). Clearly any potential ionic interactions, similar to those observed in the β adrenergic receptor, are unlikely in the GnRH-R as the Asn in this position is uncharged. However, in other GPCRs the modification of the Asp residue, through site-directed mutagenesis, has been associated with reduced agonist affinity (Chung et al, 1988; Fraser, 1989; Strader et al, 1987), altered receptor binding properties in response to pH (Neve et al, 1991), sodium (Hortsman et al, 1992; Neve et al, 1991) and GTP analogues (Chung et al, 1988) together with alterations in receptor coupling activity (Chung et al, 1988; Fraser, 1989).

In the GnRH-R, Asp318 is important in second messenger G-protein coupling. Site-directed mutagenesis studies in the $5HT_{1A}$ receptor have also highlighted a role for the equivalently positioned Asn residue in receptor binding. In the $5HT_{1A}$ receptor study, carried out by Chanda et al (1993) substitution of the TM VII conserved Asn residue to either Ala, Phe or Val resulted in a loss of agonist binding, but agonist binding was maintained when Gln was introduced at this site.

The reciprocal mutant was constructed on the rationale that if other GPCRs normally contain an Asp in TM II and an Asn in TM VII, then functional activity of the GnRH-R single mutant Asn87Asp might be restored on incorporation of an Asn in TM VII. However, the findings of this study do not support this hypothesis, as the maximum levels of GnRH-A binding in the double mutation (expressed in pcDNA 3) reached only 5% of the WT value. Although the double mutation failed to restore WT ligand binding properties, the small amount of receptor binding activity suggests that the mutation is unlikely to affect receptor membrane assembly or tertiary protein folding.

The Baldwin model of the GnRH-R structure predicts that conserved TM-located hydrophilic amino acids are positioned with their side chains orientated in towards the central pore of the receptor. The positions of Asn87 in TM II and Asp318 in TM VII in this model are illustrated in Figure 6.6 and whilst both amino acids are inwardly facing their side chains lie positioned at right angles, some distance apart. The failure of the double mutant to restore significant binding function to the receptor implies that the amino acid function is not transposable between the two residues. Furthermore, if Asn87 interacts directly with GnRH then the stereochemical configuration of the GnRH ligand is unable to support this crucial interaction when Asn is symmetrically located on the opposite side of the channel. In contrast to the results obtained for the β adrenergic receptor both Asn87Asp and the double mutation also failed to bind GnRH antagonist, implying that Asn87 may be important in the binding of both agonist and antagonist analogues.

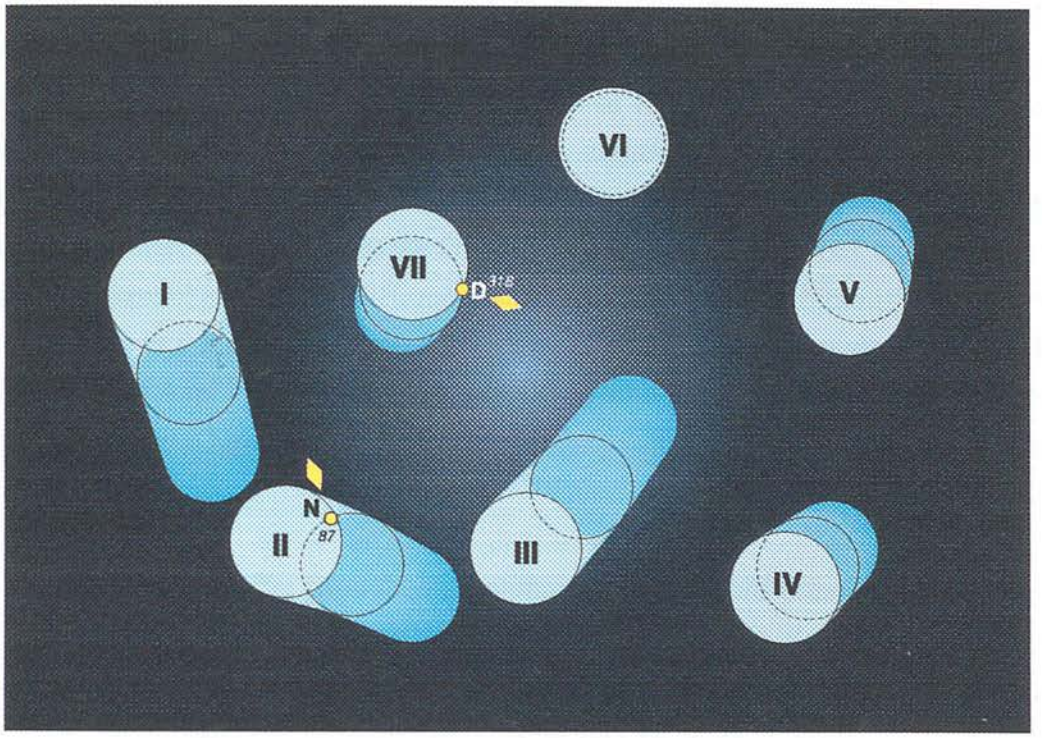

Figure 6.6 Position of Asn87 and Asp318 in the Baldwin GnRH-R model

Structural model of the TM domains of the rat GnRH-R as predicted by the Baldwin model. The model is a view from the extracellular surface of the receptor, looking inwards down the central pore, towards the intracellular face. The TM domains are represented by cylinders and the individual tilts and relative positions of the helices can be observed. Mutated amino acids are highlighted.

These experimental results have been largely substantiated by a similar study carried out by Zhou and co-workers (Zhou et al, 1993). This research group also constructed two single mutants, Asn87Asp and Asp318Asn, together with a double reciprocal mutation in the mouse GnRH-R. Again, similar observations regarding the receptor binding and functional activation of the single mutants were reported but the double reciprocal mutation appeared to have receptor binding activity of between 10% and 40% of the WT, depending on the efficiency of transfection (Dr James Davidson, personal communications). Zhou et al, have suggested that Asn87 is unlikely to be directly involved in ligand binding as (i) Asn87 is located at an amino acid position generally conserved throughout the GPCR family, (ii) the residue lies too far down the receptor channel and (iii) no differential agonist and antagonist binding was observed between the WT receptor and the double mutant. They have concluded that "the loss of binding of Asp87 mutant must be due a structural perturbation of the receptor that either distorts the binding site or disrupts the proper membrane insertion of the mutant receptor ".

These conclusions differ from the interpretation of the results presented in this study. Firstly, Asn87 is in a unique position compared to other GPCRs and therefore could mediate ligand-induced receptor specificity. Secondly, the position of the TM regions has not been absolutely defined and may in fact be quite flexible. In the Baldwin model the TM domains are represented by 26 amino acids and a value of between 20-25 amino acids is usually considered as a plausible TM domain length (Baldwin, 1993). Moreover, there is no information as to how far the ligand penetrates into the receptor pore. Thirdly, experiments have suggested that the agonist and antagonist sites are different (Janovick et al, 1993) but there is no reason why the failure to observe differential binding of both analogues should preclude Asn87 as a direct mediator of receptor binding function. For these three reasons it is possible that Asn87 has a direct functional role in GnRH-specific binding. Additional evidence supporting a putative role for Asn87 in GnRH-R binding also comes from analysis of the computer simulated model of the GnRH ligand and receptor (Figure 6.7). When GnRH is positioned in an optimal binding position, the COOH terminus of the decapeptide, implicated as an important mediator of receptor binding function, comes in close proximity to Asn87.

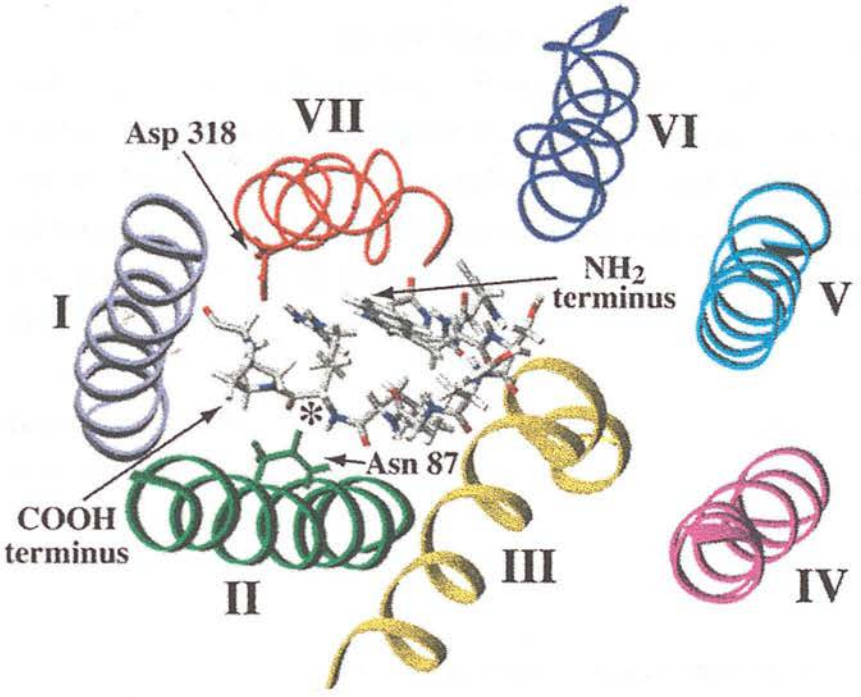

Figure 6.7 Position of Asn87 and Asp318 in the computer-derived GnRH-R model

Computer model of the TM domains of the GnRH-R with GnRH inserted in a putative binding location. The position of Asn87 in TM II and Asp318 in TM VII are highlighted. The close proximity of Asn87 and Asp318 to the GnRH ligand indicates that possible ligand-receptor interactions may be crucial for GnRH binding and receptor activation. The position of Arg8 in GnRH is marked with an *.

Zhou and colleagues also suggested that the double mutation retains functional activity through the restoration of H-bonds between the Asn and Asp residues (Zhou et al, 1993). They predicted a close spatial arrangement between TM II and TM VII, permitting a H-bonding interaction between Asn87 and Asp318. Although this bonding pattern is lost in the Asn87Asp single mutation the concurrent introduction of an Asn at the TM VII locus recreated this bonding pattern, and therefore restored the agonist binding properties of the receptor. However, in this study only 5% of WT receptor binding activity was observed for the double mutation. According to the proposed model (Figure 6.7), the distances between Asn87 and Asp318 are too great for H-bond formation. In addition, H-bonding between these amino acid residues would not be feasible if the ligand binds in the position shown between TM II, TM III and TM VII.

The differences between the findings obtained by Zhou and co-workers and this study may be due to variations in experimental procedures used. For example; (i) the use of different species of GnRH-R cDNA (rat verses mouse) (ii) alternative eukaryotic expression vectors or (iii) alternative methods of transfection.

In summary, mutant Asn87Asp prevented agonist-stimulated receptor binding activity and hence second messenger function, whilst Asp318Asn displayed normal WT receptor binding properties but was functionally uncoupled from its effector G-protein. The generation of a double reciprocal mutation did not restore full receptor binding activity and, in fact, this mutation displayed a very low level of receptor binding. The double mutation, like Asp318Asn, was also functionally uncoupled. These results indicate that Asp318 is important in receptor activation whereas Asn87 appears important in receptor binding. The position of the Asn87 residue from the molecular modelling studies locates this residue in an ideal position to make direct contact with the ligand.

Analysis of the GnRH-R amino acid sequence, relative to the sequences of other GPCRs, has provided invaluable information on the potential role of specific residues in structure-function relationships. However, an alternative molecular modelling approach has been used in the remaining experimental chapters (Chapter 7 and 8) to target amino acids potentially involved in GnRH-R ligand binding interactions.

7 Role of polar amino acids in the TM helices of the GnRH-R

7.1 Introduction

In this chapter a different approach has been utilised to target potentially important residues involved in GnRH-R binding. This strategy involved the analysis of site-directed mutagenesis data alongside information derived from the three-dimensional Baldwin model of the GnRH-R (see Chapter 4).

To predict amino acids in the receptor structure that are likely to be involved in ligand binding, both the nature and location of any putative interactions must be examined. There are three different types of bonding patterns likely to occur between a ligand and its receptor. The first type are ionic interactions, either ionic bonds between residues with opposite charges or ionic repulsion between like charged groups. The second type of interactions are hydrogen bonds (H-bonds), formed between -NH or -OH groups and the C=O groups in the peptide backbone or the $-COO^-$ group in Asp/Glu residues. Finally, hydrophobic interactions may also be important in ligand-receptor binding mechanisms (this aspect is dealt with in Chapter 8). Analysis of the ligand structure reveals the presence of a highly basic Arg residue at position 8 and therefore it is feasible that ionic interactions (either ionic bonds or repulsion forces) might play an important part in ligand binding. In addition, H bonds may also be involved in ligand-receptor interactions.

Having established possible types of bonding interactions, attention focused on putative sites within the GnRH-R where such interactions might occur. The structural elucidation of bacteriorhodopsin/rhodopsin indicated that the retinal chromophore binds in the middle regions of the TM domains (Henderson et al, 1990), hence this region of the GnRH-R was examined for potentially important ligand binding sites. Analysis of the middle cross-sectional view of the Baldwin GnRH-R model reveals the presence of polar residues Glu90, Lys121, Glu174 and Asn314, in the centre of TM II, TM III, TM IV and TM VII respectively. These residues have been highlighted in the Baldwin model as they represent TM sites

occupied by polar amino acids (either a Asn, Asp, Glu, Gln, His or Lys) in at least 10% of receptor sequences analysed. The presence of hydrophilic TM residues is unusual as the TM helices, by definition, are composed of hydrophobic amino acids. Therefore, it is possible that polar amino acids may have an important role in mediating receptor functions, as their hydrophilic nature would allow interactions with the GnRH ligand. For example, an ionic bond is possible between Glu90 and Arg8 in the ligand, ionic repulsions between Lys115 and Lys121 and Arg8, and H-bonds between Gln174/Asn314 and the carbonyl groups of the peptide backbone. In addition, these residues are ideally positioned to interact with the ligand as their side chains are directed into the centre of the receptor pore. Furthermore, GnRH-R residue Lys121 corresponds to Glu113 in rhodopsin - an amino acid important in ligand-receptor activation (Savarese and Fraser, 1992; Zhou et al, 1995). Glu113 acts as the counterion for the protonated Schiff base Lys296 and its substitution to Gln impairs ligand-receptor signal transduction mechanisms resulting in a change in the absorbance spectrum of rhodopsin from 498 nm to 380 nm (Sakmar et al, 1989).

Studies in the GnRH-R have also indicated that residues located in the TM/extracellular interface may also have a functional role in receptor binding mechanisms (Davidson et al, 1994). Therefore, the extracellular cross-sectional view of the GnRH-R Baldwin model was also examined for any suitably positioned residues. This view of the receptor highlights a further three polar amino acids, Lys115 in TM III/el 1 together with Asn304 and His305 in TM VII/el 3, which are orientated with their side chains pointing in towards the receptor pore. Furthermore, the nature of these residues would also permit suitable bonding interactions with the ligand.

In total seven amino acids were targeted, Glu90, Lys115, Lys121, Gln174, Asn304, His305 and Asn314. The position of these residues in the Baldwin GnRH-R model is illustrated in Figure 7.1 and the mutants generated summarised in Table 7.1.

Following site-directed mutagenesis, the mutant GnRH-Rs were transiently expressed in COS-1 cells and their role in GnRH-R binding and second messenger activation tested. In addition, mutants that failed to show any ligand binding function using this system were then stably expressed in HEK-293 cells for further study.

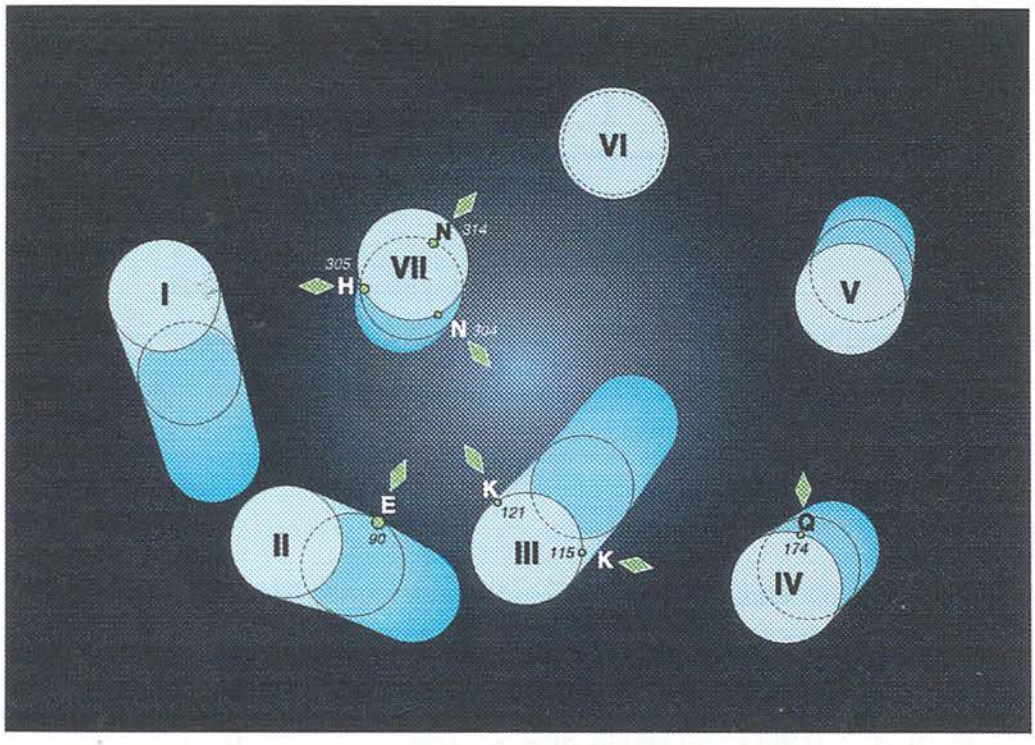

Figure 7.1 Position of TM located polar amino acids in the Baldwin GnRH-R model

Structural model of the TM domains of the rat GnRH-R as predicted by the Baldwin model. The model is a view from the extracellular surface of the receptor, looking inwards down the central pore, towards the intracellular face. The TM domains are represented by cylinders and the individual tilts and relative positions of the helices can be observed. Mutated amino acids are highlighted.

GnRH-R Mutant	TM Position	Amino acid modification
Glu90Gln	TM II	E to Q
Lys115Arg	TM III/el 1	K to R
Lys121Arg	TM III	K to R
Gln174Glu	TM IV	Q to E
Asn304Asp	TM VII/el 3	N to D
His305Arg	TM VII/el 3	H to R
Asn314Asp	TM VII	N to D

Table 7.1 GnRH-R TM-located polar mutations

Amino acids in the GnRH-R targeted for site-directed mutagenesis and their corresponding amino acid substitutions.

7.2 Results

COS-1 cells transiently expressing the GnRH-R mutants Glu90Gln (TM II), Lys115Arg (TM III/el 1), Lys121Arg (TM III), Gln174Glu (TM IV) and Asn304Asp (TM VII/el 3) showed GnRH-A receptor binding properties similar to WT. The displacement of radiolabelled GnRH-A with unlabelled GnRH-A is illustrated in Figure 7.2. Analysis of displacement curves generated IC50 values of 3.3 nM, 4.1 nM, 3.6 nM 4.5 nM 4.7 nM and 5.5 nM for the GnRH-R WT and mutants Glu90Gln, Lys115Arg, Lys121Arg, Gln174Glu and Asn304Asp respectively. In contrast, COS-1 cells transiently expressing the mutants His305Arg (TM VII/el 3) and Asn314Asp (TM VII) showed no receptor binding with either the GnRH-A or GnRH peptide. The WT and mutant GnRH-R binding data is summarised in Table 7.2.

Figure 7.2 GnRH-R WT and TM polar mutants agonist binding data (following page)

Displacement curves of GnRH-A binding to GnRH-R WT and mutants. Competitive binding assays were performed using an iodinated GnRH-A [des Gly^{10}, D-Trp^{6}, Pro^{9} NEt]-GnRH (100 000 cpm), in the presence of different concentrations of cold GnRH-A, on membrane preparations from COS-1 cells transiently expressing the GnRH-R WT and mutants. Specific binding is expressed as % of the maximum binding (Bo) minus the non-specific binding (NSB). Data points are the mean of duplicate/triplicate samples and the graph is a representative example from at least n=4 individual experiments.

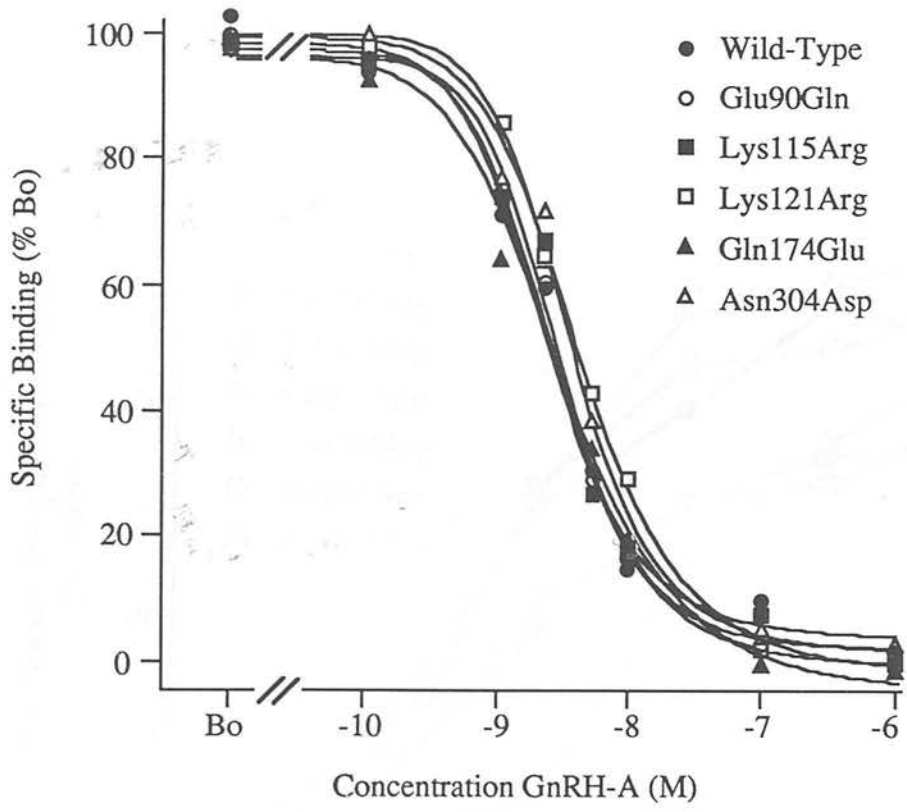

GnRH-R mutants Glu90Gln, Lys115Arg, Lys121Arg and Gln174Glu showed similar GnRH-stimulated IP production profiles to WT. The ED50 values of WT and GnRH mutant receptors Glu90Gln, Lys115Arg, Lys121Arg and Gln174Glu were 7.0 nM, 10.1 nM, 6.2 nM, 13.0 nM and 6.4 nM respectively (see Figure 7.3). Overall, the maximum levels of IP production between GnRH-R mutants and WT were comparable, although a considerable interassay variation was observed with mutants displaying maximum IP production ranging from 50% to 150% of WT activity. In general, the individual transfection efficiencies observed in second messenger activation were also displayed in the maximum receptor binding (Bo) values of the mutants. By contrast, mutant Asn304Asp, despite a similar WT IC 50 receptor binding value, showed a 10 fold increase in the GnRH concentration required to stimulate half maximal levels of total IPs (ED50 of 64 nM, Figure 7.3). In addition, this mutant showed a slight but significant decrease in maximal WT total IP production ($p < 0.05$). As expected the transiently expressing GnRH-R mutants His305Arg and Asn314Asp showed no GnRH ligand-stimulated IP response. WT and mutant GnRH-R stimulated second messenger activity is summarised in Table 7.3.

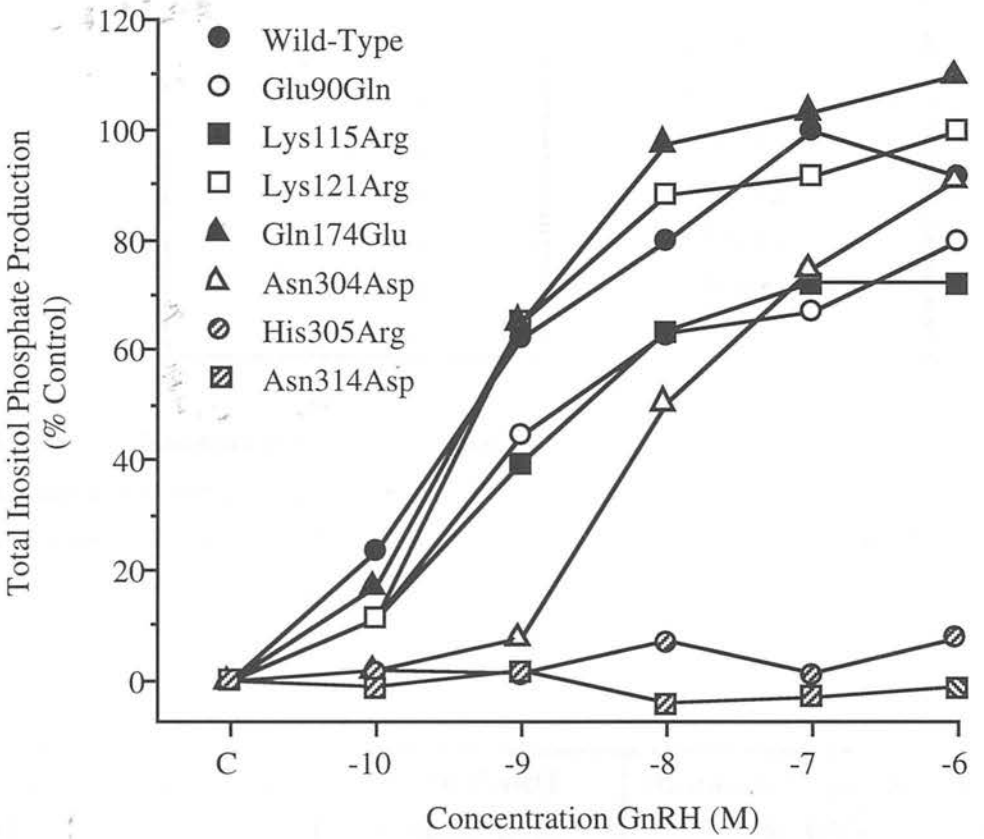

Figure 7.3 GnRH-R WT and TM polar mutants total inositol phosphate production

Total IP production in COS-1 cells transiently expressing the GnRH-R WT or mutants Glu90Gln, Lys115Arg, Lys121Arg, Gln174Glu, Asn304Asp, His305Arg and Asn314Asp following stimulation with GnRH (100pM-1μM). Untransfected COS-1 cells, negative controls, (data omitted for clarity) showed only basal stimulation at all GnRH concentrations. Data points are the mean of duplicate/triplicate samples and the graph is a representative example from n=3 individual experiments.

GnRH-R Construct	IC50 (nM) ± SEM
Wild-Type	3.3 ± 0.5
Glu90Gln	4.1 ± 0.6
Lys115Arg	3.6 ± 0.7
Lys121Arg	4.5 ± 1.0
Gln174Glu	4.7 ± 1.2
Asn304Asp	5.5 ± 1.3
His305Arg	no binding
Asn314Asp	no binding

Table 7.2 Summary of GnRH-R WT and TM polar mutant binding data

Table summarising receptor binding assay data. IC50 values were calculated from competitive binding assays, with iodinated GnRH-A displaced with cold GnRH-A. IC50 values are the average (± SEM) of at least n=3 individual experiments.

GnRH-R Construct	ED50 GnRH ± SEM (nM)	Maximum IP production (% WT)
Wild-Type	7.0 ± 0.5	100%
Glu90Gln	10.1 ± 0.1	95.8 ± 20.3
Lys115Arg	6.2 ± 1.7	100.2 ± 13.2
Lys121Arg	13.0 ± 0.3	89.2 ± 15.6
Gln174Glu	6.3 ± 2.7	96.1 ± 19.8
Asn304Asp	64 ± 20.0	75.1 ± 14.2
His305Arg	no IP stimulation	—
Asn314Asp	no IP stimulation	—

Table 7.3 Summary of GnRH-R WT and TM polar mutant total inositol phosphate data

Table summarising total IP production. The ED50 values were calculated from GnRH (100pM-1μM) stimulated IP production dose response curves. ED50 values are the average (± SEM) of at least n=3 individual experiments.

To establish whether GnRH-R mutants His305Arg and Asn314Asp completely abolished receptor binding or whether receptor binding was simply reduced to non-detectable levels, stable cell lines of both the WT and these specific mutants were constructed in HEK-293 cells. In total, two WT clones (HEK-WT clone 1 and 2), two His305Arg clones (HEK-His305Arg clone 1 and 2) and five Asn314Asp clones (HEK-Asn314Asp clone 1, 2, 3, 4 and 5) were expanded and screened for ligand binding and second messenger properties. In general, different clonal cell lines of the same mutation behaved in a similar fashion (the HEK-Asn314Asp clones were slightly more variable) and therefore, one representative example of the WT (HEK-WT clone 1) and each mutant (HEK-His305Arg clone 1 and HEK-Asn314Asp clone 3) was chosen for in-depth study. These clones were subsequently examined for GnRH-A receptor binding parameters and GnRH-stimulated total IP production. In addition, GnRH-induced single cell Ca^{2+} responses were also studied in the WT clone using dual fluorescent microscopy combined with dynamic video imaging. In order to determine any possible effects of the site-directed mutagenesis procedure on RNA transcription levels Northern Blot analysis was also carried out.

Receptor binding parameters, Kd and B max were calculated from Scatchard analysis of saturation binding data. HEK-WT cells showed a Kd (± SEM) value of 0.20 ± 0.14 nM and a B max (± SEM) value of 3.10 ± 0.63 pmol/mg protein (Figure 7.4). Saturation binding experiments on cell membrane preparations of HEK-His305Arg and HEK-Asn314Asp revealed that both these mutants exhibited a small degree of receptor binding but the level was insufficient for Scatchard analysis. To further characterise these mutants, receptor binding studies were performed using different concentrations of mutant membrane preparations. Total protein concentrations of 20, 40, 60 and 80µg were added to each tube and the specific binding calculated. Figure 7.5a shows that the receptor binding activity of these mutants is markedly reduced compared to WT, but that the linear increase in specific binding corresponds to a rise in total protein concentration (Figure 7.5a and b). At the maximum total protein concentration of 80µg per tube, the specific binding of HEK-His305Arg and HEK-Asn314Asp was approximately 1% and 6% respectively of that observed for the WT. This is an important finding as it shows that functionally active proteins are expressed at the cell surface.

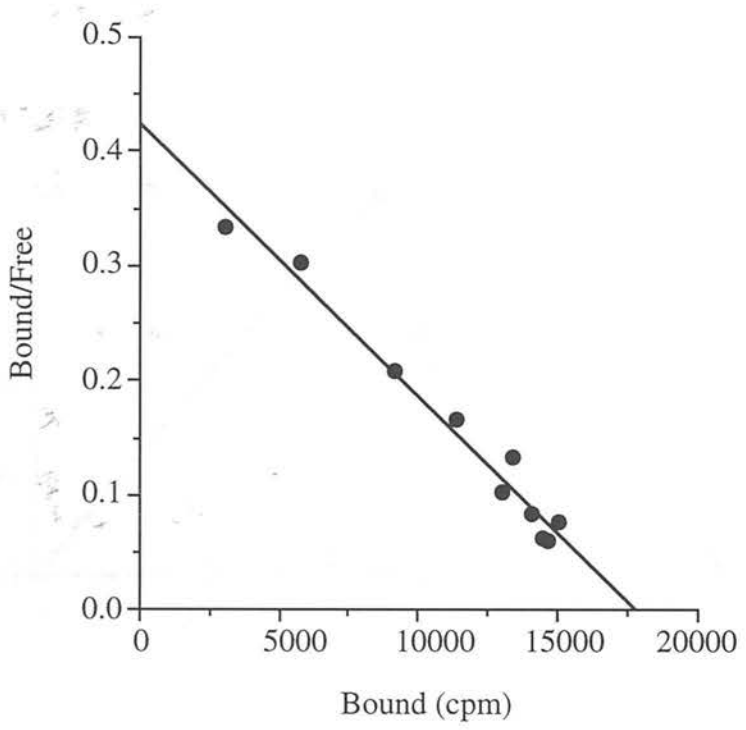

Figure 7.4 HEK-WT GnRH-R agonist binding data

Scatchard analysis of GnRH-A binding to HEK-WT GnRH-R. Saturation binding assays were performed using an iodinated GnRH-A [des Gly^{10}, D-Trp^{6}, Pro^{9} NEt]-GnRH on membrane preparations from HEK-293 cells stably expressing the rat GnRH-R WT. Data points are the mean of duplicate/triplicate samples and the graph is a representative example from n=4 individual experiments.

Figure 7.5 HEK-WT, HEK-His305Arg and HEK-Asn314Asp agonist binding data (following page)

Specific binding of GnRH-A [des Gly^{10}, D-Trp^{6}, Pro^{9} NEt]-GnRH in the presence of increasing concentrations of total protein per tube of (a) HEK-WT GnRH and mutants HEK-His305Arg and HEK-Asn314Asp (b) mutants HEK-His305Arg and HEK-Asn314Asp only. Specific binding is expressed as maximum binding (Bo) minus non specific binding (NSB) ± SEM. Binding assays were performed using the iodinated GnRH-A on membrane preparations. Data points represent the mean of triplicate samples from n=2 individual experiments

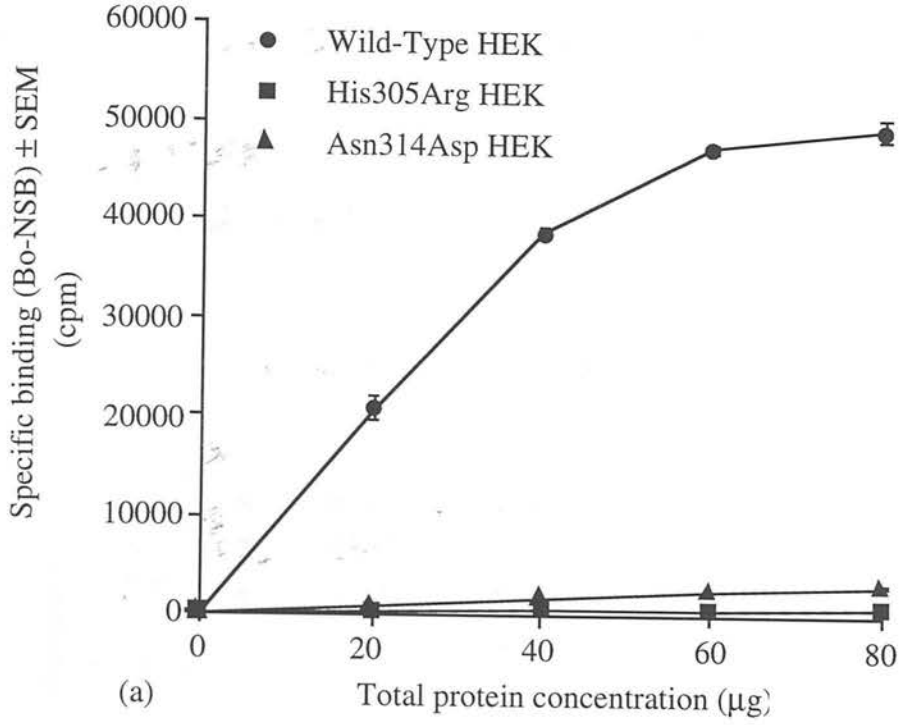
Specific binding (Bo-NSB) ± SEM (cpm)
60000
50000
40000
30000
20000
10000
0
Wild-Type HEK
His305Arg HEK
Asn314Asp HEK
0
20
40
60
80
Total protein concentration (µg)

(a)

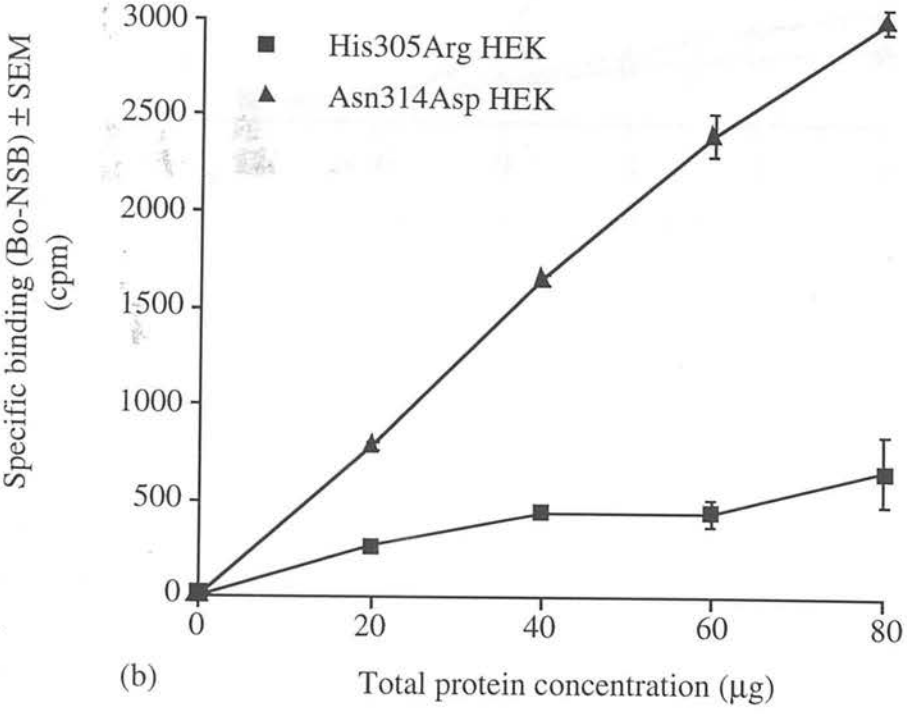
Specific binding (Bo-NSB) ± SEM (cpm)
3000
2500
2000
1500
1000
500
0
His305Arg HEK
Asn314Asp HEK
0
20
40
60
80
Total protein concentration (µg)

(b)

GnRH-stimulated second messenger production in the HEK-WT cells showed a dose-dependent increase in total IP production (Figure 7.6) with an ED50 (± SEM) value of 5.16 ± 1.0 nM. Again the two receptor mutants showed markedly reduced levels of receptor activation with the maximum level of IP stimulation at 1μM GnRH corresponding to 10% for HEK-His305Arg and 20% for HEK-Asn314Asp compared to the WT (Figure 7.6).

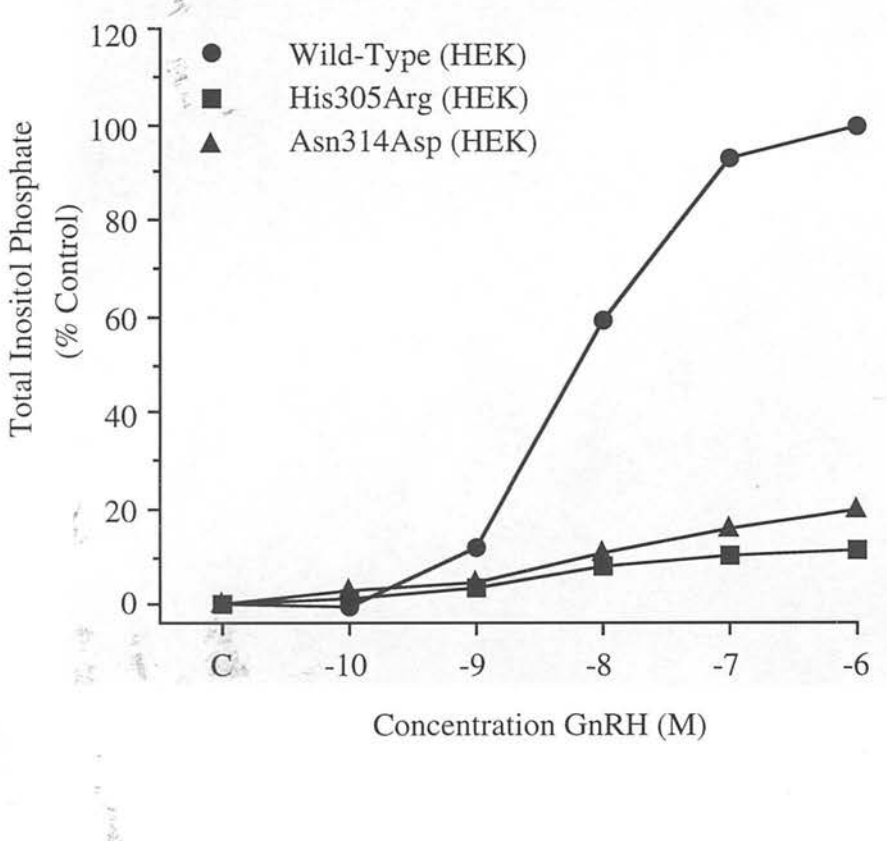

Figure 7.6 HEK-WT, HEK-His305Arg and HEK-Asn314Asp total inositol phosphate production

Total IP production in HEK-293 cells stably expressing the HEK-WT, HEK-His305Arg and HEK-Asn314Asp mutant GnRH-Rs following stimulation with GnRH (100pM-1μM). Untransfected HEK-293 cells, used as a negative control (omitted for clarity), showed only basal stimulation at all concentrations of GnRH. Data points represent the mean of duplicate/triplicate samples and the graph is a representative example from n=3 individual experiments.

In addition to monitoring GnRH induced total IP production, changes in $[Ca^{2+}]i$ were also measured in individual HEK-WT cells using fluorescent microscopy combined with dynamic video imaging (Figure 7.7). HEK-WT cells showed a monophasic rise in $[Ca^{2+}]i$ when stimulated with a concentration of 100nM GnRH. See Appendix IIIA for a description of additional methodology used.

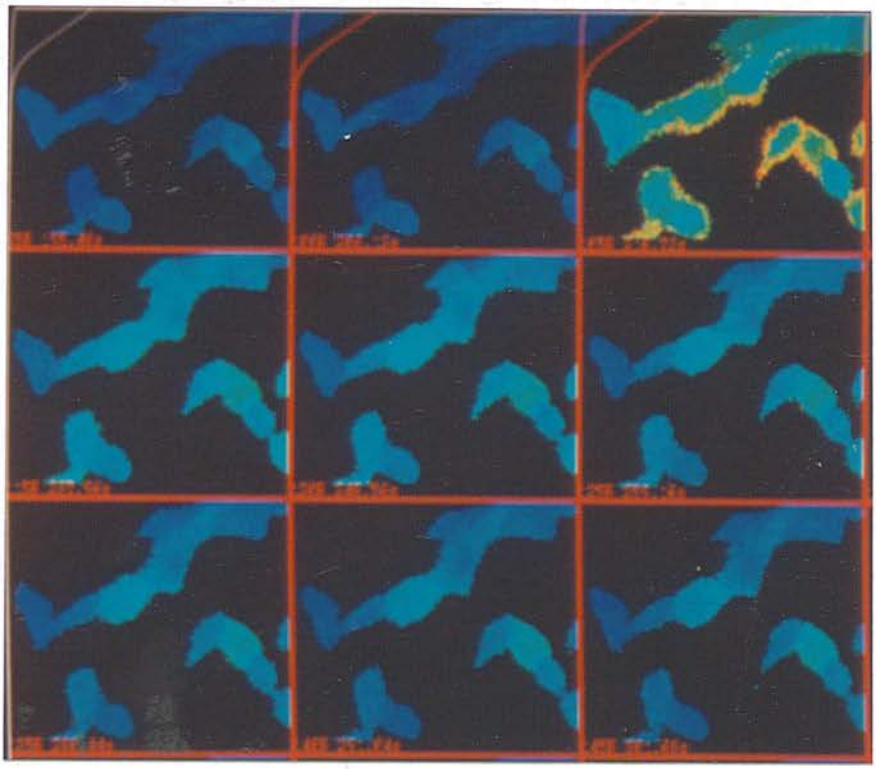

Figure 7.7 Dynamic calcium imaging of GnRH-R HEK WT

Effects of GnRH (100nM) on $[Ca^{2+}]i$ in HEK-293 cells expressing the WT GnRH-R. Data represents changes in $[Ca^{2+}]i$ in a population of cells with time (s). Fluorescent images were obtained by exposing Fura-2 loaded cells (4μM final concentration) to 320 nm and 380 nm light using dynamic video imaging. Each frame represents the ratio of 320:380 nm measurements, the frames were taken approximately 4s apart and GnRH added after frame 2 (left-right).

Northern Blot analysis was used to compare the expression of the GnRH mutant RNA with WT RNA. Figure 7.9 shows a Northern blot of total RNA extracted from HEK-293 cells stably expressing the HEK-WT GnRH-R (clones 1 and 2) and the mutants HEK-His305Arg (clones 1 and 2) and HEK-Asn314Asp (clones 1, 2, 3, 4 and 5). RNA extracted from αT3-1 cells was used as a positive control and RNA from untransfected HEK-293 and COS-1 cells were negative controls. The GnRH-R WT and mutants were cloned into the EcoRI site in the expression vector pcDNA 3. This site lies approximately 700 bp from the beginning of the CMV promoter - the transcription start site. Therefore as the size of the GnRH-R cDNA is 2.2 kb, an expected RNA transcript size would be ~ 2.9 kb. A 2.9 kb transcript was observed in the HEK-WT clone 1, HEK-His305Arg clones 1 and 2 and the HEK-Asn314Asp clones 1 and 5 (Figure 7.8a). The other clones, WT clone 2 and HEK-Asn314Asp clones 2, 3 and 4 displayed a larger transcript size of ~ 3.6 kb. A faint band corresponding to a 3.6 kb transcript size was observed in the total RNA extracted from αT3-1 cells. No hybridisation occurred in total RNA derived from the untransfected HEK-293 or COS-1 cells (Figure 7.8a).

Hybridisation of a radiolabelled 18S oligonucleotide probe with a 1.9 kb band corresponding to 18S RNA showed that equivalent amounts of RNA were loaded into each well (Figure 7.8b).

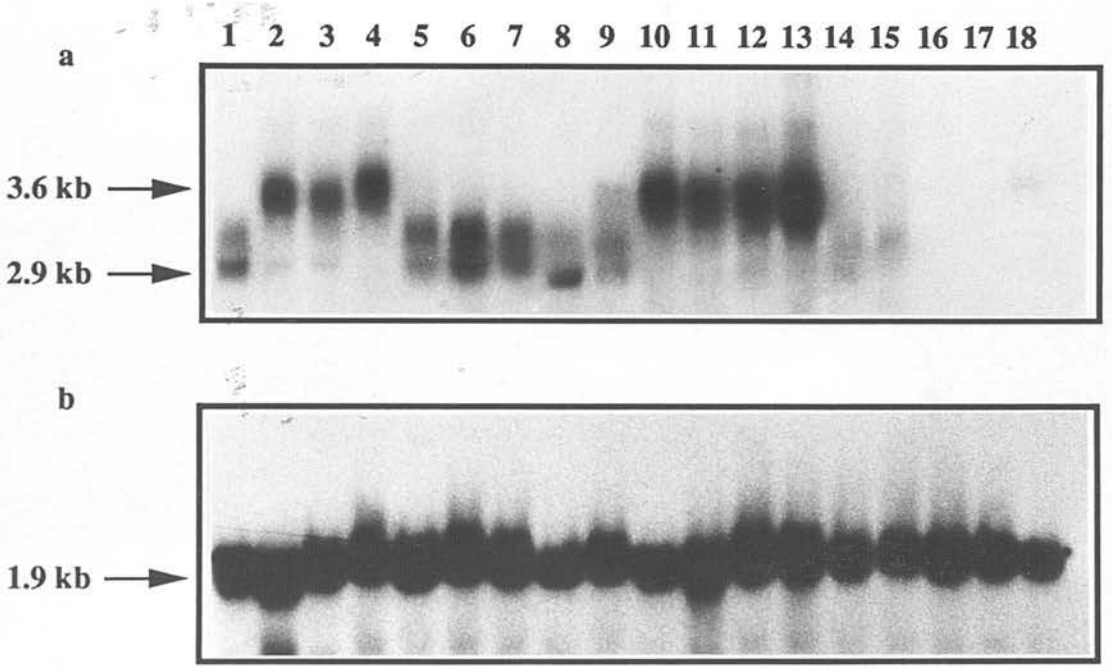

Figure 7.8 Northern Blot of GnRH-R WT and mutants stably expressed in HEK-293 cells

(a) Northern Blot probed with an [α^{32}P]dCTP labelled 2.2 kb rat GnRH-R cDNA probe showing RNA expression levels in total RNA (15μg) from GnRH-R HEK-WT and mutants HEK-His305Arg and HEK-Asn314Asp stably expressed in HEK-293 cells. The individual lanes represent HEK-His305Arg clone 5 (lane 1), clone 4 (lane 2), clone 3 (lane 3), clone 2 (lane 4) and clone 1 (lane 5), HEK-His305Arg clone 2 (lane 6 & 7) and clone 1 (lanes 8 & 9) and WT-HEK clone 2 (lanes 10-13) and clone 1 (lanes 14 & 15). COS-1 cells and untransfected HEK-293 cells (lanes 16 & 17) and αT3-1 cells (lane 18)

(b) Northern Blot probed with a [γ^{32}P]dATP labelled anti-18S oligonucleotide to check for the presence of even RNA loading in the corresponding wells. Experiments were carried out on at least n=3 independent occasions using different batches of RNA.

7.3 Discussion

The Baldwin model is a tentative model of GPCR structure with the heptahelical arrangement of the TM domains based on the analysis of GPCRs sequence data, and superimposed onto the known three-dimensional arrangement of rhodopsin. Using this model as a template, a specific model of the GnRH-R was constructed and amino acids were targeted for study based on their location within the model. In total seven residues were highlighted and mutant GnRH-Rs subsequently generated (Glu90Gln, Lys115Arg, Lys121Arg, Gln174Glu, Asn304Asp, His305Arg and Asn314Asp). All the modified amino acids were located in suitable positions to interact with the ligand, either in the middle of the TM domains or at the el/TM interface. In addition, the polar nature of these amino acids rendered them capable of forming either ionic interactions or H-bonds with the ligand.

The properties of the WT and mutant GnRH-Rs Glu90Gln, Lys115Arg, Lys121Arg, Gln174Glu, Asn304Asp, His305Arg and Asn314Asp were initially examined in a transiently expressing COS-1 cell system. Modifications of the GnRH-R structure at amino acid positions Glu90 (TM II), Lys115 (el 1/TM III), Lys121 (TM III) and Gln174 (TM IV) did not affect GnRH-R ligand binding or activation therefore implying that these sites are not involved in receptor binding processes. Alternatively, it is possible that any potential role of these residues in receptor function was maintained by the corresponding substitutions, particularly as the changes introduced at these sites were fairly conservative modifications. The rationale underlying the choice of substituting amino acids was based on the premise that residues of similar size/charge would prevent any gross changes in the tertiary folding of the receptor. Consequently, Lys residues were replaced by Arg, another highly basic amino acid, and Asp and Asn or Glu and Gln were interchanged thereby altering the charge but not the size of the residue. Studies in other GPCRs have indicated that the choice of amino acid substitutions is a critical factor in determining the outcome of site-directed mutagenesis experiments (Caron and Lefkowitz, 1993). This aspect is further explored in section 10.2.

The importance of Lys121 in GnRH-R ligand binding mechanisms has also been highlighted by Zhou and co-workers (Zhou et al, 1995). This group constructed an identical substitution Lys121Arg in the human GnRH-R, and their site-directed mutagenesis results confirmed the findings reported in this study. In addition, Zhou

and colleagues generated three more drastic substitutions, Lys121Gln, Lys121Leu and Lys121Asp. Substitution with Gln, Leu or Asp rendered agonist binding below the detection limits of the binding assay. Lys121Leu and Lys121Asp showed no GnRH-stimulated second messenger production, whilst Lys121Gln showed functional activation although this was decreased by approximately three orders of magnitude compared to WT. Further studies on the second messenger properties of Lys121Gln revealed that the GnRH-induced rise in total IP production could be inhibited by the GnRH antagonist 27 [Ac-D-$Nal_2{}^1$, D-α-Me-4-ClPhe^2, D-Trp^3, Ser^4, Isopropyl^5, D-Trp ^{6}, Leu^7, Arg^8 , Pro^9, D-Ala^{10}]-GnRH. The shift in the GnRH-stimulated IP dose-response curves in the presence of varying antagonist concentrations were comparable to those observed from the WT, despite the original decrease in the GnRH ED50 values (nM range for WT versus μM range for Lys121Gln). From these results Zhou et al, concluded that the presence of a charged strength H-bond donor, either Lys or Arg, is required at position 121 for high affinity agonist but not antagonist binding. These conclusions, however, are entirely based on the ability of antagonist 27 (co-administered with GnRH) to further reduce second messenger production in a system already partially disabled due to the Lys121Gln mutation. Moreover, these experiments failed to detect any agonist or antagonist binding in mutant Lys121Gln, a factor related to the low expression levels displayed by the human GnRH-R cDNA clone. In the absence of any direct measurement of GnRH analogue binding, these conclusions must be viewed with a degree of scepticism. However, it is clear from both studies that the functional role served by Lys at position 121 is maintained by substitution to Arg. Analysis of the computer GnRH ligand-receptor model (Figure 7.9) reveals that Lys121 lies in close proximity to the peptide, between Arg8 and Leu7, and hence it is possible that a H-bond interaction might occur between the Lys (-NH group) in the receptor and the peptide backbone of the ligand (-C=O group).

Mutant Asn304Asp at the el 3/TM VII interface showed a normal WT receptor binding IC50 value but displayed a 10 fold decrease in GnRH-stimulated IP production. The presence of a negatively charged Asp residue at this site may result in changes to the three-dimensional extracellular receptor configuration and therefore a greater peptide concentration was required to fully stimulate the G-protein coupled effector system.

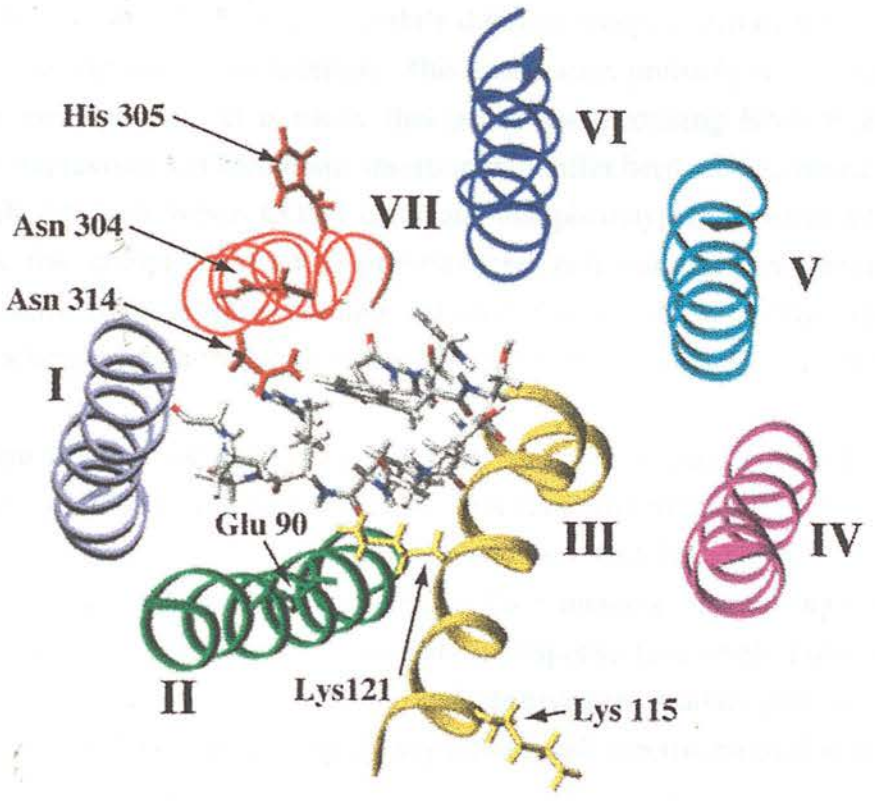

Figure 7.9 Position of TM located polar amino acids in the computer-derived GnRH-R model

Computer model of the TM domains of the GnRH-R with GnRH inserted into a putative binding location. The position of Glu90, Lys115, Lys121, Asn304, His305 and Asn314 are highlighted. The close proximity of the ligand to TM II, TM III and TM VII can be observed.

Substitution of His to Arg at position 305 (TM VII/el 3) and Asn to Asp at position 314 (TM VII) prevented ligand recognition and hence GnRH-A/GnRH-stimulated IP production. To further examine the affects of these mutations, stable cell lines of the WT and mutant receptors were generated in HEK-293 cells.

The HEK-WT GnRH-R showed a slightly different receptor affinity when compared to the transiently expressed receptor. This observation probably reflects certain cell specific mechanisms. It is likely that processes mediating RNA transcription, receptor expression and membrane insertion will differ between individual cell types (i.e. HEK-293 cells versus COS-1 cells) and that phenotypic properties of the cells, such as the complement of G-proteins and cell surface ion channels, will differentially affect receptor binding and second messenger coupling. In addition, certain cell types are intrinsically easier to transfect than others (Titus, 1991).

Two indicators of second messenger function were examined in the HEK-WT GnRH-R. HEK-WT cells showed a dose-dependent rise in total IP when stimulated with different concentrations of ligand. In addition, GnRH-induced Ca^{2+} responses were measured in single cells using dynamic Ca^{2+} imaging. Interestingly, HEK-WT cells produce monophasic Ca^{2+} transients in response to a single pulse of GnRH. This contrasts with the biphasic responses observed in pituitary gonadotroph cells (Anderson et al, 1993) and most probably reflects cell specific mechanisms.

GnRH-R binding and second messenger coupling were observed in the stably expressing GnRH-R mutant cell lines, HEK-His305Arg and HEK-Asn314Asp, but levels were markedly reduced compared to the HEK-WT. These results indicate that the mutations seriously affect ligand-receptor binding and second messenger activation mechanisms. However, the detection of small amounts of binding and functional activity implies that the mutant receptors are expressed at the cell surface.

The position of His305 at the TM VII/el 3 interface suggests that it is unlikely to be directly involved in ligand-receptor activation mechanisms. However, a recent study in the GnRH-R has implicated an extracellularly positioned amino acid in ligand modulation. Davidson and co-workers (Davidson et al, 1994) have shown that the Glu301 residue in el 3, located approximately one turn of the helix above His305, interacts with Arg8 in GnRH. The Glu301/Arg8 interaction has been postulated to conform and stabilise the ligand prior to its entry into the TM domain. It is therefore

possible that the modification of His305 to Arg may interfere with the ligand conforming role of Glu301 and hence alter the binding of GnRH to its receptor.

Levels of cell surface protein expression in GnRH-R mutant His305Arg have not been determined and, therefore, alternative explanations for the decrease in receptor binding activity displayed by this mutant must also be considered. His305Arg may interfere with receptor expression or membrane protein trafficking but the detection of some receptor binding and second messenger activity indicates that functionally active receptors are present. However, it is impossible to determine whether receptor numbers have been reduced by the mutation or if the receptor levels are unchanged and the mutation affects ligand binding function following cell membrane insertion. It is also possible that the mutation does not have a direct affect on ligand-receptor interactions but that the loss of binding is due to changes in the receptor tertiary structure. Furthermore, the substitution of a strongly basic Arg residue, in place of a weakly basic His residue, may repel the ligand and thus either preclude access of GnRH into the receptor pore or alter its correct course into the TM domains.

In contrast, the position of Asn314 in the middle of TM VII, with its side chain orientated in towards the central receptor pore, positions it in a favourable location to directly interact with the ligand. From the computer GnRH ligand-receptor simulation studies, Asn314 lies in close spatial proximity to Arg8 in GnRH and also to Phe312 (Chapter 8) and Asp318 (Chapter 6) in the receptor structure. During the course of this study, Phe312 and Asp318 have been identified as amino acids important in receptor binding and activation respectively and therefore it is possible that these three amino acids (Phe312, Asn314 and Asp318) act together as a functional unit converting ligand-induced receptor conformational changes into the activation of the second messenger effector system. However, the effects of the Asn314Asp substitution on receptor expression levels or the folding of the membrane bound protein are at present unknown. It is also feasible that the introduction of a positively charged Asp residue close to the putative binding region, distorts the shape of the ligand binding pocket or creates an unsuitable electrostatic potential around it.

In the course of this investigation two different transfection procedures were utilised. Initially, the mutant receptors were transiently expressed in monkey kidney fibroblast COS-1 cells. The mutants that failed to show ligand binding (His305Arg

and Asn314Asp) were subsequently stably expressed in HEK-293 cells, a human embryonic epithelial kidney cell line. The primary advantage of using a stable expression system is the increase in receptor numbers, a factor which facilitates the detection of very low levels of receptor expression. In addition, the clonal expansion of single cell colonies provides a homogenous cell population. However, there are also certain disadvantages from using this approach. Foremost, it is impossible to control either the position of DNA integration or the receptor copy number into the host cell genome. Both these factors may have crucial affects on transfection efficiency.

Northern Blot analysis was used to study the effects of levels of transcription of the mutant receptors. A variation in transcript sizes was observed in the WT and mutant clones with two prominent bands occurring at 2.9 kb and 3.6 kb. RNA transcription initiation from the CMV promoter is likely to account for the 2.9 kb transcript, whereas the larger transcript size probably arises from either initiation of transcription upstream of this site or its continuation past the polyadenylation site into the host cell genome. It is possible that the mutant receptor has been incorporated into the host cell at a site close to another stronger promoter signal and, therefore, RNA transcription can occur from both the CMV promoter and also at a position 700 bp upstream of this site. Alternatively, transcription may not be terminated by the mutant DNA polyadenylation signal and could continue for an additional 700 bp downstream. The size of the α-T3-1 mRNA, 3.6 kb, is in agreement with results obtained from other groups (Reinhart et al, 1992; Wu et al, 1994). However, a number of different transcript sizes have been reported in α-T3-1 cells, suggesting that RNA transcription initiation is possible at several different sites (Reinhart et al, 1992; Tsutsumi et al, 1992). Post-transcriptional modifications may also account for the differences in transcript size.

The composite Baldwin model of the GnRH-R provided the first three-dimensional image of the receptor structure. However, when this receptor model was generated, the spatial dimensions of the ligand and its possible docking site within the receptor were completely unknown. This factor made the targeting of amino acids potentially involved in receptor binding particularly difficult. Predictions were therefore based entirely on possible hypothetical bonding interactions between ligand and receptor residues, and were only limited by constraints on the location and orientation of the TM amino acids. Out of the seven amino acids targeted, five (Glu90, Lys115,

Lys121, Gln174 and Asn304Asp) appeared to have no role in receptor binding. With the exception of Lys121, these amino acids are in positions (as viewed in the computer generated GnRH-R model, Figure 7.9) outside the putative binding site, and are therefore unlikely to participate in ligand-receptor interactions. Initial site-directed mutagenesis information implied that Lys121 was also not involved in ligand-receptor binding processes. However, the position of this amino acid, with its side chain directly pointing inwards into the putative binding pocket, suggests that it may interact with the ligand. It is possible that substitution of another highly basic amino acid residue, Arg, at this site fulfils the role of the naturally positioned Lys residue. The other two GnRH-R mutants His305Arg and Asn314Asp prevented ligand-induced receptor binding and activation. The position of His305 at the TM VII/el 3 interface is likely to preclude a direct interaction with the ligand and thus the His305Arg mutation probably affects the tertiary structure of the TM/extracellular domain. In contrast, amino acid Asn314 is located in an ideal position to interact with the ligand (Figure 7.9) and the nature of the amino acid together with its location would favour a H-bond interaction with GnRH.

This chapter has examined the role of TM-located polar residues in mediating aspects of GnRH ligand binding function. It is also possible that hydrophobic bonding between the ligand and receptor plays an important part in GnRH ligand-receptor interactions and this has been explored in the following chapter.

8 Role of amino acids Phe312 and Leu83 in the GnRH-R

8.1 Introduction

In this chapter, computer-derived models of the GnRH ligand and receptor were used to predict possible hydrophobic interactions between GnRH and its receptor. Analysis of the GnRH-R model revealed a suitable site, between TM II, III and VII, capable of accommodating the biologically active GnRH hairpin structure. The position of GnRH, within the receptor model, was adjusted to orientate the ligand in a low energy conformational state. With the ligand positioned in a putative optimal binding site it was possible to simulate potential ligand-receptor interactions and identify amino acids in the receptor structure capable of interacting with the ligand. Inspection of the GnRH model shows that Trp3 and Leu7 are exposed on either side of the hairpin loop configuration, surrounded by the other eight amino acids. In the simulated ligand-receptor model, Trp3 and Leu7 of GnRH lie in close proximity to amino acid Phe312 in TM VII and Leu83 in TM II of the GnRH-R respectively (Figure 8.1). In the Baldwin model of the GnRH-R these residues are also positioned within the putative binding pocket (see Figure 8.2). Leu, Phe and Trp are all hydrophobic amino acids and therefore it is possible that the docking of GnRH with its receptor involves hydrophobic interactions between these pairs of amino acids. To test this hypothesis, six mutant GnRH-Rs were generated by site-directed mutagenesis. To establish if these specific amino acids in the receptor formed hydrophobic interactions with the ligand, each residue was substituted for an alternative hydrophobic amino acid (Leu83Val and Phe312Tyr), or for a hydrophilic residue (Leu83Lys and Phe312Arg). In addition, modification of each site to Ala, Leu83Ala and Phe312Ala, was carried out to monitor any changes in receptor function resulting from the presence of a smaller amino acid. Receptor mutants generated are shown in Table 8.1.

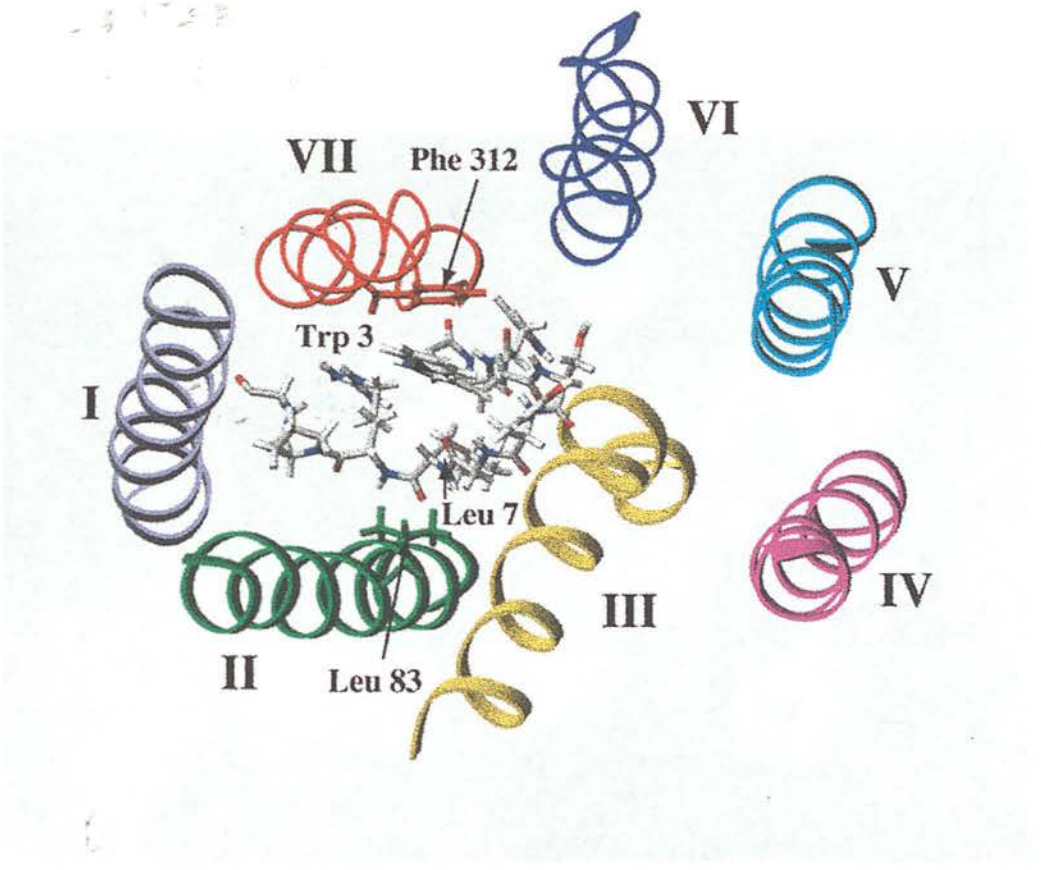

Figure 8.1 Position of Phe312 and Leu83 in the computer-derived GnRH-R model

Computer model of the TM domains of the GnRH-R with GnRH inserted into a putative binding location. The position of Phe312 in TM VII and Leu83 in TM II of the GnRH-R model are highlighted. The close proximity of Trp3 and Leu 7 in GnRH to Phe312 and Leu83 respectively can be observed.

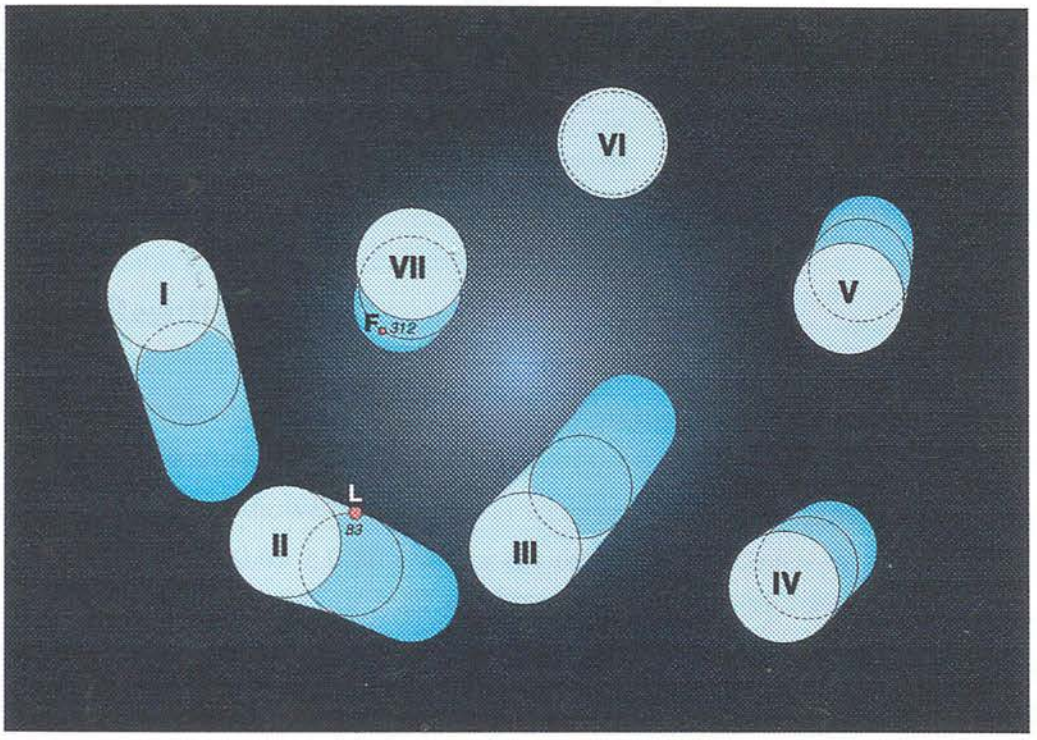

Figure 8.2 **Position of Phe312 and Leu83 in the Baldwin model**

Structural model of the TM domains of the rat GnRH-R as predicted by the Baldwin model. The model is a view from the extracellular surface of the receptor, looking inwards down the central pore, towards the intracellular face. The TM domains are represented by cylinders and the individual tilts and relative positions of the helices can be observed. Mutated amino acids are highlighted.

GnRH-R mutant	TM position	Amino acid modification
Phe312Tyr	TM VII	F to Y
Phe312Ala	TM VII	F to A
Phe312Arg	TM VII	F to R
Leu83Val	TM II	L to V
Leu83Ala	TM II	L to A
Leu83Lys	TM II	L to K

Table 8.1 GnRH-R Phe312/Leu83 mutations

Amino acids targeted for site-directed mutagenesis and their corresponding amino acid substitutions.

8.2 Results

The receptor affinity (Kd) and receptor number (B max) were calculated by Scatchard analysis of saturation binding data. COS-1 cells transiently transfected with GnRH-R mutant Phe312Tyr showed a significant increase ($p<0.05$) in receptor affinity [Kd values (± SEM) of 0.65 ± 0.38 nM] for the radiolabelled GnRH-A, compared to the WT [Kd values (± SEM) of 1.49 ± 0.38 nM] (Figure 8.3). The B max value of Phe312Tyr was ~ 50% of the WT (Table 8.2). The increase in GnRH-R affinity displayed by Phe312Tyr was also reflected in the activation of the second messenger coupling system. GnRH-stimulated total IP production of the Phe312Tyr mutant showed a significantly lower ED50 (± SEM) value of 0.25 ± 0.05 nM ($p<0.05$) compared to the GnRH-R WT value of 3.9 ± 0.9 nM (Figure 8.4a), with maximum level of IP production equivalent to that observed for the WT receptor (Table 8.3). In contrast, mutant Phe312Ala showed a comparable receptor affinity to WT with a Kd value of 1.7 ± 0.45 nM (Figure 8.3). However, the number of receptors was markedly reduced to ~ 33% relative to that observed for the WT receptor (Table 8.2). These findings are in agreement with GnRH-stimulated total IP production, as the ED50 value of 4.2 ± 0.5 nM was similar to WT (Table 8.3) but the maximum level of GnRH stimulated total IP production was reduced to ~ 28% of WT activity (see Figure 8.4a). Receptor mutant Phe312Arg showed no GnRH-A binding nor a GnRH-stimulated IP response as shown in Figure 8.4a.

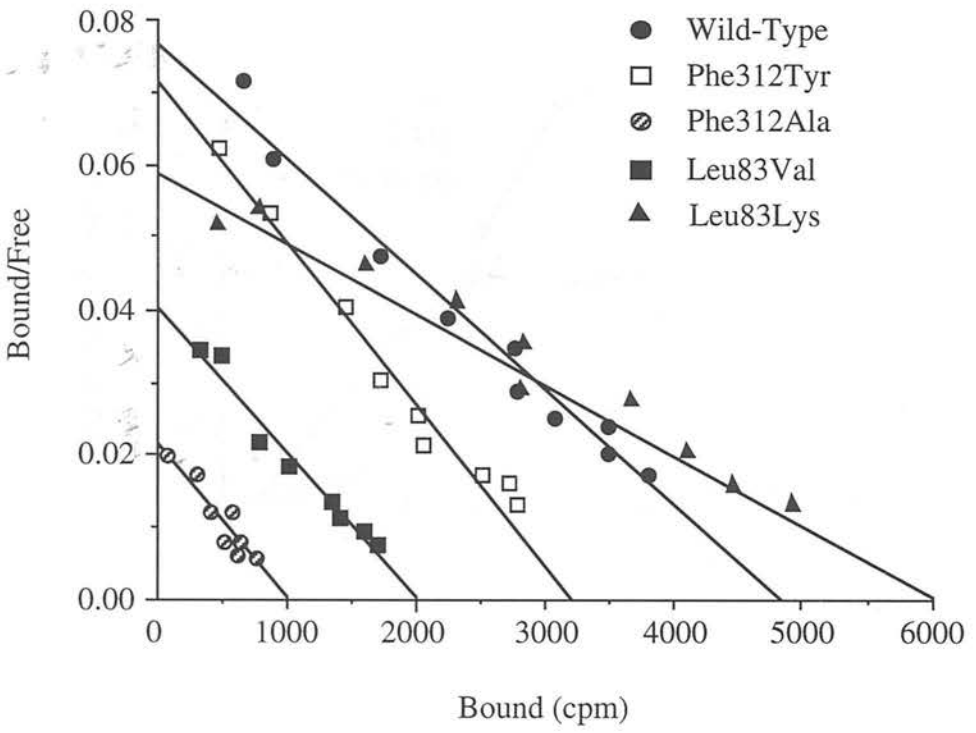

Figure 8.3 GnRH-R WT and Phe312/Leu83 mutants agonist binding data

Scatchard Plot of GnRH-A binding to GnRH-R WT and mutants Leu83 and Phe312. Saturation binding assays were performed using an iodinated GnRH-A [des Gly^{10}, D-Trp^{6}, Pro^{9} NEt]-GnRH on membrane preparations from COS-1 cells transiently expressing the GnRH-R WT or mutants. Data points are the mean of duplicate/triplicate samples and the graph is a representative example from n=4 individual experiments.

Figure 8.4 GnRH-R WT and Phe312/Leu83 total inositol phosphate production (following page)

Total IP production in COS-1 cells transiently expressing the GnRH-R WT and mutants following stimulation with GnRH (10 pM to 1 mM) (a) GnRH WT and mutants Phe312Tyr, Phe312Ala and Phe312Arg (b) GnRH WT and mutants Leu83Val, Leu83Ala and Leu83Lys. Untransfected COS-1 cells were used as a negative control showed only basal stimulation at all GnRH concentrations. Data points represent the mean of duplicate/triplicate samples and these graphs are representative examples from n=3 individual experiments.

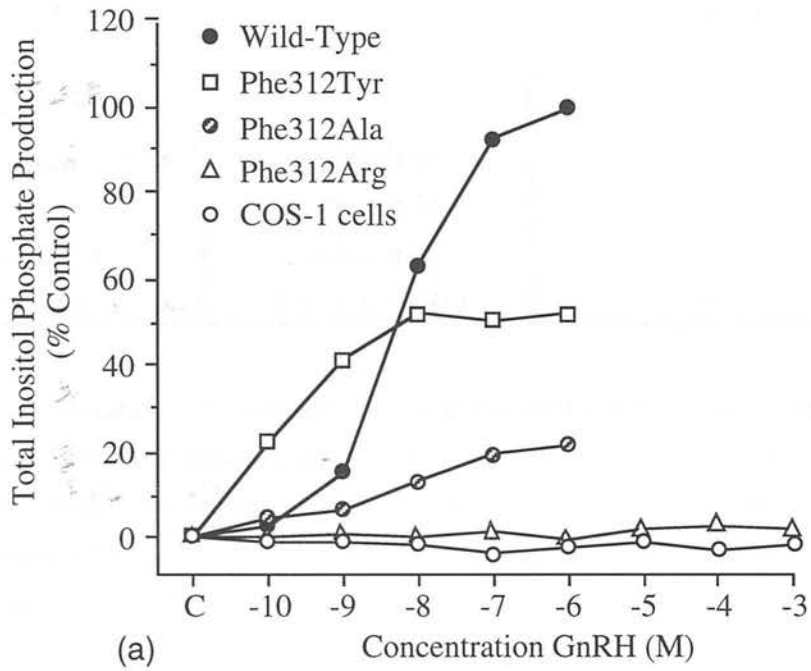
Total Inositol Phosphate Production (% Control)
120
100
80
60
40
20
0
Wild-Type
Phe312Tyr
Phe312Ala
Phe312Arg
COS-1 cells
C
-10
-9
-8
-7
-6
-5
-4
-3
Concentration GnRH (M)

(a)

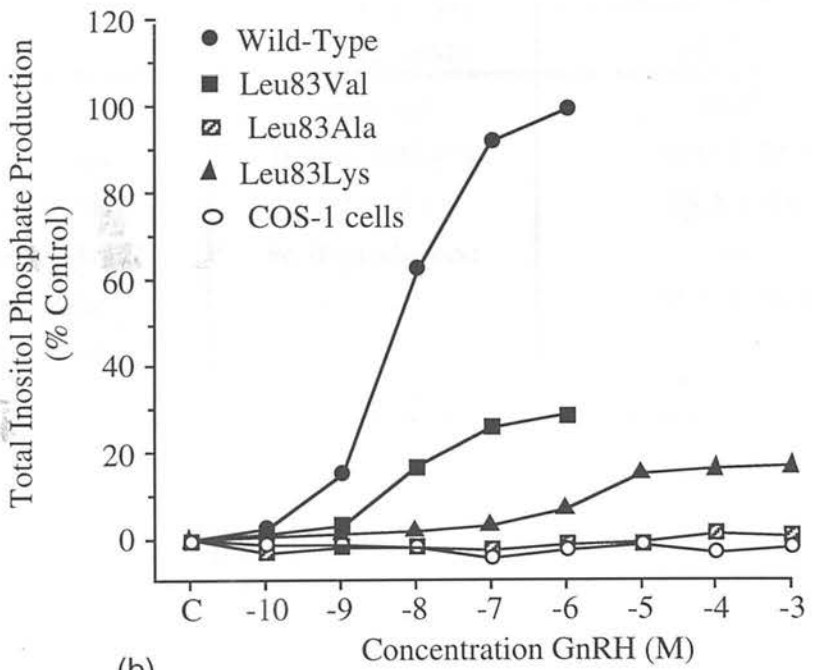
Total Inositol Phosphate Production (% Control)
120
100
80
60
40
20
0
Wild-Type
Leu83Val
Leu83Ala
Leu83Lys
COS-1 cells
C
-10
-9
-8
-7
-6
-5
-4
-3
Concentration GnRH (M)

(b)

GnRH-R Construct	Kd ± SEM (nM)	B max (% WT)
Wild-Type	1.49 ± 0.38	100%
Phe312Tyr	0.65 ± 0.35 (*)	52%
Phe312Ala	1.70 ± 0.45	33%
Phe312Arg	no binding	—
Leu83Val	1.08 ± 0.54	40%
Leu83Ala	no binding	—
Leu83Lys	2.91 ± 0.81 (*)	104%

Table 8.2 Summary of GnRH-R WT and Phe312/Leu83 mutant binding data

Table summarising receptor binding assay data. Receptor dissociation constant (Kd) and receptor numbers (B max) were calculated from Scatchard analysis of saturation receptor binding assays. Kd and B max values are the average (± SEM) of n=3 individual experiments. Statistical analysis was carried out using t-tests and (*) represents a p value of $p<0.05$.

GnRH-R construct	ED 50 GnRH ± SEM (nM)	Maximum IP production (% WT)
Wild-Type	3.6 ± 0.9	100%
Phe312Tyr	0.25 ± 0.05 (*)	89.3 ± 22.5
Phe312Ala	4.2 ± 0.5	28.2 ± 8.4
Phe312Arg	no IP production	—
Leu83Val	6.1 ± 0.7	56.9 ± 16.3
Leu83Ala	no IP production	—
Leu83Lys	1398 ± 808 (*)	21.3 ± 4.4

Table 8.3 Summary of GnRH-R WT and Phe312/Leu83 mutant total inositol phosphate data

Table summarising total IP production. The ED50 values were calculated from GnRH (10 pM to 1 mM) stimulated IP production dose response curves. ED50 values and maximum IP production are the average (± SEM) of n=3 individual experiments. Statistical analysis was carried out using t-tests and (*) represents a p value of $p<0.05$.

COS-1 cells transiently expressing the GnRH-R mutant Leu83Val showed similar receptor binding to WT with a Kd (± SEM) value of 1.08 ± 0.54 (Figure 8.3). The B max values were ~ 40% of the WT receptor. GnRH-stimulated total IP production for this mutant also yielded a similar ED50 (± SEM) value of 6.1 ± 0.7 nM, relative to WT (Table 8.3). A reduction in the maximum level of IP production to 57% of the WT value was observed (see Figure 8.4b). In contrast, receptor mutant Leu83Ala did not bind GnRH-A nor couple to the second messenger IP pathway (Figure 8.4b). GnRH-R mutant Leu83Lys showed a significant decrease ($p<0.05$) in receptor binding affinity with a Kd (± SEM) value of 2.91 ± 0.81 nM (Figure 8.3). This mutant, however, had a similar receptor number compared to WT (Table 8.2). Mutant Leu83Lys displayed a marked reduction in second messenger coupling with GnRH-stimulated total IP production detectable only above 1μM GnRH concentrations. The maximum level of total IP production reached only 21% of the WT level when COS-1 cells were stimulated with 1mM GnRH (Figure 8.4b).

Northern Blot analysis was used to compare the expression of GnRH-R mutant RNA with WT RNA. Figure 8.5 shows a Northern Blot of total RNA extracted from COS-1 cells transiently expressing the WT and mutant GnRH-Rs, Phe312Tyr, Phe312Ala, Phe312Arg, Leu83Val, Leu83Ala and Leu83Lys. RNA extracted from αT3-1 cells together with RNA from HEK-293 cells stably expressing the GnRH-R HEK-WT and mutants HEK-His305Arg and HEK-Asn314Asp were used as positive controls. RNA from untransfected COS-1 cells and HEK-293 cells were negative controls. In the Phe312 and Leu83 mutants, a major transcript size of 2.9 kb was observed (Figure 8.5a). This contrasts with the results from the WT and mutants stably expressed in HEK-293 cells (see Chapter 7, Figure 7.8). An αT3-1 RNA transcript is not visible in Figure 8.5a but further exposure of the blot to autoradiographic film (24 hours) revealed a faint band corresponding to a transcript size of 3.6 kb (as previously described in Chapter 7). Hybridisation of a radiolabelled 18S oligonucleotide probe with a 1.9 kb band corresponding to 18S RNA was used to compare the relative RNA signal between each well (Figure 8.5b).

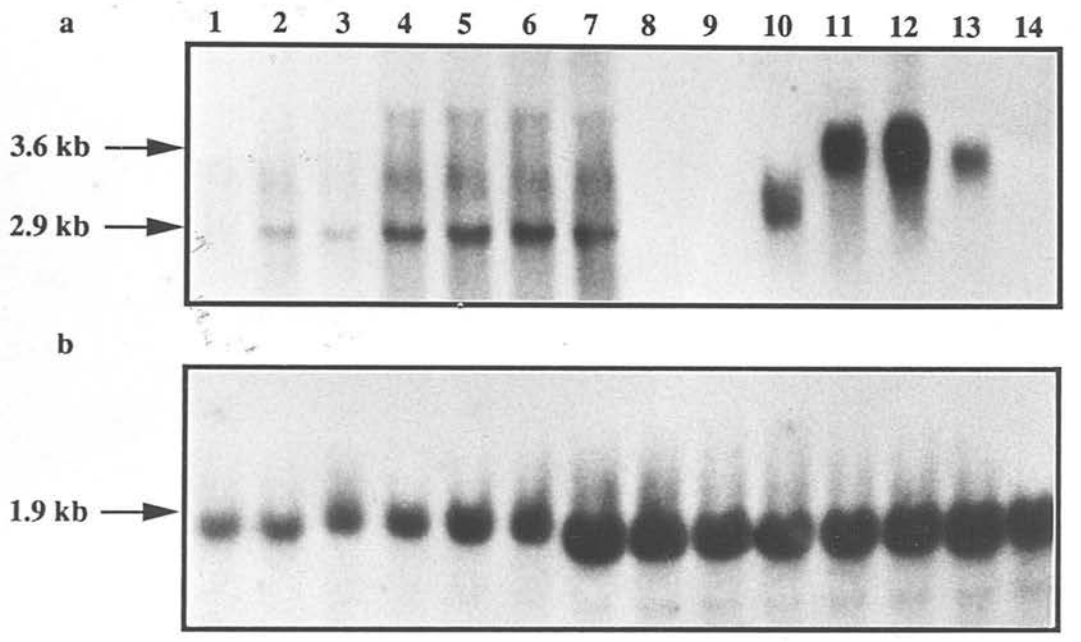

Figure 8.5 Northern Blot of GnRH-R WT and Phe312/Leu83 mutants

(a) Northern blot probed with a [^{32}P]αdCTP labelled 2.2 kb rat GnRH-R insert showing RNA expression levels in total RNA (15μg) from COS-1 cells transiently expressing GnRH-R mutants Leu83Lys (lane 1), Leu83Ala (lane 2) and Leu83Val (lane 3), Phe312Arg (lane 4), Phe312Ala (lane 5), Phe312Tyr (lane 6) and the GnRH-R WT (lane 7). Untransfected COS-1 cells (lane 8), and HEK-293 cells (lane 9) were negative controls. HEK-293 cells stably transfected with the rat GnRH-R mutants HEK-Asn314Asp clone 1 (lane 10), HEK-WT clone 2 (lanes 11 & 12) and HEK-His305Arg clone 3 (lane 13) together with αT3-1 cells (lane 14) were positive controls.

(b) Northern blot probed with [^{32}P]γ dATP labelled anti-18S oligonucleotide.

Experiments were carried out on at least n=3 independent occasions using different batches of RNA.

8.3 Discussion

Hydrophobic interactions are important in ligand-receptor binding in the β-adrenergic receptor (Strader et al, 1989). To investigate the role of similar interactions in the GnRH-R, two potentially important sites were targeted using computer simulation studies. The generation of computer-derived models of the GnRH ligand and receptor has allowed potential ligand-receptor interactions to be examined in a three-dimensional spatial orientation. With the aid of these models, possible hydrophobic interactions between Phe312 (TM VII) in the GnRH-R and Trp3 in the ligand together with Leu83 (TM II) in the GnRH-R and Leu7 in GnRH were hypothesised. To investigate these postulated interactions, Phe312 and Leu83 were targeted for site-directed mutagenesis study. Results from Chapter 7 indicated that the choice of substituting amino acid was critical in the outcome of site-directed mutagenesis experiments. Therefore, three individual mutations were constructed at each site. To examine the role of putative hydrophobic interactions between Phe312/Leu83 and GnRH, these residues were mutated to amino acids of similar hydrophobicity (Phe312Tyr and Leu83Val), and residues of a hydrophilic nature (Phe312Arg and Leu83Lys). In addition, to investigate the effects of introducing a small amino acid, Phe312 and Leu83 were also replaced by Ala.

Substitution of the hydrophobic Phe residue to Tyr at position 312 resulted in an increase in GnRH-R affinity together with an increase in coupling efficiency to the phospholipase C second messenger pathway. The number of mutant receptors was decreased to 50% of WT, whilst the maximum GnRH-induced IP production was retained at WT levels. The presence of a highly hydrophilic Arg, however, completely abolished receptor binding and activation, whilst the incorporation of Ala created a receptor displaying a WT-like receptor affinity. The second messenger coupling of the Ala substituted receptor also showed a similar profile to WT but maximum GnRH-induced IP production was decreased in accordance with the reduction in mutant receptor numbers. These results suggest that the hydropathicity of the amino acid present at position 312 plays a critical role in GnRH ligand-receptor interactions, and is involved in the functional coupling of the receptor to its appropriate G-protein.

The original hypothesis postulated a putative hydrophobic interaction between Phe312 in TM VII of the GnRH-R and Trp at position 3 in the GnRH ligand. Replacement of Phe with Tyr maintained the binding and functional activities of the receptor. In fact,

this mutant receptor showed higher receptor affinity and more efficient GnRH-induced total IP production, despite its apparent decrease in receptor numbers. Tyr, like Phe, contains an hydrophobic aromatic ring and this close structural relationship permits Tyr to function in a manner akin to the normally positioned Phe. Therefore, if Phe312 is involved in a hydrophobic interaction with Trp3 of the ligand, substitution of Tyr at this position would be expected to maintain this putative bonding role. Tyr also contains an additional hydroxyl group, and it is feasible that the increase in receptor affinity and functional activity results from stabilisation of GnRH through the interaction of the Tyr hydroxyl group with carbonyl groups of the peptide backbone.

The decrease in receptor number displayed by Phe312Tyr is a commonly observed finding in mutagenesis studies. Mutant receptors tend to express at only 40-80% of WT levels (personal observations). The reason for this phenomenon is unknown but possible alterations in receptor structure/function must occur post-transcriptionally as Northern Blot analysis revealed similar levels of RNA transcripts present in both WT and mutant GnRH-Rs. Mutagenesis may, however, have adverse effects on mRNA translation or interfere with post-translational processing, such as receptor packaging and/or the insertion of the receptor into the membrane. In addition, the mutation may also affect three-dimensional receptor folding. Site-directed mutagenesis-induced alterations in receptor structure, particularly around the ligand binding region, may reduce the accessibility of the ligand to its receptor resulting in an apparent decrease in receptor number. In this case, the receptor binding site is normal but the mutation alters the tertiary receptor structure thereby reducing ligand accessibility.

The presence of a highly hydrophobic residue at position 312 completely abolished detectable levels of receptor binding and activation implying that a hydrophobic residue is necessary for ligand binding. The lack of binding observed for mutant Phe312Arg may be due to a loss of critical interactions between the ligand and receptor. This observation is in accord with the hypothesis that a hydrophobic interaction exists between Phe312 and Trp3. If this is the case, then the presence of a highly polar Arg residue would not be expected to support such a bonding pattern. However, this provides only one explanation for the loss of receptor function displayed by Phe312Arg and it is possible that the mutation alters cell surface receptor expression (for further discussion see Chapter 9).

The size of amino acid also appears important, as the incorporation of a smaller hydrophobic Ala residue resulted in a reduced receptor number (a higher receptor concentration was required to detect receptor binding) and a corresponding decrease in the maximal second messenger production. This substitution, however, retained a receptor with WT-like properties of receptor affinity and ED50 value of GnRH-stimulated total IP production. These results suggest that the presence of Ala at position 312 maintains a functional active receptor, displaying WT characteristics, but with a reduced receptor level. In addition, this mutation may alter the three-dimensional structure of the ligand binding domain, particularly as Ala is a much smaller and less hydrophobic amino acid compared to Phe. This difference in amino acid size together with the absence of an aromatic side chain may disrupt the three-dimensional conformation of the ligand binding pocket and/or decrease any putative hydrophobic interactions with the ligand.

Together these results imply that a large hydrophobic residue is critical at position 312 in the GnRH-R in order to maintain a fully functional receptor. It is possible, as indicated by the GnRH ligand-receptor computer modelling studies, that Phe312 might interact directly with the Trp3 of the ligand. Further analysis of the models reveals that Trp3 lies in a position sandwiched between two Phe residues, Phe312 and Phe308. This arrangement would create an extremely stable structure and facilitate aromatic ring stacking interactions between π electrons of all three aromatic rings (Figure 8.6).

In addition to the importance of a hydrophobic amino acid at position 312 in the receptor, the presence of a hydrophobic residue at position 3 in the ligand is required for high affinity ligand binding. Structural modification of GnRH at position 3 reveals that the presence of a hydrophobic residue at this site is essential for the generation of active analogues. Most of the GnRH analogues constructed to date contain Trp 3 or a similar hydrophobic structure at this position, and include the agonists Tyr-OMe3, 4ClPhe-3 and 1-Nal3 (3-(-1-napthyl) alanine) (Haviv et al, 1992) and the antagonists structures D-Pal3 (D 3-pyridinyl alanine) and D-Trp3 (Janecka et al, 1993). Substitution of the indole ring by the polar photoreactive 2-nitro-4-azidophenylsulphenyl group leads to a complete loss in activity (Nikolics et al, 1988). The importance of a hydrophobic residue at position 3 in the ligand also supports the hypothesis that a hydrophobic interaction might occur between Trp 3 in the ligand and Phe312 in the GnRH-R.

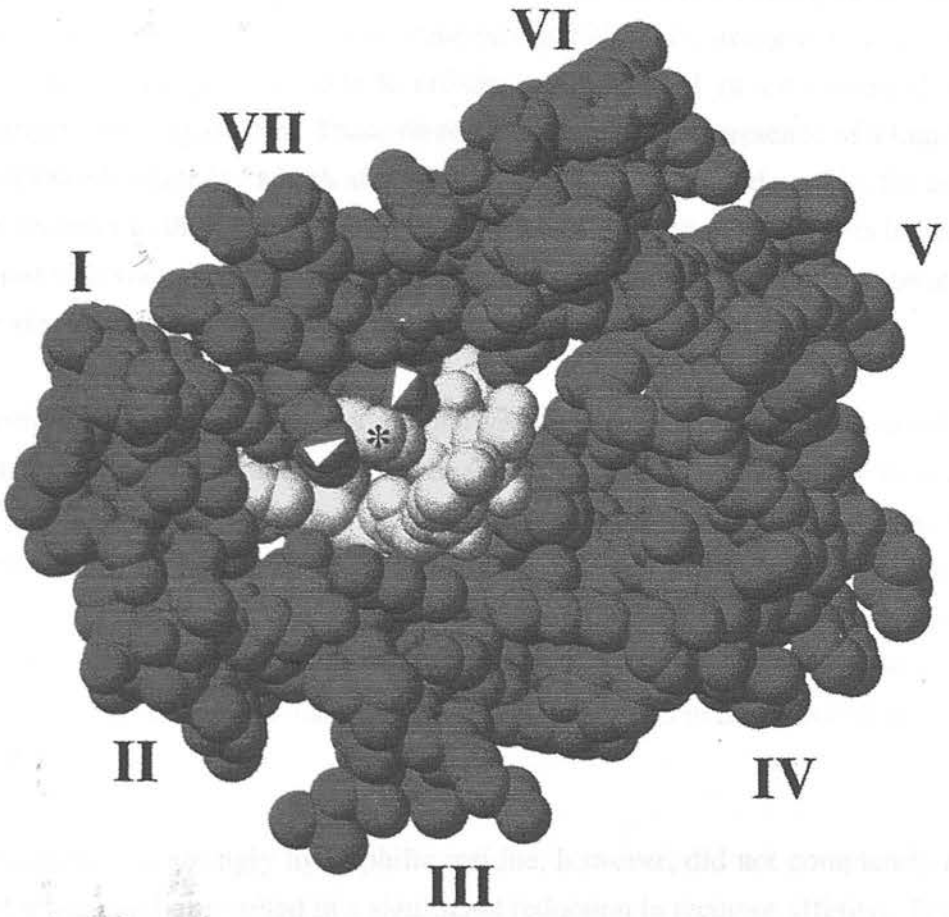

Figure 8.6 **Space-filling model highlighting GnRH ligand and receptor interactions**

Space-filling model of the GnRH-R showing a possible arrangement between the TM domains of the GnRH-R (blue) and GnRH (yellow). The position of Phe312 (left) and Phe308 (right) in the GnRH-R are marked by arrows and the position of Trp 3 in GnRH is represented by an *.

Substitution of the hydrophobic Leu83 to Val resulted in a mutant receptor displaying a similar receptor affinity and GnRH-stimulated total IP ED50 value to the WT receptor. The number of cell surface receptors and maximum GnRH-induced total IP production was decreased to 40% and 57% of the WT values respectively. The presence of a smaller Ala amino acid at this site, however, completely abolished receptor binding and activation whilst the incorporation of a strongly polar Lys residue significantly decreased GnRH-R affinity and resulted in an impaired second messenger coupling system. These findings suggest that the presence of a Leu residue at position 83 maintains a high affinity receptor binding site and permits the coupling of the receptor to the membrane bound G-protein. However, these results indicate that the most important factor mediating receptor binding and functional activation at Leu83 is the size of the amino acid residue and not its hydrophobic nature.

The original hypothesis predicted a putative interaction between Leu83 in the TM II domain of the GnRH-R and Leu 7 in the GnRH peptide. As expected, substitution of Leu83 to another hydrophobic residue Val resulted in a fully functional mutant receptor with receptor affinity and second messenger function comparable to the GnRH-R WT. The maximum level of the second messenger response decreased in accordance with the decrease in receptor number. Again, this finding was in accord with the predicted hydrophobic interaction between Leu83 in the GnRH-R and Leu7 in GnRH.

Substitution by a strongly hydrophilic residue, however, did not completely abolish receptor binding but resulted in a significant reduction in receptor affinity. The effect of this receptor mutation was primarily on second messenger coupling with ligand-induced total IP production only elevated above basal levels when the system was stimulated with high concentrations of GnRH (above 1μM). These findings imply that the putative function of the hydrophobic residue at this site may be related to receptor activation.

Modification of the receptor to incorporate Ala at position 83 gave the most surprising result. The presence of this small hydrophobic amino acid resulted in a complete loss of receptor binding and activation. It is possible that Ala alters the three-dimensional structure of the receptor binding domain to such an extent that it completely prevents ligand binding and receptor activation. Again, the possibility of a decrease in receptor

expression must be considered and without a suitable antibody it is impossible to rule out this factor (see Chapter 9).

Analysis of GnRH analogue structures substituted at position 7 also provided information as to the nature of the amino acid required at this site for high affinity binding. Substitutions yielding active analogues are also hydrophobic, with one exception, and include the substituents Phe7, cyclohexylalanine7 and cycloleucine7 (Hazum et al, 1981). Only the mammalian, chicken I and catfish GnRH peptides contain Leu7 whilst the native salmon GnRH and chicken II GnRH peptide contain another hydrophobic residue Trp in position 7 (Folkers et al, 1984). The one exception to the position of a hydrophobic amino acid involves the interchange of Leu7 and Arg8 to yield a potent antagonist with low histamine releasing properties. This substitution, however, is only active if Leu is present in position 8 (Floret et al, 1992).

Collectively, these results indicate that whilst a putative hydrophobic interaction could exist between the Leu83 in the GnRH-R and the Leu7 in GnRH any such interactions mainly affect receptor activation. The size of amino acid appears more important and this suggests that the role of Leu83 may be structural. Substitution by a much smaller amino acid may alter the three-dimensional structure of the receptor at a critical point within TM II, thereby affecting ligand binding and receptor activation. As previously highlighted in Chapter 6 Asn87, located approximately one helix turn above the Leu83, appears important in receptor binding and thus it is feasible that alterations in the protein structure at this point may have a detrimental effect on receptor function.

In conclusion, the hydropathicity of the amino acid at 312 in the GnRH-R appears important in receptor binding with high affinity binding requiring the presence of a hydrophobic amino acid at this position. In contrast, the size of the amino acid at position 83 appears to be the most critical factor for receptor binding but the presence of a large hydrophobic residue is important in G-protein activation. The three-dimensional computer-simulated models of the GnRH-R and GnRH ligand predicted a putative interaction between Phe312 and Trp3 and between Leu83 and Leu7, and from the site-directed mutagenesis data these interactions are still feasible.

Inevitably measurements of receptor protein expression at the cell surface membrane will determine whether these assumptions are valid and the monitoring of cell surface

GnRH-Rs is described in the following chapter. However, ultimately only the three-dimensional structural determination of the GnRH ligand and receptor will establish the precise nature of the interactions between them. In the meantime it is important to utilise all the tools available, including molecular modelling, to advance our understanding of the mechanisms underlying GnRH-R activation

9 Monitoring levels of receptor expression

9.1 Introduction

Site-directed mutagenesis studies are one of the first approaches used by molecular biologists to examine protein structure-function relationships. However, a major problem associated with this method is the distinction between mutational effects on local structures and those which affect more global factors such as protein folding and stability. At present there are no algorithms to predict the possible perturbations in protein structure caused by amino acid substitutions and it is possible that single base changes, in appropriate locations, may drastically affect protein expression (Sambrook et al, 1989). However, such problems can be overcome if independent measurements of receptor function can be ascertained. Several methods were used to monitor mutant receptor expression and these include (i) the development of GnRH-R antibodies, (ii) measurements of differential receptor function and (iii) epitope tagging of the GnRH-R. The development of the GnRH-R epitope tagging system is the first system which has enabled the measurement of cell surface GnRH-R protein.

9.2 Results

9.2.1 Monoclonal and polyclonal antibody screening

A polyclonal antibody, raised against a 15 amino acid sequence in the el 2 of the GnRH-R, and a monoclonal antibody raised against 1-29 residues in the NH_2 terminus were tested using Western Blot analysis. However, neither antibody detected a specific GnRH-R protein band from solubilised HEK-WT GnRH-R membrane preparations.

9.2.2 Functional Studies

In the absence of any suitable antibodies, alternative measurements of receptor expression were sought. One possible method is to examine other functional

properties exhibited by the protein. However, in the case of the GnRH-R functional properties are intrinsically tied to its ligand-receptor binding capacity. Hence, if the mutant receptor fails to bind its ligand then receptor activation properties will automatically be affected. Nevertheless, it is possible to measure some functional activation in situations where receptor binding levels are below assay detection limits by stimulating receptor mutants with very high concentrations of native ligand (Perlman et al, 1994a, b; 1995). Using this approach partial receptor second messenger function has been demonstrated in the TRH-R Cys98Ser, Cys98Ala and Cys179Ala (Chapter 5). These mutants showed no detectable levels of receptor binding activity and, therefore, total IP production at 1μM of stimulating ligand was also greatly reduced. The ability of these mutants to show a significant rise in total IP production, above basal levels, at higher peptide concentrations indicated that some functionally active receptors were present at the cell surface. It is unclear, however, if these observations reflect an amplified response in a structurally normal receptor, with low expression levels, or the activation of a receptor with normal numbers but an abnormal tertiary protein structure. Whilst this approach cannot localise the precise site of the mutational effect, it does indicate that the substituting amino acid does not completely abolish receptor trafficking to the cell surface or receptor insertion into the membrane.

Another approach testing for normal levels of receptor expression and protein folding is to examine the differential mutation effects on agonist verses antagonist binding. It has been postulated that the complement of receptor residues involved in agonist binding differs from those involved in antagonist binding and therefore whilst certain receptor amino acids may be critical for ligand-receptor activation by one analogue they may not be involved in the binding mechanisms of another (Janovick et al, 1993). Antagonist binding studies have only been carried out on the GnRH-R mutations Asn87Asp, Asp318Asn and the double mutation (Chapter 6). In this study, the agonist and antagonist binding data showed similar trends with the Asn87Asp and the double mutation unable to bind either analogue. However, only one radiolabelled antagonist was tested and to investigate this aspect more thoroughly it would be necessary to examine the binding of a large cohort of antagonist structures. Antagonist binding studies are not feasible with the TRH-R mutants as no highly specific antagonists are presently available.

9.2.3 Epitope Tagging

The final approach undertaken was the epitope tagging of the GnRH-R. This system has been used in GPCRs site-directed mutagenesis studies to monitor levels of receptor expression in mutant constructs (Kim et al, 1995; Lee et al, 1994; Ng et al, 1994; Qian et al, 1993). Two different tagging systems were tested, the Kodak Flag-tag and the human influenza hemagglutinin (HA) tag. The Kodak flag-tag was inserted into the GnRH-R sequence directly following the ATG start site, whereas both the single (HA-GnRH-R) and triple (3HA-GnRH-R) HA-tag sequences were incorporated 20 bp from the ATG start site. The positions of these epitope tags in the GnRH-R amino acid sequence are illustrated in Figure 9.1 and their protein epitope sequences shown in Table 9.1. The epitope tagging methods are described in detail in Appendix III (sections B and C).

Flag-tag protein sequence	NH_2-Asp-Tyr-Lys-Asp-Asp-Asp-Asp-Lys-COOH
HA-epitope tag protein sequence	NH_2-Tyr-Pro-Tyr-Asp-Val-Pro-Asp-Tyr-Ala-COOH

Table 9.1 The Flag-tag and single HA tag amino acid epitope sequences

The Flag-tag sequence consists of 8 amino acids and many of these residues are highly polar. The HA-tag contains a 9 amino acid epitope.

The tagged receptors were tested for receptor binding function and second messenger activation. The Flag-tag showed no receptor binding and therefore no further studies were carried out. In contrast, the HA-GnRH-R showed receptor binding and functional properties similar to the WT receptor. Receptor binding was measured using Scatchard analysis of saturation receptor binding assay data.

Figure 9.1 Position of epitope tag sequences in the rat pituitary GnRH-R (following page)

Schematic representation of the GnRH-R highlighting the position of the (a) Kodak Flag-tag (yellow) and (b) HA-Tag (green) in the rat GnRH-R. The Flag-tag sequence was incorporated in the GnRH-R directly after the ATG start site whereas the HA-tag was positioned at the Esp31 restriction enzyme site (20 bps from the ATG start site).

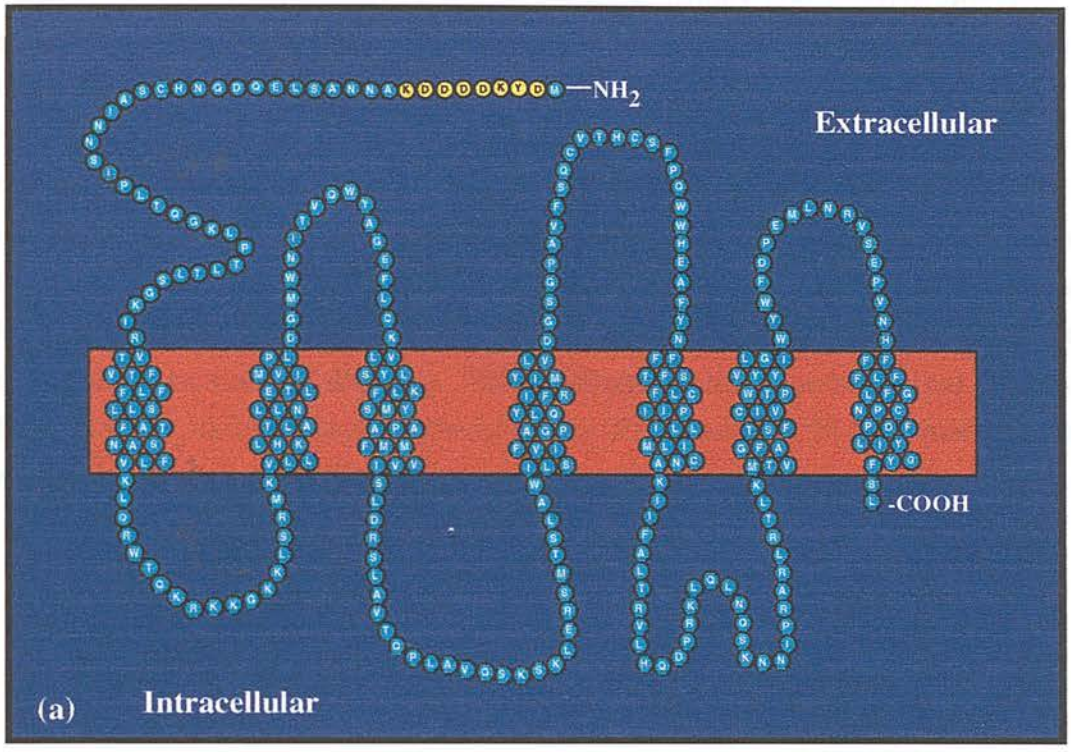
—NH2
Extracellular
-COOH
(a)
Intracellular

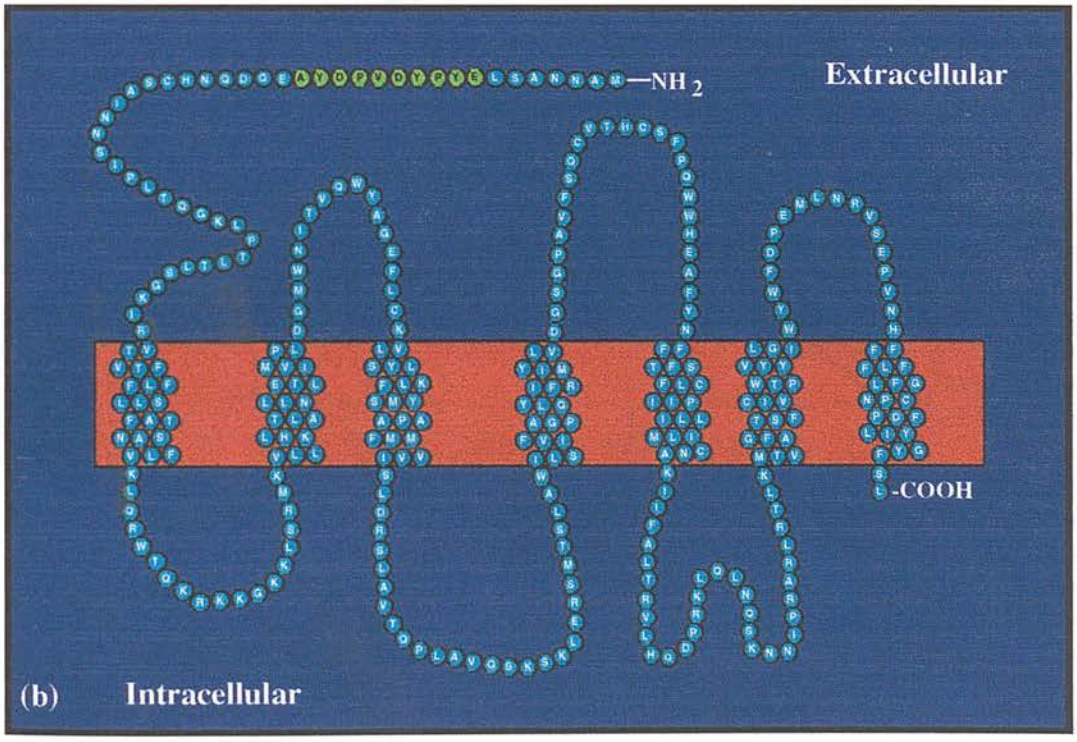
—NH 2
Extracellular
-COOH
(b)
Intracellular

The HA-GnRH-R displayed comparable receptor affinity and receptor numbers to the WT receptor (Figure 9.2). The second messenger function was assessed through GnRH stimulated $[Ca^{2+}]i$ measurements by dynamic video imaging (Figure 9.3). Like the WT receptor, GnRH induced biphasic Ca^{2+} transients in COS-1 cells transiently expressing the HA-GnRH-R. These results indicate that the incorporation of a HA-tag sequence does not interfere with normal binding and functional properties of the receptor. Following characterisation of the ligand binding and activational properties of the tagged receptor, it was necessary to optimise the methods of detection. Three different methods were utilised, Western Blot analysis, indirect immunofluorescence FITC and an ELISA method (see Appendix III, sections D, E and F).

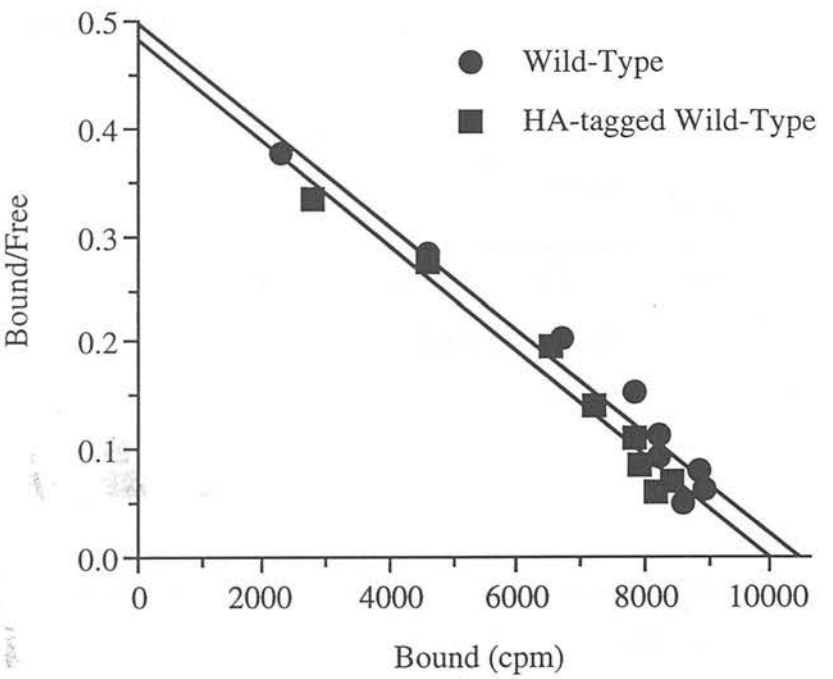

Figure 9.2 HA-tagged WT GnRH-R agonist binding data

Scatchard Plot of GnRH-A binding to GnRH-R WT and the HA-tagged GnRH-R WT. Saturation binding assays were performed using an iodinated GnRH-A [des Gly^{10}, D-Trp^{6}, Pro^{9} NEt]-GnRH on membrane preparations from COS-1 cells transiently expressing the WT or HA-tagged GnRH-R WT. Data points are the mean of duplicate/triplicate samples and the graph is a representative example from at least n=2 individual experiments.

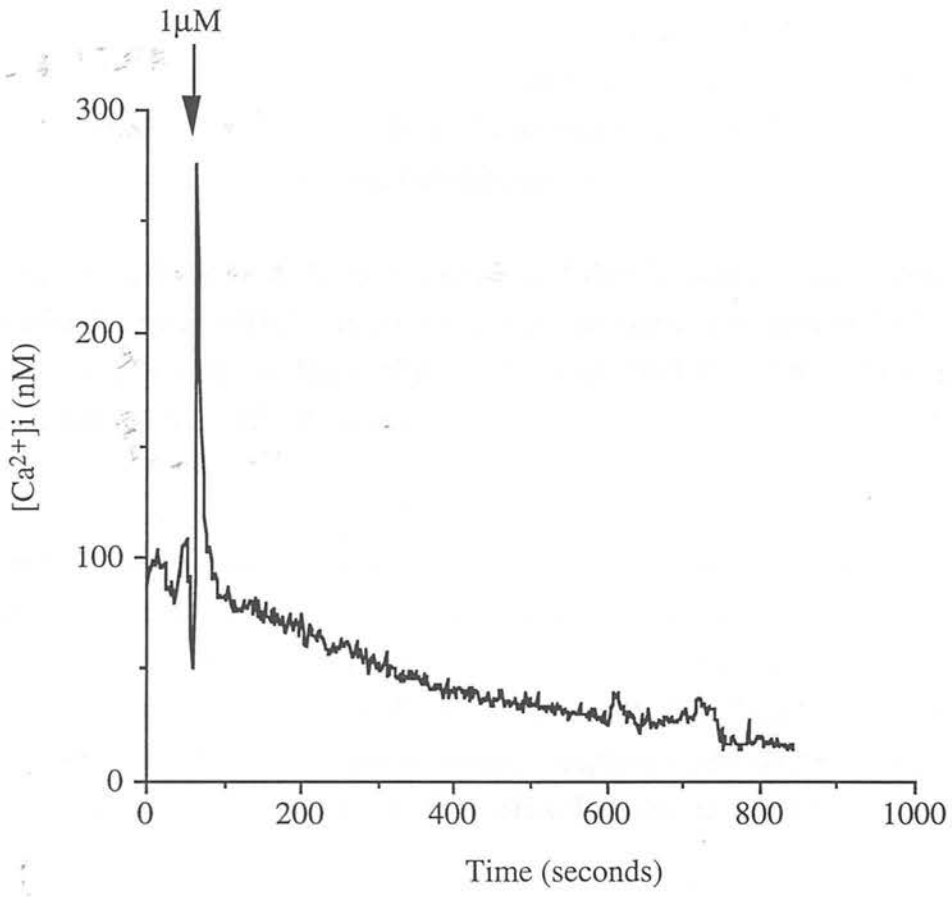

Figure 9.3 GnRH-induced calcium responses in HA-tagged GnRH-R WT

Effects of GnRH (1μM) on $[Ca^{2+}]i$ in COS-1 cells transiently expressing the rat HA-tagged GnRH-R in a population of cells with time (seconds). Graph represents an average plot of $[Ca^{2+}]i$ measurements versus time from 3 individual cells in a field of 18 cells. GnRH (1μM) added at 60 seconds produced a biphasic rise in $[Ca^{2+}]i$.

COS-1 cells transiently transfected with HA-GnRH-R and 3HA-GnRH-R were examined using Western Blot analysis (Figure 9.4). A HA-tagged Gq (HA-Gq) and a triple HA-tagged TRH-R (3HA-TRH-R) were used as positive controls (Figure 9.4). No specific band was apparent (compared to the COS-1 negative control membranes) in the HA-GnRH-R but a faint band was seen at approximately 37 kDa in the 3HA-GnRH-R. The HA-Gq showed a prominent band at 42 kDa and the 3HA-TRH-R displayed a diffuse specific banding pattern .

Detection of the HA-GnRH-R, 3HA-TRH-R and HA-Gq was also carried out using immunofluorescence (FITC). A strong fluorescent signal was seen in COS-1 cells transiently expressing the HA-GnRH-R, the 3HA-TRH-R and the HA-Gq. The untransfected COS-1 cells showed little background fluorescence (Figures 9.5 and 9.6).

Both the Western Blotting and FITC are non-quantitative analysis methods. Therefore in order to establish a quantitative detection system an ELISA method was set up. Figure 9.7 shows the ELISA results for COS-1 cells transiently transfected with the 3HA-GnRH-R, the 3HA-TRH-R and the HA-Gq. Significant differences ($p<0.01$) in the 492 nm absorbance readings, compared to the untransfected COS-1 cells, were obtained for the 3HA-GnRH-R, 3HA-TRH-R and the HA-Gq protein.

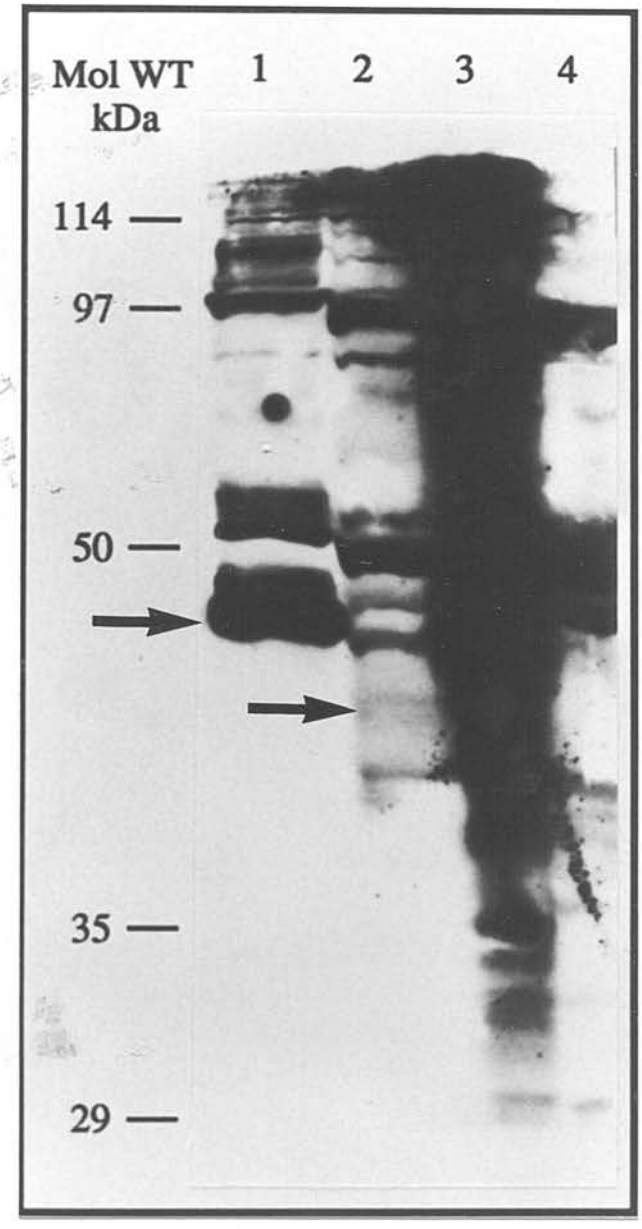

Figure 9.4 Western Blot analysis of HA-tagged Gq, GnRH-R and TRH-R

Detection of HA-tagged proteins by Western Blot analysis. Membranes were prepared from either cells expressing the Gq protein (lane 1), 3HA-tagged GnRH-R (lane 2), 3HA-tagged TRH-R (lane 3). Untransfected COS-1 cells were used as a negative control (lane 4). Arrows indicate the position of the specific 42 kDa band for Gq (lane 1) and 37 kDa band for the 3HA-tagged GnRH-R (lane 2).

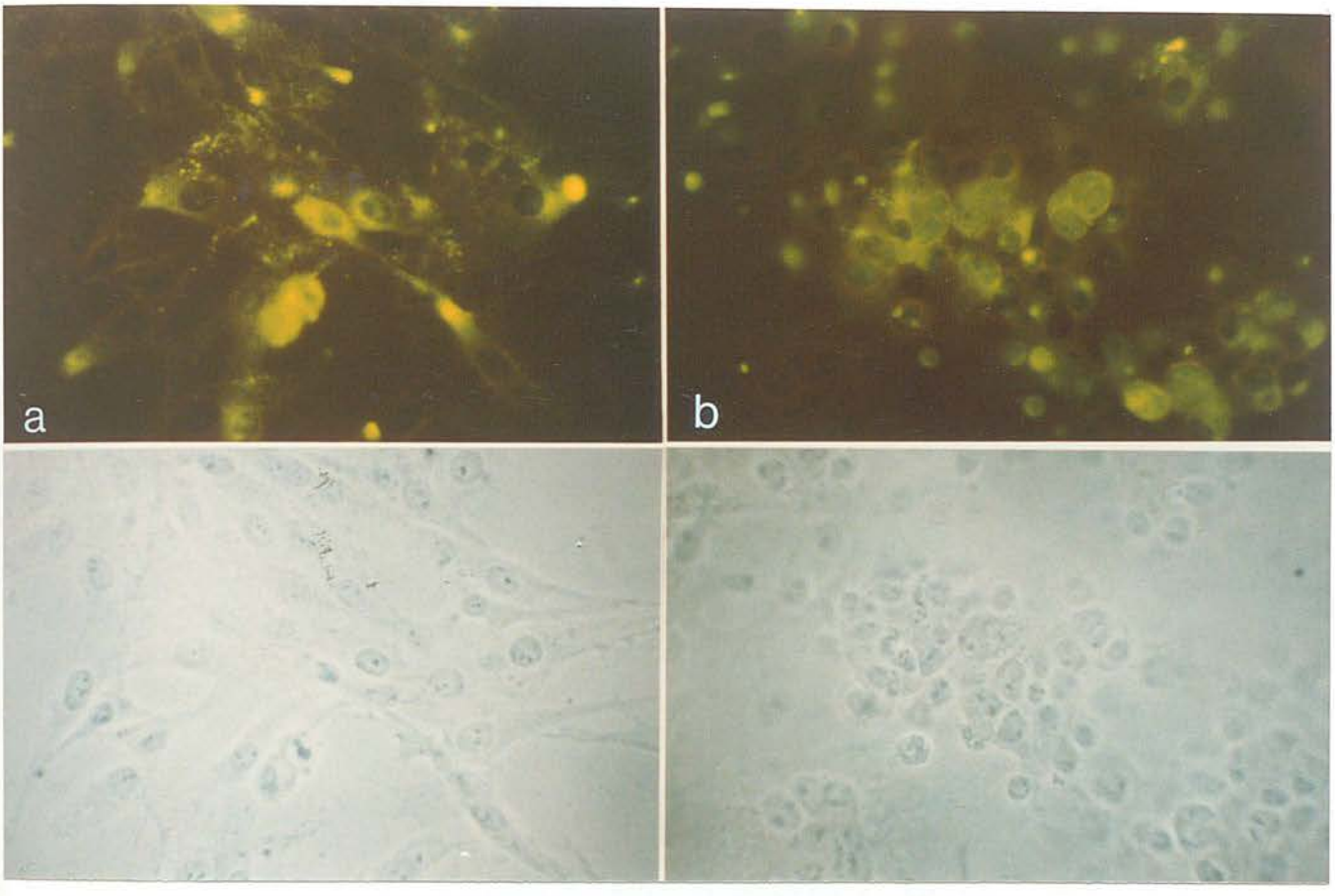

Figure 9.5 Indirect immunofluorescence detection of HA-tagged GnRH-R and TRH-R

Localisation of HA-tagged proteins in COS-1 cells transiently transfected with (a) GnRH-R and (b) 3HA-tagged TRH-R using indirect immunofluorescence (FITC). Cells are viewed by fluorescent (upper) and light microscopy (lower) and are representative pictures from n=2 experiments. Untransfected COS-1 cells demonstrated low background FITC fluorescence.

Figure 9.6 Indirect immunofluorescence detection of HA-tagged Gq and GnRH-R (following page)

Localisation of HA-tagged proteins in COS-1 cells transiently expressing (a) HA-tagged Gq (b)HA-tagged GnRH-R, and (c) untransfected COS-1 cells using indirect immunofluorescence (FITC). Cells are viewed by fluorescent (left) and light microscopy (right) and are representative pictures from n=2 experiments.

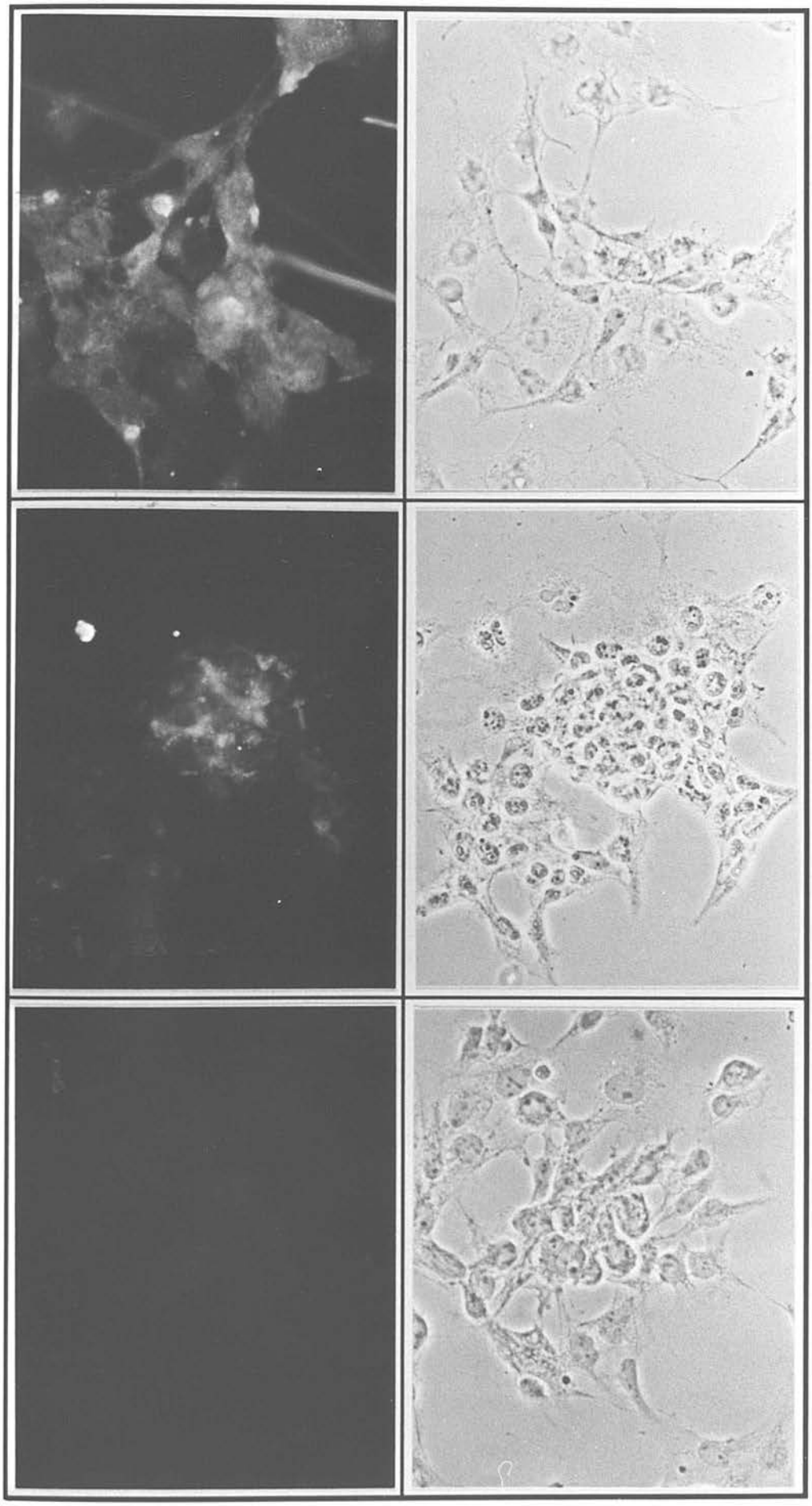
a
b
c

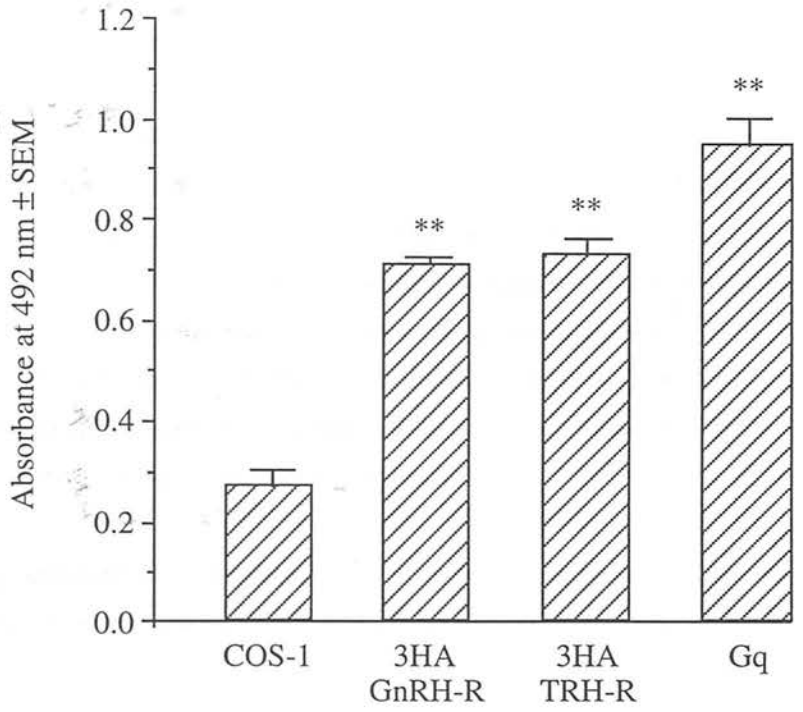

Figure 9.7 ELISA detection of HA-tagged GnRH-R, TRH-R and Gq

Detection of HA-tagged proteins using ELISA. Absorbance measurements were made at 492 nm using an anti-HA antibody dilution of 1:10 in untransfected COS-1 cells (negative control), COS-1 cells transfected with either 3HA-tagged GnRH-R, 3HA-tagged TRH-R or the HA-tagged Gq (positive control). Each sample was carried out in triplicate and this experiment is a representative example from n=2 individual experiments. Statistical analysis was carried out using t-tests and (**) represents a p value of $p<0.01$.

9.3 Discussion

To detect receptor expression in mutant receptors, three different experimental approaches were developed and tested. Initially, polyclonal antibodies raised against the GnRH-R were generated in rabbits. However, these antibodies were non-specific when tested by Western Blot analysis. This finding may be due to the complex three-dimensionalstructure of the receptor, so limiting the availability of antigenic epitopes or it may reflect the low antigenic properties of the synthetic peptides used for immunisation. A monoclonal receptor antibody was also tested but again this proved unsuccessful. Currently, a chicken host is being used for antibody production as the greater evolutionary differences between the avian and mammalian GnRH-R should increase antibody production.

Secondly, attempts were made to measure receptor function in mutant receptors with decreased receptor activity by increasing the receptor concentration in the assay systems. The generation of clonally derived stable cell lines (HEK-His305Arg and HEK-Asn314Asp) increased the receptor number/mg of total protein, allowing for the detection of low levels of receptor binding. Alternatively, it is possible to measure second messenger total IP production, in COS-1 cells transiently expressing mutant receptors, by stimulating cells with very large concentrations of peptide. This approach has been extensively used in site-directed mutagenesis studies in the TRH-R where specific antibodies are also unavailable (Perlman et al, 1994a, b; 1995). In addition, preliminary studies have been carried out to determine whether mutations affecting GnRH-R agonist binding also interfere with the binding of antagonist analogues. The demonstration of differential agonist and antagonist binding function would be particularly useful as it would show an intact receptor tertiary structure.

Finally, two different epitope tags, the Kodak Flag-tag and the HA-tag have been incorporated into the GnRH-R sequence. The Kodak Flag-tagged GnRH-R prevented receptor binding and this may have resulted from a lack of receptor expression or receptor inactivation. The small size of the GnRH-R makes it difficult to incorporate a foreign epitope without affecting ligand binding. In particular, the highly charged nature of the Flag-Tag sequence together with its position close to the ATG start site in the NH_2 terminus may have disrupted receptor expression, insertion into the membrane or protein folding. Following the failure of the Kodak

Flag-tag labelled receptors to bind radiolabelled GnRH no further studies were carried out. In contrast, the HA-GnRH-R displayed ligand binding and second messenger functions comparable to the WT GnRH-R, indicating that the HA-tag does not interfere with normal receptor binding and second messenger activation mechanisms. Western Blot analysis carried out with the single HA-GnRH-R showed a similar banding pattern to the COS-1 control cells. However, using cell membranes transfected with the 3HA-GnRH-R, a faint but specific band was detected of ~ 37 kDa in size. These results suggest that the presence of a triple HA-epitope sequence is necessary to amplify the antigenic signal to detectable levels. In contrast, the FITC HA-tag detection method showed a fluorescent signal with the single HA-GnRH-R tag, and presently other fluorescent linked fluorochromes such as Rhodamine are also under investigation. ELISA measurements of the HA-tagged receptors again revealed that detection methods improved with the triple HA-tag sequence. Using this method it will now be possible to quantify mutant receptor expression levels at the surface membrane of the cell.

These results represent preliminary data and once the system has been optimised for the WT HA/3HA-GnRH-R, then the tag sequence will be incorporated into all the receptor mutants. In the absence of suitable receptor-specific antibodies, the development of the tagging system has provided an alternative measurement of cell surface GnRH-Rs. Whilst this approach tackles the problem of monitoring mutant receptor expression, the location of the tag in the NH_2 terminus means that alterations in the three-dimensional structure of the TM domains, resulting from site-directed mutagenesis, may still go undetected.

10 Summary of results and concluding discussion

10.1 Introduction

Over the last 25 years, the action of GnRH at its specific pituitary receptor has been exploited in clinical medicine to treat a wide range of reproductive conditions. However, the molecular mechanisms underlying the interaction of GnRH with the GnRH-R remain largely unknown. Therefore, knowledge relating to ligand-induced receptor activation will aid in the development of more efficacious and therapeutically safe GnRH analogues. The aims of this study were to delineate amino acid residues in the GnRH-R which are integral in (i) stabilisation of the receptor, (ii) formation of a ligand binding pocket and (iii) ligand-induced receptor activation. Moreover, the analysis of GnRH-R structure-function relationships is imperative to understanding the molecular processes at the centre of ligand-receptor binding.

10.2 Targeting of potentially important amino acids

Potentially important amino acids within the GnRH-R and TRH-R were initially targeted based on their structure-function roles in other GPCRs. This approach provided the basis for examining the role of extracellular Cys residues in these receptors. Sequence analysis also revealed the transposed positions (relative to other GPCRs) of GnRH-R amino acids Asn87 and Asp318. The advantage of sequence homology analysis is that a great deal of mutagenesis data is already available for many different GPCRs. As GPCRs share the same topographical conformation, structural information relating to one specific receptor can often be applicable to other members of this receptor superfamily. However, comparative sequence analysis is of limited use in identifying amino acids involved in ligand receptor specificity, as individual receptors will have a different complement of residues involved in this process. To identify amino acids that interact directly with the ligand, and hence form the ligand binding pocket, it was necessary to devise an alternative targeting approach. This second strategy involved the use of three

different molecular models: (i) the Baldwin model, (ii) a computer-generated model of the GnRH-R and (iii) a simulated model of the GnRH ligand and receptor.

The Baldwin model (Baldwin, 1993) highlights the position of TM-located polar residues. By definition, the TM helices are primarily hydrophobic and so the presence of polar, hydrophilic amino acids is unusual and may have a specific functional significance. The side chains of these polar amino acids are orientated away from the hydrophobic membrane, towards the central pore of the receptor channel, and thus are positioned in an ideal location to interact with GnRH. In order to investigate the role of these residues in GnRH-R binding processes, seven amino acids located either within the TM domains or at the TM/extracellular interface were mutated.

Whilst the Baldwin model provided the first three-dimensionalview of the GnRH-R, the possible position of the ligand within the receptor structure was still completely unknown. A computer-derived model of the GnRH-R and a model of the GnRH ligand (generated at the MRC, Reproductive Biology Unit, Edinburgh) were therefore integrated to simulate potential receptor-ligand interactions. From the dynamic modelling studies of the GnRH ligand and receptor, a hypothetical interaction between Phe312 and Leu83 in the GnRH-R and Trp3 and Leu7 in the ligand was proposed.

The computer-simulated targeting approach provided greater scope (compared to the Baldwin model) for identifying amino acids crucial in receptor specificity, as it permitted the analysis of the receptor structure with direct relevance to the structure and possible positioning of the ligand. It has also allowed for a reciprocal exchange of information, whereby hypotheses based on the molecular modelling studies could be tested by site-directed mutagenesis, and the results of such studies then utilised to further redefine the model's structure. This strategy, whereby feedback information can be integrated back into the system has resulted in a dynamic model to study potential GnRH-R structure-function relationships.

However, as purely hypothetical structures, the accuracy of these models should not be overemphasised. Consequently, predictions made from computer models have to be treated with caution and it is imperative that these models are used within a framework of clearly defined parameters.

10.3 Site-directed mutagenesis

Once the amino acids had been targeted, oligonucleotides were constructed to incorporate the specific modifications required. Recent studies have demonstrated that the choice of substitute amino acids is a critical factor in determining the final outcome of site-directed mutagenesis experiments. In the β-adrenergic receptor, Lefkowitz and co-workers demonstrated that the substitution of Ala293, in the il 3, resulted in variable levels of constitutive activation depending on the nature of the amino acid introduced (Kjelsberg et al, 1992). In this study, the Ala residue was individually modified to all other 19 possible amino acids, and constitutive activation levels ranged from 21% to 250% (above basal activity). Furthermore, in the TRH-R Cys amino acid study (Chapter 5), substitution of extracellular Cys residues to Ala, favoured an increase in receptor function compared to the corresponding Cys to Ser substitutions.

In the Asn87/Asp318 experiments, the single mutations Asn87Asp and Asp318Asn introduced an amino acid of similar size but carrying a different charge, whilst the function of the double reciprocal mutation (Asn87AspAsp318Asn) was to recreate the situation normally observed in other GPCRs. In Chapter 7, the amino acids highlighted by the Baldwin model were either replaced by residues of similar charge or size. In this experimental investigation, Lys residues were modified to another highly basic amino acid Arg, Asn residues substituted for a similarly sized Asp, and Glu residues interchanged with Gln or vice versa. The only radical change was the alteration of His305 to Arg. These conservative changes were incorporated to reduce the possibility of any gross changes occurring in the receptor tertiary structure. In the final series of experiments (Chapter 8), any possible hydrophobic interactions between GnRH-R residues Leu83 and Phe312 and the ligand were examined by modifying each amino acid to either another hydrophobic amino acid, a hydrophilic amino acid or a much smaller, slightly hydrophobic, Ala residue.

10.4 Receptor binding, activation and expression of mutant receptors

Table 10.1 summarises all the effects of the mutant receptors on receptor binding and second messenger production.

Table 10.1 Summary of GnRH-R and TRH-R mutational effects

Summary of receptor binding and second messenger responses in COS-1 cells (transiently transfected) or HEK 293 cells (stably transfected) with mutant TRH-Rs and GnRH-Rs. The receptors constructed in the expression vector pcDNA 1 are indicated with the presence of a (1) after the mutation and those generated in expression vector pcDNA 3 by (3).

+++ increased receptor binding/second messenger function compared to WT

++ represents WT-like activity

+ decreased receptor binding/second messenger function compared to WT

—/+ Small amount of receptor binding/second messenger function detectable

— No receptor binding /ligand induced IP production

Note: Double mutant refers to GnRH-R mutant Asn87AspAsp318Asn

Receptor Mutant	Ligand binding	Second messenger properties
Chapter 5		
GnRH-R Cys14Ser (1)	—	—
GnRH-R Cys114Ser (1)	—	—
GnRH-R Cys195Ser (1)	—	—
GnRH-R Cys199Ser (1)	—	—
TRH-R Cys98Ser (1)	—	—
TRH-R Cys179Ser (1)	—	—
TRH-R Cys100Ser (1)	++	++
TRH-R Cys98Ala (1)	—	—
TRH-R Cys179Ala (1)	—	—
TRH-R Cys100Ala (1)	++	++
Chapter 6		
GnRH-R Asn87Asp (1)	—	—
GnRH-R Asp318Asn (1)	++	—
GnRH-R double mutant (1)	—	—
GnRH-R Asp318Asn (3)	++	—
GnRH-R double mutant (3)	-/+	—
Chapter 7		
GnRH-R Glu90Gln (3)	++	++
GnRH-R Lys115Arg (3)	++	++
GnRH-R Lys121Arg (3)	++	++
GnRH-R Gln174Glu (3)	++	++
GnRH-R Asn304Asp (3)	++	+
GnRH-R His305Arg (3)	—	—
GnRH-R Asn314Asp (3)	—	—
GnRH-R HEK-His305Arg (3)	-/+	+
GnRH-R HEK-Asn314Asp (3)	-/+	+
Chapter 8		
GnRH-R Phe312Tyr (3)	+++	+++
GnRH-R Phe312Ala (3)	++	++
GnRH-R Phe312Arg (3)	—	—
GnRH-R Leu83Val (3)	++	++
GnRH-R Leu83Ala (3)	—	—
GnRH-R Leu83Lys (3)	+	—/+

10.4.1 Role of extracellular Cys residues as determinants of GPCR tertiary structure

In both the GnRH-R and TRH-R, replacement of the extracellular Cys residues (GnRH-R, Cys14Ser, Cys114Ser, Cys195Ser, Cys199Ser and TRH-R Cys98Ser, Cys98Ala, Cys179Ser and Cys179Ala) by either Ser or Ala resulted in a loss of ligand binding and ligand-induced receptor activation (see Table 10.1). These results highlight the importance of a correct tertiary structure for the maintenance of receptor function. The majority of GPCRs contain at least one pair of conserved Cys residues, with the formation of disulphide bonds between extracellular Cys residues, integral in maintaining receptor stability. The disruption of these bonds radically alters the shape of the extracellular receptor domains and therefore prevents ligand-induced receptor activation. In the GnRH-R, the loss of receptor function displayed by all four mutant receptors suggests the presence of at least two disulphide bridges, involving both conserved and non-conserved extracellular Cys residues. In contrast, in the TRH-R, only one disulphide bond is present between conserved extracellular Cys residues, Cys98 and Cys179. TRH-R residue Cys100 does not appear to have a disulphide bonding role, as mutations generated at this site showed WT-like receptor binding and activational properties. Moreover, the retention of receptor function by mutants Cys100Ser and Cys100Ala, indicates that a normal three-dimensionalreceptor structure is maintained by these mutations, despite their close proximity to Cys98. Furthermore, this suggests that only very specific amino acids are involved in the maintenance of receptor tertiary structure. Chemical modification studies in the TRH-R have also confirmed the importance of disulphide bonding interactions.

This experimental study highlighted the role of extracellular Cys residues in disulphide bonding interactions. However, the processes which underlie the formation of disulphide bonds and the factors which determine which specific extracellular Cys residues are involved in each disulphide bridge structure (i.e. conserved or non-conserved) are unknown.

10.4.2 Role of Asn87 and Asp318 residues in GnRH-R function

Results from Chapter 6 indicate that the GnRH-R residue Asn87 (TM II) is important in mediating receptor binding function, whilst the amino acid Asp318 (TM VII) is responsible for G-protein activation. The failure of the double reciprocal

mutant, Asn87AspAsp318Asn, to restore significant receptor binding function suggests that the functional roles of these two amino acids are not interchangeable. Moreover, this implies that their positional differences, relative to other GPCRs, are linked to evolutionary mutations. Furthermore, the computer-simulation studies position Asn87 and Asp318 in favourable locations to interact with GnRH. From these computer models, Asn87 is in close proximity to Arg8 at the COOH terminus of the ligand - the amino acid thought to be responsible for mediating ligand specificity in mammalian GnRH (Davidson et al, 1994).

10.4.3 Role of TM polar amino acids in GnRH-R function

Chapter 7 identified two amino acids important for ligand-receptor binding; His305 positioned at the TM VII/extracellular interface and Asn314 in the middle of TM VII. Initial experimental work, using a transient transfection protocol, revealed that substitution of His305 to Arg and Asn314 to Asp prevented GnRH ligand binding and second messenger coupling. Further investigations, expressing these mutations in a stable cell line, showed that His305Arg and Asn314Asp had small, but detectable, levels of receptor function (binding and second messenger coupling) compared to the WT GnRH-R.

The position of His 305 at the extracellular interface suggests that is unlikely to form part of the TM-located ligand binding pocket. However, it may indirectly affect ligand-receptor binding by channelling the ligand into the receptor pore, or by maintaining the tertiary structure of the extracellular domains. The role of extracellular residues in GnRH-R binding processes has not been extensively studied. However, one residue in the el 3, Glu301, has been implicated in conforming the ligand prior to binding (Davidson et al, 1994). In other GPCRs, for example the neurokinin (Fong et al, 1992) and glycoprotein hormone receptors (Byrant et al, 1995; Ji and Ji, 1995), amino acids in the extracellular domains are important in mediating receptor binding function.

In contrast, GnRH-R residue Asn314 lies in the middle of TM VII and thus is in an ideal location to form part of the ligand binding pocket. Further analysis of the computer-derived GnRH/GnRH-R model reveals that Asn314 lies in close proximity to the amino acid side chain of Arg8 in GnRH.

10.4.4 Role of Phe312 and Leu83 in GnRH-R function

Only one GnRH-R mutant constructed to date, Phe312Tyr, showed an increase in receptor affinity and a greater production of total IPs when stimulated with low concentrations of GnRH. This finding suggests that certain structural modifications to the GnRH-R can enhance ligand binding interactions and receptor activation mechanisms. Tyr contains a hydroxyl group, capable of forming H-bonds, and it is possible that further bonding interactions between Tyr312 and the ligand, function to stabilise the ligand-receptor complex or increase its resistance to protein degradation. Mutant Phe312Arg, failed to show any ligand binding or activational properties, indicating that the presence of a hydrophobic residue was necessary at this site for maximum receptor function. Moreover, the presence of a small slightly hydrophobic residue, Ala at position 312, retained partial receptor binding and second messenger coupling properties. The computer simulation studies position Trp3 of GnRH in close proximity to both Phe312 and Phe308 in the receptor, and these locations would allow for interactions between the aromatic rings of all three residues.

GnRH-R mutant Leu83Val showed a similar receptor affinity to the WT. However, this mutation exhibited a decrease in receptor numbers and hence a decrease in the maximum level of second messenger production. During the course of this study, mutant receptors often displayed normal WT-like receptor binding (Kd) and activation (ED50) profiles but showed a decrease in receptor numbers. The reasons underlying this finding are unknown, but may be related to decreased receptor expression following transfection. Moreover, the position of the mutation appears critical, and changes in receptor residues at important loci within the receptor may have marked effects on receptor expression levels. Some mutations generated in the TM domains, however, had no effect on receptor function (TRH-R mutants Cys100Ser, Cys100Ala and GnRH-R mutants Glu90Gln, Lys115Arg, Lys121Arg, Gln174Glu), suggesting that only very specific sites within the TM domains are important for ligand-receptor binding. Furthermore, even at very critical sites for example Leu83, the radical alteration to Lys maintained some degree of receptor binding whereas the smaller change to Ala completely prevented ligand-receptor binding and activation. These factors therefore suggest that the effects of mutations are highly specific and dependent on both the nature and the position of the amino acid substitutions.

The incorporation of a smaller, less hydrophobic residue, Ala at position 83 resulted in a complete loss of ligand receptor binding and second messenger coupling. This finding may have resulted from one or more of the following factors; a decreased ability to form suitable hydrophobic interactions, a decrease in receptor expression, a partial loss of tertiary receptor structure, receptor destabilisation or increased receptor degradation. In contrast, GnRH-R mutant Leu83Lys showed a decrease in receptor affinity compared to WT but its most marked effect was on second messenger production. It is possible therefore that Leu83 forms an important link site, representing a lynchpin whereby ligand binding interactions are converted into the activation of the G-protein effector system. The position of Leu83, in the GnRH ligand receptor models, is in close proximity to Leu7 in GnRH and it is possible that hydrophobic interactions between this amino acid pair are important in ligand-receptor activation mechanisms.

10.4.5 Receptor expression

To pinpoint more accurately the site of the mutational effects, receptor mutants were examined for alterations in RNA transcription, processing and levels of cell surface receptor protein. Northern Blots were used to establish if the mutations affected RNA transcription. Results showed that the mutants had comparable levels of receptor RNA to the WT, indicating that RNA transcription was not affected following mutagenesis. Interestingly, the stably expressed GnRH-R WT and mutants showed different transcript sizes compared to the transiently expressed receptor constructs. These findings are probably reflective of the different mechanisms of DNA expression. In the transient transfection protocol, the DNA is expressed episomally whereas in the stable cell lines it becomes integrated into the host cell genome.

The detection of cell surface receptors was assessed by either antagonist binding, agonist binding (in the presence of high concentrations of total protein), or second messenger function (in the presence of high concentrations of stimulating ligand). In addition, an epitope tag has also been incorporated into the WT and mutant TRH-Rs and GnRH-Rs, so that cell surface receptor proteins can be measured directly (see Appendix V).

10.5 Conclusions

This study indicates that extracellular Cys residues are likely to be important in maintaining the three-dimensional structure of both the GnRH-R and TRH-R, through disulphide bonding interactions. Furthermore, the molecular modelling studies postulated that the ligand binding domain pocket of the GnRH-R was localised around the TM domains, TM II, TM III and TM VII. This hypothesis has been substantiated by results presented in Chapter 6, 7, and 8. Mutagenesis studies so far have highlighted Asn87 (TM II), Phe312 (TM VII) and Asn 314 (TM VII), as residues potentially important in ligand binding and amino acids Leu83 (TM II) and Asp318 (TM VII) as important in receptor activation. A pattern is already emerging whereby amino acids involved in receptor binding are positioned in the upper/middle part of the TM domains whereas those involved in receptor activation are located in the lower/middle part of the α-helices. The position of the TM domains is not absolutely defined and there may in fact be some flexibility in their positions. However, Asn87, Phe312 and Asn314 residues are all positioned approximately in the middle third of the TM domains whereas Leu83 and Asp318 are positioned much further down the receptor channel towards the intracellular side of the membrane. It is therefore possible that the GnRH ligand only penetrates half way down the receptor pore and hence amino acids critical for binding are found in this location. The observation that residues critical in activation are located further down the receptor channel is also in accord with the involvement of the il 3 in signal transduction mechanisms (Savarese and Fraser, 1992).

The lack of receptor binding activity displayed by mutations at the GnRH-R sites, Asn87, Phe312 and Asn314 could also arise from the absence of functional cell surface receptors and the answer to this question resides in the pending receptor epitope tagging studies.

10.6 Directions for future study

The epitope tagging system described in Chapter 9 (section 9.2.3) has now been characterised in the WT GnRH-R and TRH-R, and the next step is to incorporate this epitope tag into the all the receptor mutants constructed to date. The development of specific GnRH-R antibodies would also greatly aid in the measurement of GnRH-R mutant expression levels, and research is currently ongoing in this area. The use of

specific GnRH-R antibodies has advantages over the tagging system, since it would eliminate the need to modify the structure of the receptor.

Further comparative experimental studies are necessary to clarify the role of Cys residues in the GnRH-R, as has been carried out in the TRH-R. These studies could include the incorporation of the Cys/Ser mutants into a higher expression vector, the generation of corresponding Cys to Ala mutations, and chemical modification studies. Additional investigations are also necessary to identify the precise location of the disulphide bridges.

The majority of work contained within this thesis relates to mutations of the GnRH-R. In future, it may also be possible to design complementary ligand and receptor mutagenesis experimental studies, whereby direct interactions between ligand and receptor can be examined by mutating the ligand structure to complement mutations generated in the receptor. This double mutagenesis approach would be useful in the Leu83/Phe312 work.

To date, only preliminary investigations into the role of agonist verses antagonist binding sites have been carried out. Currently, there is a wide range of specific GnRH antagonists available and it would be interesting to examine variations in analogue binding between different receptor mutations. Janovick et al (Janovick et al, 1993), postulated the existence of a differential agonist and antagonist binding site in the GnRH-R. However, the majority of studies to date have been limited mainly to the delineation of GnRH/GnRH agonist ligand binding site.

The molecular modelling approach was vital to the evolution of this study and the possible use of supercomputers (for example the Cray parallel computer, Edinburgh University) would facilitate more complex molecular dynamic simulations. However, in the long term it is hoped that further developments in the overexpression and purification of the GnRH-R will enable the production of large quantities of peptide for x-ray crystallographic structural determination.

Finally, this work must be considered in terms of its potential clinical applications. Detailed structural knowledge relating to the GnRH-R should lead to an improved understanding of GnRH-R binding and second messenger activation, which in turn could permit the design of more efficacious drugs, in particular orally-active non-

peptide analogues. Furthermore, the combination of these analogues with steroid replacement could provide new contraceptive agents and improve positive health care, for example in the treatment of breast and prostate cancer and osteoporosis.

In the light of the extensive use of GnRH analogues in the regulation of human reproduction and in the treatment of a wide range of endocrine related disorders, this study provides important new insights into the mechanisms underlying GnRH-R function.

Appendix I Buffers and Stock Solutions

A Bacterial media

1. LB (Luria-Bertani Media) broth

12.5g Luria Broth Base in 500ml of H_2O (autoclaved).

2. LB agar

12.5g Luria Broth Base in 500ml of H_2O, 7.5g agarose (autoclaved).

3. SOC medium

2% Bactotryptone (w/v), 0.5% Bacto yeast extract (w/v), 10mM NaCl, 2.5mM KCl, 10mM $MgCl_2$, 10mM $MgSO_4$, 20mM glucose. Autoclave and then add glucose.

4. 2xYT Medium

1.6% Bacto tryptone (w/v), 1% Bacto yeast extract (w/v), 100mM NaCl (autoclaved).

B Antibiotics

1. Ampicillin: 50mg/ml in H_20, filter-sterilised, stock solutions stored at -20°C.
2. Chloramphenicol: 34mg/ml in ethanol, stock solutions stored at -20°C.
3. Kanamycin: 10mg/ml in H_20, filter-sterilised, stock solutions stored at -20°C.
4. Tetracycline: 5mg/ml in ethanol, stock solutions stored at -20°C.

C General reagents

1. 10M Ammonium Acetate

Dissolve 770g of ammonium acetate in 1000ml of H_20.

2. Chloroform

24:1 (v/v) mixture of chloroform and isoamyl alcohol. Stored at room temperature.

3. 50xDenhardt's

2% (w/v) Ficoll™, 2% (w/v) polyvinylpyrrolidone, 2% (w/v) bovine serum albumin (BSA), Pentax Fraction V. Stored at -20°C.

4. 0.5M EDTA

Add 186.1g of disodium ethylenediaminetetraacetate.$2H_20$ in 1000 ml H_20. Adjust pH to 8.0 with 20g of NaOH pellets.

5. 6xGel-Loading buffer (Agarose Gels)

0.25% (w/v) bromophenol blue, 0.25% (w/v) xylene cyanol FF, 30% (v/v) glycerol in H_2O, stored at 4°C.

6. Phenol (TE-saturated)

Phenol is removed from -20°C, warmed to room temperature and melted at 68°C. Add hydroxyquinoline to final concentration of 0.1% (w/v). To melted phenol, add an equal volume of buffer (0.5M Tris/HCl, pH8.0) at room temperature, stir for 15minutes and leave to separate. Remove upper layer and add an equal volume of 0.1M Tris/HCl, pH8.0, repeat extractions until pH of the phenol is >7.8. After equilibration, add 0.1% (v/v) 0.1M Tris/HCl, pH8.0 containing 0.2% β-mercaptoethanol. Store in dark at 4°C for 1 month.

7. Phenol/chloroform

1:1 (v/v) phenol and chloroform equilibrated with TE buffer (pH8.0). Stored at 4°C, protected from light.

8. Phosphate buffer pH 7.2

Add 400ml of 1M Na_2HPO_4 solution to 150ml 1M $NaH_2PO_4.2H_20$ while stirring and monitoring pH (autoclaved).

9. Phosphate-buffered saline (PBS)

Dissolve 8g NaCl, 0.2g KCl, 1.44g Na_2HPO_4 and 0.24g KH_2PO_4 in 1000 ml. Adjust to pH 7.4 with HCl.

10. 3M Sodium acetate

Dissolve 408.1g of sodium acetate.$3H_20$ in 800ml H_20. Adjust pH to 5.2 with glacial acetic acid or pH to 7.0 with dilute acetic acid. Adjust volume to 1000ml.

11. 20% SDS (sodium dodecyl suphate/lauryl sulphate)

20% SDS (w/v) in distilled of H_2O (autoclaved).

12. 20XSSC (sodium salt citrate)

3M NaCl, 0.3M Na_3 citrate.$2H_20$, 0.02M EDTA, pH 7.0 (autoclaved).

13. TE buffer

10mM Tris/HCl, pH7.8, 0.1mM EDTA (autoclaved).

14. 1M Tris

Dissolve 121.1g of Tris base in 800ml of H_20. Adjust to desired pH with concentrated HCl (pH7.4, 70ml HCl/ pH7.6, 60ml HCl/pH8.0, 42ml HCl)

15. 10XTBE Electrophoresis Buffer

108g Tris base, 55g boric acid, 40ml 0.5M EDTA in 1000ml of H_2O (autoclaved).

D Tissue culture solutions

1. DMEM complete medium

To a 500ml bottle of Dulbecco's modified Eagle's medium (DMEM) add 10ml stock L-glutamine (0.3mg/ml final concentration), 5ml stock penicillin/streptocmycin (P/S) solution (100IU penicillin final concentration, 100µg streptomycin final concentration) and 10% (v/v) heat-inactivated foetal calf serum (HIFCS).

2. Inositol-free DMEM media for IP assays

To a 500ml bottle of Special DMEM add 10ml stock L-glutamine (0.3mg/ml final concentration), 5ml stock penicillin/streptocmycin (P/S) solution (100IU penicillin final concentration, 100µg streptomycin final concentration) and 1% (v/v) dialysed heat-inactivated foetal calf serum (HIFCS).

3. Trypsin-EDTA solution

Trypsin-EDTA is available as a X10 liquid solution (GIBCO-BRL) containing 5.0g trypsin (0.5% w/v) and 2g EDTA in 100ml and is stored at -20°C. The working concentration of trypsin is 0.1% w/v and the stock solution is diluted 1/5 with phosphate buffered saline (PBS). Aliquots are stored at -20°C.

4. G418 Sulphate

Stock solution of 100mg/ml in H_20, filter sterilised.

E β Galactosidase detection assays

1. Glutaraldehyde solution

0.1M phosphate buffer, pH 7.0, 1mM $MgCl_2$ and 0.25% glutaraldehyde.

2. X-gal solution

0.2% X-gal, 1mM $MgCl_2$, 150mM NaCl, 3.3mM $K_4Fe(CN)_63H_2O$, 3.3mM $K_3Fe(CN)_6$, 60mM Na_2HPO_4 and 40mM NaH_2PO_4.

F Buffers and solutions for IP assays and calcium imaging

1. Buffer A

1mg/ml Fatty acid-free BSA, 140mM NaCl, 20mM Hepes, 4mM KCl, 8mM D-Glucose, 1mM $MgCl_2$ and 1mM $CaCl_2$. Adjust to pH 7.2 with concentrated NaOH.

2. 2%Perchoric acid (PCA)/ 0.5M EDTA Stopping solution

Dissolve 1.86g of EDTA in 800ml of H_2O add 28.6ml of PCA, adjust volume to 1000ml.

3. 0.5M KOH/60mM Hepes Neutralisation Buffer

Dissolve 28.055g KOH and 14.3g Hepes in 1000ml of H_2O.

4. 0.6M Ammonium formate/500mM sodium tetraborate

Dissolve 37.83g of ammonium formate and 19.07g of sodium tetraborate in 1000ml of H_2O.

5. 1M Ammonium formate/0.1M formic acid

Dissolve 31.53g ammonium formate in 500ml of H_2O. Add 2.56 ml of formic acid.

6. Calcium imaging buffer

NaCl (127mM), KCl (5mM), $MgCl_2$ (2mM), NaH_2PO_4 (0.5mM), $NaHCO_3$ (5mM), $CaCl_2$ (1.8mM), HEPES (10mM), and BSA (0.1%) pH 7.2.

G Buffers and solutions for receptor binding assays

1. Membrane buffer

20mM Tris-HCl pH 7.2, 2mM $MgCl_2$.

2. TRH-R binding assay buffer

20mM Tris-HCl pH 7.2, 2mM $MgCl_2$.

3. GnRH-R binding assay buffer

40mM Tris-HCl pH 7.4, 2mM $MgCl_2$.

4. 1M Dithiothreitol (DTT)

Dissolve 1g DTT in 6.49ml of distilled H_2O.

5. 50mM p-chloromercuribenzoic acid (p-CMB)

Dissolve 89.3mg of p-CMB in 1M NaOH.

H Buffers and solutions for RNA extraction/Northern Blots

1. DEPC (diethylpyrocarbonate) treated solutions

Solutions were treated with 0.1% DEPC for at least 12 hours at 37°C prior to autoclaving.

2. Dye solution - RNA gel electrophoresis

7.5% (w/v) Ficoll 400, 0.1% (v/v) bromophenol blue, 1mg/ml ethidium bromide.

3. 10xMOPS/EDTA running buffer - RNA gel electrophoresis

8.36g MOPS (3-[N-morpholino]propranesulfonic acid) (200mM), 0.744g EDTA (10mM), 0.82g sodium acetate (50mM), dissolved in 150ml DEPC-treated H_2O and adjusted to pH 7.0 with sterile 5M NaOH.

4. Sample buffer - RNA gel electrophoresis

200µl (10X) MOPS/EDTA running buffer, 1ml deionised formamide, 356µl formaldehyde (37% v/v).

5. 50% Formamide hybridisation buffer (cDNA probes)

50% (v/v) deionised formamide, 5XSSC, 1XDenhardt's, 20mM sodium dihydrogen orthophosphate (NaH_2PO_4) pH 6.8, 0.1% SDS, 10% dextran sulphate, 10µg/ml polyadenylic acid, 10µg/ml polycytidylic acid. Add 100µg/ml freshly boiled, sonicated salmon sperm DNA just before use.

6. 15% Hybridisation buffer (oligonucleotide probes)

15% (v/v) deionised formamide, 200mM phosphate buffer pH 7.2, 1mM EDTA, 7% (w/v) SDS, 1% (w/v) BSA.

7. Washing buffer (oligonucleotide probes)

40mM phosphate buffer pH 7.2, 1mM EDTA pH 8.0 and 1% SDS.

Appendix II Chemical and Equipment Suppliers

Advanced Protein Products Ltd., Premier partnership estate, Leys Road, Brockmoor, Brierly Hill, Westmidlands, DY5 3UP UK.

American Type Culture Collection, Maryland USA.

Amersham International plc, Amersham Place, Little Chalfont, Bucks. HP7 9NA, UK.

Applied Biosystems, Kevin Close, Birchwood Science Park, Warrington, Cheshire, UK.

BDH Ltd., Burnfield Avenue, Thornliebank Glasgow G46 7TP, UK.

Bio-Rad Laboratories Ltd., Bio-Rad House, Maylands Ave. Hemel Hempstead, Herts. HP2 7TD, UK.

Biosoft, Cambridge, Cambs, UK.

Boehringer Mannheim UK (Diagnostics and Biochemicals) Ltd., Bell Lane, Lewes, E.Sussex BN7 1LG, UK.

Cambridge Research Biochemicals Ltd., Gadbrook Park, Northwich, Cheshire.

Costar, 205 Broadway, Cambridge, MA 02139, USA.

Dupont (UK) Ltd., Medical Products, NEN products, Wedgewood Way, Stevenage, Herts. UK.

Falcon, Becton Dickinson UK Ltd., Between Towns Road, Cowley, Oxford, UK.

Flow Laboratories Ltd., PO Box 17, Second Avenue, Industrial Estate, Irvine, Ayrshire, Scotland.

Flowgen, FMC Bioproducts, High Wycombe, Bucks, UK.

GIBCO-BRL, Life Technologies Ltd., PO Box 35 Trident House, Renfrew Road, Paisley PA3 4EF, Scotland, UK.

Invitrogen - British Bio-technology Products Ltd., 4-10 The Quadrant, Barton Lane, Abingdon, Oxon OX14 3YS, UK.

Joyce Loebl Ltd., Dukesway, Team Valley, Gateshead, Tyne and Weir, UK.

Kodak - IBI Ltd., 36 Clifton Road, Cambridge CB1 4ZR, UK.

Kontron Instruments, 52 Telford Road, Lenziemill, Cumbernauld, UK.

Northumbria Biologicals Ltd., Enzymes Division, South Nelson Industrial Estate, Cramlington, Northumberland NE23 9HL, UK.

Nunc, A/S Nunc, Kamstrupvej 90, Kamstrup, DK-4000 Roskilde, Denmark.

Pharmacia Biotechnology Ltd., 23 Grosvenor Road, St Albans, Herts, AL1 3AW, UK.

Peninsula, 611 Taylor Way, Belmont, CA 94002, USA.

Promega Ltd., 2800 Woods Hollow Road, Madison, WI 53711-5399, USA.

Semat Technical (UK) Ltd., 1 Executive Park, Hatfield Road, St. Albans, Herts. AL1 4TA, UK.

Sigma Chemical Company Ltd., Fancy Road, Poole, Dorset BH17 7NH, UK.

Stratagene Ltd., Cambridge Innovation Centre, Cambridge Science Park, Milton Road, Cambridge CB4 4GF, UK.

Vilber Lourmat, 77202 Marne la Vallee, Cédex 2, France.

Whatman LabSales Ltd., Unit 1 Coldred Road, Parkwood, Maidstone, Kent UK.

Appendix III Additional Methodology

A Fluorescent microscopy and dynamic calcium imaging

Trypsin-treated cells were plated on sterilised glass coverslips and after 48 hours washed twice with buffer containing 127 mM NaCl, 5 mM KCl, 2 mM $MgCl_2$, 0.5 mM $NaHCO_3$, 1.8 mM $CaCl_2$, 10 mM Hepes and 0.1% (w/v) BSA, (pH 7.2). Cells were then loaded with Fura-2 pentaacetoxymethylester (Fura-2AM), to a final concentration of 4 µmol/L, for 30 minutes at 37°C in a 5% (v/v) CO_2 humidified incubator and any unincorporated dye removed by washing three times with buffer. The coverslips were subsequently transferred to a heated stage (37°C) of an inverted Nikon Diaphot epifluorescent microscope. Cells where incubated in a fixed volume of buffer (1ml). Drug solutions (5ml) could be added directly to the coverslip chamber and 1ml volumes automatically obtained through suction. Dynamic video imaging of changes in $[Ca^{2+}]i$ were carried out in single cells using MagiCal hardware and tardis software (Applied Imaging). The fluorescent images were obtained by exposing cells to filtered 340 nm and 380 nm light, alternating under computer control. Video images were captured and the changes in the $[Ca^{2+}]i$ under the two different light wavelengths calculated. Fluorescent excitation shifts occur when Fura 2 binds Ca^{2+} i.e. the excitation increases at 340 nm and decreases at 380 nm and therefore alterations in these dual wavelength ratios represent changes in $[Ca^{2+}]i$ levels.

B Kodak-Flag tag method

The Kodak-Flag tag sequence was inserted into the rat GnRH-R using a PCR based approach. A 5' oligonucleotide incorporating ATG and the Flag-tag DNA sequence (5' AGAAATATG**GACTACAAGGACGACGATG**ACAAG 3' was designed together with a 3' oligonucleotide 5' GATTCTTATTCAGCAACA 3' matching nucleotides 1780-1795 in the 3' untranslated region of the GnRH-R cDNA sequence). A PCR reaction was carried out, the PCR products run on a 1% agarose gel and the 1.8 kb band excised for purification. The purified DNA was subsequently cloned into the TA cloning vector (Invitrogen) and then subcloned into the expression vector

pcDNA 3. The sequence of the Kodak Flag-tag was confirmed by automated DNA sequencing.

C HA-tag method

1 GnRH-R

DNA oligonucleotides (5' TGAG**TATCCATATGATGTTCCAGATTATGC** 3' and 5' CTCA**GCATAATCTGGAACATCATATGGATA** 3') were annealed together by boiling 10 nmol of each oligonucleotide, in a total volume of 300µl for 2 minutes, and then allowing the reaction mixture to cool slowly. The double-stranded oligonucleotide fragment was then ligated in frame into the rat GnRH-R cDNA, at the unique Esp31 restriction site in the NH_2 terminus of the sequence. GnRH-R cDNA (3µg) was digested using 3µl (4 units/µl) of Esp31 (Immunogen) in a total volume of 30µl for 16 hours at 37°C. EGTA was then added to a final volume of 10mM, the digestion products treated with proteinase K (50µg/ml final concentration) for 10 minutes at 37°C and the DNA purified using phenol/chloroform extraction. The annealed double-stranded oligonucleotide (13.3 pmols) was then ligated into the purified Esp31 cut GnRH-R cDNA in a ratio of 24:1 (oligo to cDNA), using 1µl of ligase. The ligation mixture was subsequently transformed into Top10 F' *EColi* cells by electroporation. The colonies were grown in LB broth and the DNA was extracted using the Promega miniprep DNA isolation system. The sequence of the HA-tagged GnRH-R was confirmed by automated DNA sequencing.

2 TRH-R

The TRH-R cDNA was modified by addition of a Sal I linker to the 5' end (5' ACG CGT CGA CGA GAA TGA AAC CGT CAG TGA AC 3') and a Xba 1 linker to the 3' end (5' GCT CTA GAG CTC ATA TTT TCT CCT GTT TGG CAG 3'). PCR was performed, using 200ng of TRH-R cDNA as a template, with pfu polymerase (Stratagene) (95°C 42 seconds, 58°C 1minute, 72°C 3 minutes for 30 cycles followed by 95°C 42 seconds, 58°C 1 minute and 72°C 5 minutes for 1 cycle). This PCR product was then subcloned between the Xho 1 and Xba 1 sites in the pcDNA 3 expression vector, previously modified to encode the triple HA tag sequence immediately after the ATG codon (YPYDVPDYAGYPYDVPDYAYPYDVPDYA).

This construct was then transformed into DH5α cells and the presence of the construct confirmed by restriction enzyme digests and automated DNA sequencing.

D Western Blotting

Cell membranes (3x60mm plates for COS-1 cells transiently expressing the HA-tagged GnRH-R and the 3HA-TRH-R and 1x60mm plate for the COS-1 cells transiently expressing the HA-tagged Gq) were resuspended with 200µl of loading buffer containing 0.5% Triton-X114 (Sigma) and boiled for 3 minutes prior to loading (20µl per sample) onto a 10% SDS polyacrylamide gel. The gel was run in 5x running buffer overnight at 60V and the protein transferred onto a Hybond C nitrocellulose membrane (Amersham). Non-specific binding sites on the membrane were blocked by immersing the membrane in non-fat milk diluted in TTBS (20mM Tris-HCl, 500mM NaCl, pH 7.5 and 0.005% Tween-20) for 1 hour at room temperature with shaking and the excess blocking solution removed by washing in TTBS. A primary mouse monoclonal anti-HA antibody 12CA5 (Boehringer Manniheim) was preabsorbed against a membrane blotted with COS-1 cells to remove any non-specific binding and then added in a 1:80 dilution (in TTBS) for 1 hour at room temperature or overnight at 4°C. The membrane was rinsed in TTBS, washed x1 for 15 minutes and then x2 for 5 minutes in TTBS. The sheep antimouse horseradish peroxidase secondary antibody (Amersham) was diluted 1:6000 in TTBS, added to the membrane for 1 hour at room temperature and immunodetection carried out using an ECL detection method (Amersham).

E Fluorescein isothiocyanate conjugate (FITC) immunoassay

Twenty-four hours post-transfection cells were transferred into 4 well chamber slides (Nunc) incubated for a further 48 hours, then fixed with 4% formaldehyde, washed with PBS and the non-specific binding sites blocked with DMEM/HIFCS. The primary mouse monoclonal anti-HA antibody 12CA5 was added in a 1:10 dilution in DMEM overnight at 4°C and subsequently removed by washing with (x2) PBS. The second antibody, a FITC conjugated goat anti-mouse IgG, was then added at a 1:50 dilution in DMEM for 2 hours. This antibody is light-sensitive so the chamber slides were kept in the dark. Citifluor was added to the cells to prevent quenching of the fluorescent signal. This reaction was observed under a fluorescence microscope at a wavelength 495nm.

F Enzyme Linked Immunosorbent Assay (ELISA)

COS-1 cells in 60mm plates were transfected with either 3µg of Control WT, HA-tagged receptor DNA or sham untransfected plates. Twenty-four hours later, cells were trypsinised, then transferred into 96 well plates (50, 000 cells/well) and after a further 48 hours fixed using 4% formaldehyde in PBS (30 minutes at room temperature). Following fixation the cells were washed (x3) with PBS, the non-specific binding sites blocked with DMEM containing 10% HIFCS and a primary mouse monoclonal anti-HA antibody 12CA5 added in 1:10 or 1:250 dilutions in DMEM. This anti-HA antibody recognises the HA peptide sequence (YPYDVPDYA) derived from the human influenza hemagglutinin protein. Cells were incubated with anti-HA overnight at 4°C, subsequently washed with PBS (x3) and then further incubated with a 1:1000 dilution of a peroxidase conjugated goat/sheep anti-mouse IgG (Sigma) in DMEM for 1 hour at 37°C. The final substrate (200µl), 5mM o-phenylenediamine/0.03% H_2O_2 in 0.1M citrate/phosphate buffer (pH 5.0), was added in a light-sensitive environment for 30 minutes at room temperature and the enzymatic reaction stopped with 50µl of 2N H_2SO_4 solution. An orange colour reaction was produced when the substrate reacted with the peroxidase enzyme conjugated on the second antibody and the colour density of each well measured using a Labsystems Multiscan MCC/340 reader at 492 and 639 nm wavelengths.

Appendix IV Publications and Presentations

Publications:

JV Cook, E Faccenda, L Anderson, KA Eidne and PL Taylor: Effects of Asn^{87} and Asp^{318} mutations on ligand binding and signal transduction in the rat GnRH receptor. J. Endocrinol. (1993) **139**, R1-R4

JV Cook and KA Eidne: A disulfide bonding role for extracellular cysteine residues cysteine 98 and cysteine 179 in the rat thyrotropin-releasing hormone receptor. Endocrinology (accepted subject to review) *

Presentations to Scientific meetings:

JV Cook, PL Taylor and KA Eidne: Effects of GnRH receptor transmembrane region mutations on GnRH recognition and signal transduction. American Endocrine Society 77th Annual Meeting, June 1995, Washington, DC, USA.

L Anderson, **JV Cook**, K Chatzati and KA Eidne: Studies on the intracellular responses of pituitary and extrapituitary GnRH receptors. American Endocrine Society 77th Annual Meeting, June 1995, Washington, DC, USA.

JV Cook, E Faccenda, L Anderson, PL Taylor and KA Eidne: The GnRH receptor ligand binding domain: Molecular modelling and site-directed mutagenesis studies. American Endocrine Society 76th Annual Meeting, June 1994, Anaheim, California, USA.

JV Cook, L Anderson, PL Taylor , G Couper and KA Eidne: Site Directed Mutagenesis of the Extracellular Domains of the Rat Thyrotropin Releasing Hormone Receptor (TRH-R). International Congress of Physiological Sciences, August 1993, Glasgow, UK.

L Anderson, GC Couper, G Milligan, **JV Cook**, PL Taylor and KA Eidne: Characterisation of the G-protein coupled events of the rat Thyrotropin Releasing Hormone receptor (TRH-R). The Endocrine Society, June 1993, Las Vegas, USA.

L Anderson, GC Couper, G Milligan, **JV Cook**, PL Taylor and KA Eidne: Putative intracellular phosphorylation sites within the rat Thyrotropin Releasing Hormone Receptor (TRH-R) which are potentially involved in receptor desensitisation. The 3rd International Pituitary Congress, June 1993, Los Angeles, USA.

KA Eidne, R Sellars, PL Taylor, **JV Cook** and L Anderson: Cloning, expression and site-directed mutagenesis of the rat GnRH receptor. The 3rd International Pituitary Congress, June 1993, Los Angeles, USA.

* In the interim the results of this study have been confirmed by Gershengorn and co-workers in a manuscript entitled

'A disulphide bond between conserved extracellular cysteines in the thyrotropin-releasing hormone receptor is critical for receptor binding'.

published in The Journal of Biological Chemistry, Volume 270, No.42, Issue of October 20th, pp. 24682-24685, 1995.

Appendix V Measurements of expression in TRH-R mutants (Chapter 5)

The measurement of protein receptor expression levels has since been achieved in the extracellular TRH-R Cys mutation study (Chapter 5). Western Blot analysis of membranes prepared from COS-1 cells expressing the 3HA-tagged TRH-R WT and mutants is illustrated in Figure A1. Receptor expression levels similar to WT are maintained in the TRH-R mutants Cys98Ser, Cys98Ala, Cys179Ala, Cys100Ser (Note mutant Cys100Ala has not been included, but this mutation showed normal WT receptor binding levels). In contrast, the Cys179Ser mutant shows no TRH-R expression. This data confirms the results obtained from the ligand-induced total IP measurements, whereby Cys179Ser showed no increase in second messenger production when stimulated with concentrations of TRH above 1μM (Figure 5.7). These results indicate that mutating Cys179 to Ser interferes with the normal expression of the receptor at the membrane. In conclusion, the loss of receptor binding displayed by mutants Cys98Ser, Cys98Ala and Cys179Ala does not result from a decrease in receptor expression and must therefore be attributable to a loss of disulphide bridge formation.

Bibliography

1. Abe H, Endler D, Molitch M E, Bollinger-Grober J and Reichlin S. Vasoactive intestinal peptide is a physiological mediator of prolactin release in the rat. Endocrinology 1985; 116:1383-1390.

2. Albarracin C T, Kaiser U B and Chin W W. Isolation and characterization of the 5' flanking region of the mouse gonadotropin-releasing hormone receptor gene. Endocrinology 1994; 135:2300-2306.

3. Amarant T, Fridkin M and Kosh Y. Luteinizing hormone-releasing hormone and thyrotropin-releasing hormone in human and bovine milk. European Journal of Biochemistry 1982; 127:647-650.

4. Anderson L, Holland J, Mason W T and Eidne K A. Characterisation of gonadotropin-releasing hormone calcium response in single αT3-1 pituitary gonadotroph cells. Molecular and Cellular Endocrinology 1992; 86:167-175.

5. Anderson L, McGregor A, Cook J V F, Chilvers E and Eidne K A. Rapid desensitisation of GnRH-stimulated intracellular signalling events in αT3-1 and HEK-293 cells expressing the rat GnRH receptor. Endocrinology 1995; 136:5228-5231.

6. Anderson L, Milligan G and Eidne K A. Characterisation of the gonadotropin-releasing hormone receptor in α-T3-1 pituitary gonadotroph cells. Journal of Endocrinology 1993; 136:51-58.

7. Andreason G L and Evans G A. Introduction and expression of DNA molecules in eukaryotic cells by electroporation. Biotechniques 1988; 6:650.

8. Aragay A M, Katz A and Simon M I. The $G\alpha_q$ and $G\alpha_{11}$ proteins couple the thyrotropin-releasing hormone receptor to phospholipase C in GH3 rat pituitary cells. Journal of Biological Chemistry 1992; 267:24983-24988.

9. Arora K K, Saki A and Catt K J. Effects of second intracellular loop mutations on signal transduction and internalization of the gonadotropin-releasing hormone receptor. Journal of Biological Chemistry 1995; 270:22820-22826.

10. Asa S L, Kovacs K and Melmed S. The hypothalamic pituitary axis. In: The pituitary. Melmed S, ed. Cambridge, Massachusetts: Blackwell Science, 1995:3-41.

11. Aten R F, Willams T, Behrman H R and Wolin D L. Ovarian gonadotropin-releasing hormone-like peptide(s): Demonstration and characterisation. Endocrinology 1986; 118:961-967.

12. Baldwin J M. The probable arrangement of the helices in G-protein coupled receptors. The EMBO Journal 1993; 12:1693-1703.

13. Baldwin J M. Structure and function of receptors coupled to G-proteins. Current Opinion in Cell Biology 1994; 6:180-190.

14. Barbieri R L. Clinical application of GnRH and its analogues. Trends in Endocrinology and Metabolism 1992; 3:30-34.

15. Barnhart K M and Mellon P L. The orphan nuclear receptor, SF-1, regulates the glycoprotein hormone α subunit gene in pituitary gonadotropes. Molecular Endocrinology 1994; 8:878-885.

16. Baumann K H, Keisel L, Kaufmann M, Bastert G and Runnebaum B. Characterization of binding sites for a GnRH-agonist (Buserelin) in human breast cancer biopsies and their distribution in relation to tumor parameters. Breast Cancer Research Treatment 1993; 25:37-46.

17. Ben-Menahem D and Noar Z. Regulation of gonadotropin mRNA levels in cultured rat pituitary cells by gonadotropin-releasing hormone (GnRH): Role for Ca^{2+} and protein kinase C. Biochemistry 1994; 33:3698-3704.

18. Benovic J L, Mayor J F, Staniszewski C, Lefkowitz R J and Caron M G. Purification and characterisation of β-adrenergic receptor kinase. Journal of Biological Chemistry 1987; 262:9026-9032.

19. Berridge M J. Cytosolic calcium oscillations. FASEB Journal 1988; 2:3074-3082.

20. Bhasin S and Swerdloff R. Follicle-stimulating hormone and luteinizing hormone. In: The pituitary. Melmed S, ed. Cambridge, Massachusetts: Blackwell Science, 1995:230-276.

21. Billing H, Furuta I and Heush A J W. Gonadotropin-releasing hormone directly induces apoptotic cell death in the rat ovary: Biochemical and in situ detection of the deoxyribonucleic acid fragmentation in granulosa cells. Endocrinology 1994; 134:245-252.

22. Braden T D and Conn P M. Altered rate of synthesis of gonadotropin-releasing hormone receptors: Effects of homologous hormone appear independent of extracellular calcium. Endocrinology 1990; 126:2577-2582.

23. Braden T D and Conn P M. Activin-A stimulates the synthesis of gonadotropin-releasing hormone receptors. Endocrinology 1992; 130:2101-2105.

24. Bramley T A, Menzies G S and Baird D T. Specific binding of gonadotrophin-releasing hormone and an agonist to human corpus luteum homogenates: Characterisation, properties and luteal phase levels. Journal of Clinical Endocrinology and Metabolism 1985; 61:834-841.

25. Brazeau P, Vale W and Burges R. Hypothalamic polypeptide that inhibits the secretion of immunoreactive pituitary growth hormone. Science 1973; 179:77-79.

26. Brooks J, Taylor P L, Saunders P, Eidne K A, Struthers W J and McNeilly A S. Cloning and sequencing of the sheep pituitary gonadotropin-releasing hormone receptor and changes in expression of its mRNA during the estrous cycle. Molecular and Cellular Endocrinology 1993; 94:R1-R6.

27. Burgus R, Butcher M, Amoss M, Ling N, Monahan M, Rivier J, Fellows R, Blackwell R, Vale W and Guillemin R. Primary structure of the ovine hypothalamic luteinizing hormone-releasing factor (LRF). Proceedings of the National Academy of Sciences: USA 1972; 69:278-282.

28. Burrin J M and Jameson J L. Regulation of the transfected glycoprotein α gene expression in primary pituitary cell cultures. Molecular Endocrinology 1989; 3:1643-1651.

29. Byrant W P, Berget E R and Morris J C. Delineation of amino acid residues within hTSHr 256-275 that participate in hormone binding. Journal of Biological Chemistry 1995; 269:30935-30938.

30. Calogero A E, Weber R F A, Raiti F, Burrello N, Moncada M L, Mongioi A and Dagata R. Involvement of corticotropin-releasing hormone and endogenous opioid peptides in prolactin suppression of gonadotropin releasing hormone release in vitro. Neuroendocrinology 1994; 60:291-296.

31. Caron M G and Lefkowitz R J. Catecholamine receptors: Structure, function and regulation. Recent Progress in Hormone Research 1993; 48:277-290.

32. Chanda P K, Minchin M C, Davis A R, Greenburg L, Reilly Y, McGregor W H, Bhat R, Lebeck M D, Mizutani S and Hung P. Identification of residues important for ligand binding to the human 5-hydroxytryptamine$_{1A}$ serotonin receptor. Molecular Pharmacology 1993; 43:516-520.

33. Chandran U R, Attardi B, Friedman R, Dong K W, Roberts J L and DeFranco D B. Glucocorticoid receptor mediated repression of gonadotropin-releasing hormone promoter activity in GT1 hypothalamic cell lines. Endocrinology 1994; 134:1467-1474.

34. Chang Y L, Gutell R, Noller H F and Wool I G. The nucleotide sequence of the rat 18S ribosomal ribonucleic acid gene and a proposed secondary structure of 18S ribosomal ribonucleic acid. Journal of Biological Chemistry 1984; 259:224-230.

35. Chi L, Zhou W, Prikhozhan A, Flanagan C, Davidson J S, Golemba M, Illing N, Millar R P and Sealfon S C. Cloning and characterization of the human GnRH receptor. Molecular and Cellular Endocrinology 1993; 91:R1-R3.

36. Chung F-Z, Wang C-D, Potter P C, Venter J C and Fraser C M. Site-directed mutagenesis and continuous expression of human β-adrenergic receptors. Journal of Biological Chemistry 1988; 263:4052-4055.

37. Clay C M, Nelson S E, Di Gregorio G B, Campion C E, Wiedermann A L and Nett R J. Cell specific expression of the mouse gonadotropin-releasing hormone (GnRH) receptor gene by elements residing within 500 bp of the proximal 5' flanking region. Endocrine 1995; 3:615-622.

38. Clayton R N and Catt K J. Gonadotropin-releasing hormone receptor: Characterisation, physiological response and relationship to reproductive function. Endocrine Reviews 1980; 2:189-209.

39. Clayton R N, Solano A R, Gracia-Vela A, Dufau M L and Catt K J. Regulation of pituitary receptors for gonadotropin-releasing hormone receptor during the rat estrous cycle. Endocrinology 1980; 107:699-706.

40. Conn P M and Crowley W F. Gonadotropin-releasing hormone and its analogues. Annual Review of Medicine 1994; 45:391-405.

41. Conn P M, Rodgers D C and Seay S G. Biphasic regulation of the gonadotropin-releasing hormone receptor by microaggregation and intracellular Ca^{2+} levels. Molecular Pharmacology 1984; 25:51-55.

42. Cook J V, Faccenda E, Anderson L, Cooper G C, Eidne K A and Taylor P L. Effects of Asn87 and Asp318 mutations on ligand binding and signal transduction in the rat GnRH receptor. Journal of Endocrinology 1993; 139:R1-R4.

43. Corbin A and Beatty C W. Inhibition of the pre-ovulatory proestrus gonadotropin surge, ovulation and pregnancy with a peptide analogue of luteinising hormone releasing hormone. Endocrine Research Communications 1975; 2:1-6.

44. Crowley W F, Filicori M, Spratt D I and Santoro N F. The physiology of gonadotropin releasing hormone secretion in men and women. Recent Progress in Hormone Research 1985; 41:473-526.

45. Currie A J, Fraser H M and Sharpe R M. Human placental receptors for luteinising hormone releasing hormone. Biochemical Biophysical Research Communications 1981; 99:332-338.

46. Davidson F F, Loewen P C and Khorana H G. Structure and function in rhodopsin: Replacement by alanine of cysteine residues 110 and 187, components of a conserved disulfide bond in rhodopsin, affects the light-activated metarhodopsin II state. Proceedings of the National Academy of Sciences: USA 1994; 91:4029-4033.

47. Davidson J S, Flanagan C A, Becker I I, Illing N, Sealfon S C and Millar R P. Molecular function of the gonadotrophin-releasing hormone receptor: Insights from site-directed mutagenesis. Molecular and Cellular Endocrinology 1994; 100:9-14.

48. Davidson J S, Flanagan C A, Zhou W, Becker I I, Elario R, Emeran W, Sealfon S C and Millar R P. Identification of the N-glycosylation sites in the gonadotropin-releasing hormone receptor: Role in receptor expression but not in ligand binding. Molecular and Cellular Endocrinology 1995; 107:241-245.

49. DeBlasi A, O'Reilly K and Moutulsky H J. Calculating receptor number from binding experiments using the same compound as radioligand and competitor. Trends in Pharmacological Science 1989; 19:227-229.

50. Dohlman H G, Caron M G, Deblasi A, Frielle T and Lefkowitz R J. Role of extracellular disulfide-bonded cysteines in the ligand binding function of the β2 adrenergic receptor. Biochemistry 1990; 29:2335-2342.

51. Donnelly D and Findlay J B C. Seven-helix receptors: Structure and modelling. Current Opinion in Structural Biology 1994; 4:582-589.

52. Donnelly D, Findlay J B C and Blundell T L. The evolution and structure of aminergic G-protein coupled receptors. Receptors and Channels 1994; 2:61-78.

53. du Vingneud V, Gish D T and Katsoyannis P G. A synthetic preparation possessing the biological properties associated with arginine vasopressin. Journal of American Chemical Society 1954; 76:4751-4752.

54. Eidne K A, Flanagan C A, Harris N S and Millar R P. Gonadotropin-releasing hormone (GnRH) binding sites in human breast cancer cell lines and inhibitory effects of GnRH antagonists. Journal of Clinical Endocrinology and Metabolism 1987; 64:425-432.

55. Eidne K A, Flanagan C A and Millar R P. Gonadotrophin-releasing hormone binding sites in human breast carcinomas. Science 1985; 229:989-991.

56. Eidne K A, Sellar R E, Couper G, Anderson L and Taylor P L. Molecular cloning and characterisation of the rat pituitary gonadotrophin-releasing hormone (GnRH) receptor. Molecular and Cellular Endocrinology 1992; 90:R5-R9.

57. El Etr M, Akwa Y, Fiddes R J, Robel P and Baulieu E E. A progesterone metabolite stimulates the release of gonadotropin-releasing hormone from GT1-1 hypothalamic neurons via the gamma aminobutyric acid type A receptor. Proceedings of the National Academy of Sciences: USA 1995; 92:3769-3773.

58. Emons G, Portmann O, Becker M, Irmer G, Springer B, Laun R, Holzel F, Schulz K D and Schally A V. High affinity binding and direct antiproliferative effects of LHRH analogues in human ovarian cell lines. Cancer Research 1993; 53:5439-5446.

59. Emons G and Schally A V. The use of luteinizing hormone releasing hormone agonists and antagonists in gynaecological cancers. Human Reproduction Update 1994; 9:1364-1379.

60. Fallest P C, Trader G L, Darrow J M and Shupnik M A. Regulation of the rat luteinising hormone β gene expression in transgenic mice by steroids and a gonadotrophin-releasing hormone antagonist. Biology of Reproduction 1995; 53:103-109.

61. Fan N C, Jeng E-B, Peng C, Olofsson J I, Krisinger J and Leung P C K. The human gonadotropin-releasing hormone (GnRH) receptor gene: Cloning, genomic organization and chromosomal assignment. Molecular and Cellular Endocrinology 1994; 103:R1-R6.

62. Farnworth P G. Gonadotrophin secretion revisited. How many ways can FSH leave a gonadotroph. Journal of Endocrinology 1995; 145:387-395.

63. Feinburg A P and Vogelstein B. A technique for labelling DNA restriction endonuclease fragments to high specificity. Addendum: Annuals of Biochemistry 1984; 137:266-267.

64. Feinburg A P and Vogelstein B. A technique for radiolabelling DNA fragments to high specificity. Annuals of Biochemistry 1983; 132:6-13.

65. Fekete M, Bajusa S, Groot K, Csernus V J and Schally A V. Comparison of different agonist and antagonists and of luteinizing hormone-releasing hormone for receptor-binding ability to rat pituitary and human breast cancer membranes. Endocrinology 1989; 124:946-955.

66. Finch E A, Turner T J and Goldin S M. Calcium as a coagonist of inositol 1,4,5-trisphosphate-induced calcium release. Science 1991; 252:443-446.

67. Floret G, Mahon K and Majewski T. Decreased histamine release by luteinising hormone releasing hormone antagonists obtained upon translation of the cationic amino acid from position 8 to position 7. Journal of Medicinal Chemistry 1992; 35:636-640.

68. Folkers K, Bowers C Y and Sheih H M. Antagonists of the luteinising hormone releasing hormone (LHRH) with the emphasis on the Trp7 of the salmon and chicken II LHRH's. Biochemical and Biophysical Research Communications 1984; 123:1121-1226.

69. Fong T M, Huang R C and Strader C D. Localisation of agonist and antagonist binding domains in the human Neurokinin-1 receptor. Journal of Biological Chemistry 1992; 267:25664-25667.

70. Fonseca M I, Lunt G G and Aguilar J S. Inhibition of muscarinic cholinergic receptors by disulfide reducing reagents and arsenicals: Differential effect on locust and rat. Biochemical Pharmacology 1991; 41:735-742.

71. Fraser C M. Site-directed mutagenesis of β-adrenergic receptors. Journal of Biological Chemistry 1989; 264:9266-9270.

72. Fraser H M and Eidne K A. Extrapituitary actions of LHRH analogues and LHRH-like peptides. In: Shaw R W and Marshall J C, ed. LHRH and its analogues: Their use in gynaecological practice. London: Wright, 1989: 64-69.

73. Fujino M, Kobayashi S, Obayashi M, Shinagawa S, Fukuda T, Kitada C, Nakayaga R, Yamazaki I, White W F and Rippel R H. Structure-activity relationships in the C-terminal part of the luteinising releasing hormone (LHRH). Biochemical Biophysical Research Communications 1972; 49:863.

74. Gharib S D, Wierman M E, Shupnik M A and Chin W W. Molecular biology of the pituitary gonadotropins. Endocrine Reviews 1990; 11:177-199.

75. GonzalesBarcena D, VadilleBuenfil M, GomezOrta F, Garcia M F, CardenasCornejo I, GraefSanchez A, ComaruSchally A M and Schally A V. Responses to antagonistic analogs of the LH-RH SB-75, (cetrorelix) in patients with benign prostatic hyperplasia and prostatic cancer. Prostate 1994; 24:84-92.

76. Green J D and Harris G W. Observations of the hypophyseal-portal vessels in the living rat. Journal of Physiology 1949; 108:359-361.

77. Grosser P M, O'Byrne K T, Williams C L, Thalabard J C, Hotchkiss J and Knobil E. Effects of naloxone on estrogen-induced hypothalamic gonadotropin releasing hormone pulse generator activity in the rhesus monkey. Neuroendocrinology 1993; 57:115-119.

78. Grotzinger J, Engels M, Jacoby E, Wollmer A and Strabburger W. A Model for the $C5_a$ receptor and for its interaction with the ligand. Protein Engineering 1991; 4:767-771.

79. Guillemette G, Balla T, Baukal A J and Catt K J. Inositol 1,4,5 trisphosphate binds to a specific receptor and releases microsomal calcium into the anterior pituitary gland. Proceedings of the National Academy of Sciences: USA 1987; 84:8195-8199.

80. Guillemin R, Brazeau P, Bohlen P, Esch F, Ling N and Wehrenburg W P. Growth-hormone releasing factor from a human pancreatic islet tumor that caused acromegaly. Science 1982; 218:585-587.

81. Guillemin R, Burgus R and Vale W. The hypophysiotrophic thyrotropin releasing factor. Vitamins and Hormones 1971; 29:1-39.

82. Guo C-H, Janovick J A, Kuphal D and Conn P M. Transient transfection of GGH3-1 cells [GH3 cells stably transfected with gonadotropin-releasing hormone (GnRH) receptor complementary deoxyribonucleic acid] with the carboxy-terminal of the β-adrenergic receptor kinase 1 blocks prolactin release: Evidence for a role of the G-protein βγ-subunit complex in GnRH signal transduction. Endocrinology 1995; 136:3031-3036.

83. Gupta H M, Talwar G P and Salunke D M. A novel computer modeling approach to the structure of small bioactive peptides: The structure of the gonadotropin-releasing hormone. Proteins: Structure, Function and Genetics 1993; 16:48-56.

84. Hargrave P A and McDowell J H. Rhodopsin and phototransduction: A model system for G protein-linked receptors. FASEB Journal 1992; 6:2323-2331.

85. Harris N, Dutlow C, Eidne K E, Dong K-W, Roberts J and Millar R P. Gonadotropin-releasing hormone gene expression in MDA-MB-231 and ZR-75-1 breast carcinoma cell lines. Cancer Research 1991; 51:2577-2581.

86. Hauger R L, Karsch F J and Foster D L. A new concept for the control of the estrous cycle of the ewe based on the temporal relationships between LH, estradiol, and progesterone in peripheral serum and evidence that progesterone inhibits tonic LH secretion. Endocrinology 1977; 101:807-817.

87. Hauser F, Meyerhor W, Wulfsen I, Schonorock C and Richter D. Sequence analysis of the promoter region of the rat somatostatin receptor subtype 1 gene. FEBS Letters 1994; 345:225-228.

88. Havelka W A, Henderson R and Oesterhelt D. Three-dimensional structure of halorhodopsin at 7Å resolution. Journal of Molecular Biology 1995; 247:726-738.

89. Haviv F, Fitzpatrick T D, Nichols C J, Swenson R E, Bush E N, Diaz G, Nguyen A, Nellons H N, Hoffman D J, Ghanbari H, Johnston E S, Love S, Cybulski V and Greer J. Stabilisation of the N-terminal residues of the luteinising-hormone releasing hormone agonists and the effects on pharmacokinetics. Journal of Medicinal Chemistry 1992; 35:3890-3894.

90. Hazum E. Binding properties of solubilised gonadotropin-releasing hormone receptor: Role of carboxyl groups. Biochemistry 1987; 26:7011-7014.

91. Hazum E, Fridkin M, Baram T and Kosh Y. Synthesis, biological activity and resistance to enzyme degradation of luteinising-hormone releasing hormone analogues modified at position 7. FEBS Letters 1981; 213:300-302.

92. Henderson R, Baldwin J M, Ceska T A, Zemlin F, Beckmann E and Downing K H. Model for the structure of bacteriorhodopsin based on high-resolution electron cryo-microscopy. The Journal of Molecular Biology 1990; 213:899-929.

93. Hille B, Tse A, Tse F and Bosma M M. Signalling mechanisms during response of pituitary gonadotrophs to GnRH. Recent Progress in Hormone Research 1995; 50:75-95.

94. Hoflack J, Trumpp-Kalmeyer S and Hibert M. Re-evaluation of bacteriorhodopsin as a model for G-protein coupled receptors. Trends in Pharmacological Science 1994; 15:7-9.

95. Horn F, Bilezikjian L M, Perrin M H, Bosma M M, Windle J J, Huber K S, Blount A L, Hille B, Vale W and Mellon P L. Intracellular responses to the gonadotropin-releasing hormone in a clonal cell line of gonadotrope origin. Molecular Endocrinology 1991; 5:347-355.

96. Horn F, Windle J J, Barnhart K M and Mellon P L. Tissue specific gene expression in the pituitary: The glycoprotein hormone α-subunit gene is regulated by a gonadotrophe-specific protein. Molecular Cell Biology 1992; 12:2143-2153.

97. Hortsman D A, Brandon S, Wilson A L, Guyer C A, Cragoe E J and Limbard L E. An aspartate conserved among G-protein receptors confers allosteric regulation of the α2 adrenergic receptors by sodium. Journal of Biological Chemistry 1992; 265:21590-21595.

98. Horvath E and Kovacs K. Anatomy and histology of the normal and abnormal pituitary gland. In: DeGroot L J, ed. Endocrinology. 3rd ed. Philadelphia: W B Saunders Company, 1995: 160-177.

99. Hsieh K-P and Martin T F J. Thyrotropin-releasing hormone and gonadotropin releasing hormone receptors activate phospholipase C by coupling to the guanosine triphosphate-binding proteins G_q and G_{11}. Molecular Endocrinology 1992; 6:1673-1681.

100. Huhtaniemi I T, Eskola V, Pakarinen P, Matikainen T and Sprengel R. The murine luteinizing hormone and follicle-stimulating hormone receptor genes: Transcription initiation sites, putative promoter sequences and promoter activity. Molecular and Cellular Endocrinology 1992; 88:56-66.

101. Hunting A L, Lindgreen J A, Hokfelt T, Eneroth P, Werner S, Patrono C and Samuelsson B. Leukotriene C4 as a mediator of luteinizing hormone release from rat pituitary cells. Proceedings of the National Academy of Sciences: USA 1985; 82:3834-3838.

102. Iida T, Stojikovic S S, Izumi S-I and Catt K J. Spontaneous and agonist induced calcium oscillations and secretory responses in pituitary gonadotrophs. Molecular Endocrinology 1991; 5:949-958.

103. Iino M and Endo M. Calcium dependent immediate feedback control of inositol 1,4,5-trisphosphate-induced Ca^{2+} release. Nature 1992; 360:76-78.

104. Ikeda Y, Luo X, Abbud R, Nilson J H and Parker K L. The nuclear receptor steroidogenic factor 1 is essential for the formation of the ventromedial hypothalamic nucleus. Molecular Endocrinology 1995; 9:478-486.

105. Illing N, Jacobs G F M, Becker I I, Flanagan C A, Davidson J S, Eales A, Sealfon S C and Millar R P. Comparative sequence analysis and functional characterization of the cloned sheep gonadotropin-releasing hormone receptor reveals differences in primary structure and ligand specificity among mammalian receptors. Biochemical and Biophysical Research Communications 1993; 196:745-751.

106. Janecka A, Janecki T, Bowers C and Folkers K. Effective antagonists with luteinizing hormone releasing hormone modified at position one. Amino Acids 1993; 5:359-365.

107. Janecka A, Janecki T, Bowers C and Folkers K. The structural features of effective antagonists of the luteinising releasing hormone. Amino Acids 1994; 6:111-130.

108. Janovick J A and Conn P M. A cholera toxin-sensitive guanyl nucleotide binding protein mediates the movement of pituitary luteinising hormone into a releasable pool: loss of this event is associated with the onset of homologous desensitization to gonadotropin-releasing hormone. Endocrinology 1993; 132:2131-2135.

109. Janovick J A, Haviv F, Fitzpatrick T F and Conn P M. Differential activation of a GnRH agonist and antagonist in the pituitary GnRH receptor. Endocrinology 1993; 133:942-945.

110. Jennes L and Conn P M. Gonadotropin-releasing hormone and its receptors in rat brain. Frontiers in Neuroendocrinology 1994; 15:51-77.

111. Jennes L, Dalati D and Conn P M. Distribution of gonadotropin-releasing hormone agonist binding sites in the rat central nervous system. Brain Research 1988; 452:156-164.

112. Ji I and Ji T H. Differential role of the exoloop1 of the human follicle-stimulating hormone receptor in hormone binding and receptor activation. Journal of Biological Chemistry 1995; 270:15970-15973.

113. Johnson M H and Everitt B J. The regulation of gonadal function. In: Essential Reproduction. 4th ed. Oxford: Blackwell Science, 1995: 79-108.

114. Johnson R M, Wasilenko W J, Mattingly R R, Weber M J and Garrison J C. Fibroblast transformed with v-src show enhanced formation of an inositol tetrakisphosphate. Science 1989; 246:121-124.

115. Jonathan B. Dopamine: A prolactin inhibiting hormone. Endocrine Review 1985; 6:564-589.

116. Kaiser U B, Jakubowiak A, Steinberger A and Chin W W. Regulation of rat pituitary gonadotropin-releasing hormone receptor mRNA levels in vivo and in vitro. Endocrinology 1993; 133:931-934.

117. Kaiser U B, Zhao D, Cardona R G and Chin W W. Isolation and characterization of the cDNAs encoding the rat pituitary gonadotropin-releasing hormone receptor. Biochemical and Biophysical Research Communications 1992; 189:1645-1652.

118. Kakar S S, Grantham K, Musgrove L C, Devor D, Sellars J C and Neill J D. Rat gonadotropin-releasing hormone (GnRH) receptor: Tissue expression and hormonal regulation of its mRNA. Endocrinology 1994; 101:154-157.

119. Kakar S S, Musgrove L C, Devor D C, Sellers J C and Neill J D. Cloning, sequencing and expression of the human gonadotropin-releasing hormone (GnRH) receptor. Biochemical and Biophysical Research Communications 1992; 189: 289-295.

120. Kakar S S, Rahe C H and Neill J D. Molecular cloning, sequencing and characterizing the bovine receptor for the gonadotropin-releasing hormone (GnRH). Domestic Animal Endocrinology 1993; 10:335-342.

121. Kamel F, Balz J A, Kubajak C L and Scheider V A. Gonadal steroids modulate pulsatile luteinizing hormone secretion by perifused rat anterior pituitary cells. Endocrinology 1987; 120:1651-1657.

122. Karnik S S and Khorana H G. Assembly of functional rhodopsin requires a disulfide bond between cysteine residues at 110 and 187. Journal of Biological Chemistry 1990; 265:17520-17524.

123. Karnik S S, Sakmar T P, Chen H-B and Khorana H G. Cysteine residues 110 and 187 are essential for the formation of the correct structure of bovine rhodopsin. Proceedings of the National Academy of Sciences: USA 1988; 85:8859-8459.

124. Karten M J and Rivier J E. Gonadotropin-releasing hormone analog design. Structure-function studies towards the development of agonists and antagonists: Rationale and perspectives. Endocrine Reviews 1986; 7:44-66.

125. Katt J A, Duncan J A, Herbon L, Barkan A and Marshall J C. The frequency of gonadotrophin releasing hormone stimulation determines the number of pituitary gonadotrophin releasing hormone receptors. Endocrinology 1985; 116:2113-2115.

126. Keinan D and Hazum E. Mapping of the gonadotropin-releasing hormone receptor binding site. Biochemistry 1985; 24:7728-7732.

127. Kepa J K, Wang C, Needly C I, Raynolds M V, Gordon D F, Woods W M and Wierman M E. Structure of the rat gonadotropin-releasing hormone (GnRH) gene promoter and functional analysis in hypothalamic cells. Nucleic Acid Research 1992; 20:1393-1399.

128. Khodr G S and Siler-Khodr T M. The effect of luteinising hormone factor on the human chorionic gonadotropin secretion. Fertility and Sterility 1978; 30:301-314.

129. Kim J, Wess J, Van Rhee A M, Schoneberg T and Jacobson K A. Site-directed mutagenesis identifies residues involved in ligand recognition in the human A_{2a} adenosine receptor. Journal of Biological Chemistry 1995; 270:13987-13997.

130. King J A, Hassan F, Mehl A I and Millar R P. Gonadotropin-releasing hormone molecular forms in the mammalian hypothalamus. Endocrinology 1988; 122:2742-2752.

131. Kjelsberg M A, Cotecchia S, Ostrowski J, Caron M G and Lefkowitz R J. Constitutive activation of the α_{1B} adrenergic receptor by all amino acid substitutions at a single site. Journal of Biological Chemistry 1992; 267:1430-1433.

132. Knobil E. Neuroendocrine control of the menstrual cycle. Recent Progress in Hormone Research 1980; 36:53-88.

133. Kosh Y, Goldhaber G, Fireman I, Zor U, Shani J and Tal E. Suppression of prolactin and thyrotropin secretion in the rat by antiserum to thyrotropin-releasing hormone. Endocrinology 1977; 100:1476-1478.

134. Kreiger D T. Brain peptides: What, where, why? Science 1983; 222:975-985.

135. Krsmanovic L Z, Stojilkovic S S, Mertz L M, Tomic M and Catt K J. Expression of gonadotropin-releasing hormone receptors and autoregulation of neuropeptide release in immortalised hypothalamic neurons. Proceedings of the National Academy of Sciences: USA 1993; 90:3908-3912.

136. Kumar T R and Low M J. Gonadal steroid hormone regulation of the mouse follicle stimulating hormone β-subunit expression in vivo. Molecular Endocrinology 1994; 7:898-906.

137. Kunkel T A. Rapid and efficient site-specific mutagenesis without phenotypic selection. Proceedings of the National Academy of Sciences: USA 1987; 82:488-492.

138. Le Blanc P, Crumetrolle M, Latouche J, Jordan D, Fillion G, L'Heritier A, Kordon C, Dussaillant M, Rostene W and Haour F. Characterization and distribution of receptors for gonadotropin releasing hormone in the rat hippocampus. Neuroendocrinology 1988; 48:482-488.

139. Lee C, Gardella T J, AbouSamra A-B, Nussbaum S R, Segre G V, Potts J T, Kronenberg H M and Juppner H. Role of the extracellular regions of the parathyroid hormone (PTH)/PTH-related peptide receptor in hormone binding. Endocrinology 1994; 135:1488-1495.

140. Lee T W, Anderson L A, Eidne K A and Milligan G. Comparison of the signalling properties of the long and short forms of the rat thyrotropin-releasing hormone receptor following expression in Rat 1 fibroblasts. Biochemical Journal 1995; 310:291-298.

141. Lemay A, Surrey E S and Friedman A J. Extending the use of gonadotropin-releasing hormone agonists: The emerging role of steroidal and non-steroidal agents. Fertility and Sterility 1994; 61:21-34.

142. Leong D and Thorner M D. A potential code of LHRH-induced calcium ion responses in the regulation of luteinizing hormone secretion among individual gonadotrophs. Journal of Biological Chemistry 1991; 266:9016-9022.

143. Lerrant Y, Kottler M-L, Bergametti F, Moumni M, Blumberg-Tick J and Counis R. Expression of gonadotropin-releasing hormone (GnRH) receptor is altered by GnRH agonist desensitisation in a manner similar to that of the gonadotropin β-subunit genes in normal and castrated rat pituitary. Endocrinology 1995; 136:2803-2808.

144. Li Y-X, Rinzel J, Keizer J and Stojilkovic S S. Calcium oscillations in pituitary gonadotrophs: Comparison of experiment and theory. Proceedings of the National Academy of Sciences: USA 1994; 91:58-62.

145. Limor R, Schvartz I, Hazum E, Ayalon D and Naor S. Effects of guanine nucleotides on stimulus secretion and coupling mechanisms in permeabilised pituitary cells: Relationship to gonadotropin-releasing hormone action. Biochemical and Biophysical Research Communications 1989; 159:51-58.

146. Lu R, Hubbard J R, Martin B R and Kalimi M Y. Roles of sulfhydryl and disulfide groups in the binding of CP-55,940 to rat cannabinoid receptor. Molecular and Cellular Biochemistry 1993; 121:119-126.

147. Lui T C and Jackson G L. Differential effects of cyclic nucleotide analogues and GnRH on LH synthesis and release. American Journal of Physiology 1981; 241:E6-E13.

148. Lui X, Davis D and Segaloff D. Disruption of potential sites N-linked glycosylation does not impair hormone binding to the lutropin/choriogonadotropin receptor if Asn-173 is left intact. Journal of Biological Chemistry 1993; 268:1513-1516.

149. Mahachoklertwattana P, Black S M, Kaplan S L, Bristow J D and Grumbach M M. Nitric oxide synthesized by gonadotropin-releasing hormone neurons is a mediator of N-methyl-D-aspartate (NMDA) induced GnRH secretion. Endocrinology 1994; 135:1709-1712.

150. MaMahon S B and Monroe J G. Role of primary response genes in generating cellular responses to growth factors. FASEB 1992; 6:2707-2715.

151. Matsuo H, Baba Y, Nair R M, Arimura A and Schally A V. Structure of the porcine LH- and FSH-releasing hormone I. Proposed amino acid sequence. Biochemical Biophysical Research Communications 1971; 43:1334-1339.

152. McCardle C A and Poch A. Dependence on gonadotropin-releasing hormone stimulated luteinizing hormone release upon intracellular Ca^{2+} pools is revealed by desensitisation and thapsigargin blockade. Endocrinology 1992; 130:3567-3574.

153. Melcangi R C, Galbiata M, Messi E, Piva F, Martin L and Motta M. Type 1 astrocytes influence luteinizing hormone releasing hormone release from the hypothalamic cell line GT1-1: Is transforming growth factor-beta the principle factor involved? Endocrinology 1995; 136:679-686.

154. Mellon P L, Windle J J, Goldsmith P C, Padula C A, Roberts J L and Weiner R I. Immortalization of hypothalamic GnRH neurons by genetically targeted tumorigenesis. Neuron 1990; 5:1-10.

155. Merchenthaler I, Setalo G, Csontos C, Petrusz P, Flerko B and Negro-Vilar A. Combined retrograde tracing and immunocytochemical identification of luteinizing hormone-releasing hormone and somatostatin-containing neurons projecting to the median eminence. Endocrinology 1990; 125:2812-2821.

156. Merrifield R B. Solid phase peptide synthesis I. The synthesis of a tetrapeptide. The Journal of the American Chemical Society 1963; 85:2149.

157. Metcalf G and Jackson I M D. Thyrotropin-releasing hormone receptor: Biomedical significance. New York Academy of Science: New York, 1989:631pp.

158. Mignery G A, Newton C L, Archer B T and Sudhof T C. Structure and expression of the rat inositol 1,4,5 trisphosphate receptor. Journal of Biological Chemistry 1990; 265:12679-12685.

159. Millar R P, Davidson J S, Flanagan C, Golembo M, Illing N, Jacobs G, Becker I, Wakefield I, Eales A, Tsutsumi M, Chi L, Zhou W and Sealfon S C. Towards the direct design of GnRH analogues: Insights from cloned GnRH receptors. In: Current Topics in Andrology. Oshima H and Burger H G, ed. Tokyo: Japan Society for Andrology, 1993:1-12.

160. Miller W R, Scott W N, Morris R, Fraser H M and Sharpe R M. LHRH agonists and human breast cancer cells. Nature 1985; 329:770.

161. Milligan G. Mechanisms of multifunctional signalling by G-protein linked receptors. Trends in Pharmacological Sciences 1993; 14:239-244.

162. Milovanovic S R, Radulovic S and Schally A V. Evaluation of binding of cytotoxic analogs of luteinizing hormone-releasing hormone to human breast cancer and mouse MTX mammary tumor. Breast Cancer Research and Treatment 1992; 24:147-158.

163. Monahan M W, Amoss M S, Anderson H A and Vale W. Synthetic analogs of the hypothalamic luteinising hormone releasing factor with increased agonist and antagonist properties. Biochemistry 1973; 12:4616.

164. Morgan R O, Chang J P and Catt K J. Novel aspects of gonadotropin-releasing hormone action on inositol polyphosphate metabolism in cultured pituitary gonadotrophs. Journal of Biological Chemistry 1987; 262:1166-1171.

165. Moro O, Lameh J, Hogger P and Sadee W. Hydrophobic amino acid in the i2 loop plays a key role in receptor-G protein coupling. Journal of Biological Chemistry 1993; 268:22273-22276.

166. Moro O, Shockley M S, Lameh J and Sadee W. Overlapping multi-site domains of the muscarinic cholinergic Hm1 receptor involved in signal transduction and sequestration. Journal of Biological Chemistry 1994; 269:6651-6655.

167. Morrison N, Sellar R E, Boyd E, Eidne K A and Connor J M. Assignment of the gene encoding the human gonadotropin-releasing hormone receptor to 4q13.2-13.3 by fluorescence in-situ hybridization. Human Genetics 1994; 93:714-715.

168. Nagy G, Mulchahey J J and Neill J D. Autocrine control of prolactin secretion by vasoactive intestinal peptide. Endocrinology 1988; 122:364-366.

169. Naor Z. Signal transduction mechanisms in Ca^{2+} mobilising hormones: The case of gonadotropin-releasing hormone. Endocrine Reviews 1990; 11:326-353.

170. Naor Z, Fawcett C P and McCann S M. Differential effects of castration and testosterone replacement on basal and LHRH-stimulated cAMP and cGMP accumulation and on gonadotropin release from the pituitary gland of the male rat. Molecular and Cellular Endocrinology 1979; 14:191-198.

171. Naor Z, Keiser L, Vanderhoek J Y and Catt K J. Mechanism of action of gonadotropin-releasing hormone: Role of the lipoxygenase products arachadonic acid in luteinizing hormone release. Journal of Steroid Biochemistry 1985; 23:711-717.

172. Nazian S J, Landon C S, Muffly K E and Cameron D F. Opioid inhibition of adrenergic and dopaminergic but not serotonergic stimulation of luteinizing releasing hormone released from immortalised hypothalamic neurons. Molecular and Cellular Neuroscience 1994; 5:642-648.

173. Neve K A, Cox B A, Henningson R A, Spanoyannis A and Neve R L. Pivotal role for aspartate-80 in the regulation of dopamine D2 receptor affinity for drugs and the inhibition of adenylate cyclase. Molecular Pharmacology 1991; 39:733-739.

174. Ng G Y K, Mouillac B, George S R, Caron M, Dennis M, Bouvier M and O'Dowd B F. Desensitisation, phosphorylation and palmitoylation of the human dopamine D1 receptor. European Journal of Pharmacology 1994; 267:7-19.

175. Nikolics K, Shonyi E and Ramachandran Y. Photoaffinity labeling of pituitary GnRH receptors: significance and position of photolabel on the ligand. Biochemistry 1988; 27:1425-1432.

176. Noda K, Saad Y, Graham R M and Karnik S S. The high affinity state of the β2-adrenergic receptor requires unique interaction between conserved and non-conserved extracellular loop cysteines. Journal of Biological Chemistry 1994; 269:6743-6752.

177. Nunn D L and Taylor C W. Luminal Ca^{2+} increases the sensitivity of Ca^{2+} stores to inositol 1,4,5-trisphosphate. Molecular Pharmacology 1992; 41:115-119.

178. O'Dowd B F, Hanatowich M, Caron M G and Lefkowitz R J. Palmitoylation of the human β2-adrenergic receptor. Journal of Biological Chemistry 1989; 264:7564-7569.

179. Parini A, Homcy C J and Graham R M. Structural properties of the α1-Adrenergic receptor: Studies with membrane purified receptor preparations. Circulation Research 1987; 61:I100-I104.

180. Pelvin R A and Boarder M R. Stimulation of formation of inositol phosphates in primary cultures of bovine adrenal chromaffin cells by angiotensin II, histamine, bradykinin and carbachol. Journal of Neurochemistry 1988; 51:634-641.

181. Perlman J H, Thaw C N, Laakkonen L, Bowers C Y, Osman R and Gershengorn M C. Hydrogen bonding interaction of thyrotropin-releasing hormone (TRH) with transmembrane tyrosine 106 of the TRH receptor. Journal of Biological Chemistry 1994a; 269:1610-1613.

182. Perlman J H, Laakkonen L, Osman R and Gershengorn M C. A model of the thyrotropin-releasing hormone (TRH) receptor binding pocket. Journal of Biological Chemistry 1994b; 269:23383-23386.

183. Perlman J H, Laakkonen L, Osman R and Gershengorn M C. Distinct roles for arginines in the transmembrane helices 6 and 7 of the thyrotropin-releasing hormone receptor. Molecular Pharmacology 1995; 47:480-484.

184. Perrin M H, Bilezikjian L M, Hoeger C, Donaldson C J, Rivier J, Haans Y and Vale W W. Molecular and functional characteristics of GnRH receptors cloned from rat pituitary and mouse pituitary tumor cell lines. Biochemical and Biophysical Research Communications 1993; 191:1139-1144.

185. Pfaff D W, Schwanzel-Fukuda F, Parhar I S, Lauber A H, McCarthy M M and Kow L-M. GnRH neurons and other cellular and molecular mechanisms for simple mammalian reproductive behaviors. Recent Progress in Hormone Research 1994; 49:1-25.

186. Poletti A, Melcangi R C, NegriCesi P, Maggi R and Martini L. Steroid binding and metabolism in the luteinizing-hormone releasing hormone producing neuronal cell line GT1-1. Endocrinology 1994; 135:2623-2628.

187. Popkin R, Bramley T A, Currie A, Shaw R W, Baird D T and Fraser H M. Specific binding of luteinising hormone releasing hormone to human luteal tissue. Biochemical Biophysical Research Communications 1983; 14:750-756.

188. Prevost G, Mormont C, Gunning M and Thomas F. Therapeutic use and perspectives of synthetic peptides in oncology. Acta Oncologica 1993; 32:209-215.

189. Probst W, Synder L A, Schuster D I, Brosius J and Sealfon S C. Sequence alignment of the G-protein coupled receptor superfamily. DNA and Cell Biology 1992; 11:1-20.

190. Qian X-X, Winitz S and Johnson G L. Epitope-tagged G_q α subunits: Expression of GTPase deficient α subunit persistently stimulates phosphatidylinositol-specific phospholipase C but not mitogen activated protein kinase activity by the m1 muscarinic acetylcholine receptor. Proceedings of the National Academy of Sciences: USA 1993; 90:4077-4081.

191. Quyam A, Gullick W J, Mellon K, Krausz T, Neal D, Sikora K and Waxman J. The partial purification and characterisation of GnRH-like activity from prostatic biopsy specimens and prostatic cancer cell lines. Journal of Steroid Biochemistry and Molecular Biology 1990a; 37:899-902.

192. Quyam A, Gullick W, Clayton R C, Sikora K and Waxman J. The effects of gonadotropin releasing hormone analogues in prostate cancer are mediated through specific tumour receptors. British Journal of Cancer 1990b; 62:96-99.

193. Radovick S, Wray S, Muglia L, Westphal H, Olsen B, Smith E, Patriquin E and Wondisford F E. Steroid hormone regulation and tissue-specific expression of the human GnRH gene in cell culture and transgenic animals. Hormones and Behaviour 1994; 28:520-529.

194. Rand E, Candelore M R, Cheung A H, Hill W S, Strader C D and Dixon R A F. Mutational analysis of β-adrenergic receptor glycosylation. Journal of Biological Chemistry 1990; 265:10759-10764.

195. Redding T W, Schally A V, Radulovic S, Milovanovic S, Szepeshazi K and Isaacs J. Sustained release formulations of luteinizing hormone-releasing hormone antagonist SB-75 inhibits proliferation and enhance apoptotic death of human prostate carcinoma (PC-82) in male nude mice. Cancer Research 1992; 52:2539-2544.

196. Reichlin S. Neuroendocrine control of pituitary function. In: Besser G M and Cudworth A G, ed. Clinical Endocrinology. London: Chapman and Hall, 1987: 1.2-1.14.

197. Reinhart J, Mertz L M and Catt K J. Molecular cloning and expression of cDNA encoding the murine gonadotropin releasing hormone receptor. Journal of Biological Chemistry 1992; 267:21281-21284.

198. Reissmann T, Diedrich K, Comaru-Schally A M and Schally A V. Introduction of LHRH-antagonists into the treatment of gynaecological disorders. Human Reproduction 1994; 9:767-769.

199. Reubi J C, Palacios J M and Maurer R. Specific luteinising hormone-releasing hormone receptor binding sites in hippocampus and pituitary. Neuroscience 1987; 21:847-856.

200. Russo D, Chazenbalk G D, Nagayama Y, Wadsworth H L and Rapoport B. Site-directed mutagenesis of the human thyrotropin receptor: Role of asparagine-linked oligosaccharides in the expression of a functional receptor. Molecular Endocrinology 1991; 5:29-33.

201. Sakmar T F, Franke R R and Khorana H G. Glutamic acid-113 serves as the retinylidine schiff base counterion in bovine rhodopsin. Proceedings of the National Academy of Sciences: USA 1989; 86:8309-8313.

202. Sambrook J, Fritsch E F and Maniatis T. Molecular Cloning A Laboratory Manual. 2nd ed. Cold Spring Harbor Laboratory Press: New York, 1989; 16.1-16.72.

203. Sandow J. Clinical applications of LHRH and its analogues. Clinical Endocrinology 1983; 18:571-592.

204. Sankararamakrishnan R, Sreerama N and Vishveshwara S. Characterization of proline containing right-handed α-helical regions by molecular dynamics. Biophysical Chemistry 1991; 40:97-108.

205. Savarese T M and Fraser C M. In vitro mutagenesis and the search for structure-function relationships among G-protein coupled receptors. Biochemical Journal 1992; 283:1-19.

206. Savarese T M, Wang C-D and Fraser C M. Site-directed mutagenesis of the rat m1 muscarinic acetylcholine receptor. Journal of Biological Chemistry 1992; 267:11439-11448.

207. Schally A V, Comaru-Schally A M and Redding T W. Antitumor effects of analogs of hypothalamic hormones in endocrine-dependent cancers. Proceedings of the Society for Experimental Biology and Medicine 1984; 175:259-281.

208. Schertler G F X, Villa C and Henderson R. Projection structure of rhodopsin. Nature 1993; 362:770-772.

209. Schertler G F X and Hargrave P A. Projection structure of frog rhodopsin in two crystal forms. Proceedings of the National Academy of Sciences: USA 1995; 92: 11578-11582.

210. Schmidt F, Sundaram K, Thau R B and Bardin C W. [Ac-D-Nal^{1},4FD-Phe^{2},D-Trp^{3},D-Arg^{6}]-LHRH, a potent antagonist of LHRH, produces transient edema and behavioural changes in rats. Contraception 1984; 29:283-289.

211. Schwanzel-Fukuda F, Bick D and Pfaff D W. Luteinizing hormone-releasing hormone (LHRH) expressing cells do not migrate normally in inherited hypogonadal (Kallmann) syndrome. Brain Research 1989; 6:311-326.

212. Schwanzel-Fukuda F and Pfaff D W. The origin of luteinizing-hormone-releasing hormone neurons. Nature 1989; 338:161-164.

213. Schwanzel-Fukuda M, Zheng L M, Bergen H, Weesner G and Pfaff D W. LHRH neurons: Function and development. Progress in Brain Research 1992; 93:189-203.

214. Sealfon S C and Millar R P. The gonadotrophin-releasing hormone receptor: Structural determinants and regulatory control. Reviews of Reproductive Biology 1995; 17:255-283.

215. Seeburg P H and Adelman J P. Characterization of a cDNA precursor of human luteinising hormone releasing hormone. Nature 1984; 311:666-668.

216. Seeburg P H, Mason A J, Stewart T A and Nikolics K. The mammalian GnRH gene and its pivotal role in reproduction. Recent Progress in Hormone Research 1987; 43:69-91.

217. Sellar R E, Taylor P L, Lamb R F, Zabavnik J, Anderson L and Eidne K A. Functional expression and molecular characterization of the thyrotrophin-releasing hormone receptor from the rat anterior pituitary gland. Journal of Molecular Endocrinology 1993; 10:199-206.

218. Seprodi J, Coy D H, Vilchez-Martinez J A, Pedroza E and Schally A V. Branched-chain analogues of luteinizing hormone releasing-hormone. Journal of Medicinal Chemistry 1978; 21:276.

219. Sharpe R M and Fraser H M. Leydig cell receptors for luteinising hormone releasing hormone and its agonists and their modulation by administration or depriving of the releasing hormone. Biochemical and Biophysical Research Communications 1980; 95:256-262.

220. Shears S B. Metabolism of inositol phosphates. Advances in Second Messenger Phosphoprotein Research 1992; 26:63-92.

221. Sherwood N M, Lovejoy D A and Coe I R. Origin of mammalian gonadotropin-releasing hormone. Endocrine Review 1993; 14:241-254.

222. Shupnik M A. Effects of GnRH on rat gonadotropin-gene transcription in vitro: Requirement for pulsatile secretion for LH beta gene stimulation. Molecular Endocrinology 1990; 4:1444-1451.

223. Shupnik M A, Gharib S D and Chin W W. Divergent effects of estradiol on gonadotropin gene transcription in pituitary fragments. Molecular Endocrinology 1989; 3:474-478.

224. Sielecki A R, Hendrickson W A, Broughton C G, Delbaere L T, Brayer G D and James M N. Protein structure refinement: Streptomyces griseus serine protease A at 1.8Å resolution. Journal of Molecular Biology 1979; 134:781-804.

225. Silverman A J, Krey L C and Zimmerman E A. A comparative study of the luteinising hormone releasing hormone (LHRH) neuronal networks in mammals. Biology of Reproduction 1979; 20:98-110.

226. Soules M R, Steiner R A, Clifton D K, Cohen N L, Aksel S and Bremmer W J. Progesterone modulation of pulsatile LH secretion in normal women. Journal of Clinical Endocrinology and Metabolism 1984; 58:378-83.

227. Speigel A M, Shenker A and Weinstein L S. Receptor-effector coupling by G-proteins: Implication for normal and abnormal signal transduction. Endocrine Reviews 1992; 13:536-565.

228. Spergel D J, Krsmanovic L Z, Stojilkovic S S and Catt K J. Glutamate modulates $(Ca^{2+})(i)$ and gonadotropin releasing hormone secretion in immortalised hypothalamic GT1-7 neurons. Neuroendocrinology 1994; 59:309-317.

229. Stojilkovic S S and Catt K J. Calcium oscillations in anterior pituitary cells. Endocrine Reviews 1992; 13:256-280.

230. Stojilkovic S S, Kukulijan M, Tomic M, Rojas E and Catt K J. Mechanism of agonist-induced $[Ca^{2+}]i$ oscillations in pituitary gonadotrophs. Journal of Biological Chemistry 1993; 268:7713-7720.

231. Stojilkovic S S, Krsmanovic L Z, Spergel D L and Catt K J. Gonadotropin-releasing hormone neurons: Instrinsic pulsatility and receptor mediated regulation. Trends in Endocrinology and Metabolism 1994a; 5:201-208.

232. Stojilkovic S S, Reinhart J and Catt K J. Gonadotropin-releasing hormone receptors: Structure and signal transduction pathways. Endocrine Reviews 1994b; 15:462-499.

233. Strader C D, Sigal I S, Register R B, Canderlore M R, Rands E and Dixon R A F. Identification of residues required for ligand binding to the β-adrenergic receptor. Proceedings of the National Academy of Sciences: USA 1987; 84:4384-4388.

234. Strader C D, Sigal I S, Canderlore M R, Rands E, Hill W S and Dixon R A F. Conserved aspartate residues 79 and 113 of the β-adrenergic receptor have different roles in receptor function. Journal of Biological Chemistry 1988; 263:10267-10271.

235. Strader C D, Sigal I S and Dixon R A F. Structural basis of β-adrenergic function. FASEB Journal 1989; 3:1825-1832.

236. Tan L and Rousseau P. The chemical identity of the immunoreactive LHRH-like peptide biosynthesized in the human placenta. Biochemical Biophysical Research Communications 1982; 109:1061-1071.

237. Thompson J D, Higgins D G and Gibson T J. CLUSTAL W: Improving the sensitivity of progressive multiple sequence alignment through sequence weighting, position-specific-gap penalties and weight matrix choice. Nucleic Acid Research 1994; 22:4673-4680.

238. Thompson M A, Adelson M D and Kaufman L M. Lupron retards proliferation of ovarian epithelial tumor cells cultured in serum free medium. Journal of Clinical Endocrinology and Metabolism 1991; 72:1036-1041.

239. Titus D E, ed. Promega Protocols and applications guide. 2nd ed. Madson: Promega Corporation, 1991:422.

240. Tsutsumi M, Zhou W, Millar R P, Mellon P L, Roberts J L, Flanagon C A, Dong K, Gillo B and Sealfon S C. Cloning and functional expression of a mouse gonodotrophin-releasing hormone receptor. Molecular Endocrinology 1992; 6:1163-1168.

241. Tsutsumi M, Lewis S C and Sealfon S C. Homologous up-regulation of the gonadotropin-releasing hormone receptor in αT3-1 cells is associated with unchanged receptor messenger RNA (mRNA) levels and altered mRNA activity. Molecular Endocrinology 1993; 7:1625-1633.

242. Tsutsumi M, Laws S C, Rodic V and Sealfon S C. Translational regulation of the gonadotropin-releasing hormone receptor in αT3-1 cells. Endocrinology 1995; 136:1128-1136.

243. Turzillo A M, Jeugel J L and Nett T M. Pulsatile gonadotropin-releasing hormone (GnRH) increases concentrations of GnRH receptor messenger ribonucleic acid and number of GnRH receptors during luteolysis in the ewe. Biology of Reproduction 1995; 53:418-423.

244. Vale W, Grant G, Rivier J, Amoss M, Blackwell R, Burgus R and Guillemin R. Synthetic polypeptide antagonists of the hypothalamic luteinising hormone releasing factor. Science 1972; 176:933.

245. Vale W, Spiess J, Rivier C and Rivier J. Characterisation of a 41 residue ovine hypothalamic peptide that stimulates the secretion of corticotropin and β endorphins. Science 1981; 213:1394-1397.

246. Van-Vugt D A, Lam N Y and Ferin M. Reduced frequency of pulsatile LH secretion in the luteal phase of the rhesus monkey: Involvement of endogenous opioids. Endocrinology 1984; 115:1095-1101.

247. Wang O F, Farnworth P G, Findlay J K and Burger H G. Effect of purified 31K bovine inhibin on specific binding of gonadotropin releasing hormone to rat anterior pituitary cells in culture. Endocrinology 1988; 123:2161-2166.

248. Weick R F and Noh K A. Inhibitory effects of estrogen and progesterone on several parameters of pulsatile LH release in the ovariectomized rat. Neuroendocrinology 1984; 38:351-356.

249. Whitelaw P F, Eidne K A, Sellar R, Symth C D and Hillier S G. Gonadotropin-releasing hormone receptor messenger ribonucleic acid expression in the rat ovary. Endocrinology 1995; 136:172-179.

250. Wray S, Zoller R T and Gainer H. Differential effects of estrogen on LHRH expression gene expression in slice explant cultures prepared from specific forebrain regions. Molecular Endocrinology 1989; 3:1197-1203.

251. Wu J S, Sealfon S C and Miller W L. Gonadal hormones and gonadotropin-releasing hormone alter mRNA levels of GnRH receptors in sheep. Endocrinology 1994; 134:1846-1850.

252. Xu B, Sahu A, Crowley W R, Leranth C, Horvath T and Kalra S P. Role of neuropeptide Y in episodic luteinizing hormone release in ovariectomized rats: An excitatory component and opioid involvement. Endocrinology 1993; 133:747-754.

253. Yamaji T, Dierschke D J, Bhattacharya A N and Knobil E. The negative feedback control of estradiol and progesterone on LH secretion in ovariectomized rhesus monkey. Endocrinology 1992; 90:771-777.

254. Yamamoto Y, Kamiya K and Terao S. Modeling of the human thromboxane A_2 receptor and analysis of the receptor ligand interactions. Journal of Medicinal Chemistry 1993; 36:820-825.

255. Yamano Y, Ohyama K, Chaki S, Guo D-F and Inagami T. Identification of amino acid residues of the rat angiotensin II receptor for ligand binding by site directed mutagenesis. Biochemical and Biophysical Research Communications 1992; 187:1426-1431.

256. Yen S C C. The hypothalamic control of pituitary hormone secretion. In: Reproductive Endocrinology. Yen S S C and Jaffe R B, ed. 3rd ed. Philadelphia: W B Saunders Company, 1991: 65-104.

257. Zhang D and Weinstein H. Signal transduction by a $5HT_{2A}$ receptor: A mechanistic hypothesis from molecular dynamics simulations of the three-dimensional model of the receptor complexed to ligands. Journal of Medicinal Chemistry 1993; 36:934-938.

258. Zhang D and Weinstein H. Polarity conserved positions in transmembrane domains of G-protein coupled receptors and bacteriorhodopsin. FEBS Letters 1994; 337:207-212.

259. Zhang R, Tsai-Morris C H, Kitamura M, Bucako E and Dufau M L. Changes in binding activity of luteinizing hormone receptors by site-directed mutagenesis of potential glycosylation sites. Biochemical and Biophysical Research Communications 1991; 181:804-808.

260. Zheng L, Stojilkovic S S, Hunyady L, Krsmanovic L Z and Catt K J. Sequential activation of phospholipase C and phospholipase D in agonist-stimulated gonadotrophs. Endocrinology 1994; 134:1446-1454.

261. Zhou W, Flanagan C, Ballesteros J A, Konvicka K, Davidson J S, Weinstein H, Millar R P and Sealfon S C. A reciprocal mutation supports helix 2 and helix 7 proximity in the gonadotropin-releasing hormone receptor. Molecular Pharmacology 1993; 45:165-170.

262. Zhou W and Sealfon S C. Structure of the mouse gonadotropin-releasing hormone receptor gene: Variant transcripts generated by alternative processing. DNA and Cell Biology 1994; 13:605-614.

263. Zhou W, Rodic V, Kitanovic S, Flanagan C A, Chi L, Weinstein H, Maayani S, Millar R P and Sealfon S C. A locus of the gonadotropin-releasing hormone receptor that differentiates agonist and antagonist binding sites. Journal of Biological Chemistry 1995; 270:18853-18857.